Exploring Brain CSF-Mediated Clearance in Major Depressive Disorder using Neuroimaging

Althubaity, Noha

Awarding institution:
King's College London

Exploring Brain CSF-Mediated Clearance in Major Depressive Disorder using Neuroimaging

Noha Saad Althubaity

A thesis submitted for the degree of Doctor of Philosophy in Neuroimaging Analysis

First Supervisor: Dr. Mattia Veronese
Second Supervisor: Dr. Danai Dima

Department of Neuroimaging
King's College London
London, UK
July 2023

Acknowledgements

My PhD journey has been unforgettable. Every moment of my PhD life was filled with happiness, challenges, and brightness. I have appreciated every day since I started my PhD in 2019 until now. A huge thanks to the incredible people who made this dream come true. A massive thanks to my first supervisor, Dr Mattia Veronese, and second supervisor, Dr Danai Dema, who believed in me and kept supporting and helping me until this moment. They made my journey amazing, as well as full of passion and prosperity. They improved my learning and my research skills. They taught me how to think critically and outside of the box. They were always there for me and stood beside me at all times, especially during the difficult period of COVID-19. I would not have been able to finish my PhD and publish my papers without them. Through their supervision, I learned professionalism, they provided me with a safe space, and were full of patience to allow me to grow and develop to be an independent researcher. Their comments and guidance were always valued and helpful. I always felt very comfortable asking them for help whenever I needed it. I would like to thank Professor Federico Turkheimer for his thoughts, support, help, and co-operation on this project. I am so lucky to have such wonderful supervisors and a research team who made this work on a very interesting and new topic enjoyable.

I would like to thank all the co-authors who were involved in published papers, including the research group at NIMA consortium and BIODEP project that provided data involved in my analysis as well as useful feedback throughout my project.

A huge thanks to my family who encouraged and motivated me every time. I could not have completed this project without the enormous love and support provided by my parents, sisters, and brothers from Riyadh all the way to London. It was so hard to be away from family and my home while doing such a challenging task, but my family was always full of faith and trust

that I will make it through this adventure. I am so grateful that I have an amazing family who believed in me and are always by my side.

The period of COVID-19 was very difficult in that it affected my studies and health. I would like to thank my family, supervisors, and dearest friends, both in London and in Riyadh, who helped me to recover during the lockdown and feel well enough to continue my studies and complete my PhD. Also, I would like to thank my colleagues in the research team who offered their assistance during the distance learning period. I would like to thank every person who participated in all my happy and challenging moments during my PhD and sent me love, support, and prayers.

I am thankful for my decision to move to London, have a new experience, and take the opportunity to do scientific research and enhance my research skills, which I loved.

Finally, I would like to acknowledge the King Saud bin Abdulaziz University for Health Science in Riyadh, which sponsored my PhD, and the Saudi Arabia Cultural Bureau in London, which supported me. A special thanks to Dr Ali Dhebaib, the head of the department of Radiology Science at the Kings Saud bin Abdulaziz University for Health Science.

Abstract

Major Depression Disorder (MDD) is a significant neuropsychiatric disorder which leads to disabilities worldwide. Considerable evidence has shown links between peripheral inflammation and MDD pathophysiology, but how these peripheral inflammation changes are incorporated into the brain remains poorly understood. Peripheral and central immune interactions are discussed in the literature, which suggests a mechanism for developing neuroinflammation linked to the disruption of the brain solute clearance and fluid homeostasis in the brain. In this model, the dysregulation of the dynamic or the production of cerebrospinal fluid (CSF) may contribute to the dysfunction of the brain's waste clearance pathways.

A few studies on neurological conditions have indirectly examined the CSF-mediated clearance alteration by assessing the CSF dynamic in the lateral ventricles using Positron Emission Tomography (PET). Other studies have used the Magnetic Resonance Imaging (MRI) to evaluate the alteration in the solute clearance. However, no previous studies have investigated CSF-mediated clearance and its relevance for neuroinflammation in MDD. This PhD thesis aims to examine indirect measurements of the brain CSF-mediated clearance using neuroimaging data to quantify their link to neuroinflammation in depression.

Study1: This study aimed at testing the immune-mediated model of depression that proposes a direct effect of peripheral cytokines and immune cells on the brain to elicit a neuroinflammatory response via a leaky blood–brain barrier and ultimately depressive behaviour. The blood-to-brain and blood-to-CSF perfusion rates for two TSPO radiotracers collected in two separate studies and were estimated, in two datasets normal and depressed cohorts and 7 healthy controls where peripheral inflammation was induced via subcutaneous injection of interferon (IFN)-α. In both studies we observed a consistent negative association between peripheral inflammation, measured with C-reactive protein (CRP), and radio tracer

perfusion into and from the brain parenchyma and CSF. These results suggest a different model of peripheral-to-central immunity interaction whereas peripheral inflammation may cause a reduction in BBB permeability.

Study 2: this study aimed to investigate choroid plexus (CP) volume alterations in depression and their associations with inflammation depressed participants and age- and sex-matched healthy controls using [^{11}C]PK11195 PET/structural MRI imaging for measuring neuro-inflammation and CP volume respectively. A significantly greater CP volume in depressed subjects compared to HCs was found which positively correlated with [^{11}C]PK11195 PET binding in the anterior cingulate cortex, prefrontal cortex, and insular cortex, but not with the peripheral inflammatory markers. The CP volume correlated with the [^{11}C]PK11195 PET binding in CP. This result supports the hypothesis that changes in brain barriers may cause reduction in solute exchanges between blood and CSF, disturbing the brain homeostasis and ultimately contributing to inflammation in depression.

Study 3: This paper aimed to explore the use of a free water (FW) measurement taken from the Neurite Orientation Dispersion and Density Imaging (NODDI) MRI process as an alternative to TSPO PET to quantify neuroinflammation in patients with depression.
No significant associations were observed between the FW fraction and peripheral and central inflammation markers, nor between the FW fraction and the depression clinical scores. Although we found evidence of changes in the FW in depression, there is no clear link between the FW and the immune response or depression.

These overall results indicate that CSF-mediated clearance alterations can be assessed using neuroimaging and explore a modified model of the peripheral-to-central immune axis.

The changes in the CSF clearance are associated with peripheral and central inflammation, but not necessarily with MDD.

Statement of Authorship

I hereby declare that all progress made in this project has been performed by Noha Althubaity. The original project was designed by Dr. Mattia Veronese and Dr. Danai Dima. All published papers and conference proceedings were circulated for co-author review before submission. All data analyzed for this project were previously collected for other studies as part of the Biomarkers in Depression Study (BIODEP, NIMA consortium, https://www.neuroimmunology.org.uk/). Julia Schubert helped to extract the PET signal in the lateral ventricles and choroid plexus. Daniel Martins run on the transcriptome analysis in study 2 in Chapter 3. Samira Bouyagoub performed the primary analysis of the NODDI map in study 3 in Chapter 4. Each study chapter is involved a contribution statement.

Ethics

All procedures performed in studies involving human participants were in accordance with the ethical standards of the institutional and/or national research committee and with the 1964 Helsinki declaration and its later amendments or comparable ethical standards. Written informed consent was obtained from all individual participants included in the studies. The BIODEP study was approved by the NRES Committee East of England Cambridge Central (REC reference:15/EE/0092) and the UK Administration.

List of abbreviations

Aβ	β-amyloid
ACC	Anterior cingulate cortex
AD	Alzheimer's disease
ANOVA	Analysis of variance
AQP1	Aquaporin-1
AQP4	Aquaporin-4
AUC	Area under curve
BBB	Blood-brain barrier
BCSFB	Blood-cerebrospinal fluid barrier
BIODEP	Biomarkers in Depression
11 C	Carbon 11
CRP	C-reactive protein
CNS	Central nervous system
CP	Choroid plexus
DVR	Distribution volume ratio
FLIRT	FMRIB Linear Image Registration Tool
FMRIB	Oxford Centre for Functional Magnetic Resonance Imaging of the Brain
FSL	FMRIB software library
FW	Free water volume

IFN- α	Interferon- α
IL-6	Interleukin-6
HC	Healthy controls
INS	Insular cortex
MCI	Mild cognitive impairment
MDD	Major Depression Disorder
MRI	Magnetic resonance imaging
MS	Multiple sclerosis
PBR	Peripheral benzodiazepine receptor
PET	Positron emission tomography
PFC	Prefrontal cortex
ROI	Region of interest
SD	Standard deviation
SPM	Statistical parametric mapping
SUV	Standardized uptake value
SUVR	Standardized uptake value ratio
TAC	Time activity curve
TBI	Traumatic brain injury
TNF- α	Tumour Necrosis Factor- α
TSPO	Translocator protein
V_T	Distribution volume

Table of Contents

List of Tables

List of Figures

Publications

Turkheimer FE, Althubaity N, Schubert JJ, Nettis MA, Cousins O, Dima D, Mondelli V, Bullmore ET, Pariante C, Veronese M. Increased serum peripheral C- reactive protein is associated with reduced brain barriers permeability of TSPO radioligands in healthy volunteers and depressed patients: implications for inflammation and depression. Brain Behav Immun. 2021; 91: 487-497.

Althubaity N, Schubert JJ, Yousaf T, Nettis MA, Mondelli V, Pariante C, Bullmore ET, Dima D, Turkheimer FE, Veronese M, NIMA Consortium. Choroid plexus enlargement is associated with neuroinflammation and reduction of blood brain barrier permeability in depression. Neuroimage. 2021; 33:

Conference proceedings:

Althubaity N, Schubert JJ, Yousaf T, Nettis MA, Mondelli V, Pariante C, Bullmore ET, Dima D, Turkheimer FE, Veronese M, NIMA Consortium. Choroid plexus enlargement is associated with neuroinflammation and reduction of blood brain barrier permeability in depression. Neuroimage. 2021; 33: 13th International Symposium of Functional Neuroreceptor Mapping of the Living Brain; 2021 Dec 14-16; virtual meeting, oral presentation.

Althubaity N, Schubert JJ, Yousaf T, Nettis MA, Mondelli V, Pariante C, Bullmore ET, Dima D, Turkheimer FE, Veronese M, NIMA Consortium. Choroid plexus enlargement is associated with neuroinflammation and reduction of blood brain barrier permeability in depression. Neuroimage. 2021; 33: International Webinar on Neurology & Neuro Disorders; March 13, 2023; virtual meeting, oral presentation.

1 Chapter 1: Introduction

In this introductory chapter we will briefly cover Major Depression Disorder (MDD) in terms of its diagnosis, symptoms, and treatment. Then, the role of the immune process and the inflammation of the aetiology in MDD will be discussed. Multiple and replicable evidence indicates that there is communication between the peripheral and central immune system, which may reflect the biological mechanism involved in developing brain inflammation or neuroinflammation. Peripheral inflammatory markers are found in patients suffering from depression. The different pathways of the proinflammatory markers crossing the brain tissue are explained, as well as the role of brain barriers to maintain the brain homeostasis of the depressive brain. After that, the role of the glial cells in developing neuroinflammation will be covered. Non-invasive measures to investigate neuroinflammation are now possible using neuroimaging procedures, including PET imaging and MRI. Neuroinflammation has been found to impact the microglia, astrocyte, and brain barriers, which exhibits a link to CSF mediating clearance. The process of CSF-mediating clearance has recently been discovered to be a process of Glymphatic Function. The glymphatic pathways and the dysfunction in different neurodegenerative disorders are described. Finally, different research examines the glymphatic pathways and the CSF clearance by using an indirect method to assess CSF mediated clearance.

1.1 Major Depression Disorder

Major Depression Disorder (MDD) is the most common mental disorder, ranked as the top cause of disability worldwide (Friedrich, 2017) in contributing to the international burden of disease (Ferrari et al., 2013).The World Health Organization states that MDD affects approximately 280 million people globally, and is expected to be the leading cause of disability by 2030 (World Health Organization, 2022)(Bains and Abdijadid, 2022). The predicted

economic cost of MDD globally between 2011 and 2030 is estimated to be approximately 5.36 trillion USD (Richards et al., 2016, Bloom et al., 2012). This includes the care, the pharmacological and cognitive behavioural therapy, as well as the resultant loss of employment caused globally (McCrone et al., 2018, Richards et al., 2016, Larson et al., 2022). The high cost-effect is estimated to increase in line with changes in demographic features, including sex and age (Ferrari et al., 2013). The rates of MDD are increasing in females compared to males, and in people with low-income and lower educational backgrounds (Annequin et al., 2015).

The two main symptoms used to identify MDD are mood dysregulation and anhedonia (Kennedy, 2022). MDD has at least five confirmed symptoms in addition to mood impairment or anhedonia based on the DSM-5 (Otte et al., 2016). Other symptoms not covered by the DMS, such as irritability and anxiety, can be measured using different rating scales, such as the Hamilton Rating Scale for Depression (HAMD), the Beck Depression Inventory (BDI), and the Center for Epidemiological Studies Depression Scale (Fried et al., 2016). Depression symptoms, including low mood, anhedonia and sadness, crying, feeling unpleasant and guilty, having no desire to do most daily activities, appetite/weight disturbance, fatigue, anxiety, insomnia or excessive sleep, and suicidal thoughts or attempts, must be present on most days or every day (Fried et al., 2016, Otte et al., 2016) . The presence of MDD can either be a single episode (2 weeks minimum) or recurrent episodes with no drug or alcohol abuse or other medical condition. MDD patients also demonstrate cognitive impairment, such as memory defect, impairment in attention, and verbal fluency (Sierksma et al., 2010).

MDD treatment is dependent on the severity and the characteristics of the depressive episode, as well as the symptoms displayed. The first line of treatment for MDD includes psychological therapy such as cognitive behavioural therapy and/or antidepressant medication (Wong and Licinio, 2001). Treatment using one method for MDD patients has an equivalent remission rate of approximately 30 to 40% (Gelenberg et al., 2010). Although a combination

of treatments including medication and cognitive therapies has a higher remission rate, this entails higher costs and effort (Craighead and Dunlop, 2014).

Less than 50% of depressed patients who were treated with antidepressant drugs demonstrated poorer responses to the standard antidepressant treatment (Petralia et al., 2020). Depression patients who were treated with at least two different antidepressants of a sufficient dose and for a sufficient period of time and failed to develop a significant response to the brain stimulation or improvement in the clinical outcomes are considered resistant to the antidepressant (Sackeim et al., 2019). One third of MDD patients who show resistance to antidepressants exhibit high peripheral inflammatory markers, such as cytokines, acute phase proteins, chemokines, adhesion molecules, and inflammatory mediators, such as prostaglandins in plasma and cerebrospinal fluid (CSF) (Strawbridge et al., 2015, Miller et al., 2009, Dantzer et al., 2008). It is important to note that a meta-analysis of randomised clinical trials which used an anti-inflammatory agent alongside antidepressant drugs approved for MDD sufferers, reveals that participants showed a better response to antidepressant treatment, with higher levels of remission, when using an anti-inflammation treatment compared to those receiving the placebo(Köhler et al., 2014, Bai et al., 2020). Studies in which the peripheral inflammatory markers were blocked showed a reduction in the depressive symptoms in pathologies accompanied by chorionic inflammation (Tyring et al., 2006, Abbott et al., 2015).

1.2 The role of peripheral inflammation in the aetiology of depression

Different studies have confirmed the role of inflammation and the immune system in the aetiology of depression (Raison et al., 2010, Nettis et al., 2020).The association between peripheral inflammation and depression has been investigated in a number of studies (Dantzer et al., 2006, Dantzer et al., 2008, Felger et al., 2018, Howren et al., 2009). Depression has been shown to be prevalent and comorbid with different autoimmune diseases (Gavard et al., 1993, Sartorius, 2022, Siegert and Abernethy, 2005, Matcham et al., 2013). These autoimmune

diseases, such as diabetes mellites Type 1 (Korczak et al., 2011), rheumatoid arthritis (Nerurkar et al., 2019), and multiple sclerosis (MS) (Feinstein et al., 2014) are associated with chronic inflammation. Chronic inflammation is characterised by slow and long-term inflammation which lasts for months or years. Many risk factors which have been found to contribute to chronic inflammation, such as stress, sleep disorders, obesity, a diet rich in saturated fat, ageing, and low sex hormones (Pahwa et al., 2021), have also been found in MDD patients (Fried and Nesse, 2015, Motivala et al., 2005, Meyers et al., 2005).

MDD patients who have experienced a history of early life trauma such as childhood sexual abuse – the most predictive risk factor for depression – demonstrated increased proinflammatory markers, including Tumour Necrosis Factor (TNF)-α, C-reactive protein (CRP), and Interleukin (IL)-6 (Baumeister et al., 2014). Moreover, the administration of immune challenges, such as interferon- α (IFN- α), which is used for the treatment of infectious diseases such as hepatitis C or a malignant disease, exhibited an association of up to 60% with the onset of mild to moderate depressive symptoms (Golden et al., 2005, Raison et al., 2005). Developing symptoms such as fatigue, anxiety, discomfort, loss of appetite, sleepiness, and loss of concentration during treatment for infection emulate depressive symptoms in MDD (Stieglitz et al., 2015). Increased peripheral inflammation cytokines and evolving sickness behaviour such as fatigue, confusion, and less desire to do daily activities, following a single injection of peripheral immune challenges, were identified in normal human volunteers (Nettis et al., 2020).

Patients with depression exhibit high levels of proinflammatory cytokines, including IL-6, TNF-α, and CRP (an acute inflammatory protein synthase in the liver in response to the IL-6) (Pasco et al., 2010). The proinflammatory cytokines are tiny proteins secreted by different nucleated cells (cells with a nucleus) and contribute to the development, homeostasis, and regulation of the immune process (Lackie, 2010). Low-grade inflammation measured by

the concentration of CRP in plasma has been found in MDD patients (Osimo et al., 2019), and predicted the onset of a depressive episode (Gimeno et al., 2009). Notably, the CRP in plasma, which is associated with depressive symptoms, is strongly correlated with the CRP and inflammatory cytokines in the CSF (Felger et al., 2018). Despite the fact that considerable evidence has shown links between peripheral inflammation and MDD pathophysiology, how these peripheral inflammation changes are incorporated into the brain remains poorly understood.

1.3 Peripheral immune system versus central immune system

The central nervous system (CNS) is known to be immuno-privileged, as it is isolated from the circulation and peripheral immune system by the blood-brain barrier (BBB) and blood CSF barriers (BCSFB), and its maintenance and homeostasis are independent (Croese et al., 2021). However, bone marrow-derived immune cells (myeloid cell) are involved in the central immune and neuroprotective processes (Croese et al., 2021) and play a significant role in neurological diseases and neuroinflammation (Passaro et al., 2021). The central immune system is composed of innate immune cells, including the microglia, resident macrophages, astrocytes, and ependymal and mast cells, which maintain the homeostasis and neuron plasticity (Passaro et al., 2021). The dysregulation on the CNS homeostasis due to injury, inflammation, bacterial, or viral infection will activate the immune cells. The microglia are the primary immune cells in the CNS which maintain homeostasis and are involved in the phagocytosis process (Ousman and Kubes, 2012). In terms of neuroinflammation, the activation of the microglial cells is promoted by the stimuli which either release proinflammatory phenotypes that induce neural damage, or anti-inflammatory phenotypes which help to repair neurons (Mosser and Edwards, 2008). This classification of the glial activation was considered an oversimplification as the microglial activation presented greater complexity (Mosser and Edwards, 2008). The proinflammatory cytokines released from

activation microglia are activated astrocyte, the tight junctions regulation in BBB, which therefore release proinflammatory or anti-inflammatory phenotypes derived from microglia activation (Passaro et al., 2021). The dysregulation of the barriers permeability allowed the infiltration of peripheral cytokines and monocytes into the CNS crossing the BBB in a neuroinflammation state and revealed either proinflammatory or anti-inflammatory functions derived from macroglia activation.

Furthermore, the ependymal cells in the choroid plexus (CP) contain immune cells such as macrophages and memory T-cells, which are able to recognise the CNS antigens and produce anti-inflammatory markers, including IFN-**γ** and IL-10. (Passaro et al., 2021, Croese et al., 2021). The CP also adjusts the immune composition of the CSF, which presents low numbers of bone marrow-derived immune cells (Ousman and Kubes, 2012). Moreover, the meninges host many antigen-presenting cells (APCs), including macrophages and dendritic cells derived from the bone marrow in the skull, which migrate to the parenchyma without crossing the blood (Herisson et al., 2018). All macrophages found in the CP, meninges, and perivascular spaces expressed proinflammatory cytokines in response to the neuroinflammation (Jordão et al., 2019). The disturbance of brain homeostasis will enhance the infiltration of the cytokines and monocytes into the brain parenchymal, and this process is involved in tissue damage and neuroinflammation (Varvel et al., 2016, Song et al., 2020); nevertheless, they may support the CNS by producing anti-inflammatory phenotypes (Shechter et al., 2009).

In a healthy brain, the peripheral monocyte does not present in the CNS parenchyma, even when examined in different neuroinflammation states, trafficking from the blood stream into the brain tissue (Prinz and Priller, 2017). The peripheral immune system comprises collections of cells, tissue, and organs, which respond to the pathogens through innate and adaptive immunity (Paul, 2012). The innate immune cells comprise white blood cells such as

dendritic cells, macrophages, mast cells, neutrophils, basophils and eosinophils, and lymphocytes without specific antigens (Akira et al., 2006). The innate immune cells can circulate freely through the blood stream and express cytokines or activate the adaptive immune cells by interaction with other cells (Liaskou et al., 2012). The adaptive immune cells involve lymphocytes with specific antigen receptors, usually T- and B-cells (Medzhitov and Janeway Jr, 1997). The responses of the peripheral immune cells are very important for protecting and repairing body tissues, as well as controlling infections in the critical early period (Liaskou et al., 2012). It has recently been shown that the peripheral immunity cells communicate with the central immune system by passing brain barriers into the brain tissue during neuroinflammation (Quan and Banks, 2007). There are different routes for peripheral leukocytes crossing the brain parenchyma: through the BCSFB, perivascular space, and postcapillary venules (Ransohoff et al., 2003). The literature confirms that patients who have experienced neuroinflammation diseases demonstrated elevation of the CSF and plasma cytokines (Brosseron et al., 2014, Sosvorova et al., 2015, Sun et al., 2019, Dahl et al., 2014), as well as activated microglia (Enache et al., 2019, Werry et al., 2019)

1.4 The communication between the peripheral immune system and central nervous system

Peripheral and central immune system interactions have been implicated as a mechanism for developing neuroinflammation. However, the CNS is separated from plasma by tight junctions found in the BBB and BCSFBs in epithelial cells in the choroid plexus (CP) (Johanson and Johanson, 2018). There are different pathways for the proinflammatory cytokines to infiltrate brain tissue from the bloodstream (Dantzer, 2018). The cytokine pathways, which include the humoral, neural, and cellular pathways, were suggested by some animal studies. The humoral pathways were identified on cytokines across a leaky BBB, as

found in the circumventricular structures, while the neural pathways where the cytokines bind saw the active transport of molecules in the BBB. The cytokine receptors found in peripheral afferent nerve fibres as vagus nerves are represented in the neural pathway. In terms of the cellular pathway, the activated immune cells in the perivascular, parenchyma, and CP, which infiltrate into the CSF and brain parenchyma indicated other pathways into the brain (Miller and Raison, 2016).

The CP forms BCSFB, which work alongside the BBB to control the traffic between the blood and the CSF and the brain parenchyma (Saunders et al., 2012). The BBB is comprised of an endothelial cell with very low transcytotic vesicles, a vascular allowing macromolecules to move across the cell membrane, and a high restrictive paracellular diffusion barrier (Wolburg and Lippoldt, 2002). The BBB contains tight endothelial cells that form a restrictive barrier to limit the entry of substances into the brain interstitial fluid (ISF) (Abbott, 2005). However, the BCSFB fenestrations in the choroid plexus vascular are less restricted and allow ions and small molecules to diffuse into CP epithelial cells (Maharaj et al., 2008).

The immune cells in CP work with the intraventricular immune cells to form the initial defensive action against brain infection, and acute and chronic inflammation (Yang et al., 2021). The CP is considered the main brain structure that responds to chronic and acute inflammation (Marques and Sousa, 2015, Turner et al., 2014). Chronic inflammation is thought to increase the transport of immune cells from the plasma into the CP, and consequently into the brain parenchyma (Marques and Sousa, 2015). Importantly, the study of post-mortem MDD tissue found an alteration in the transforming growth factor-beta (TGF-$\boldsymbol{\beta}$) pathways and a downregulation of the CP transcriptome link to the interaction with the CP extracellular matrix and cytoskeleton, which may indicate a dysregulation in CP functions (Turner et al., 2014). Additionally, the permeability of the BBB was found to be inconsistent in depression studies (Wengler et al., 2019, Maharaj et al., 2008). Finally, a meta-analysis of the vascular endothelial

growth factor (VEGF), a plasma protein measuring the BBB permeability produced by CP endothelial cells, identified mixed results in depression patients ((Clark-Raymond and Halaris, 2013). Taking all of the above into account, CP can be considered a brain structure that plays an important role in immune responses in the nervous system, where the peripheral and the central immune systems communicate (Meeker et al., 2012).

1.5 Markers of neuroinflammation in depression

Once the peripheral cytokines cross the brain, they activate their receptors in the vascular endothelial cells, perivascular immune cells, glial cells including microglia, astrocyte, and oligodendrocytes, and neurons in several brain regions linked to mood regulation (Woelfer et al., 2019). Microglia are resident microphages in the brain and spinal cord which play a role in the immune process (Spindler and Hsu, 2012), where the astrocytes – immunocompetent cells – preserve the tight junction of the BBB and maintain the water and ion balance (Enache et al., 2019, Watzlawik et al., 2010). The oligodendrocyte is a glial cell which has a main role in the myelination as well as releasing pro-inflammatory cytokines following brain injury (Mechawar and Savitz, 2016). The activation of microglia and astrocyte in the brain may contribute to developing a neuroinflammation (Maeng and Hong, 2019). Neuroinflammation is a process where increasing immune responses of microglia and astrocytes release proinflammatory chemokines and cytokines, including the TNF-α and IL-6, consequently impairing brain functions (Maeng and Hong, 2019). Different neurological diseases and neuropsychiatric disorders, including depression, demonstrated high peripheral cytokines as well as the activation of glial cells (Haapakoski et al., 2015). In addition to the heightening of the peripheral inflammatory markers in depression patients, gene expression studies have supported the role of inflammation in depression in demonstrating an increase of the messenger RNA in genes expressing the proinflammatory mediator in mood disorders (Savitz et al., 2013, Pandey et al., 2015, Drexhage et al., 2011). Also, central inflammatory markers have been

explored in several research studies on depression and exhibited immune dysregulation markers in the brain (Enache et al., 2019).The dysregulation of the immune system in the brain has been investigated in depression studies and showed a high level of CSF cytokines obtained from lumber punctures, as well as an alteration of the amount and function of immune regulation cells such as microglia, astrocytes and oligodendrocytes, which have been demonstrated in many post-mortem studies (Enache et al., 2019, Mechawar and Savitz, 2016). In order to detect neuroinflammation in humans in-vivo and non-invasively, neuroimaging has been used to investigate neuroinflammation through either measuring the radioactive signals of Positron Emission Tomography (PET) in activated microglia (Enache et al., 2019), or by using Magnetic Resonance Imaging MRI to investigate structural alterations in depressed patients (Oestreich and O'Sullivan, 2022).

1.6 Neuroimaging for neuroinflammation

1.6.1 PET Imaging

Positron Emission Tomography (PET) is a nuclear imaging technique using radionuclides such as Carbon-11, Fluorine-18 or Oxygen-15, which emit positrons during isotope decay (Brownell, 1999). A positron is a subatomic particle with the same mass as an electron but with the opposite charge (Faulstich, 1991). Radionuclides are manufactured in a particle accelerator called a cyclotron and combined with biologically active molecules to create a labelled compound, which may be referred to as a radioactive tracer, radiotracer or radioligand. Radioactive tracers mimic the biological behaviours, pharmacokinetics, and pharmacodynamics of the unlabelled equivalent compound (Bloomfield *et al*., 2017). Following intravenous injection, radioactive tracers circulate around the bodily tissues via the blood circulation system. Upon interaction of the positron with an electron, annihilation occurs producing two gamma rays with an energy of ~511 keV (Faulstich, 1991). The two gamma rays are detected by opposing detectors placed within the PET scanner around the anatomical structures of the participant to be imaged (Cherry *et al*., 2006). The imaginary line connecting

the PET scanner detectors is termed the 'line of response' and is used to identify the location of an annihilation event. Several lines of response are recorded during a PET measurement, which are ultimately used to reconstruct the PET image (Bloomfield *et al*., 2017).

False events may occur during emission detection, including photon attenuation, non-linearity of the detection system, photon deflection, and random coincidences. Once these are corrected, the number of coincident counts assigned to each line of response reflects the overall isotope activity. The detected signals represent a 2/3- dimensional projection of the tracer distribution, which are combined to generate a sinogram (Bloomfield *et al*., 2017). The sinogram is converted to images to determine the distribution of radioactivity by using a reconstruction algorithm either via filter back-projection or iterative reconstruction.

Quantification of the PET signal by measuring area-specific tracer activity or analysing radiotracer exchanges is determined to establish the behaviour of the radiotracer within the target tissue compartments (Bloomfield *et al*., 2017). The monitoring of radiotracer exchanges requires dynamic acquisition to measure tracer activity over time. Dynamic PET imaging is commonly conducted alongside the collection of arterial blood samples to ascertain the uneven distribution of the tracer in the plasma and blood, and to assess tracer-protein binding and tracer metabolites in the plasma. This presents a reliable method of quantitatively analysing tracer kinetics, and different techniques such as compartmental modelling can be used to generate specific outcomes. Compartmental modelling involves the creation of a mathematical model of the biological system, using the radioligand concentration in arterial plasma as a model input. Conversely, if a reference region time activity curve is available, this may be used as a substitute for the arterial input function in receptor studies (Lammertsma and Hume, 1996). Currently, this is the only process validated for comprehensively understanding a disease or physiological system (Bloomfield *et al*., 2017).

The peripheral benzodiazepine receptor (PBR), recently named the 18-kDa translocator protein (TSPO), is a translocator protein found extensively in the outer membrane of the mitochondrial, although not exclusively (Cagnin et al., 2007). In its normal physical state, the TSPO was found at low levels in the brain, and increased with neuroinflammation and brain injury, mainly in the activated microglia (Chen and Guilarte, 2008). The PK11195 is a particular ligand of the TSPO and is combined with radioactive molecules to quantify brain function as a characteristic of the activated microglia in neuroinflammation (Enache et al., 2019, Chen and Guilarte, 2008). Several studies on depression have shown mixed results regarding the radioligand PET signal targeting the TSPO. Some have found an increase of the TSPO radioligand PET signal in some brain regions involving the anterior cingulate cortex (ACC), prefrontal cortex (PFC), and insula in the MDD group (Schubert et al., 2021c, Setiawan et al., 2018, Richards et al., 2018). However, some studies did not find an elevation of the TSPO radiotracer in the activation microglia in different brain regions in the MDD cohorts (Hannestad et al., 2013), nor in the subjects of experimental tests after the injection of an immune challenge marker (IFN-α), even with high peripheral cytokines and transient depressive behaviour (Nettis et al., 2020).

1.6.2 MRI Imaging

Magnetic Resonance Imaging (MRI) is a non-invasive, less expensive compared to the PET, and easily accessible neuroimaging procedure that characterises biophysical changes in brain tissue related to in-vivo neuroinflammation (Oestreich and O'Sullivan, 2022). MRI uses a strong magnetic field and radiofrequency to create well-defined structural and functional images depending on the magnetic properties of the hydrogen protons (H^+) which are abundant in the human body. The H^+ at the centre of the magnetic pore are aligned with the direction of the strong magnetic field. Then, the radiofrequency is turned on and off on the hydrogen protons at a specific degree, a net magnetisation, which changes their orientation. When the net magnetisation returns to equilibrium, a radiofrequency signal is released and detected by

the gradient coils placed in the MRI scanner. The signals are reconstructed and transformed into electronic images with differing image contrast. The image contrast is dependent on the physiological properties of the tissue, including the T1, which represents the relaxation time (the time taken for the H^+ to realign to the magnetic field direction) and the T2, which is the dephasing time (the time for the H^+ to dephase). Usually, structural MRI is used with a T1 spin echo to create a well-defined anatomical image used for segmentation and registration. The echo planer pulse sequence (gradient echo) is used for the diffusion and perfusion of images to investigate the functional properties of water molecules.

MRI has been used to assess the micro and macro changes in brain tissue during neuroinflammation (Oestreich and O'Sullivan, 2022). MDD patients have shown a reduction in the volume of some regions in the grey matter (GM), measured by structural MRI, which are associated with a high CRP level (Opel et al., 2019). Other structural MRI research has found changes in the macrostructures of the brain tissue in depressed patients (Zhang et al., 2018b, Ramezani et al., 2015), and confirmed a consistent reduction in the cortical thickness of ACC and PFC in patients who suffered multi-depressive episodes compared to the healthy control group (Bora et al., 2012). Similarly, the volume of the frontal cortex, including the prefrontal cortex, orbitofrontal cortex, middle prefrontal cortex, and dorsolateral prefrontal cortex, was decreased in drug-naïve MDD patients (Zhang et al., 2018b). MRI contrast enhancement has also been used for multiple sclerosis (MS) subjects with depression, compared to MS subjects without depression (Kallaur et al., 2016). A reduction in the contrast enhancement and an increase of the peripheral inflammatory cytokines were seen in MS patients with depression, compared to MS subjects without depression (Kallaur et al., 2016). Other MRI procedures using a diffusion-weighted image (DWI) were applied to investigate microstructure changes in brain tissue, as well as the movement of water molecules (Bloomfield et al., 2017). The diffusion tensor image (DTI) is one DWI technique, and has

been used to investigate the microstructure in regional white matter (WM) (Bergamino et al., 2016). The DTI was used to explore a reduction in the white matter integrity of depression patients compared to healthy control subjects (Bergamino et al., 2016). These structural changes detected by MRI in the brain tissues of depression sufferers may suggest a mechanism for developing neuroinflammation. The neuroinflammation also showed a contribution to the dysregulation of the dynamic, or the production of CSF, which may point to the dysfunction of the brain's waste clearance pathways and ultimately the disruption of brain homeostasis.

1.7 Cerebral Spinal Fluid (CSF) and its role in preserving brain homeostasis

1.7.1 CSF Production

CSF is a proteinaceous fluid composed of 99% water and 1% other compounds, which include proteins, ions, growth factors, glucose (Amann et al., 2016), neuropeptides (Mizui et al., 2019), hormones (Sullivan et al., 2006), neurotrophic factors (Gerner et al., 1984), and neurotransmitters (Lindström, 1985). Compared to plasma, CSF contains a higher concentration of sodium and magnesium, but a lower concentration of potassium and calcium (Sakka et al., 2011). CSF is produced by specialised ependymal cells found in the CP in the basal lamina of the four brain ventricles (Shen, 2018, Brown et al., 2004). The CP is a folded structure which produces 75% of the CSF (430 - 530 mL), with a 150 mL constant flow volume within the CNS (Kress et al., 2014). CP epithelial cells have two borders: an apical border facing the ventricular side, which is covered by microvilli to increase the surface area for CSF secretion and diffusion, and a basolateral border facing the blood supply, which has several folds and creases to increase absorption (Brinker et al., 2014). Changes in the concentrations of the plasma and the CSF presented by the active transporters enable the exchange of sodium (Na) and chlorine (Cl) by basolateral transport proteins (Brown et al., 2004). The CP epithelial cells are surrounded by stroma, blood vessels, and immune cells (Marques et al., 2009). The

CP produces the CSF in two stages: through the passive diffusion of the plasma via fenestrated choroidal capillaries, driven by the different osmatic pressure gradient between the two surfaces, and through the ultrafiltration of the active transporters and channels via the choroid plexus epithelial cells in the ventricles (Brown et al., 2004, Ghersi-Egea et al., 2018b), See Figure 1.1 .

Figure 1.1 Choroid plexus (CP) and brain-CSF-barriers (BCSFB)

A B

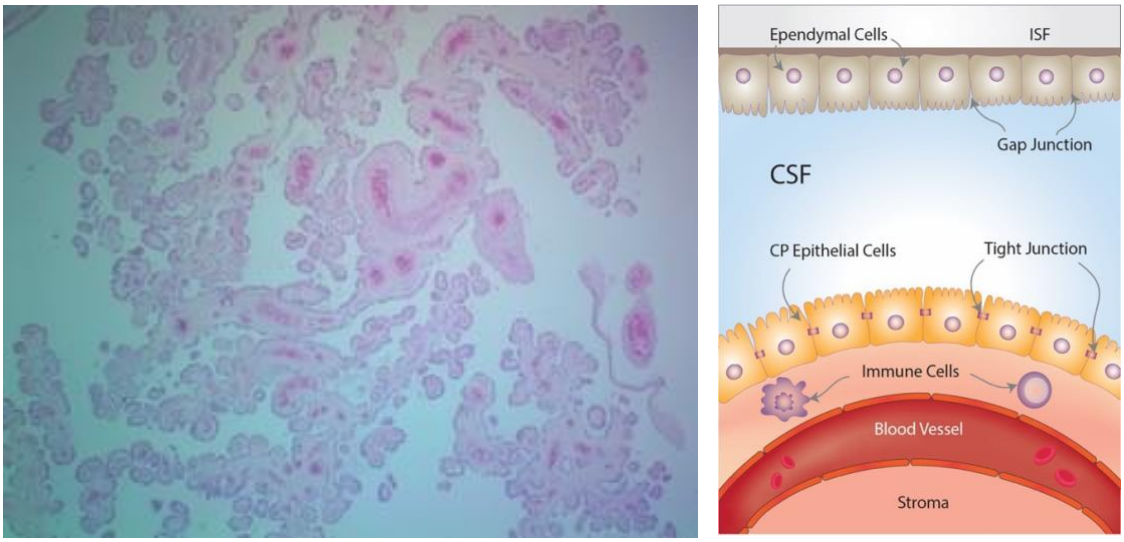

A. *CP histology: A single layer of cuboidal epithelial cells (dark purple) surrounding the choroidal stroma and comprising bundles of choroidal capillaries (red) and connective tissues (pink).*

B. *The CP epithelial cells are connected by tight junctions in the apical border facing the cerebrospinal fluid (CSF) and are covered by microvilli, while the basolateral border faces the blood vasculature. The ependymal cells cover the roof of the ventricles and are connected by gap junctions, which facilitate the exchange of electrolytes and some solutes between the CSF and the interstitial fluid (ISF).*

The CP has numerous mitochondria to provide the energy to control the movements of macromolecules including hormones, growth factors, drugs, and ions, from and into the CSF (Damkier et al., 2013), as well as into and out of the brain through particular channels in the tight junctions of the CP epithelial cells (Plog and Nedergaard, 2018). Moreover, the Osmotic pressure gradient promotes the movement of water molecules, which are facilitated by the water channel Aquaporin-1 (AQP1), found on the apical surface of CP epithelial cells (Khasawneh et al., 2018, Mobasheri and Marples, 2004). Also, the gap junctions between the ependymal cells lining the lateral ventricles facilitate the diffusion of small molecules into the ventricular CSF from the interstitial fluid (ISF), which contributes to the production of a small amount of the CSF (Saunders et al., 2012). The tight junctions in the CP epithelial cells which form the BCSFBs, control the movement of substances and regulate the trafficking of the immune cells into the ventricles in the normal physical state (Meeker et al., 2012). An alteration of the CP can result in a reduction in the BCSFB integrity which alters the trafficking of the immune cells as well as the pathogens into the CNS (Szmydynger-Chodobska et al., 2012), and is linked to several neurodegenerative diseases including Alzheimer's disease (AD), autoimmune diseases such as multiple sclerosis (MS), and following strokes and brain trauma (Solár et al., 2020). Interestingly, the CP volume was found to be increased in AD (Tadayon et al., 2020) and MS patients (Ricigliano et al., 2021).

1.7.2 CSF Dynamic

CSF flows unidirectionally through the ventricular system, moving from the two lateral ventricles located on each hemisphere into the third ventricle placed between thalami via the foramen of Monro, and into the fourth ventricle located within the brainstem through the cerebral aqueduct (the aqueduct of Sylvius). CSF leaves the ventricular system into the subarachnoid space, cisterns, and central canal of the spinal cord through the two lateral apertures (the foramina of Luschka) and the median aperture (the foramen of Magendie), respectively, where CSF movement becomes slow and multidirectional. The cisterna and

subarachnoid spaces reach the perivascular space that surrounds the extension arteries and veins supplying the brain parenchyma (Zhang et al., 1990, Ghersi-Egea et al., 2018b). Ultimately, the CSF is reabsorbed by the venous system through specialised cells, arachnoid granulations, or villi found along the brain surface drained into the dural venous sinuses (Johnston and Papaiconomou, 2002, Bradbury and Cserr, 1985). The CSF exits the brain through the cribriform plate into the cervical lymphatic vessels and/or to the meningeal lymphatic vessels that run along the dura sinuses (Chen et al., 2015), see Figure 1.2.

Figure 1.2 CSF pathways and blood-brain barriers (BBB)

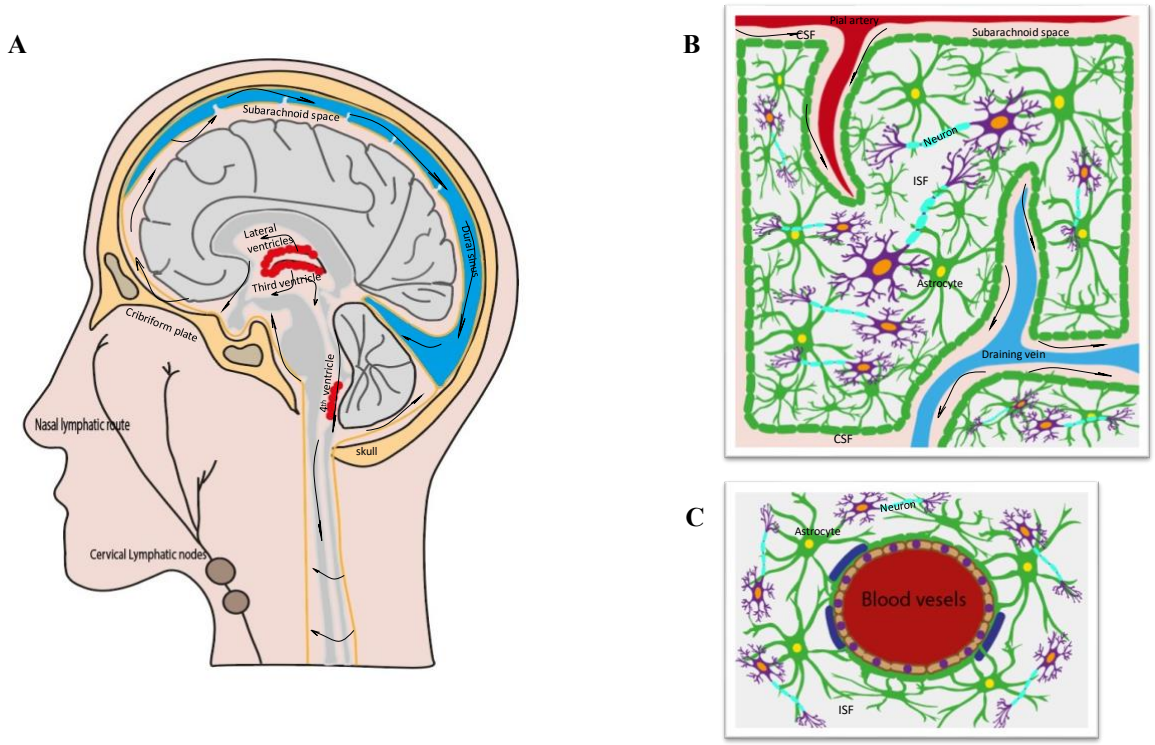

A. *CSF is produced by the CP and flows through the four brain ventricles to the subarachnoid space and into the brain parenchyma, ultimately exiting the brain. CSF is absorbed by dura sinuses via the arachnoid granulation and drain into cervical lymph nodes by the meningeal lymphatic vessels and the nasal lymphatic route across the cribriform plate.* ***B.*** *CSF circulates through the brain parenchyma and removes waste products via direct CSF/ISF exchange, mediated by the astrocyte end-feet AQP-4. CSF clearance is*

facilitated by the bulk flow of fluid through the AQP4, which assists the CSF influx at the para-arterial space into the ISS and removes parenchymal waste via the ISF efflux along the para-venous space. ***C.*** *The BBB contains tight endothelial cells that form a restrictive barrier to limit the entry of substances into the brain ISF.*

All the brain ventricles and the central canal of the spinal cord are lined with ciliated ependymal cells, which are composed of cuboidal glial cells with a ciliated surface, contributing to the CSF flow (Del Bigio, 1995). The arachnoid membrane is also considered a part of the BCSFB, despite the unidirectional exchange between the CSF and the periphery (Siyahhan et al., 2014). The CSF flow is encouraged by the pressure gradient, motivated by cardiac and pulmonary pulsation (Vinje et al., 2019) in addition to the choroid plexus arterial pulses (Takizawa et al., 2018, Bering, 1962) assisted by the movement of the ependymal cilia (Siyahhan et al., 2014). The CSF protects the brain and spinal cord and plays a significant role in the nutrient supply and mediation of tissue clearance, despite the lack of conventional lymphatics in the brain (Iliff et al., 2012, Iliff et al., 2013).

1.8 The glymphatic pathways

The recent discovery of the brain glymphatic system (GS) has provided new perspectives on the waste clearance mechanisms in the central nervous system (CNS), as well as new insights into the neuropathological mechanisms common in several brain disorders (Louveau et al., 2017). This recently-identified clearance pathway has been termed the glymphatic system, due to the important role of glial cells and their similarity with the lymphatic system in the peripheral tissues (Iliff et al., 2012). The CSF removes cellular waste within the perivascular space, also known as the Virchow–Robin space, via the water channels at the astrocytes end-feet, which are called aquaporin-4 (AQP4) (Schubert et al., 2019, Jessen et al., 2015, Bakker et al., 2016). The CSF clearance is facilitated by the bulk flow of fluid

through the AQP4, which assists CSF influx at the para-arterial space into the interstitial space (ISS) and removes parenchymal waste via the interstitial fluid (ISF) (Iliff et al., 2012). ISF is a fluid formed and secreted by the capillary endothelial cells (Nagelhus and Ottersen, 2013) that effluxes along the para-venous space (Iliff and Nedergaard, 2013, Iliff et al., 2012). The ISF and its components are mixed with the CSF, a process which can present across the ependymal layer of the ventricular system (Del Bigio, 1995, Saunders et al., 2012), either recirculating in the subarachnoid space, or exiting the cranial cavity through absorption via the arachnoid granulations to the sinuses and meningeal lymphatic vessels (Johnston and Papaiconomou, 2002, Westman et al., 2012).

The function of the GS is more active during natural sleep and general anaesthesia: research shows increases in the ISS and therefore increases in the convicted exchange between the CSF and the ISF during sleep (Xie et al., 2013). Furthermore, sleep disorders are associated with several psychiatric disorders, including anxiety disorders, MDD, and schizophrenia (Baglioni et al., 2016). In addition, a chemical imbalance in the CSF of patients with psychiatric disorders (Huang et al., 2006) and with depression (Martinez et al., 2012, Heilig, 2004, Soleimani et al., 2014) has been found.

1.9 CSF alterations in Depression

The CSF of MDD patients exhibited increases in some neuropeptides (Martinez et al., 2012, Heilig, 2004, Soleimani et al., 2014), along with the immunoreactive hormone corticotropin-releasing factor (Nemeroff et al., 1984). In contrast, transthyretin, a carrier protein produced by the CP and secreted into the CSF, is significantly reduced in patients with MDD (Sullivan et al., 2006). CSF proinflammatory cytokines were also found to be higher in MDD patients (Enache et al., 2019). An alteration of the CSF production and dynamic may alter the process of CSF-mediated clearance and consequently unbalance the CNS homeostasis (Khasawneh et al., 2018).

1.10 Neuroimaging of CSF-mediating brain clearance

Glymphatic function has been investigated in biotechnology experiments in animal models (Jessen et al., 2015). The first in-vivo study to examine CSF clearance as a direct measurement of glymphatic pathways involved the injection of a fluorescent tracer into the cisterna magnum of mice. The study revealed that CSF influx in brain parenchyma through the periarterial space is mediated by the AQP4 on astrocyte end-feet (Iliff et al., 2012), and that excessive Aβ protein is removed from the ISF through the perivenous space (Iliff and Nedergaard, 2013). Previous studies have revealed that CSF clearance was impaired in AQP4 null mice, resulting in the accumulation of amyloid plaques and tau tangles (Iliff et al., 2013, Iliff et al., 2012). Furthermore, changes in the AQP4 in reactive astrocytes have been observed in rats with a subarachnoid haemorrhage and acute ischemic stroke (Gaberel et al., 2014). Alterations in the AQP4 result in changes in the perivascular space polarisation and increase Aβ and tau protein accumulation (Jessen et al., 2015, Gaberel et al., 2014).

Furthermore, glymphatic function was investigated in mice with a subarachnoid haemorrhage and acute ischemic stroke using MRI contrast enhancement (Gaberel et al., 2014), finding a decrease in CSF clearance. Similarly, a rat model of ischemic stroke has demonstrated that intraventricular contrast enhancement is associated with BCSFB impairment (Renú et al., 2017). Likewise, patients with ischemic stroke showed a contrast enhancement in the ventricles after intravenous thrombolysis treatment to remove the thrombosis (Park et al., 2017). An accumulation of the contrast enhancement on the lateral ventricles of a stroke patient may reveal an alteration of the BCSFB (Park et al., 2017). Interestingly, neuroinflammation may contribute to the dysfunction of BCSFB and BBB integrity (Kaur et al., 2016, Raison et al., 2006), impairing the process of CSF-mediated brain clearance.

The measurement of CSF clearance can be obtained either invasively, through a lumbar puncture, or through neuroimaging, which serves as a non-invasive alternative procedure (De Leon et al., 2017). Several studies have reported an impairment of CSF clearance in the pathology of neurodegenerative diseases (De Leon et al., 2017, Schubert et al., 2019), with no direct biomarkers monitoring these parameters in humans. De Leon et al. (2017) used PET imaging as an indirect method to investigate the CSF dynamic in the lateral ventricles as a marker of CSF-mediated clearance, finding a reduction in ventricular CSF clearance which was inversely proportional to the Aβ deposition in patients with AD. AD and MS patients also exhibited a decrease in CSF-mediated tissue clearance compared with matched healthy controls (Schubert et al., 2019). The CSF-mediated clearance pathway is critical for the removal of potentially harmful molecules such as Aβ, which is a pathological hallmark of AD (Rasmussen et al., 2018). The mechanisms underlying decreased CSF clearance have not yet been fully explained, but the inflammation of the CP and ventricular ependymal cells, as seen in MS (Vercellino et al., 2008, Lisanti et al., 2005), AD, and PD (Doorduin et al., 2008), may play an important role in the alteration of the clearance process.

Depression is known to be a risk factor for AD (Green et al., 2003) and comorbid with MS (Feinstein, 2011), where there is a reduction in the marker of CSF-mediated clearance. There have yet been no studies investigating CSF-mediated clearance in depression. This PhD project investigated the CSF-mediated clearance in an MDD group using CSF dynamics in lateral ventricles – measured by a PET signal – and the choroid plexus volume as indirect proxies of CSF-mediated clearance.

1.11 Aim and Objectives

Overall Aim

The primary aim of this research project is to explore, through indirect measurement, the brain CSF-mediated clearance and its link to peripheral and central inflammation in depression, compared to healthy controls, using PET imaging and MRI, to establish an indirect proxy of CSF clearance.

Specific Aims

Study 1**:** To explore the clinical relevance of the [^{11}C]PK11195 PET signal of the lateral ventricles as a proxy of CSF dynamics by comparing the signal magnitudes of MDD patients and healthy controls. The study also sets out to assess the link between the CSF clearance marker and peripheral inflammatory markers, as well as with clinical MDD symptoms.

Study 2**:** To investigate the choroid plexus volume and its relationship to the peripheral and central inflammation using structural MRI in depressed and healthy controls. It was also anticipated that the CP enlargement would be associated with the reduction of the CSF clearance markers measured in the study, as well as the clinical scores relating to depression.

Study 3**:** To investigate the free water volume extracted from the multiple shell diffusion weight image of an MRI for three regions of interest (the anterior cingulate cortex, prefrontal cortex, and insula cortex) as a biomarker for neuroinflammation, as well as its relation to clinical scores in depressed and healthy control subjects. The study also sets out to assess the link between the free water volume and the indirect marker of CSF-mediated clearance measured in the first study, and the choroid plexus volume measured in the second study.

1.12 Hypotheses

1. A reduction of the lateral ventricle PET measure is sensitive to the alterations of the CSF dynamic in depressed patients compared to healthy control subjects.

2. Mild inflammation in depressed patients reduces the CSF dynamic by closing the brain barriers in response to peripheral inflammation.

3. Reduction of CSF clearance mediates depressive symptoms.

4. CP volume is larger in depressed patients compared to healthy control subjects.

5. Alterations in barriers structure mediates depressive symptoms.

6. CP volume enlargement links to high peripheral inflammatory markers and high central inflammatory markers, measured by the TSPO PET uptake in key regions of depression: the anterior cingulate cortex, the prefrontal cortex, and the insular.

7. The free water volume measured with MRI increases in the key regions of depression (anterior cingulate cortex, the prefrontal cortex, and the insula), as well as in the total grey matter in depressed patients compared to healthy control subjects.

8. The free water volume links to the marker of CSF clearance, including the TSPO PET signal perfused in the lateral ventricles and CP enlargement, as well as to the peripheral and central inflammatory markers.

2 Chapter 2

<u>Study 1</u>: Increased serum peripheral C-reactive protein is associated with reduced brain barriers permeability of TSPO radioligands in healthy volunteers and depressed patients: implications for inflammation and depression

This study is published in the *Brain, Behavior, and Immunity*, 91 (2021), 487-497.

2.1 INTRODUCTION

The relationship between peripheral and central inflammation and depressed behaviour has been investigated by a number of in vivo studies using Positron Emission Tomography (PET) and radioligands targeting the 18 kDa translocator protein (TSPO) in patients with depression. The TSPO is a mitochondrial protein that is expressed in a number of cells (endothelial, astrocyte as well as neurons) of the central nervous system (CNS) (Notter et al., 2020) but is particularly enriched in activated microglia, the brain-resident macrophages (Betlazar et al., 2018, Tournier et al., 2019). However, TSPO PET studies in depressed cohorts have returned mixed results demonstrating either negative (Zhang et al., 2018a), null(Hannestad et al., 2013) or mild TSPO elevations (Setiawan et al., 2015, Su et al., 2016, Holmes et al., 2018, Richards et al., 2018), with elevation being more evident in unmedicated subjects (Richards et al., 2018) and in those with suicidal thoughts (Holmes et al., 2018). More importantly, so far no study has demonstrated a consistent and replicable association between TSPO brain concentration and peripheral inflammatory mediators (Mondelli et al., 2017, Enache et al., 2019). A positive association was found in a sample of 48 patients with major depressive disorder between plasma adiponectin (an anti-inflammatory protein) and TSPO PET imaging in anterior cingulate cortex, but the analysis was only exploratory and did not survive

correction for multiple comparisons (Richards et al., 2018). More recently, a negative association between CRP and brain TSPO expression was found by Attwells (Attwells et al., 2019), suggesting that patients with depression and high peripheral inflammation would have less microglia activation than those with normal level blood CRP. This disagrees with the immune-mediated model of depression for which depressive symptoms can be induced by peripheral cytokines and immune cells acting on the brain to elicit a neuroinflammatory response via a leaky blood-brain barrier (BBB) (Miller and Raison, 2016, Dantzer, 2009, Schedlowski et al., 2014). The evidence above prompted us to re-evaluate the data collected in TSPO imaging studies in normal and depressed cohorts by focusing on the relationship with one particular peripheral inflammatory marker, C-reactive protein (CRP), in order to propose an alternative model for the mechanism of action between peripheral and CNS immunity.

Meta-analysis of cross-sectional and longitudinal studies on the relationship between peripheral immunity and depression have highlighted the relevance of pro-inflammatory cytokines such as tumour necrosis factor-α (TNF-α), interleukin-1β (IL-1β) and interleukin-6 (IL-6) but also of the acute phase protein, CRP (Valkanova et al., 2013). CRP is an acute phase reactant, a protein primarily made by the liver that is released into the blood within a few hours after tissue injury, the start of an infection or other inflammatory insults (Sproston and Ashworth, 2018). The concentration of CRP in blood has been increasingly used to quantify levels of systemic inflammation and associated levels of risks for a number of conditions, with concentrations greater than 3 mg/L indicating a high risk of cardiovascular disease (Smith, 2004).

In-vitro and preclinical models have shown that high concentrations of CRP (10 to 20 mg/L) are associated with BBB disruption, increasing its permeability (Hsuchou et al., 2012).

However, the clinical relevance of this literature to the in-vivo human context remains to be shown, as in most instances CRP levels in depressed cohorts are below the 10 mg/L mark, which is on the low to moderate spectrum of the peripheral inflammatory range (Elwood et al., 2017); in particular, we note that higher CRP levels increase BBB porosity to plasma proteins (measured as cerebrospinal fluid/serum albumin ratio) but only in those instances when CSF also exhibited abnormalities (Elwood et al., 2017). At the same time, other in-vitro work has reported that milder CRP plasma concentrations may stiffen endothelial cells and reduce endothelial permeability (Kusche-Vihrog et al., 2011a, Tomiyama et al., 2005).

Hence, we hypothesized that, in normal volunteers and patients with depression but no other BBB impairment, the levels of CRP in the range observed in these cohorts (range 3-10 mg/l, equivalent to 'low-grade inflammation') are associated with reduced blood to brain permeability. To test this hypothesis, we evaluated previously acquired data on the perfusion of TSPO radiotracers across the blood-brain interface (e.g., the BBB) and the blood cerebrospinal fluid (CSF) interface (e.g., the choroid plexus).

Specifically, we quantified radiotracer perfusion from blood into parenchyma (via the BBB) and from blood and parenchyma into the CSF (via epithelial barriers and the choroid plexus) from TSPO PET data collected in two separate studies, one large cross-sectional study of neuroinflammation in normal controls and depressed patients (Schubert et al., 2020) and a second study where peripheral inflammation in normal volunteers was induced via subcutaneous injection of interferon (IFN)-α and CNS inflammation was measured with PET (Nettis et al., 2020).

2.2 METHODS

2.2.1 Datasets

Two independent TSPO PET datasets collected from two separate neuroimaging studies were considered in this work.

Dataset 1 includes 51 subjects with major depressive disorder (MDD) (36/15 women/men; mean age: 36.2 ± 7.4 years) and 25 matched healthy controls (HC) (14/11 women/men; mean age: 37.3 ± 7.8 years) without statically different in mean age and sex as part of the Biomarkers in Depression Study (BIODEP, NIMA consortium, https://www.neuroimmunology.org.uk/) to investigate the contribution of neuroinflammation in depression. The data for the BIODEP project was collected in two phases. The primary cohort involved HC and MDD subjects matched for age, sex, and BMI, while the secondary cohort the HC and MDD matched for age and sex but not for BMI. Patients aged 25 to 50 (inclusive) that were taking anti-depressant treatment and had a total Hamilton Depression (HAMD) score>13 or were untreated and had a total HAMD>17 were included. The final sample consisted of 9 untreated patients and 42 taking medications. MDD patients were further classified based on their blood CRP level, CRP >3mg/L corresponding to the *high CRP group* (20 patients, 36.9 ± 7.6 years) and CRP<=3mg/L corresponding to *low CRP group* (31 patients, 35.7 ± 7.2 years). Of the 9 untreated patients 4 were in the high CRP group and 5 in the low CRP group. In the treated group, 17 were in the high CRP group, 25 in the low CRP group. 33 patients were treatment resistant (15 and 18 respectively in the high and low CRP group) while of the remaining 9, 2 had high CRP values and 7 low. CRP concentrations for controls were no different to the ones for low CRP group ($t = 0.017$, $p = 0.99$). MDD cases and HC with a lifetime history of other neurological disorders, active drug and/or alcohol abuse, participation in clinical drug trials within the previous year, concurrent medication or medical disorder that could compromise the interpretation of results, and those who were pregnant or breastfeeding were excluded. HC subjects had no personal history of clinical depression requiring treatment

and were age- and sex-matched with the patient group. On the contrary, BMI was significantly higher for the depression group (BMI_{MDD}: 27.2±4.0) kg/m; BMI_{HC} 24.2±4.8 kg/m^2; p value=0.001). For patients detailed characteristics and demographics please refer to the original publication (Schubert et al., 2021b), Table 2.1.

Table 2.1 Demographic and Clinical Characteristics for Depressed and Healthy Control Subjects

Variable	Depressed Subjects (n = 51)	Healthy Control Subjects (n = 25)	p Value
Age, Years, Mean (SD)	36.2 (7.3)	37.3 (7.8)	.561
Male, n (%)	15 (29%)	11 (44%)	.208
BMI, kg/m^2, n, Mean (SD) **All** **High CRP** **Low CRP**	 51, 27.2 (4.0) 20, 30.0 (3.8) 31, 26.2 (3.4)	 24.2 (4.8) NA NA	 .001* NA NA
CRP, mg/L, n, Mean (SD) **All** **High CRP** **Low CRP**	 51, 2.9 (2.8) 20, 5.6 (2.6) 31, 1.1 (0.7)	 0.6 (0.9) NA NA	 001* NA NA
Medication Status, n (%) **Untreated** **Treatment resistant** **No grouping**	 9 (17.5%) 33 (65%) 9 (17.5%)	 NA NA NA	 NA NA NA
HDRS, Mean (SD)	18.5 (3.7)	0.6 (0.9)	.001*

BMI, body mass index; CRP, C-reactive protein; HDRS, Hamilton Depression Rating Scale; NA, not applicable. *p < .05

Dataset 2 includes data from 7 healthy males to image microglia activation in the CNS before and ~24 hours after one subcutaneous injection of the immune challenge IFN-α (Roferon-A 3 million IU/0.5 ml solution for injection). The mean age and BMI for the 7 healthy males are 29.85 ± 6.44 and 23.46 ± 1.75, respectively. The study aimed to investigate putative changes in brain microglia activity and their relationship with changes in peripheral inflammation and in mood. Eligible participants were non-smokers, drank no more than 5

alcohol drinks per week, had no history of significant medical illness and did not meet the criteria for any current or past psychiatric or substance-dependence diagnosis. Subjects were excluded if they had an infection in the last month or had regularly used anti-inflammatory drugs. All subjects were TSPO high-affinity binders (HABs) as determined by single nucleotide polymorphism rs6971 genotyping (Owen et al., 2012).

All imaging protocols were approved by the local ethics committee and participants gave written informed consent prior to data collection.

2.2.2 Image acquisition and analysis

Dataset 1 - All subjects underwent 60-minute dynamic PET scan on a GE SIGNA PET/MR scanner (GE healthcare, Waukesha, USA) after an intravenous bolus injection of [^{11}C]PK11195 (target dose ~350 MBq, injected dose 361±53MBq). Data were reconstructed using multi-subject atlas method and improvements for the MRI brain coil component (Burgos et al., 2014). Data were corrected for scatter, randoms and deadtime using the scanner GE software. No arterial blood data was collected during the PET imaging consistent with best practice of [^{11}C]PK11195 PET imaging (Turkheimer et al., 2007). Full experimental details are reported in the original reference (Schubert et al., 2021a).

Dataset 2 – All the subjects underwent two 90-minute dynamic PET scans on a Siemens Biograph™ True Point™ PET/CT scanner (Siemens Medical Systems, Germany) after receiving a bolus injection of [^{11}C]PBR28 (target dose ~350 Mbq, injected dose 341±15). Images were reconstructed using filtered back projection and corrected tissue attenuation, scatter and random coincidences, and deadtime using scanner software. In parallel to the PET acquisition, arterial blood sampling was performed to generate metabolite-free arterial input function consistently with previous studies using the same tracer (Bloomfield et al., 2016).

Ligand free-plasma fraction (fp), or the portion of [^{11}C]PBR28 unbound to plasma proteins, was determined for all scans using ultrafiltration-based method as previously described (Hannestad et al., 2013).Full experimental details are reported in the original reference (Nettis et al., 2020).

In both datasets, all subjects also had structural T1-weighted brain MRI, either collected during the PET acquisition as in *dataset 1* or acquired just before the PET session as in *dataset 2*. These MRI images were used for PET data processing including grey matter (GM) and white matter (WM) tissue segmentation, brain masking, and atlas-based region extraction. These pre-processing steps as well as the PET inter-frame motion correction were performed using MIAKAT^{TM} (www.miakat.org) a MATLAB-based software combining tools from SPM12 and FSL for PET/MRI imaging analysis. For the [^{11}C]PK11195 PET studies TSPO density was assessed using BPnd parameter calculated by using a supervised clustering reference region approach (Turkheimer et al., 2007). For the [^{11}C]PBR28 PET study, instead, the tracer tissue kinetics was described with full compartmental modelling (Rizzo et al., 2019, Rizzo et al., 2014). The tracer blood to tissue exchange rate (K_1) and tracer volume of distribution (V_T) were used as main parameters of interest to measure the tracer perfusion and TSPO availability, respectively.

2.2.3 Quantification of blood to CSF tracer exchange

TSPO tracer exchange between blood and CSF through CP was calculated from the PET imaging using the validated analysis protocol defined in (De Leon et al., 2017, Schubert et al., 2019). The method has shown to be sensitive to CSF dynamics, returning evidence for altered CSF-mediated clearance in dementia and multiple sclerosis (De Leon et al., 2017, Schubert et al., 2019). Briefly, manual lateral ventricle ROIs were generated for all subjects using the subject T1-weighted structural MRI data and the ITK-SNAP (Yushkevich et al., 2006)

(itksnap.org) snake tool, following previously described guidelines for lateral ventricle extraction (Acabchuk et al., 2015). The lateral ventricle ROIs were then eroded by two voxels (5.2 mm) using the erode function given by FSL 'fslmaths' utility package in order to reduce partial volume effects of the surrounding tissues.

For both datasets, standardized uptake value ratios (SUVRs) at 60 minutes (activity at 60 mins normalized to counts of a reference region) and the area-under-curve from 30 to 60 minutes (AUC30-60, e.g. integrated activity between 30 and 60 mins) were calculated from the PET images using the eroded lateral ventricle activity as target region and supervised reference region (dataset 1) or whole brain grey matter (dataset 2) as normative region.

In certain circumstances, reference regions may be unavailable. TSPO is expressed throughout the entire brain, hence a true reference region exhibiting no TSPO expression is not possible to obtain. The use of whole brain grey matter as a normative region has been proposed as a solution to the problem, although this has limitations (Albrecht *et al.,* 2018). In particular, this method may prove effective for the analysis of focal inflammatory disease but not widespread inflammation (Schubert et al., 2021a). Nevertheless, a normative region can assist in the quantification of the PET signal without applying a plasma input function, and facilitates the PET procedure by avoiding the discomfort caused by arterial blood sampling (Turkheimer *et al*., 2012). Furthermore, the use of a normative tissue region in TSPO PET imaging reportedly reduced between-subjects variability when compared to blood-based quantification (Schubert et al., 2021a).

In dataset 2, for which metabolite-free arterial input function was also available, we implemented the compartmental modelling approach to quantitatively describe the rates of exchanges of the tracer from blood to lateral ventricle (*K1*), from tissue into lateral ventricle and clearance (*kClearance*) as well as the tracer specific biding in the lateral ventricle (*kon* and

koff) (Figure 2.1). The volume of distribution of the [^{11}C]PBR28 into lateral ventricles was calculate as $V_T = K_1$/kClearance*(1+kon/koff). Interestingly, it was not possible to model a specific tracer exchange from tissue to CSF as in the original paper describing [^{11}C]PIB kinetics into lateral ventricles (Schubert et al., 2019); this may be possibly due to a poorer extraction of the radiotracer whereas the radioactivity in tissue is ~1% of the one in blood hence its contribution to the kinetics in the ventricles is undetectable (Sander et al., 2019). Consistent with a previous publication the model was implemented using SAAM II software (Barrett et al., 1998).

Figure 2.1 Compartmental modelling of [^{11}C]PBR28 tracer kinetic in lateral ventricles and parenchyma.

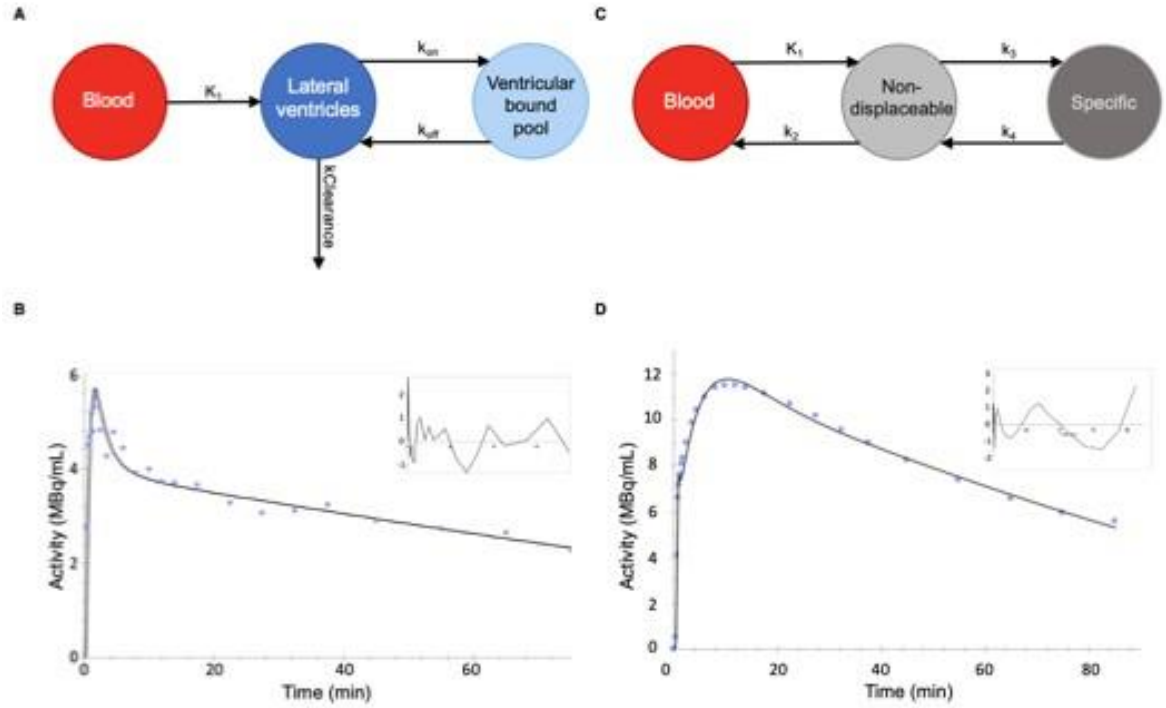

Figure 2.1 1

A) Compartmental model and kinetic parameters for lateral ventricles. K1 represents the rate of transfer from plasma to the lateral ventricles. Given the low extraction of the tracer into parenchyma in respect to blood (1%) the rate of transfer of the tracer from parenchyma into the lateral ventricles was not detectable. The parameters kon and koff represent the potential binding on and off to binding sites in the ventricles; These binding sites are so far unknown and could be specific to cells lining the ventricles or simply non-specific (lipids) due to the lipophilicity of PET tracer. The parameter KClearance compounds the rate of flux of the tracer back into blood or, potentially in parenchyma – the two not being identifiable by the model in this context B) Representative data fit for a ventricle time-course (healthy control, baseline). C) Compartmental model and kinetic parameters for brain parenchyma. K1 and k2 represent the rates of transfer from blood to tissue and viceversa while k3 and k4 denote the on and off rate of rate of binding to the TSPO. D) Representative data fit for a tissue time-course (healthy control, baseline).

2.2.4 High sensitivity C-reactive protein measurement

For both datasets venous blood samples were collected from each participant for the CRP analysis in study 1, a venous blood sample was collected after an overnight fast between 08:00 and 10:00 on the day of clinical assessment. Participants had refrained from exercise for 72 h and had been lying supine for 0.5 h prior to venepuncture (Chamberlain et al., 2019). For study 2, blood samples were collected at the time of PET scans, i.e. at baseline and ~24 hours after IFN-α injection. High sensitivity CRP (hsCRP) was used to assess peripheral inflammation. For both projects, blood samples were collected in clot activator containing tubes for measurement. The samples were allowed to coagulate for 30–60 minutes, then centrifuged at 1600 Relative Centrifugal Force (RCF) for 15 min. For the first project (BIODEP), serum samples were separated and transported to a central laboratory (Q2Solutions) where analyzed on the day of receipt. Samples were exposed to anti-CRP-antibodies on latex particles, and the increase in light absorption due to complex formation was used to quantify hsCRP levels, using Turbidimetry on Beckman Coulter AU analyzers. Inter

and intra-assay coefficients of variation were<10%. For the second project (FLAME) after blood collection, the serum was separated, aliquoted and stored at −80 °C before use. It was later assayed on the Siemens Advia 2400 Chemistry analyser (Siemens Healthcare Diagnostics, Frimley, UK) (Mason et al., 2013). Inter and intra-assay co-efficient of variations were also<10%. In both datasets there were no missing data or values below detection limit.

2.2.5 VEGF and S100B measurement

Forth both datasets, VEGF-A was measured using Meso Scale Discovery (MSD) VPLEX sandwich immunoassays (Dabitao et al., 2011, King et al., 2019), and plates read on an MSD QuickPlex SQ 120. The results were analyzed using MSD DISCOVERY WORKBENCH analysis software. Intra-assay and inter assay coefficients of variation were 7% and 15% respectively, and in both datasets there were no missing data or values below detection limit. In dataset 2 (FLAME), levels of serum S100B protein were also measured in serum using a S100B kit distributed by Diasorin, Charles House, Toutley Road, Wokingham, Berkshire, run on the Liaison XL chemiluminescence analyser (Wunderlich et al., 2004, Townend et al., 2002). Intra assay and inter assay coefficients of variation were <7% and < 11% respectively. 7% of the values were undetected, so they we replaced with the lowest detectable validated value (0.02 µg/L).

2.3 Statistics

SPSS (version 24.0, Chicago, IL) was used to perform all statistical analyses. Normality of the data was tested using Shapiro-Wilk W test. For *dataset 1*, blood to CSF exchange measures (i.e. SUVR and AUC30-60) were investigated using analysis of variance (ANOVA) to test for group differences between MDD at different CRP levels and HC, while covarying for possible confounding factors (e.g. age, BMI, tracer injected dose, or lateral ventricle

volume). Group differences were further investigated using independent samples t tests, while association between CSF-mediated clearance measures and clinical scores (i.e. HAMDI, Childhood trauma, and Perceived Stress Score) were investigated with bivariate correlations. Correlation of these metrics with the blood brain barrier permeability marker (VEGF) was also explored. For *Dataset 2*, we explored the relationship between CRP changes and blood to CSF exchange measures (i.e. SUVR and AUC30-60) before and after IFN-α challenge. We also compared K_1 and V_T, both into lateral ventricles and GM parenchyma between conditions. The latter was chosen as representation of the parenchymal tracer uptake independent from lateral ventricles. Correlation of these metrics with CRP levels, peripheral tracer plasma protein binding and the blood brain barrier integrity markers (VEGF and S100b) were also explored. We implemented the Durbin-Watson test to exclude outliers.

2.4 RESULTS

2.4.1 Marked inverse association between blood-to-CSF exchange measures and CRP in patients with depression

Results from the analysis of dataset 1 indicated the presence of a reduction in blood to CSF small-molecule perfusion as shown by an inverse association between blood-to-CSF exchange parameters and CRP, with higher CRP levels corresponding to both lower SUVR and lower AUC30-60 (Figure 2.2) in both MDD patients and HC. Considering the whole population (HC and MDD cases) the association remained significant, once corrected for lateral ventricle volumes using partial correlations, for both SUVR ($r=-0.233$, $p=0.045$) and AUC30-60 ($r=-0.277$, $p=0.016$). There was no effect of age, tracer injected dose and subject BMI on SUVR and AUC30-60 ($p>0.4$).

These associations between CRP and CSF radiotracer activity became stronger when considering MDD patients only, both in SUVR (partial correlation r: -0.300, p=0.034) and AUC30-60 (partial correlation r: -0.338, p=0.016). The relationship between these variables became more evident by restricting the analysis to the MDD-high CRP group only. Controlling for lateral ventricle volume SUVR-CRP partial correlation was -0.447 (p=0.048) while AUC30-60-CRP partial correlation was -0.579 (p=0.007). As for the whole sample, there was no effect of age, tracer injected dose and subject BMI on SUVR and AUC30-60 correlation with CRP.

No correlations between CSF-mediated clearance measures and HAMD score, Childhood trauma or Perceived Stress Score were found. The only exception was a significant inverse association between AUC30-60 and Childhood trauma score (Spearman's rho = -0.32, p: 0.02) although it did not survive to multiple comparison correction.

No correlation between VEGF and CSF-mediated clearance measures or CRP was found ($p>0.5$) although MDD cases reported a significantly lower VEGF value compared to HC (t_{44}: 2.90, $p<0.01$).

Figure 2.2 CSF-mediated clearance parameters and peripheral CRP in MDD.

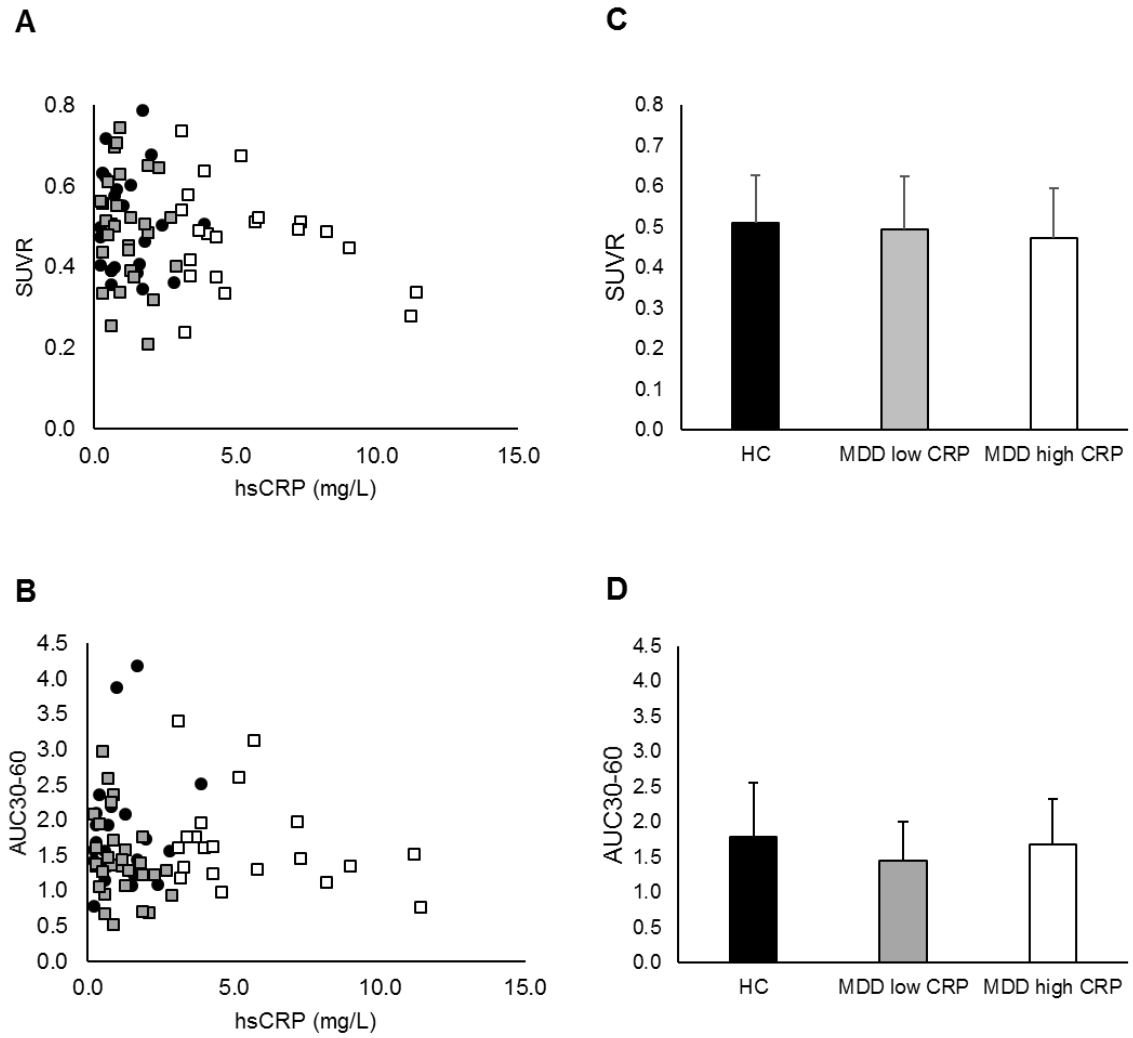

The results refer to [^{11}C]PK11195 PET study (dataset 1). Patients are identified by low CRP group (<3mg/L, grey bar) and high CRP group (>3mg/L, white bar). Healthy matched controls are reported in black. Panel A and B show the distribution of SUVR and AUC30-60 as function of CRP, respectively. Panel C and D show the SUVR and AUC30-60 group averages and standard deviations.

2.4.1 Peripheral CRP increase is associated with reduction of blood to brain tracer percolation after IFN-α injection

In dataset 2, we found that the CRP increase following the peripheral IFN-a challenge was inversely associated with lateral ventricular SUVR measure (R^2: 0.72, p=0.015) (Figure 2.3A) indicating a reduction on blood-to-CSF small molecule transfer. This association was not replicated by AUC30-60 (Figure 2.3B).

The most interesting results were obtained for the compartmental modelling analysis (Figure 2.3 C and D). When we considered the tracer kinetics into lateral ventricle CSF we found that V_T was significantly reduced after IFN-a injection (-18±12%, p=0.01) while the difference in blood to CSF tracer transportation K_1 almost reached significance (-23±20%, p=0.05). No significant difference was found for the other kinetic parameters (kClearance: 1±49%, kon: 19±56%; koff: 2±10%).

Figure 2.3CSF-mediated clearance after IFN-a immune challenge.

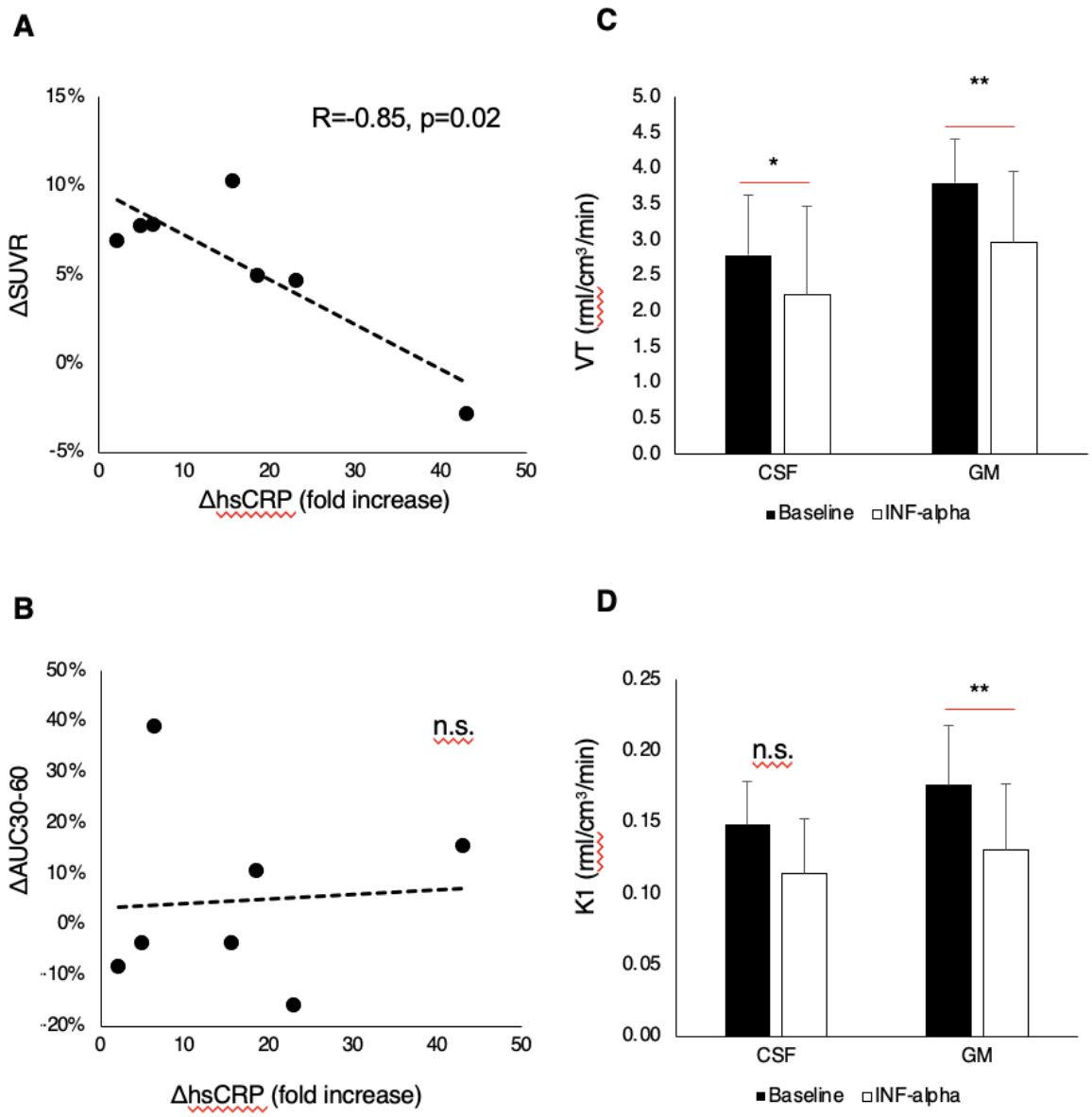

The results refer to [^{11}C]PBR28 PET study (dataset 2). A) Association between CRP and SUVR variations at baseline and after 24 hours IFN-a injection. B) Association between CRP and AUC30-60 variations at baseline and after 24 hours IFN-α injection. C)Comparison of the volume of distributions (V_T) for GM and lateral ventricle CSF at baseline and after 24 hours IFN-a injection. D) Comparison of blood to tissue rates (K_1) for GM and lateral ventricle CSF at baseline and after 24 hours IFN-α injection.

A stronger effect of interferon-a was found also for the kinetic parameters describing tracer kinetics with brain GM. Particularly we found that both blood to GM tracer transportation K_1 (-27±15%, $p<0.01$) and GM V_T (-22±10%, $p<0.01$) were significantly reduced after the challenge. Given the effect that blood proteins have on the TSPO tracer availability (Lockhart et al., 2003), we explored whether these reductions were associated with CRP changes or with tracer plasma protein binding (Figure 2.4). We found that both variables were associated with reduction of tracer percolation into GM (Figure 2.4A and B) and into lateral ventricle CSF (Figure 2.4D and E).

Given the collinearity between plasma protein binding and CRP ($R^2=0.32$, $p=0.03$) we studied their interaction with K_1 as the dependent variable. Partial regression between K_1 and CRP controlling for plasma protein binding (fp) showed significant association for GM tissue (Pearson's $R=-0.65$,$p<0.01$) but not for CSF (Spearman rho=-0.37, $p=0.11$). However, when we directly corrected the transfer rate K_1 by multiplication with fp, we found significant associations between the tracer perfusion and CRP for both CSF and GM (Figure 2.4C and F).

Figure 2.4Association between blood to tissue tracer percolations, plasma protein binding and CRP

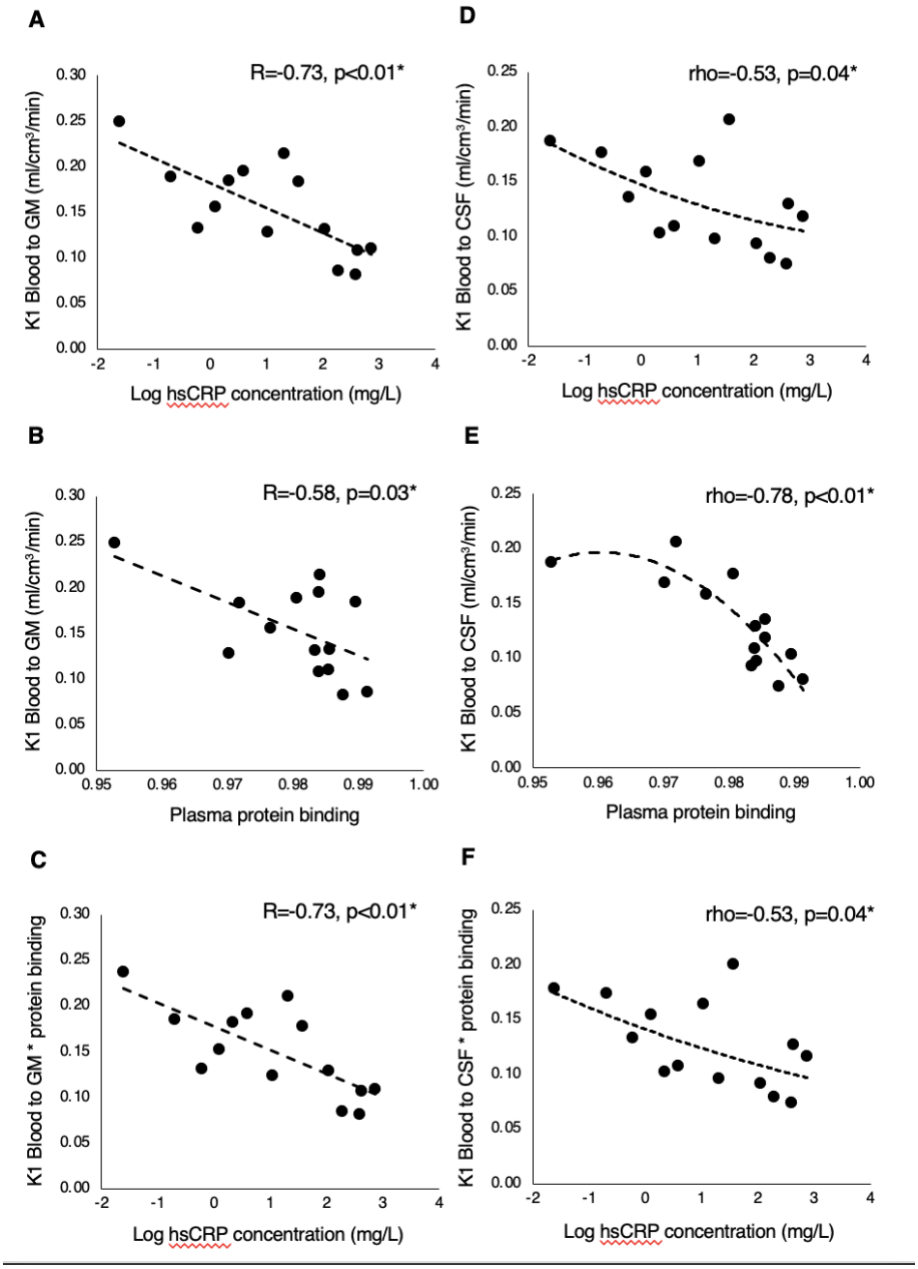

A-C) Blood to tissue transport into brain GM. D-F) Blood to tissue transport into lateral ventricle CSF.

In terms of BBB permeability markers, there were positive associations between VEGF and K_1 parameters (R=0.63, p=0.02 for CSF and R=0.53, p=0.05 for GM) but no association

was found between S100β and any kinetic parameter (both K_1 and tracer clearance from lateral ventricle) (Figure 2.5). Interestingly S100β and VEGF were positively associated (R=0.55, p=0.04) but only VEGF was significantly reduced after interferon-α (from 134.5±52.5 at 1 h before IFN-α to 93.5±34.9 at 24 hours after; paired t-test, t=5.15, p=0.002).

Figure 2.5Association between blood to tissue tracer percolations and BBB integrity (VEGF and S100β)

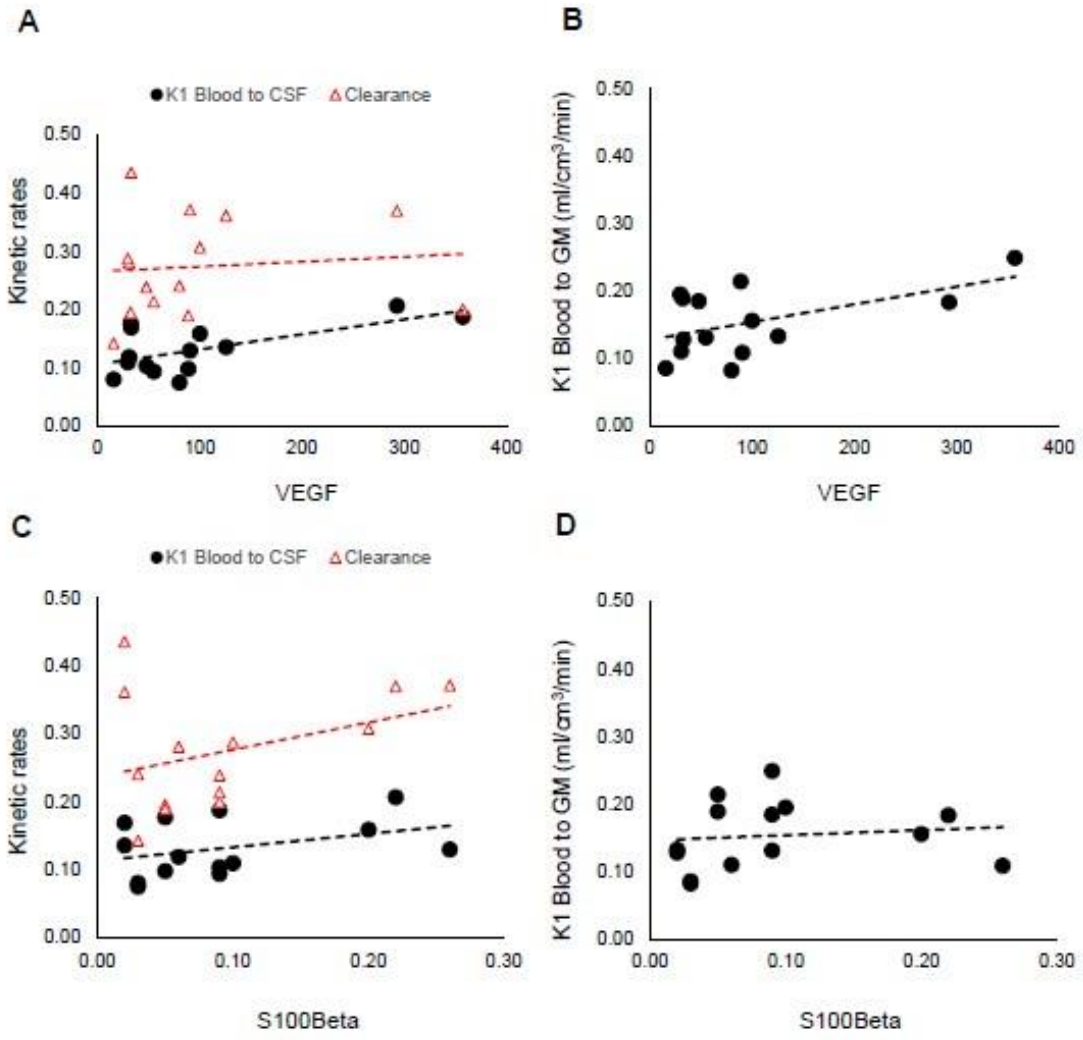

A) Tracer kinetics in lateral ventricles (black circles = K_1, red triangle = kClearance). B) Blood to GM transport (black circles = K_1)

2.5 DISCUSSION

This work has demonstrated that, contrary to expectations, high levels of the peripheral inflammatory marker CRP are associated with reduced influx of TSPO PET radiotracers into brain spaces. Influx rates K1, whether they represent the rate of transfer of the tracer from plasma to parenchyma through the BBB or from blood to the CSF through the choroid plexus, are the product of two factors: cerebral blood flow (*CBF*) and tracer extraction (*E*). Hence reduction in influx in the MDD cohorts can be explained by reduction of either *CBF* or *E* or both. A review of the literature seems to point to a likely reduction in extraction; a very recent MRI imaging technique called IDEALS (intrinsic diffusivity encoding of arterial labeled spin) (Wengler et al., 2019) now allows the direct and simultaneous measurement of *CBF* and BBB water extraction. Preliminary data obtained with IDEALS indicate that in MDD *CBF* is unchanged but *E* is reduced by about 20% (Wengler et al., 2019).

It is important to note that BBB permeability of water is not the same as the permeability of a PET radioligand. The BBB is constituted by three layers; the endothelial layer where cell-to-cell contact is through the tight junctions, the basal membrane upon which the endothelial cells lie, and the final layer made of pericytes and the astrocytic end-feet (Hladky and Barrand, 2016). Aqueous transport across the endothelial layer is thought to be paracellular across the tight junction while PET radioligands, that are generally quite lipophilic, are thought to use a transcellular route (Bagchi et al., 2019). Less is known about the transfer of substances through the remaining layers and a number of models considering passage through the clefts between astrocytic end-feet or through aquaporin channels have been proposed (Hladky and Barrand, 2016). Data so far do not allow the clarification of the mechanism involved in the observed changes in permeability in MDD and further studies are granted.

However, it is very worth noting that TSPO ligands have molecular weight (~300 g/mol) and lipophilicity similar to that of other lipid-soluble drugs like antidepressants (Frisk-Holmberg and van der Kleijn, 1972) and thus it is interesting to consider the possibility that reduced paracellular perfusion of small lipophilic molecule into the brain could be a mechanism of drug resistance. In fact, in those instances where MDD cohorts demonstrate increases in BBB porosity, drug response seems associated with increased levels of the marker S100β (Arolt et al., 2003, Ambree et al., 2015) although this is debated (Jang et al., 2008)

In addition, on a technical level, our findings are relevant in the context of the difficulties encountered in the quantification of the binding of TSPO PET tracers in the study of patient cohorts with inflamed peripheral status where the volume of distribution, e.g. the estimated ratio between the target and the plasma tracer concentrations, will be lowered by the decreased perfusion and this may be mistakenly interpreted as a reduction in the target TSPO density. This further complicates the interpretation of TSPO neuroimaging studies, which is already methodological challenging (Turkheimer et al., 2015).

It is notable that the findings here do not fit with the previous models of peripheral-to central immune interaction in depression. For example, depression's main environmental risk factor is chronic stress and one prevalent model proposes that peripheral myeloid cells or proinflammatory cytokines generated during prolonged stress conditions can diffuse into the brain due to stress-induced increase of BBB permeability (Quan and Banks, 2007); a large body of literature exists on this matter (Menard et al., 2017, Hodes et al., 2015, Wohleb et al., 2013, Weber et al., 2017, Esposito et al., 2001, Santha et al., 2015, Friedman et al., 1996) although this link is still controversial (Roszkowski and Bohacek, 2016). Clinical evidence is very sporadic with only a few reports on the subject; association between BBB leakage and

depression has been demonstrated with higher CSF albumin concentration in small patients' subgroups (Bechter et al., 2010) and in elderly women (Gudmundsson et al., 2007). Another marker of BBB integrity is the astrocytic marker S100β protein that has been reported as increased in MDD (Tsai and Huang, 2016, Arora et al., 2019) and reduced after medication (Schroeter et al., 2002), although elevated levels S100β have been shown to be correlated positively with therapeutic response in depressed patients (Arolt et al., 2003, Ambree et al., 2015), with few exceptions (Tsai and Huang, 2016). Contrary to this, in MDD cohorts, high levels of CRP in plasma and CSF are not associated with increased BBB permeability as measured by albumin plasma-to-CSF ratio (Felger et al., 2018). Indeed, even in this paper, patients in the BIODEP cohort did not demonstrate biomarkers of BBB disruption. In the FLAME study, the HC after the IFN-α challenge did not exhibit evidence of BBB leakage as measured by serum levels of S100β (Figure 2.5).

If the reduction in BBB permeability in MDD extends beyond lipophilic molecules then a different model can be put forward positing a reduction of the permeability of the healthy BBB in reaction to increased peripheral inflammation as indexed by CRP.

Hence, we may then speculate that the mild inflammatory state observed by PET imaging in the brain of clinically depressed patients may be the result of disturbed homeostasis due to the much-reduced transfer of solutes across the BBB. This reduction of BBB permeability may be protective on the short-term but may lead to disturbed homeostasis in the case of prolonged/chronic inflammatory states. If this were proven to be the case, then the mechanism of interaction between peripheral cytokines and CNS immune activity would be indirect, e.g., mediated by the BBB closure and ensuing disturbance to CSF dynamics.

Importantly, the activation of microglia in MDD would be the secondary outcome of disturbed homeostasis. To support further this model, Dantzer and colleagues have very recently demonstrated that sickness behaviour generated in mice and rats by peripheral immune challenges is not mediated by microglia (Vichaya et al., 2020).

Further support to this model comes from the observation that in MDD peripheral circulating glucocorticoidsare increased (Lombardo et al., 2019), and conditions with high endogenous glucocorticoids, such as Cushing's disease, are associated with depression (Sonino et al., 1998). Within neuroinflammatory diseases such as multiple sclerosis use of high dose glucocorticoid treatment is thought to reduce BBB permeability and therefore reduce the flow of inflammatory mediators from the blood into the CNS (Miller et al., 1992). Anti-glucocorticoid treatments have also been used with some benefit in the treatment of MDD in patients with high serum glucocorticoids (Lombardo et al., 2019). Therefore, increases in circulating glucocorticoids in MDD, although not measured in this study, could potentially explain the reduction in BBB permeability demonstrated and therefore changes in BBB permeability could explain the mechanism of their actions.

The observation of reduced transfer across the choroid plexus into CSF also supports our proposed model; amongst its various functions, the choroid plexus regulates the access for chemical substances from blood to the CSF playing a key role in neurotransmitter volumetric transmission (Skipor and Thiery, 2008). Molecular and gene-expression analysis of choroid plexus gene expressions in MDD has suggested alterations to calcium signalling as well as to immune activity in MDD (Turner et al., 2014, Devorak et al., 2015).

Finally, it is also of note the significant negative correlation between reduced CSF tracer exchange in ventricles and increased childhood trauma scores observed in the secondary analysis; this correlation did not survive multiple comparison correction but it is suggestive that early life events may translate into BBB porosity becoming a trait in the following years, most likely because of an increased inflammatory state (Baumeister et al., 2016), and become a risk factor for adult depression. Further investigations on the issue are needed in a much larger dataset.

2.5.1 Methodological Issues

To measures the perfusion of the tracers from blood to CSF we focused on the amount of radioactivity percolating into the lateral ventricles. Generally, the source of this radioactivity is both the fraction of the radiotracer in parenchyma flowing in the interstitial spaces and then across the ependymal cells that line the ventricular spaces and the radiotracer flowing directly from blood through the choroid-plexus (Schubert et al., 2019). Kinetic modelling of the [^{11}C]PBR28 data evidenced that in the case of TSPO tracers, likely due to their poor tissue extraction, radioactivity in the lateral ventricles is predominantly sourced from blood.

Given the variability across subjects in the BIODEP dataset as well as the unavailability of arterial blood data for [^{11}C]PK11195 study, we then turned to another dataset where inflammation was experimentally controlled via IFN-α challenge in normal volunteers and measured with [^{11}C]PBR28 with arterial sampling. Here we also observed a strong inverse linear relationship between peripheral CRP levels and radioactivity in ventricles measured both with SUVR and via kinetic modelling through the blood to lateral ventricle CSF transport. In these data as in the previous set, the effect was amplified non-linearly for abnormal CRP levels. Although we do not know whether CRP is directly inducing the observed reduction in tracer delivery, this modulation, that was consistently observed across the two datasets, possibly

indicates a threshold effect with barriers becoming less permeable for inflammatory states corresponding to CRP levels greater than 3-5 mg/L.

In the [^{11}C]PBR28 dataset, the same association between CRP and reduction in tracer delivery to the lateral ventricles was observed in the blood-to-brain transfer constant K_1. This also suggests that in the BIODEP dataset the SUVR for the lateral ventricles may actually underestimate the reduction of delivery into those spaces given that is likely that the delivery to parenchyma was also reduced; this would explain the lack of group difference between controls and patients. Note that an alternative explanation is that the observed associations are confounded by changes in the free fraction of the radiotracer in plasma. Lockart et al., (Lockhart et al., 2003) demonstrated an affinity of PK11195, a quinoline, to the reactant alpha1-acid glycoprotein which, although not measured in these two datasets, is also likely to be positively associated with peripheral inflammatory states. There was indeed an association between tracer delivery into brain and CSF and plasma free fractions of [^{11}C]PBR28, the latter being highly collinear with CRP levels. However, the range of changes in free fractions did not explain a significant portion of the variability of blood-to-tissue transport (as measured by K_1) either in CSF or in GM.

The inverse association between TSPO tracer perfusion and peripheral inflammatory status indexed by CRP may explain why brain TSPO density quantified with a plasma input function has shown reductions or no differences in MDD cases versus HC as the parameter used, the volume of distribution, is dependent on the target TSPO density but also on the perfusion of the tracer into tissue. Reference tissue approaches to quantification, that are not dependent on plasma-to-tissue transfer, may be more suitable for the quantification task in these cohorts (Marques et al., 2019).

Overall, the observed changes in free plasma fraction and brain perfusion, combined with the moderate-to-low variations observed in MDD and psychiatric cohorts, underlie the difficulty of obtaining robust quantification in these studies.

2.6 Limitations

The use of PET tracer percolation into lateral ventricle is an indirect way to quantify CSF dynamics and suffers from the low PET signal measurable in this anatomical area. However, when we tested the reproducibility of our metrics (both SUVR and AUC30-60) in a test-retest [^{11}C]PBR28 brain PET dataset of 5 patient with mild AD (Nair et al., 2016) we found good performances: for SUVR parameter the test-retest absolute variability was 8%±4%, corresponding to an intra-class correlation coefficient (ICC) = 0.97, while for AUC30-60 test-retest absolute variability was 12%±7% (ICC = 0.86). These numbers are in line with those obtained for SUV in whole GM for which absolute variability was 6%±3% and ICC = 0.94 (Nair et al., 2016).

2.7 Conclusion

We have demonstrated a strong association between (increased) peripheral inflammation indexed by CRP and (reduced) blood-to-brain and blood-to-CSF transfer of TSPO-PET radiotracers. These results may be expanded to implicate a mechanism of reduced permeability of the BBB and BCSFB that may be harmful if protracted by chronic inflammatory states. This mechanism should be further tested to assess the effect of peripheral inflammatory messengers on BBB permeability for a wider range of molecules as well as antidepressant medication.

2.8 Contributions to Study 1

The lateral ventricle segmentations were created by Noha Althubaity. All data collection was conducted for use in original studies and the data was re-analysed for this work. All data analysis and the reporting of the results were conducted by Noha Althubaiy.

3 Chapter 3

<u>Study 2</u>: Choroid plexus enlargement is associated with neuroinflammation and reduction of blood brain barrier permeability in depression

This study was published in *NeuroImage: Clinical*, 33 (2022), 102926.

3.1 INTRODUCTION

Major Depressive Disorder (MDD) is a neuropsychiatric disorder associated with significant psychosocial impairment, recognized by the World Health Organization (WHO) as the leading cause of disability worldwide (Petralia et al., 2020). MDD is associated with mood changes such as sadness, crying, irritability, and anhedonia as well as psychophysiological symptoms such as insomnia, slowness of speech and action, loss of appetite, constipation, diminished sexual desire, and suicidal thoughts (Belmaker and Agam, 2008). Available antidepressant medications, which largely target monoamine pathways, are effective; however, more than 30% of depressed patients fail to achieve remission despite multiple treatment trials (Nettis et al., 2021a). Treatment resistance in MDD has been associated with heightened peripheral immunity (Bekhbat et al., 2018).

MDD patients who experienced treatment resistance exhibit most of the cardinal features of inflammation, including elevations in inflammatory cytokines, acute phase proteins, chemokines, adhesion molecules, and inflammatory mediators such as prostaglandins in peripheral blood and CSF (Miller et al., 2009). Different studies have shown significant associations between inflammatory cytokines, in particular IL-1, TNF- α, and IL-6 that are markers of innate immune response, and depressive symptoms (Miller and Raison, 2016, Enache et al., 2019). Evidence of direct relationship between peripheral heightened immunity and MDD is supplied by the reproducible observation that the acute and chronic administration of cytokines (or cytokine inducers such as lipopolysaccharide (LPS) or vaccination) can cause

behavioural symptoms that overlap with those found in MDD (Miller and Raison, 2016). For example, 20% to 50% of patients receiving chronic IFN-alpha therapy for the treatment of infectious diseases or cancer develop MDD (Lotrich, 2009). Moreover, inducing acute IFN-α in healthy subjects results in the elevation of peripheral inflammation immune markers such as C-reactive protein, TNF-α, and IL-6 and is accompanied with depressive symptoms (Nettis et al., 2020).

The mechanisms linking peripheral immunity to changes in central nervous system and mood changes in MDD are still under investigation. The hypothesis of a potential direct action of peripheral cytokines trespassing the blood brain barrier (BBB) to activate brain microglia (D'Mello et al., 2009) has spurred a number of imaging studies of neuroinflammation in the central nervous system (CNS) in MDD that have been conducted using positron emission tomography (PET) and radiotracers targeting the 18kDa mitochondrial translocator protein (TSPO), a protein that is consistently upregulated in activated microglia (see review in (Mondelli et al., 2017)). These have revealed mild microglial activity in depressed subjects (Schubert et al., 2021b); however, evidence of a relationship between central and peripheral inflammation for PET imaging has been lacking (Schubert et al., 2021b). Instead, there is very recent evidence of a relationship between heightened peripheral immunity and the reduction of the brain barriers permeability, both for the BBB and blood-CSF barrier (BCSFB) at the choroid plexus (CP) (Turkheimer et al., 2020).

This has led us to hypothesize a different model of peripheral-to-central inflammatory interaction whereas brain barriers react to increases in circulating inflammatory messengers by reducing peripheral-to-central solute transfer (Turkheimer et al., 2020). This may be protective in the short term but, if the inflammatory status becomes chronic, may disturb brain homeostasis and induce microglia to react to the disturbed environment. Very recent work on immune peripheral activation via LPS in mice and rats supports this view by showing that

sickness behaviour is not mediated by microglia, hence their activation is a secondary result of the peripheral immune challenge (Vichaya et al., 2020).

The model above leads to a novel focus on a particular brain structure, the CP, that is an important part of the brain barriers, plays an active role in immune responses in the nervous system (Meeker et al., 2012), and, importantly, can be measured in-vivo using MRI imaging: the choroid plexus, **see Figure 1.1 in Chapter 1**.

The primary role of the CP is to produce the cerebrospinal fluid (CSF) and form the BCSFB (Liddelow, 2015). The CP is an epithelial-endothelial convolute, consisting of a highly vascularised stroma with connective tissue and epithelial cells and is located in the basal lamina of the four brain ventricles (Shen, 2018, Brown et al., 2004, Khasawneh et al., 2018). It is responsible for producing 75% of CSF, and through the action of active transporters and channels mediates the movement of water and solutes across the epithelium (Ghersi-Egea et al., 2018a). CP epithelial cells are connected via tight junctions, which play a fundamental role in regulating the permeability and integrity of the BCSFB (Ghersi-Egea et al., 2018a). The fenestrations in the choroidal plexus vessels are less restricted compared to cerebral vessels, and allow ions and small molecules such as amino acids to diffuse into the CP epithelial cells, which can then be actively transported actively into the CSF (Maharaj et al., 2008, Liddelow, 2015). The BCSFB together with the BBB control the traffic between the blood, the CSF, and the brain parenchyma (Saunders et al., 2012). There has been a recent increase of interest in the CP due to its important role in regulating brain homeostasis and, particularly, the neuroinflammatory response (Schwartz and Baruch, 2014). CP immune cells and intraventricular macrophages provide the first line of defence against brain infections and inflammation (Pollak et al., 2018, Yang et al., 2021). Prolonged inflammation may contribute to the infiltration of the CP by immune cells, and subsequently into the CSF and into the brain parenchyma (Marques and Sousa, 2015).

There is a growing body of literature that recognises the importance of CP morphology in psychiatric conditions. In subjects with schizophrenia, CP enlargement has been found to be associated with chronic stress (Zhou et al., 2020), a condition often associated with MDD and inflammation. A more direct correlation between CP volume and levels of peripheral IL-6 has been documented by Lizano and colleagues in psychosis (Lizano et al., 2019) whereas CP enlargement was also associated with reductions in gray matter and amygdala volume as well as ventricle enlargement and consequential deteriorated cognitive status (Lizano et al., 2019). Note that CP enlargement is also observed in patients with mild cognitive impairment and Alzheimer's disease, for which MDD is a known prodrome (Tadayon et al., 2020). However, few studies suggest a potential direct link between CP structural and functional alterations and depression. Gene expression analysis from a cross-sectional post-mortem study has identified multiple differential mRNA expression in CP samples obtained from MDD patients (Turner et al., 2014, Devorak et al., 2015). ICAM-1 and VEGF transcripts are notable examples as they are known to play an important role in depression, being part of the tissue inflammatory response. They are also known to affect BBB permeability and in fact their peripheral measures serve as inflammatory markers (Müller, 2019, Clark-Raymond and Halaris, 2013).

In this study we wanted to test the model of peripheral-to-central inflammation sketched above by investigating for the first time the association between CP volume and neuroinflammation in a depressed cohort, using structural MRI and 18kDa translocator protein (TSPO) positron emission tomography (PET) data. We hypothesized that if the BCSFB were indeed a mediator between peripheral and central inflammation in depression, we would observe a direct correlation between central inflammation, here marked by TSPO parenchymal expression, and CP volume.

3.2 Methods

3.2.1 Dataset

Data for this study were collected from a network of clinical research sites in the United Kingdom as part of the Biomarkers in Depression Study (BIODEP, NIMA consortium, https://www.neuroimmunology.org.uk/) and included 51 depressed participants and 25 healthy controls (HCs). Depressed subjects who had taken anti-depressive treatment with Hamilton Depression Rating scale (HDRS)>13 and untreated subjects with HDRS>17 were included. In total, there were 9 untreated subject and 42 were medicated. An overview of demographic and clinical characteristic data is reported in **Table 3.1**, while full details of the dataset are outlined in the previous publication (Schubert et al., 2021b). Participant's inclusion criteria were as follows: no history of other neurological disorder, no current alcohol and/or drug abuse, no contribution in any clinical drug trials during the previous year. Participants were not experiencing any other medical disorders or undergoing any treatment that could affect the accuracy of the study's results. Pregnant or breastfeeding women were excluded. HC subjects were age- and sex-matched with the depressed subjects, and they did not have a history of clinical depression or antidepressant treatment. Ethical approval was obtained from the local ethics committee. All participants provided written informed consent prior to the study.

Table 3.1 Demographics and clinical characteristics for depressed subjects and healthy controls (HCs)

Variable	**Depressed subjects (n = 51)**	**Healthy controls (n = 25)**	**p Value**
Demographics			
Age, mean ± SD, years	36.2 ± 7.3	37.3 ± 7.8	0.56
Male, No. (%)	15 (29)	11 (44)	0.21
Weight, mean ± SD, kg	80.3 ± 14.4	73.7 ± 15.1	0.10
BMI, mean ± SD, kg/m^2	27.2 ± 4.0	24.2 ± 4.8	<0.01*
Blood Variables, (MDD No.; HC No.), mean ± SD:			
CRP mg/L (51; 25)	2.9 ± 2.8	1.1 ± 0.9	<0.01*
IL6 (35;12)	1.1 ± 1.63	0.6 ± 0.4	0.35
TNF-α (34;11)	2.7± 0.9	2.3 ± 0.5	0.25
IFN-γ (35;11)	4.0 ± 0.7	4.2 ± 0.0	0.26
IP-10 (49;22)	402 ± 152	428 ± 101	0.46
Lymphocytes (47;23)	30.9 ± 7.2	30.2 ± 10.2	0.79
Monocytes (47;23)	6.8 ± 2.1	6.6 ± 2.5	0.78
Neutrophils total (47;23)	58.8 ± 8.3	59.3 ± 11.3	0.80
Neutrophils absolute (47;23)	3.9 ± 1.5	4.1 ± 1.4	0.48
Albumin (47;23)	44.8 ± 2.7	45.3 ± 2.1	0.44
Cholesterol (47;23)	5.2 ± 1.2	4.9 ± 1.2	0.35
VEGF (35;11)	82 ± 55.5	136 ± 47.8	<0.01*

Depressive Clinical Scores, (MDD No.), mean ± SD:			
HDRS (51)	18.5 ± 3.7	0.6 ± 0.9	<0.001*
Childhood Trauma score (50)	54.3 ± 14	38.2 ± 5.4	<0.001*
Perceived Stress score (48)	26.7 ± 4.3	10 ± 5.9	<0.001*
ICV, mean ± SD, mm^3	1,562,594 ± 137,333	1,550,724 ± 185,887	0.76

Abbreviations: NA, not applicable

3.2.2 Clinical Assessments

For the clinical evaluation of depression, HCs and depressed subjects underwent a number of psychiatric assessments: the Hamilton Depression Rating scale (HDRS), the Standard Clinical Interview for DSM-5, the Beck Depression Inventory, the Spielberger StateTrait Anxiety Rating Scale, the Chalder Fatigue Scale, the Snaith-Hamilton Pleasure Scale, the Childhood Trauma score, and the Perceived Stress score. A venous blood sample was collected from all participants to assess peripheral blood parameters including interlukin-6 (IL-6), tumor necrosis factor-alpha (TNF-α), interferon gamma (IFN-γ), interferon gamma-induced protein 10 (IP-10), lymphocytes, monocytes, neutrophil's total, neutrophils absolute, albumin, cholesterol, VEGF, and C-reactive protein (CRP) concentration. CRP was used as the main marker of a peripheral inflammation, consistent with other studies in MDD (Howren et al., 2009, Haapakoski et al., 2015).

3.2.3 MRI and PET Imaging

For all the subjects, imaging data were obtained using a GE SIGNA simultaneous PET/MR scanner (GE Healthcare, Waukesha, USA). All MRI acquisitions included a high resolution T1-weighted image for structural imaging. PET imaging consisted in a bolus injection of [^{11}C]PK11195 (target dose ~350 MBq, mean injected dose 361± 53MBq) followed by a 60-minute dynamic acquisition. A multi-subject atlas method was used for attenuation

correction and included improvement for the MRI brain coil component (Burgos et al., 2014). Additional corrections (including scatter, random, normalisation, and deadtime correction), were performed using the standard console software that applied PET/MR reconstruction algorithm correction. Additional information on the PET and MRI protocols can be found in the original report on these data (Schubert et al., 2021b).

3.2.4 CP Volume and brain volume measurement

The CP of the lateral ventricles of all subjects was manually segmented on the axial, sagittal, and coronal planes of the high resolution T1- weighted image using the Analyze software (v.12, https://analyzedirect.com) **(Figure 3.2)**. The image intensity was adjusted to assist in the localization of the region of interest and its anatomical boundaries. The CP was traced slice by slice starting from the axial plane followed by coronal and sagittal planes. After the region contouring, the CP volume was calculated for each subject using the Analyze software. The SPM12 (http://www.fil.ion.ucl.ac.uk/spm) was used to perform tissue segmentation for grey matter, white matter, and CSF (Heinen et al., 2016). High resolution T1 weighted images were smoothed and normalised into MNI standard space using the DARTEL algorithm via the SPM12 for brain volume calculation (Ashburner, 2007). The total brain volume was obtained by the sum of gray and white matter volume (Heinen et al., 2016). Additionally, the Freesurfer software (v.6.0, http://surfer.nmr.mgh.harvard.edu/), was used to estimate the total intracranial volume (ICV) (Fischl et al., 2002, Jovicich et al., 2009), which was used as a covariate in the statistical analysis (Pintzka et al., 2015).

Figure 3.1 Choroid plexus (CP) segmentation in HCs and depressed subject

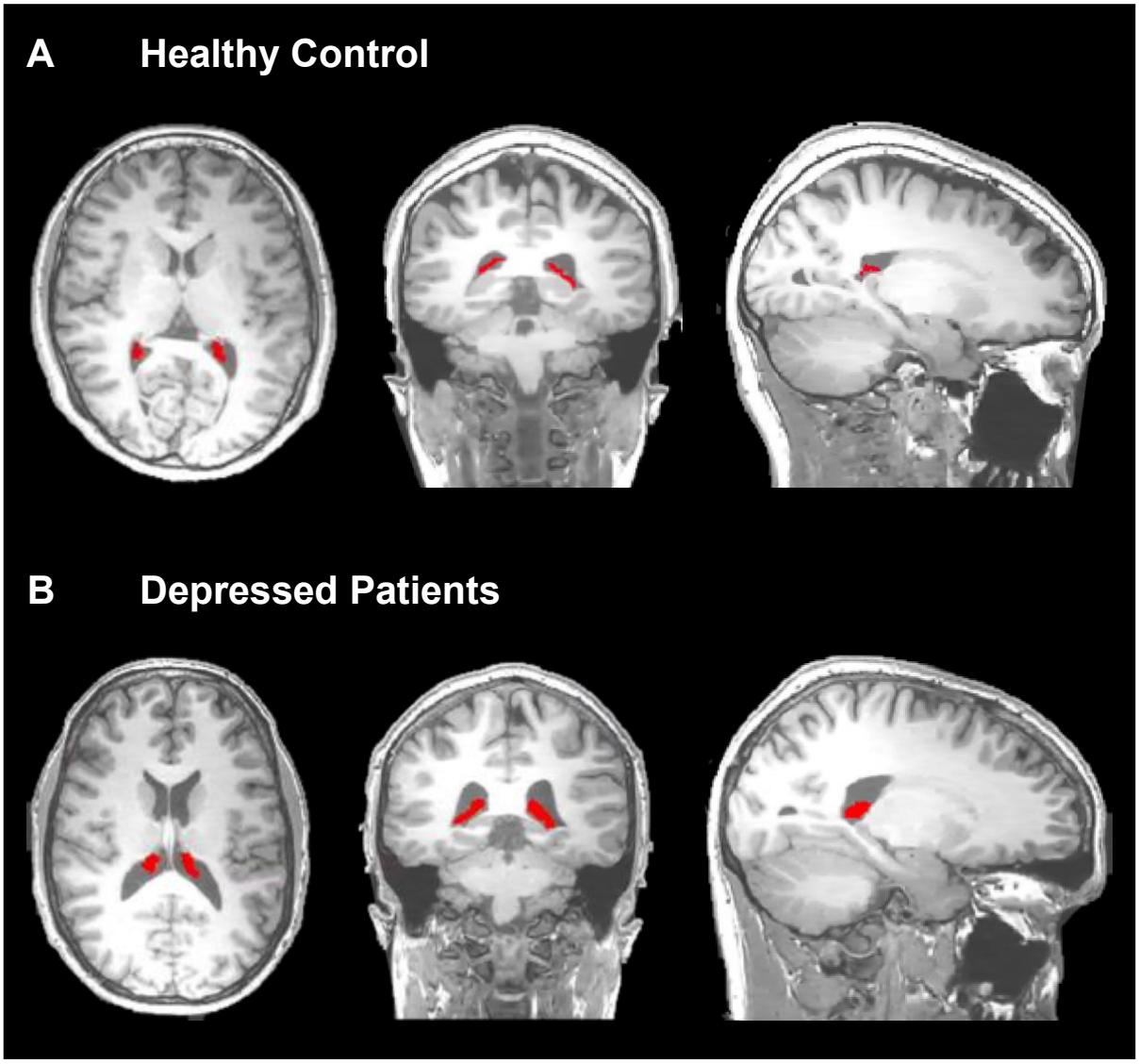

T1-weighted MRI images with the manual segmentation of the left and right CP (red) on the axial, coronal, and sagittal planes for one representative control (A) and one depressed subject (B).

3.2.5 PET Analysis

The pre-processing of the [^{11}C]PK11195 PET imaging including frame-by-frame motion correction, PET-MRI alignment, brain masking, and atlas-based region extraction was

performed using the MIAKAT software (www.miakat.org). Processed data were hence used for both the quantification of TSPO distribution in brain parenchyma (as a proxy of neuroinflammation) as well as to assess the tracer exchange between blood and CSF in the lateral ventricles. This second method had been previously validated and used to demonstrate CSF dynamic alterations in Alzheimer's disease (De Leon et al., 2017, Schubert et al., 2019) and multiple sclerosis (Schubert et al., 2019). The lateral ventricles were manually segmented using T1-weighted structural MRI and ITK-SNAP software as was done in the original reference (Schubert et al., 2019, Acabchuk et al., 2015), and then eroded by two voxels in native space (5.2 mm) to reduce the effect of the partial volume(Yushkevich et al., 2006, Turkheimer et al., 2020). The [^{11}C]PK11195 PET activity extracted from the eroded lateral ventricles was used to calculate the standardized uptake value ratio (SUVR) normalized by a reference region at 60 minutes, and the area-under-curve (AUC) which included activity of the lateral ventricles between 30 and 60 minutes ($AUC_{30\text{-}60}$) (Turkheimer et al., 2020). For the quantification of TSPO, the simplified reference tissue model was used to calculate the distribution volume ratio (DVR) of [^{11}C]PK11195 in brain (Turkheimer et al., 2007). The DVR estimates for the anterior cingulate cortex (ACC), prefrontal cortex (PFC), and insula (INS), were extracted to assess the level of brain inflammation as these regions serve important roles in mood regulation (Goldin et al., 2008), and the ACC has been previously shown to be involved in inflammation-associated mood deterioration (Harrison et al., 2009, Torres-Platas et al., 2014). For both methods, the same reference region derived from a supervised clustering of dynamic PET images was applied (Schubert et al., 2021a). Additional details about the PET image processing and quantification are found in our previous studies (Turkheimer et al., 2020, Schubert et al., 2021b).

3.3 Statistical Analysis

Statistical analyses were performed using SPSS software (version 25.0, Chicago, IL). The Shapiro-Wilk's test was used to test for normality of the data. An independent sample ttest was used to examine the difference of CP volume between the HCs and depressed subjects. Partial correlations were used to analyse the relationship between CP volume and depressive clinical scores (HDRS, the Childhood Trauma, and Perceived Stress score), while covarying for ICV. Partial correlation tests were used to investigate the association between the CP volume and blood to CSF exchange measures (SUVR and $AUC_{30\text{-}60}$) while covarying for the ICV and group. Partial correlation of CP volume measures and brain TSPO values (ACC, PFC, and INS) and brain volume were also investigated while covarying for possible confounding factors including ICV and group. The same analyses were repeated voxelwise with SPM12, using FWE for multiple comparison corrections.

3.4 Imaging transcriptomics

We leveraged transcriptomic data from the Allen Human Brain Atlas (AHBA) (Hawrylycz et al., 2012) to explore possible associations between the brain map depicting the correlations between CP volume and TSPO and post-mortem brain gene expression. With this analysis, we aimed to gain further insight about potential biological pathways explaining regional vulnerability to spatial variability in the association between CP volume and brain TSPO across subjects.

We used the *abagen* toolbox (https://github.com/netneurolab/abagen) to process and map the transcriptomic data to 83 parcellated brain regions from the DK atlas (Desikan et al., 2006), as described in Martins et al. (Martins et al., 2021). We applied the normalization for cortical and subcortical regions separately, as suggested by *Arnatkeviciute et al., 2019*

(Arnatkeviciute et al., 2019). After pre-processing, we retained regional gene expression data from 15,633 genes, corresponding to genes with expression higher than background noise. We then used partial least square regression (PLS) to investigate associations between the t-statistics quantifying the regional correlations between CP volume and TSPO and brain gene expression. We focused on both cortical and subcortical regions from the left hemisphere only. This choice was motivated by scarcity of data in the AHBA for the right hemisphere.

Partial least square regression ranks all genes by their multivariate spatial alignment with the regional strength of the association between CP volume and TSPO. The first PLS component (PLS_1) is the linear combination of the weighted gene expression scores that have a brain expression map that covaries the most with the map of the association between CP volume and TSPO. We confirmed PLS_1 explained the largest amount of variance by testing across a range of PLS components (between 1 and 15) and quantifying the relative variance explained by each component. The statistical significance of the variance explained by each PLS model was tested by permuting the response variables 1,000 times, while considering the spatial dependency of the data by using a spin test (Alexander-Bloch et al., 2013a, Alexander-Bloch et al., 2013b, Vasa et al., 2018). Since PLS_1 alone explained the largest amount of variance in the imaging dependent variable, we focused our following analyses on this component.

The error in estimating each gene's PLS_1 weight was assessed by bootstrapping (resampling with replacement of the 34 brain regions), and the ratio of the weight of each gene to its bootstrap standard error was used to calculate the *Z* scores and, hence, rank the genes according to their contribution to PLS_1 (Whitaker et al., 2016). Genes with large positive PLS_1 weights correspond to genes that have higher than average expression in regions where the association between CP volume and TSPO is more strongly positive. Mid-rank PLS weights

showed expression gradients that are weakly related to the pattern of the regional association between CP volume and TSPO.

We then used the list of genes ranked by the respective weights according to the PLS_1 component to perform gene set enrichment analyses for biological pathways (gene ontology) and genes expressed in different brain cell types, as identified in a previous single-cell transcriptomic study of the human brain (Lake et al., 2018). We implemented these analyses using the GSEA method of interest of the Web-based gene set analysis toolkit (*WebGestalt*) (Zhang et al., 2005).

For comparative purposes, we used the same method to understand the spatial variability of changes in brain TSPO between subjects with depression and HCs.

3.5 RESULTS

3.5.1 Demographic and Clinical Characteristics

Subjects with depression and HCs were matched in terms of age (p=0.56) and sex (p=0.21), and no difference was shown in terms of the ICV between groups (p=0.76). BMI was significantly higher in depressed subjects compared to HCs ($t_{(76)}$=3.52, p=0.001).

Peripheral blood parameters were all comparable between two groups (**Table 3.1**), with the exception of CRP and VEGF levels. Depressed subjects had higher blood CRP ($t_{(76)}$ =3.14, p=0.002) and lower VEGF ($t_{(46)}$ =-2.90, p=0.006) levels compared to HCs. While CRP differences were expected given the recruitment parameters (Schubert et al., 2021b), the difference in VEGF level was not.

In terms of clinical variables, the HDRS, Childhood Trauma scores, and the Perceived Stress score were significantly higher in depressed subjects compared to HCs ($t_{(76)}$ =23.6, p<0.001), ($t_{(75)}$ =5.5, p<0.001), ($t_{(73)}$ =13.8, p<0.001) respectively **(Table 3.1)**.

3.5.2 Depressed subjects have larger CPs compared to HCs

The CP volume was log10-transformed to induce normality in the data distribution as confirmed by Shapiro-Wilk's test ($W_{(76)}$ =0.98, p=0.23). The CP volume was greater in patients with depression compared to HCs (mean value of depressed patients:1710.29 ±408.80; mean value HCs: 1513.96±459.80; $t_{(76)}$=2.17, p=0.03) (**Figure 3.3)**. In both groups, the CP volume was strongly correlated with ICV (r=0.25, p=0.03) and sex (F=4.7, p=0.03), but not with age (p=0.72) or BMI (p=0.19). However, when both ICV and sex were included as covariates, only ICV remained significant. After adjusting for ICV, the CP volume remained significantly higher in depressed subjects compared with HCs ($F_{(76)}$=4.6, p=0.04) (**Figure 3.3)**.

After adjusting for ICV, the CP volume of depressed subjects showed a negative association with Perceived Stress score (r=-0.30, p=0.05); however, the association was not significant following multiple comparisons correction. No association was found with any other clinical variable.

Figure 3.2 Choroid plexus (CP) volume in depressed subjects and healthy controls (HCs)

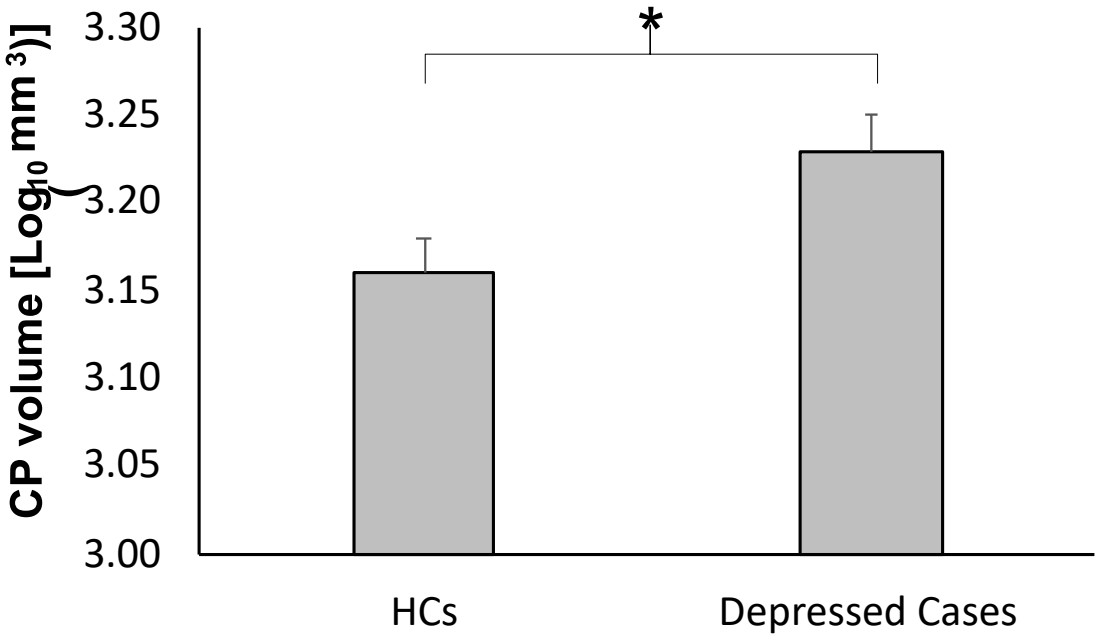

Mean difference of CP volumes between HC and depressed groups (F=5.30, p=0.02). Error bars indicate standard error. The analysis is corrected for the intracranial volume.

3.5.2 CP volume is not associated with peripheral inflammatory markers

When using the full sample, the CP volume was not associated with the CRP levels (r=0.07, p=0.53), IL-6 (r=-0.08, p=0.61), TNF-α (r=-0.06, p=0.70), or VEGF (r=0.12, p=0.39). Similarly, no association between CP volume and peripheral inflammatory markers was found when depressed and HC groups were analysed separately.

3.5.3 CP volume is positively associated with central inflammation and inversely with CSF clearance

Using the full dataset (N=76), CP volume measures were positively correlated with [^{11}C]PK11195 DVR in the ACC (r=0.28, p=0.02), PFC (r=0.24, p=0.04) and INS (r=0.24, p=0.04) (**Figure 3.4)**. All these correlations were corrected for group and ICV, although only ICV was a significant covariate in the regression for ACC and INS (**Figure 3.4)**. When analysis was repeated in the depression cohort only, no correlation was detected between the CP volume and [^{11}C]PK11195 DVR in any of the main ROIs (ACC: r=0.20, p=0.40; PFC: r=0.18, p=0.18; INS: r=0.17, p=0.2). No correlation was found between CP volumes and total cortical [^{11}C]PK11195 DVR (r=-0.21, p=0.07) nor with whole brain [^{11}C]PK11195 DVR (r=-0.05, p=0.56).

Figure 3.3 Correlation between the choroid plexus (CP) volume and brain inflammation in healthy controls (HCs) and depressed subjects in ACC (A), PFC (B) and INS (C).

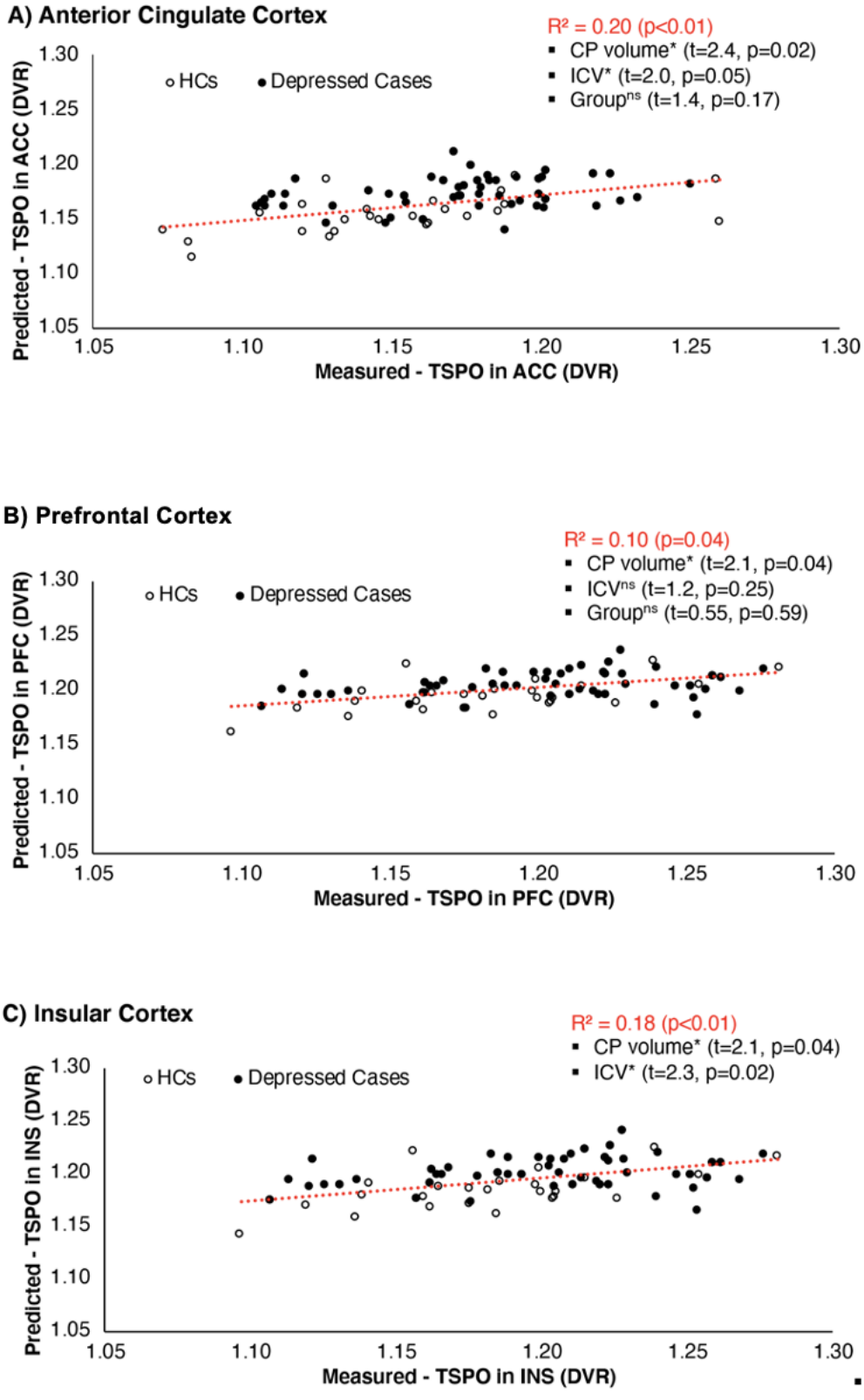

Group^{ns} (t=0.9, p=0.35) **indicates statistical significance (p-value<0.05). ^{ns} indicates non-significant results.*

The CP volume exhibited a negative association with the blood-to-CSF radiotracer exchange as measured by the lateral ventricle SUVR (r=-0.23, p=0.05), following correction for group and ICV. A similar association was found for radiotracer $AUC_{30\text{-}60}$ in lateral ventricle (r=-0.26, p=0.02) (**Figure 3.5)**. However, the depression cohort did not show a significant association between the CP volume and the SUVR (r=-0.19, p=0.19) nor $AUC_{30\text{-}60}$ (r=-0.20, p=0.16).

Figure 3.4Inverse association between choroid plexus (CP) volume and CSF-blood tracer exchange measured by [^{11}C]PK11195 PET uptake (SUVR and AUC, respectively) in lateral ventricles (LV).

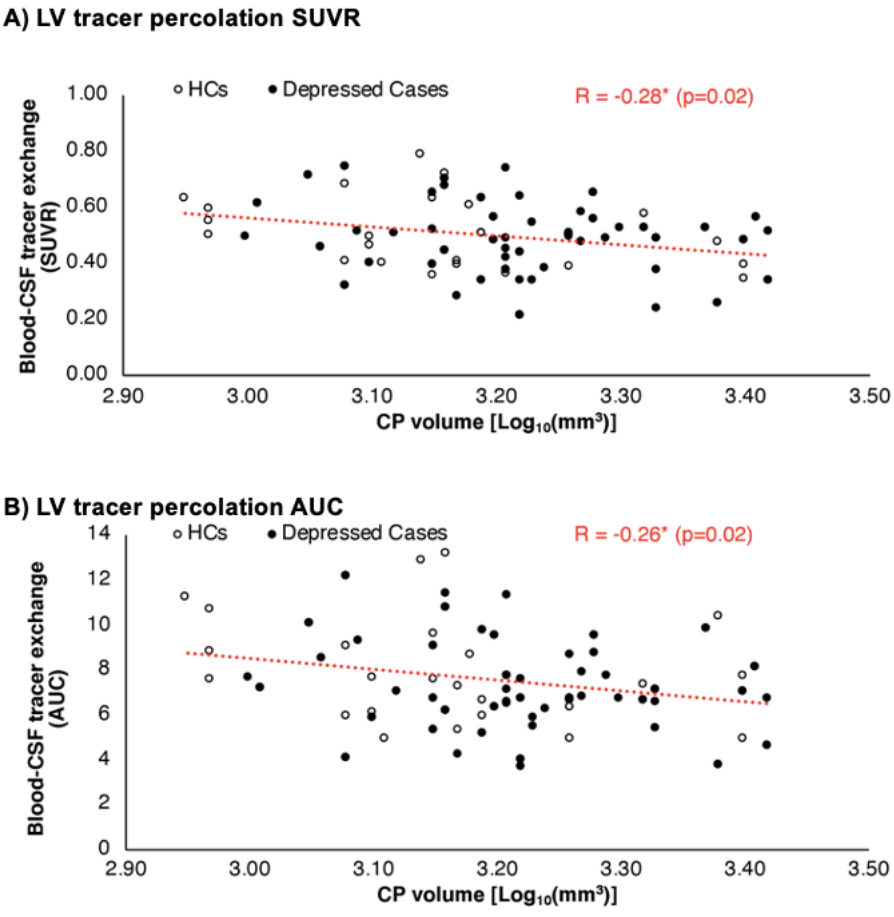

** indicates statistical significance (p-value<0.05).*

3.5.4 CP volume is not associated with brain volume

No association was detected between the CP volume and brain volume (r=0.16, p=0.17), nor with total grey matter volume (r=0.10, p=0.38) when depression and control groups were combined. Results were consistent with and without group and ICV as covariates.

3.5.5 Imaging transcriptomics

The first PLS component explained 26.01% of the spatial variability in the strength of the association between CP volume and TSPO and did so above chance (r=0.51, $p_{spatial}$ =0.006) (**Figure 3.6**). The list of genes ranked by the respective PLS1 weights can be found in "Supplementary data - [*PLS1_weights_CP_TSPO_Corr*]". We found significant enrichment for six gene ontology (i.e. biological pathways terms among the top positively weighted genes), including "protein localization to endoplasmatic reticulum", "leukocyte activation involved in inflammatory response", "serotonin receptor signalling pathway", "gamma-aminobutyric acid signalling pathway", "neuroinflammatory response", and "interleukin-1 response". In the brain cell type enrichment analysis, we found enrichment among the top positively weighted genes mostly for genes from excitatory and inhibitory neurons, where the strongest positive enrichment hit was the subclass of excitatory neurons "Ex3e" (**Figure 3.6**) (Full statistics can be found in "Supplementary data - [*GSEA_PLS1_CP_TSPO_Corr*]").

For the analyses on case-control differences in TSPO, PLS_1 explained 33.64% of the spatial variability in TSPO differences and did so above chance (r=0.58, p_{boot}=0.001) (Supplementary - Figure 3.1). In the gene set enrichment analysis, we did not find significant enrichment for any gene ontology. In the brain cell type enrichment analysis, we also did not find significant enrichment among positively weighted genes for genes from any of the cell types we tested (Full statistics can be found in Supplementary [*PLS1_weights_TSPO_Differences*] and [*GSEA_PLS1_TSPO_Differences*]).

Figure 3.5Imaging transcriptomics decoding of regional variation in the association between choroid plexus (CP) volume and TSPO.

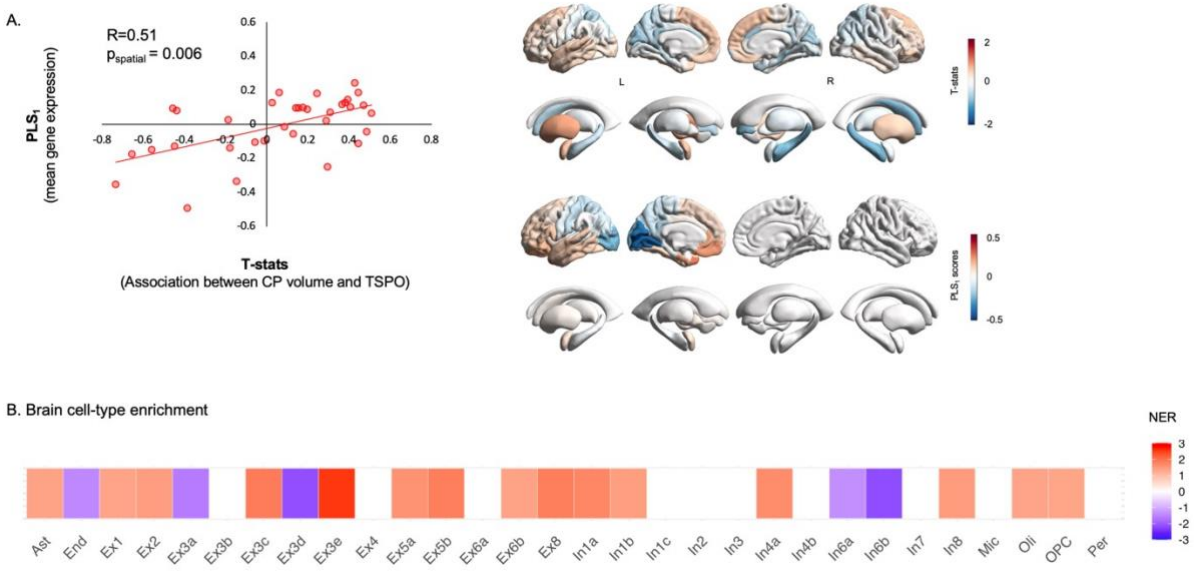

Panel A: Left - scatter plot depicting a significant positive correlation between PLS1 gene expression weights and the t-statistics quantification the association between CP volume and TSPO for each region of the left hemisphere. Right – the upper brain map depicts the cortical distribution of the t-statistics quantifying the association between CP volume and TSPO; the lower brain map depicts the cortical distribution of the weights of PLS_1. Panel B: Table showing the results of the brain cell-type gene enrichment analysis. The colours depict normalized enrichment ratios; positive ratios indicate enrichment for genes of a specific cell class among those genes with the highest positive PLS_1 weights; the reverse applies to negative enrichment ratios. White squares indicate cell classes where enrichment did not survive $p_{FDR}<0.05$. NER – Normalized enrichment ratio; CP – Choroid plexus.

Figure 3.6Supplementary Figure 3.1 - Imaging transcriptomics decoding of regional variation in the TSPO differences (Depressed cases (MDD) > control cases).

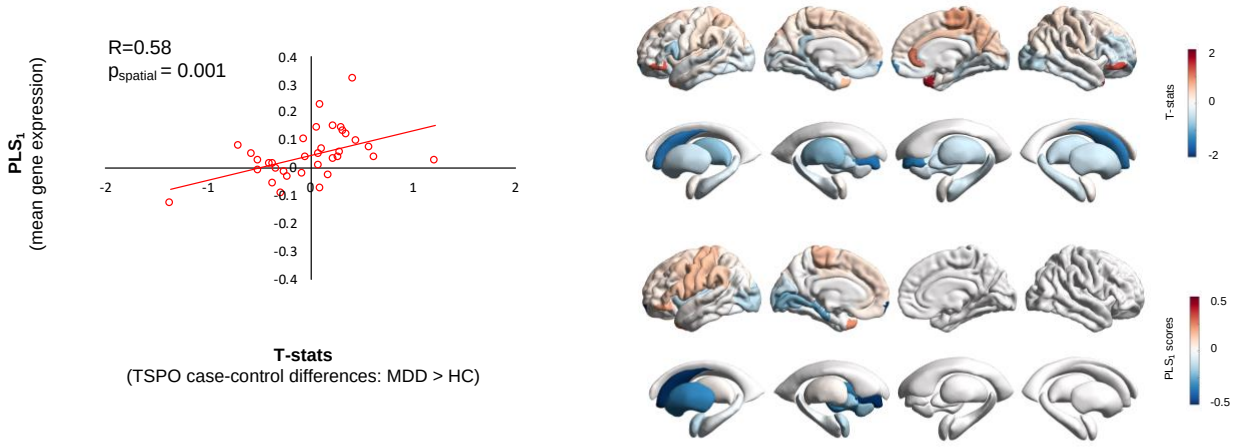

Left - scatter plot depicting a significant positive correlation between PLS_1 gene expression weights and the t-statistics quantification of TSPO regional differences. Right – the upper brain map depicts the cortical and subcortical distribution of the t-statistics quantifying TSPO differences (as measured by [11C]PK11195 PET distribution volume ratio); the lower brain map depicts the distribution of the weights of PLS_1.

3.6 Discussion

We demonstrated for the first time the association between CP enlargement in depression and a reduction of brain barrier permeability reflected by blood-to-CSF radiotracer exchange parameters (SUVR). Moreover, we have also demonstrated that in the same patients CP volume is positively associated with increases in brain inflammation as measured by TSPO PET in key regions (ACC, PFC and Insular Cortex). There was no association between CP volume and peripheral inflammatory markers (CRP, IL6, and TNF-α) nor depression clinical scores (HDRS, Childhood Trauma score), but there was an association with Perceived Stress score. However, as this result was from exploratory analysis and did not survive multiple comparison testing correction, it should be taken with caution. Our results support the hypothesis that CP enlargement occurs in depressed cohorts, and this enlargement is associated with central inflammation.

The finding that CP volume is correlated with inflammation of the CNS but not with peripheral inflammation fits into the proposed model of the relationship between peripheral and central inflammation. We can speculate that CP volume may increase with time, likely together with the BBB dysfunction (Kealy et al., 2020) as a reaction to a heightened concentration of peripheral immune mediators. The lack of correlation between CP volume and CRP (which trends towards a positive association but does not achieve significance) is probably due to the CRP concentrations being an instantaneous measurement (Felger et al., 2018), while CP volume increase is likely the result of the integrated series of peripheral immune events across time (Marques and Sousa, 2015, Turner et al., 2014). Interestingly, CP volume increases were associated with reductions in plasma albumin which is a well established marker of chronic inflammation (Don and Kaysen, 2004). The enlargement of the CP volume in our result is associated with the reduction of the BCSFB permeability, which was identified as a reaction to the chronic inflammatory events in depressed subjects (Turkheimer et al., 2020). Similarly, the correlation between CP volume and brain inflammation may indicate that microglial activation is also the result of disturbed homeostasis across time (Enache et al., 2019). In our study, we did not see any elevation of CP [^{11}C]PK11195 in depression, but we were able to replicate the association between CP volume and CP TSPO uptake as reported by in relapsing remitting multiple sclerosis patients (Ricigliano et al., 2021). The specificity to TSPO of tracer activity in CP was investigated in an independent [^{11}C]PBR28 PET blocking study with XBD173(Veronese et al., 2018). A significant reduction of tracer activity (-42%, $t(7) = 2.6$, $p = 0.04$) was found after XBD173 administration. Unfortunately, we cannot comment on the origin of tracer specific binding in CP, as it could be endothelial, vascular, or infiltration of immune cells (Veronese et al., 2018).

The spatial profile of the correlation pattern between CP volume and TSPO brain expression was positively associated with neuron distribution, twice stronger for excitatory

neurons than for inhibitory ones (supplementary data). In general, this result indicates that those brain areas metabolically more active are also those where inflammation is likely the result of reduced permeability of the barriers. These areas are known as "neotenic" as they contain a disproportionate density of synapses that have exceptionally high energy requirements and matching needs of efficient transport and clearance of metabolic substrates and products (Goyal et al., 2014, Vaishnavi et al., 2010). These results confirm an associative link between brain metabolism, brain barriers, permeability, and neuroinflammation. But further research is required to establish a causal link between these factors in MDD.

It is important to note that imaging data on the structure of CP do not explain the functional mechanism underlying such morphological modifications. Previous gene expression analysis from a cross-sectional post-mortem study has identified multiple differences in CP samples obtained from patients with depression, particularly in the downregulation of genes related to the "transforming growth factors- beta" (TGF-$\boldsymbol{\beta}$) pathway, which are known to interact with the production of the extracellular matrix, suggesting changes in the cytoskeleton of CP epithelial cells in patients with MDD (Turner et al., 2014). Reduction of VEGF, a neurotrophic factor which is produced by the CP epithelial cells and responsible for angiogenesis and vascular fenestration permeability, were found in serum of suicide victims with MDD (Isung et al., 2012) and in plasma of MDD patients (Dome et al., 2009). To date, however, CP alterations remain poorly understood and multiple mechanisms are put forward that include CP ependymal cell proliferation (Barkho and Monuki, 2015), infiltration of CP by peripheral immune cells or oedema (Johanson and Johanson, 2018).

Finally, it is important to note that the findings above do not seem to be specific to depression. Hence, this peripheral-to-central immunity mechanism seems to be generalizable

to all pathologies where peripheral inflammatory states are observed, in particularly those where the BBB is not disrupted such as in schizophrenic cohorts (Lizano et al., 2019, Zhou et al., 2020). Recently, strong evidences from multiple sclerosis patients, a cuprizone diet-related demyelination mouse model and the experimental autoimmune encephalomyelitis model demonstrated a cross-dependency between neuroinflammation and choroid plexus functional, cellular and morphological characteristics which included volume enlargement, glia hyperactivity and the upregulation of functional pathways primary related to neuroinflammation and cell-to-cell interactions (Fleischer et al., 2021). Taken together, these results further support the use of CP volume as a reliable, trans-diagnostic marker of neuroinflammation.

3.7 Limitations

Some limitations have to be considered regarding our results. Manual CP segmentation is operator dependent but reanalysis of the CP volume with a second operator (JS) lead to an intraclass correlation coefficient ICC = 82% indicating robustness in our estimation. Automatic methods to measures CP volume exists but do not match well with manual extraction (Lizano et al., 2019) especially when applied to structural T1-weighted MRI data. The sample size in this study was small compared to recent big-data structural MRI studies in depression (N>1,000) (Schmaal et al., 2020). However, this is one of the largest samples ever published in depression that combines MRI with TSPO PET imaging. Future studies should investigate the use of automatic methods for CP segmentation in order to scale up these analyses to a larger sample size. Moreover, the collection of TSPO PET data with arterial input function to quantify tracer kinetic exchange though BCSFB would be more accurate than static SUVR and AUC parameters (Schubert et al., 2019) for measuring CSF dynamics.

3.8 Conclusion

This study has identified for the first time in vivo a relationship between CP volumetric and brain inflammatory alterations in depression. The change on the CP morphology has been found in different neuroinflammation disorders, with no clear interpretation of CP enlargement. This study also provides further evidence to the model that reduced permeability of the BBB and BCSFB could alter brain homeostasis, becoming harmful if protracted by chronic inflammatory states. These findings do not seem to be specific to depression, but rather explain a more general mechanism of brain immune defence, in which CP plays a fundamental role.

3.9 Contributions to Study 2

The manual segmentation and the choroid plexus volume techniques were conducted by Noha Althubaity. All data collection was conducted for a previous study and the data were reanalysed for this work. All data analysis and the reporting of these results were conducted by Noha Althubaity.

4 Chapter 4

Study 3: An investigation of brain free-water MRI in depression: the relevance for neuroinflammation

This study is currently under review among co-authors.

4.1 Introduction

Depression is a common neuropsychiatric disorder and a leading cause of disability worldwide (Iancu et al., 2020). It is characterised by different psychophysiological features, including reduced appetite and slowness in speech, as well as mood swings, anhedonia, tearfulness, psychomotor problems, sleep issues and suicidal thoughts (Fried and Nesse, 2015).

Much of the evidence in the literature suggests that inflammation is an important process in the aetiology of depression (Green et al., 2021). Depressed patients show a consistent elevation in innate immune response cytokines, including interleukin 6 (IL-6), tumour necrosis factor-alpha (TNF-α) and acute phase C-reactive protein (CRP), a systemic inflammation marker produced by the liver in response to high levels of IL-6 (Strawbridge et al., 2015, Osimo et al., 2019, Osimo et al., 2020). Importantly, patients who show resistance to antidepressant treatments have high peripheral inflammatory markers such as cytokines, acute phase proteins, chemokines, adhesion molecules, and inflammatory mediators in the plasma and cerebrospinal fluid (CSF) (Miller et al., 2009, Dantzer et al., 2008, Enache et al., 2019). The observed increased levels of cytokines in the CSF are also suggestive of the activation of microglia, the immune cells of the central nervous system (CNS). In relation to depression, microglia activation has been investigated in several neuroimaging studies targeting the 18k Dalton translocator protein (TSPO) with Positron Emission Tomography (PET) (Richards et al., 2018, Enache et al., 2019). A consistent but modest increase in the TSPO radioligand PET signal has been detected in the anterior cingulate cortex (ACC) across a number of cohorts, including medicated and unmedicated major depressive disorder (MDD) patients (Schubert et al., 2021b).

Unmedicated depressed patients have also shown increases in TSPO in the prefrontal cortex (PFC) and the insular cortex (INS) when compared to healthy controls (Setiawan et al., 2015, Richards et al., 2018). Unfortunately, the cost and the methodological and logistical complexities of TSPO PET imaging (Turkheimer et al., 2015) have impeded the use of this biomarker beyond small-sized experimental medical studies, driving the need to discover alternative methods to quantify brain immune response.

Magnetic Resonance Imaging (MRI) is a non-invasive, less expensive technique comparing to the PET, and easily accessible procedure that has been proposed as an alternative to PET for characterising biophysical changes in the brain tissue which are related to neuroinflammation (Oestreich and O'Sullivan, 2022). Among the different MRI modalities, free water (FW) imaging taken from single shell diffusion MRI has been used to investigate microstructural changes in the presence of brain immune activation (Oestreich and O'Sullivan, 2022). Among the different MRI modalities, fraction anisotropy (FA) taken from a single shell diffusion MRI and corrected for the free water (FW) has been used to investigate microstructural changes in depression patients (Bergamino et al., 2017, Bergamino et al., 2016). So far, evidence relating to the alteration of FW in depression has been mixed. A study in unmedicated MDD patients revealed no difference in FW levels compared to healthy controls (Bergamino et al., 2016). In contrast, post-stroke depression patients have been identified as showing increases in the FW in the reward system, including the nucleus accumbens, the prefrontal cortex, the amygdala, and the hippocampus (Oestreich et al., 2020). Interestingly, these regions have also shown an association between a reduction in cortical volume and systemic inflammation in depressed patients (Zhang et al., 2018b, Green et al., 2021).

One significant limitation of the FW imaging process is its inability to distinguish between increased FW due to neuroinflammation and increased FW due to brain atrophy (Oestreich and O'Sullivan, 2022). As an alternative to FW imaging, there is a growing body of

literature investigating neuroinflammation using multi shell diffusion MRI by running Neurite Orientation Dispersion and Density Imaging (NODDI). NODDI is a two-shell high-angular resolution diffusion MRI process that can be applied to model diffusion signals in three tissue compartments (Zhang et al., 2012). The three compartmental model provides specific estimates for the extracellular space that corresponds to the FW signal, the orientation of axons and dendrites represented by the orientation dispersion index, and the densities of the cell bodies and glial cells represented by the neurite density index (Yi et al., 2019, Kraguljac et al., 2019).

There is little published information about FW levels in comorbid depression (Kallaur et al., 2016, Oestreich et al., 2020), and no previous study has investigated FW in depression using NODDI. This paper aims to explore the use of NODDI FW as an alternative neuroimaging biomarker to TSPO PET for detecting neuroinflammation. Specifically, we hypothesised that the FW signals measured in the ACC, PFC, and the INS, would be significantly increased in depressed patients because of the relationship of these regions with neuroinflammation (Schubert et al., 2021b). We also tested the link between FW-NODDI with biomarkers of peripheral inflammation and CSF-mediated brain clearance measurements which have been demonstrated as being impaired in patients with clinical depression. We further examined the association of FW-NODDI with structural choroid plexus volume alterations, which have been demonstrated in depressed patients as well as in relation to clinical measures of depression.

4.2 Methods and Materials

4.2.1 Participants

Data from 79 depressed patients (27 men and 52 women; mean age: 37 ± 7.2 years) and 45 age-matched healthy controls (HCs) (19 men and 26 women; mean age: 35 ± 7.7 years) from the BIODEP (Biomarkers in Depression) study (NIMA Consortium; https://www.neuroimmunology.org.uk/biodep/) were analysed for this study. All the subjects were recruited from a network of clinical research sites in the UK as part of the NIMA consortium, and were tested for symptoms of depression using the Structured Clinical Interview for DSM-5 (SCID) screening questionnaire (Shankman et al., 2018). The full details of the subjects' recruitment were reported by Kitzbichler et al (Kitzbichler et al., 2021). Each depressed patient had a total Hamilton Depression Rating Scale (HDRS) score of greater than 13 (Hamilton, 1960). Participants were categorised into high and low CRP groups based on the CRP concentrations in the blood using 3mg/L as a threshold. This threshold was defined prior to the study recruitment, and has been shown to identify differential inflammatory loads and treatment responses in depression (Nettis et al., 2020). The depression cohort was divided into two groups, 47 low-CRP and 32 high-CRP subjects. Depressed patients were tested using the Beck Depression Inventory, the State-Trait Anxiety Inventory questionnaires, the Chalder Fatigue Scale, the Snaith-Hamilton Pleasure Scale, the Perceived Stress Scale (PSS), and the Childhood Trauma Questionnaire (CTQ).

All HCs and depressed patients who were recruited to the study conformed to the following inclusion criteria: no history of depression for the HCs, no history of other neurological disorders, no history of drug or alcohol abuse, no previous participation in any clinical drug trials, no previous or ongoing medication history or medical conditions that could affect the interpretation of the study results, and no current pregnancy or breastfeeding regime.

The ethical approval for the BIODEP study was confirmed by the Cambridge Central NRES Committee for the East of England (REC reference: 15/EE/0092) and the UK Administration of Radioactive Substances Advisory Committee. All participants gave their written and informed consent before participation in the study.

4.2.2 Neuroimaging and blood data acquisition

4.2.2.1 MRI data acquisition

As part of the study imaging protocol, each subject had a 90-minute MRI scan comprised of both structural and functional imaging (Kitzbichler et al., 2021).The data was obtained from 3T MRI scanners (SEIMENS Prisma and GE MEDICAL SYSTEMS DISCOVERY MR750) at three different MRI imaging centres (University of Cambridge Central; King's College Hospital Clinical Research Facility, London; the John Radcliffe, Oxford). Individual neuroimaging data included a multi-parameter structural MRI using a 3D T1-weighted sequence (parameters: repetition time (TR) = 1900ms, echo time (TE) = 4ms, field of view (FOV) 174x192mm^2, and voxel size 1x1x1mm^3), and a multi-shell diffusion weighted imaging sequence, in which diffusion-weighted images were acquired using an echoplanar sequence (parameters: repetition time, 8200ms; echo time, 95ms; flip angle, 90°; bvalues, 0, 800, and 2000 s/mm^2; 30 and 60 non-colinear diffusion-weighted directions; field of view, 768 × 768 mm; resolution 2.5 × 2.5 × 2.5 mm^3). The latter method was used to create single subject FW maps (Bouyagoub et al., 2021).

4.2.2.2 Image analysis

All multiband diffusion images were corrected for susceptibility and eddy currents using the FMRIB software library (FSL, version 5.0.7, Oxford, UK). The FSL top-up corrected the susceptibility, while the eddy current distortion was corrected by the FSL Eddy command (Andersson et al., 2003). The corrected images were fitted into the NODDI model using the toolbox (http://www.nitrc.org/projects/noddi_toolbox) run in MATLAB 2012b (MathWorks,

Inc., Natick, MA). The NODDI parameters used to obtain the free-water (FW) fraction were generated as voxel-wise whole brain maps for free-water isotropic volume fractions (ISOVF) (Kamagata et al., 2017). The ISOVF maps were normalised to the Montreal Neurological Institute (MNI152) space and mean FW values and in regions of interest (ROI) analyses were then extracted for further analysis (Kamagata et al., 2017). The ROIs were ACC, PFC, and the INS, and these were chosen based on their role in modes and emotional demands, as well as their previously demonstrated changes in depression (Stuhrmann et al., 2011, Goldin et al., 2008) as well as links to neuroinflammation (Holmes et al., 2018, Harrison et al., 2009). ROI masks were created using the Harvard-Oxford Cortical Structural Atlas in the MNI space, and the mean values for each of the ROI volumes were extracted for all subjects (Pantangco et al., 2016).

As well as free water analysis, the lateral ventricle choroid plexus (CP) was automatically segmented from T1 weighted images using Free Surfer software (v.6.0, http://surfer.nmr.mgh.harvard.edu/). CP segmentation was improved further using the Gaussian Mixture Model (GMM) (Tadayon et al., 2020) to evaluate the CP volume. For validation purposes, a subset of 70 individual automated CP volume estimates was compared with those obtained by manual segmentation (Althubaity et al., 2022). Meanwhile, the Free Surfer analysis was used to estimate total intracranial volumes (TIV), which were then included as a covariate of interest in the statistical analysis.

4.2.2.3 PET data acquisition and image analysis

A subset of 70 subjects (22 HC and 48 MDD) also received 60 minutes of dynamic PET imaging using [^{11}C]PK11195, a TSPO radioligand that was used as a putative marker of glia activation. All the data was collected from the simultaneous PET/MR scanner (GE Healthcare, Waukesha, WI) using the same experimental protocol, and processed using a common analytical function (Schubert et al., 2021b). More details of the PET acquisition can be found in the original reports on this data (Schubert et al., 2021b, Turkheimer et al., 2020).

The quantification of the TSPO distribution in the brain parenchyma was used as a proxy for neuroinflammation, using a supervised clustering approach for the extraction of a pseudo-reference region (Turkheimer et al., 2006). The distribution of the TSPO in the brain was assessed using the simplified reference tissue model, and the distribution volume ratio (DVR) was used as the primary parameter of interest. The [^{11}C]PK11195 radioactive uptake in the lateral ventricles was calculated and used as an indirect CSF-blood exchange marker (De Leon et al., 2017, Schubert et al., 2019). The lateral ventricles were manually segmented using a T1-weighted structural MRI and ITK-SNAP software (Schubert et al., 2019, Turkheimer et al., 2020, Acabchuk et al., 2015). To reduce the partial volume effect, the lateral ventricles were eroded by 2mm (corresponding to two voxels) in the native space, and the [^{11}C]PK11195 PET activity was extracted from the eroded ventricles. The tracer uptake in the eroded lateral ventricles was then normalised to the same reference region used for the quantification of the brain PET TSPO, and the standardised uptake value ratio (SUVR) at 60 minutes and the area-under-curve (AUC) at between 30 to 60 minutes were computed from the PET images using the eroded lateral ventricle activity (Schubert et al., 2019) which were used as the main parameter of interest to express the CSF-brain tracer exchange (Turkheimer et al., 2020).

4.2.2.4 Peripheral inflammatory markers

A venous blood sample was collected from all participants at the time of the MRI scan to calculate the concentration of the peripheral inflammation markers, including interleukin-6 (IL-6), interleukin-10 (IL-10), tumour necrosis factor-alpha (TNF-α), interferon-gamma (IFN-γ), interferon gamma-induced protein 10 (IP-10), lymphocytes, monocytes, total and absolute neutrophil, albumin, cholesterol, vascular endothelial growth factor (VEGF), and C-reactive protein (CRP) (Schubert et al., 2021b). The CRP was considered to be the primary peripheral inflammation marker in this study (Chamberlain et al., 2019) .

4.3 Statistical Analysis

The statistical analysis was performed using SPSS (Version 27, IBM). To answer the primary research question, a comparison between the ISOVF and TSPO PET was undertaken using the mean values extracted from the ACC, PFC, and INS ROIs. The Shapiro-Wilk W test was used to examine the normality of the data. The differences between the HC and MDD in these dependent variables were tested using an analysis of the variance by running a general linear model analysis to explore case-control differences, while covarying for subjects' ages, total intracranial volume (TIV), and scan sites. Exploratory secondary analysis investigating possible links between FW measures with clinical scores, peripheral inflammatory markers, and CSF-blood exchange parameters was carried out using Pearson's and partial correlation tests.

4.4 Results

4.4.1 Demographic and clinical characteristics

The demographic and clinical details of the depressive patients and HCs are shown in Table 1.4. The groups were matched in terms of age ($p = 0.1$), sex ($p = 0.7$), and TIV ($p = 0.1$). Significant differences were detected in terms of the BMI ($p< 0.001$), IL-6 ($p< 0.001$) and CRP levels ($p< 0.001$) between depressive subjects and HCs. All clinical scales were significantly higher for the group with depression ($p< 0.001$). When comparing high CRP patients to low CRP patients, the groups were matched for age ($p = 0.5$), TIV ($p = 0.1$), HDRS ($p = 0.3$) and PSS ($p = 0.9$), but differentiated by BMI ($p = 0.02$), sex ($p = 0.003$), CRP ($p< 0.001$), and CTQ ($p = 0.03$).

Table 4.1 The Demographic and Clinical Characteristics of the Depressed and Healthy Control Subjects

Variable	**Healthy Control Subjects (n = 45)**	**Depressed Subjects (n=79)**	**P value HC vs. MDD**	**Depressed Subjects, Low CRP (n = 47)**	**Depressed Subjects, High CRP (n = 32)**	**P Value Low CRP vs. High CRP**
Age, Year, Mean (SD)	35 (7.5)	37 (7.2)	0.11	36 (6.9)	37 (7.7)	0.54
Sex (Male/Female)	19/26	28/52	0.79	23/25	5/27	0.003
BMI, Kg/m2, Mean (SD)	24 (4.8)	27 (3.9)	<0.001	25.9 (3.3)	28.7 (4.1)	0.001
CRP, mg/L, Mean (SD)	0.9 (0.7)	3 (2.9)	<0.001	1.0 (0.7)	5.9 (2.6)	< 0.001
IL-6, n, Mean (SD)	41, 0.57 (0.29)	76, 0.78 (0.50)	0.01	45, 0.61 (0.38)	31, 1.02 (0.50)	< 0.001
VEGF, n, Mean (SD)	42, 103,3 (61.9)	77, 95 (61.1)	0.5	45, 94.3 (64.1)	32, 95.1 (57.6)	0.9
TIV, cm3, Mean (SD)	1400 (200)	1438.7 (183)	0.14	1,464 (180)	1,401(185)	0.14
HDRS, Mean (SD)	0.49 (0.87)	19 (4.5)	<0.001	18.6 (4.6)	19.7 (4.5)	0.33
CTQ, Mean (SD)	38.3 (5.2)	53.5 (16)	<0.001	56.7 (17.5)	48.7 (12.3)	0.03
PSS, Mean, (SD)	11.87 (5.4)	26.2 (6)	<0.001	26.1 (6.7)	26.3 (5.2)	0.89

Abbreviations: BMI = body mass index; CRP = C-reactive protein; TIV = total intracranial volume; HDRS = Hamilton Depression Rating Scale; CTQ = childhood trauma questionnaire; PSS = perceived stress score; ns = not significant.

4.4.1 NODDI FW in depression

No difference was found in the FW fractions between HCs and depressed patients in any of the primary ROIs: ACC ($F = 2.69$, $p = 0.09$), PFC ($F = 0.67$, $p = 0.8$), and INS ($F = 0.25$, $p = 0.6$). Age and TIV were significant covariates ($p< 0.001$ and $p< 0.05$, respectively), while sex and scan sites were not significantly associated with FW in any ROIs.

When the depressed patients were split into high and low CRP subgroups, statistical differences in the FW were found in the ACC ($F = 3.36$, $p = 0.04$) between the three groups (HC, low, and high CRP). In contrast, no differences were found in the PFC ($F = 1.91$, $p = 0.15$) and INS ($F = 1.10$, $p = 0.33$) (Figure 4.1). In the post hoc analysis, depressed patients with low CRP showed a significant reduction in the FW of the ACC ($F= 5.88$, $p=0.02$), but not in the PFC ($F= 1,12$, $p=0.3$), or INS ($F= 1.3$, $p=0.3$), compared to the HC after controlling for covariates. This result may be affected by the collinearity or controlled variables that correlated with the FW. However, no significant difference was found in the FW of the ACC between HC and depressive patients with high CRP ($F = 0.08$, $p = 0.8$).

When considering only the depressed cohort (high CRP vs. low CRP), a significant difference in the FW was found in the ACC ($F = 4.46$, $p = 0.04$), but not in the PFC ($F = 0.06$, $p = 0.08$) or INS ($F = 0.50$, $p = 0.48$). These results were obtained after controlling for age, TIV, sex, and scan site.

In terms of the correlation with depression clinical scores, FW was not associated with any of the clinical scales, including HRDS, childhood trauma scores (CTQ), and preserved stress score (PSS), in any of the ROIs.

Figure 4.1The estimated mean of the free-water fraction in the anterior cingulate cortex (ACC), prefrontal cortex (PFC), and insula (INS) regions

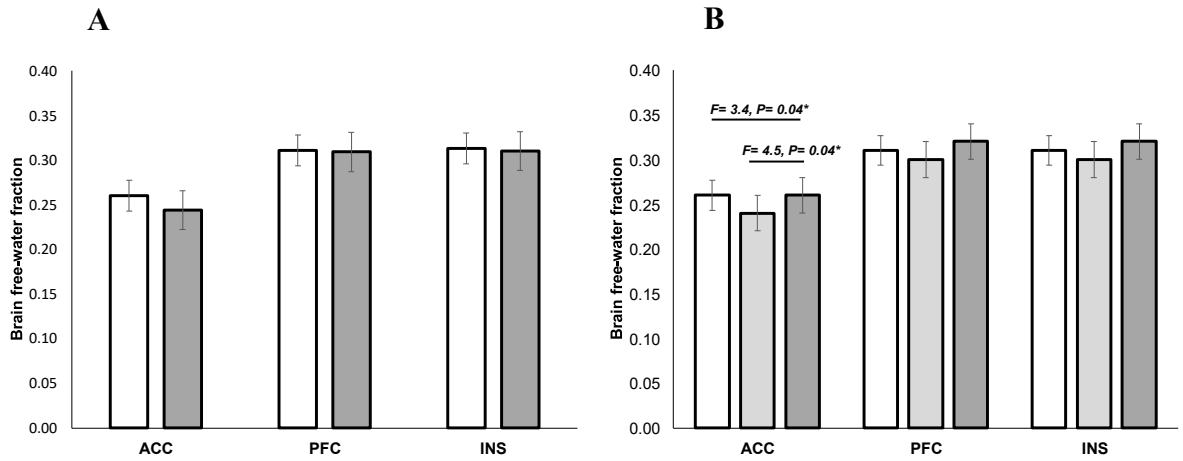

(A) Comparison between the healthy control (white bars) and the depression groups (grey bars). (B) Comparison between the healthy controls (white bars) and depressed patients with low CRP (< 3 mg/L, light grey bar) and high CRP (> 3 mg/L, dark grey). Error bars represent SE, and analyses have been corrected for age, TIV, and different scan sites. Asterisks indicate significant differences (p< 0.05).

4.4.2 Links between NODDI FW and inflammation measures

When considering peripheral inflammation, no significant correlations between FW fraction, CRP, and blood inflammatory markers (IL6, or TNF-α) were found in any of the main ROIs.

The subset of participants with both TSPO PET and FW MRI data consisted of 22 healthy controls and 48 depressed patients (28 low CRP, 20 high CRP). No significant links were observed between the FW estimates and the TSPO PET DVR estimates in any of the main ROIs: the ACC (r = -0.14, p = 0.3), the PFC (r = -0.19, p = 0.1), and the INS (r = 0.16, p= 0.2). The results remained unaltered after controlling for covariates.

4.4.3 Relationships between NODDI FW and CSF-blood exchange parameters

At the regional level, no significant associations were found between the CP volume and FW in the ACC (r = 0.14, p = 0.1), the PFC (r = 0.18, p = 0.05), or the INS (r = 0.13, p = 0.2). The results remained the same after controlling for age, TIV, and scan sites.

In terms of the CSF-mediated clearance markers, a significant inverse association was observed between the lateral ventricular SUVR and FW fraction in the INS (r = -0.31, p = 0.01, Figure 2). However, no associations were found between the lateral ventricular SUVR and the FW fraction in the ACC (r = -0.12, p = 0.3) or the PFC (r = -0.18, p = 0.1). After controlling for age, TIV, and scan site, no associations were detected between the lateral ventricular SUVR and the FW fraction in any of the ROIs. No significant association was found between the CSF dynamic measured by the AUC (30-60) in the lateral ventricles and the FW in any ROIs.

Figure 4.2Association between the free water fraction in insula and lateral ventricles SUVR

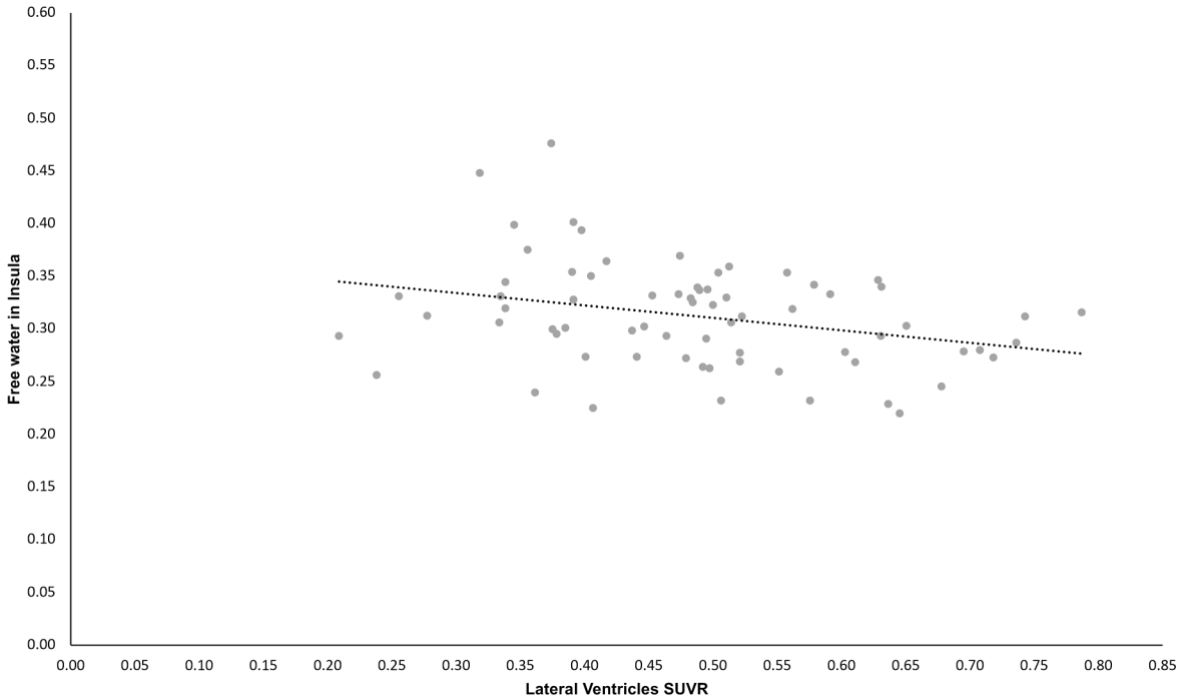

Scatterplot of the free-water fraction (y-axis) for the insula (INS) regions vs. 11C-PK11195 lateral ventricles SUVR for 60 minutes in depression patients and healthy controls with no covariates (r = -0.31, p = 0.01).

4.5 Supplementary Results

4.5.1 S1: The results of the free water differences between the healthy control and depression groups in grey matter and white matter

There was a significant reduction in the FW levels in the GM of the depression patients compared to the healthy control subjects after controlling for covariates (F = 4.05, p = 0.046). When the depression sufferers were divided into high and low CRP categories, the trend's difference was significant (F = 3.08, p = 0.05). See Supplementary Figure 4.3.

There was also no significant difference in the FW in the GM in the depression patients only (F = 1.92, p = 0.2). No significant difference was observed between the groups in terms of the FW in the WM.

Supplementary Figure 4.3 The estimated mean of the free-water fraction in the total grey matter

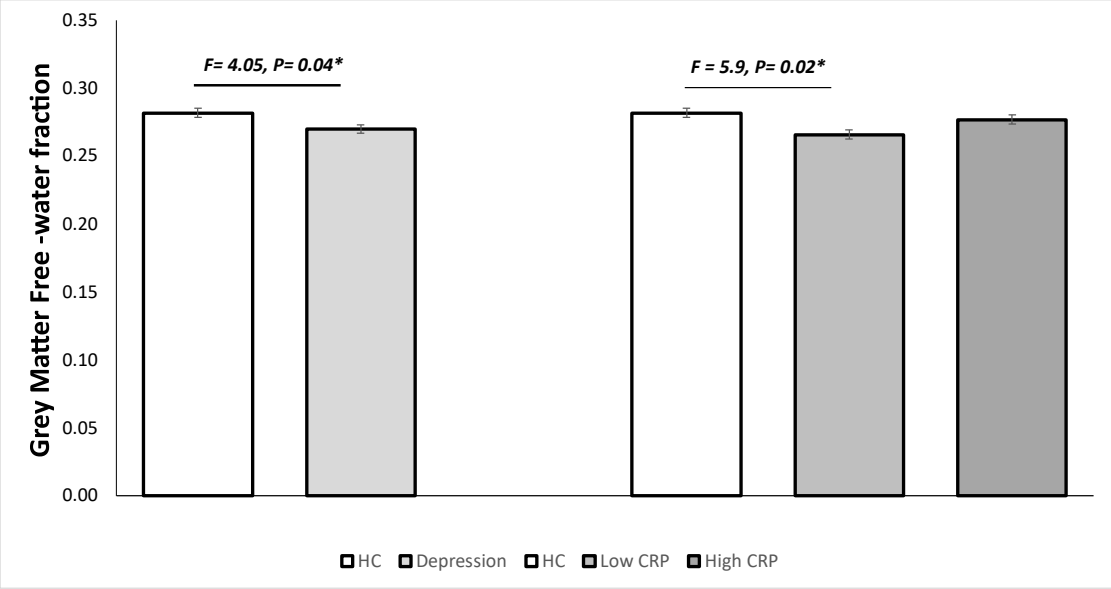

The first comparison is between healthy control (white bars) and the depression groups (grey bars). The second comparison is between the healthy controls (white bars) and the depressed patients with low CRP (< 3 mg/L, light grey bar) and high CRP (> 3 mg/L, dark grey). Error bars represent SE, and analyses have been corrected for age, TIV, and different scan sites. Asterisks indicate significant differences (p< 0.05).

4.5.2 *S2: The whole brain voxel-wise analysis for differences in the free water map between the healthy control and depression groups*

The whole brain analysis of FW maps and the differences between depressed patients and healthy controls showed no significant clusters. When the ANOVA analysis was repeated after the patients were divided into low and high CRP categories and the healthy control group, significant differences in the FW estimate clusters were found in multiple areas, including the right viso-motor coordination, the right primary motor, and the right dorsal posterior cingulate cortex. More differences between the clusters were found when a grey matter mask was applied to the free-water map, including the right frontal field and the right primary sensor association. When the analysis was restricted to the depression groups, the high CRP group showed significant increases in FW compared to the low CRP group in two brain regions, including the right frontal field (32, 27, 48, number of voxels = 26, T = 5.29, $p_{FWE\ corrected} = 0.02$) and in the right dorsal posterior cingulate cortex (12, -30, 40, number of voxels = 26, T= 4.5, $p_{FWE\ corrected} <0.03$). See Supplementary Figure 4.4, Table 4.2.

Supplementary Figure 4.4

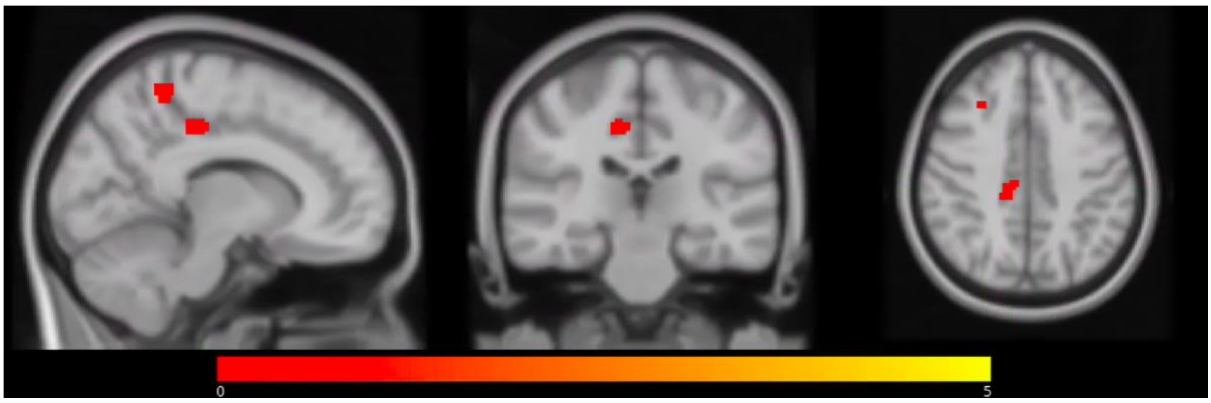

The voxel-wise difference analysis of the brain free-water MRI. The colour map represents significantly different clusters in the free water in depressed patients with high and low CRP in sagittal, coronal, and axial planes. The tow clusters show a significant increase in the free

water in the right frontal field and the right dorsal posterior cingulate cortex. The colour bar indicates the T value, and the corrected threshold is p<0.05.

Supplementary Table 4.2 voxel-wise analysis of a brain free-water MRI in depression: different significant clusters in the depression group compared to the healthy control group.

Region	**MNI coordinate**	**Number of voxels**	**F values**	**$P_{FWE\ (corrected)}$ values**
Right vis motor	14, -46, 56	191	18.7	p< 0.00
Right dorsal posterior cingulate cortex	12, -38, 48	53	12.8	p< 0.00
Right sensor association	12, -38, 66	51	12.6	p< 0.00
Right primary motor	24, -30, 64	30	11.6	p= 0.02
Right frontal field	32, 26, 48	19	14,1	p= 0.03

4.5.3 S3: Voxel Based Morphometry (VBM) analysis for different free water cluster

To control for the possible confounding of tissue loss, the brain tissue volume of the significantly different clusters was calculated using the VBM and tested using the General Linear Model. After controlling for age, TIV, and scan site, no significant difference in the cluster volume was detected between the HC and the high or low CRP groups (F = 2.37, p = 0.10). When restricted to the subjects with depression, no significant difference was detected in the cluster volume (F = 0.55, p = 0.5) after correction for age, TIV, sex, and scan site.

4.5.4 *S4: Association of free water in white matter and lateral ventricles SUVR, AUC 30-60*

In terms of the CSF-mediated clearance markers, significant inverse associations were observed between the lateral ventricular SUVR and the FW fraction in the WM ($r = -0.34$, $p = 0.004$) and the FW in the WM and the AUC (30-60) ($r = -0.29$, $p = 0.02$). See Supplementary Figure 4.5. After controlling for age, TIV, and scan site, no associations were detected between the lateral ventricular SUVR and the FW fraction in the WM or with the AUC (30-60).

Supplementary Figure 4.5

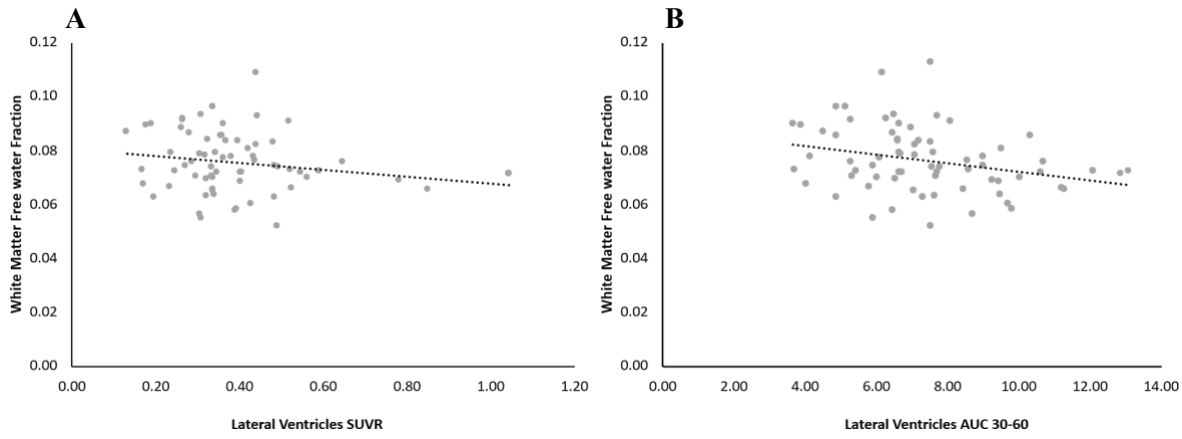

Scatterplot of the free-water fraction (y-axis) of the white matter vs the 11C-PK11195 lateral ventricles: (A) the free water in the white matter vs the lateral ventricles SUVR for 60 minutes in depression patients and the healthy controls; (B) the free water in the white matter vs. the lateral ventricles Area Under Curve (AUC) at 30 to 60 minutes in depression patients and the healthy controls.

4.5.5 *S5: A whole brain voxel-wise analysis of the association between the free water map and the choroid plexus volume*

A voxel-wise regression analysis was used to examine the association between the choroid plexus (CP) volume and free water (FW) maps in the whole brain. No significant

clusters were associated with the CP volume in the free water map after controlling for covariates. However, when the expletory analysis was performed without controlling for covariates, only the right primary motor was significantly associated with the CP volume (26, -24, 58, number of voxels = 31, T = 4.5, $p_{FWE\ corrected} = 0.001$). Several clusters were significantly correlated when the expletory analysis was expanded to apply the GM mask. (Supplementary Figure 4.6, Table 4.3). No significant clusters were correlated with the CP volume in the free water maps when applied to the GM mask and controlled for covariates.

Supplementary Figure 4.6

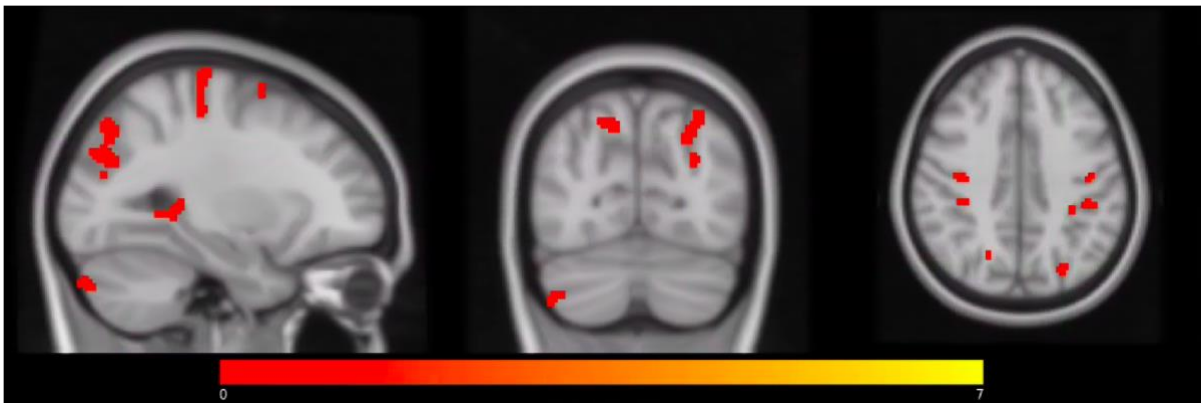

The voxel-wise correlation of the brain free water map and the CP volume in the depressive and healthy control groups. The colour map represents the significant association clusters in the free water map and the CP volume of the sagittal, coronal, and axial MRI planes. The colour bar indicates the T values, and the corrected threshold is p<0.05.

Supplementary Table 4.3 Voxel-wise correlation of the brain free water map and the CP volume in depressive patients: significant clusters.

Region	**MNI coordinate**	**Number of voxels**	**T values**	**$P_{FWE\ (corrected)}$ values**
Left visual association	-12, -62, 8	28	5.4	p= 0.002
Right supramarginal gyrus	38, -38, 52	85	4.8	p< 0.00
Right primary motor	42, -14, 54	66	4.6	p< 0.00
Cerebellum	6, -80, -28 36, -82, -40 -26, -88, -36	41 87 32	4.6	p< 0.01
Right vis motor (Brodmann area 7)	24, -68, 50	54	5.1	p< 0.00
Left primary sensory	-48, -34, 48	48	4.5	p= 0.01

4.6 Discussion

The primary aim of this study was to investigate whether NODDI FW measurements could be used as a marker of neuroinflammation in depression. Based on the free water studies in the literature and the association of FW with neuroinflammation, we hypothesised that we would see an increased FW signal in depressed patients in comparison to the healthy control group. However, we found an unexpected reduction in the FW in the anterior cingulate cortex in depressed patients with low peripheral inflammation, compared to both the healthy control group and compared to patients with high peripheral inflammation, while no differences were found in the prefrontal regions nor in the insular cortex. After extending the analysis to the whole brain, the level of FW was also found to be generally reduced in the grey matter ($F = 4.05$, $p = 0.046$) of the depression group compared to the healthy control (Supplementary 1). Meanwhile, a voxel-wise analysis in our study showed differences in the free water map in some clusters involving the motor cortex of depressed patients compared to healthy controls (Supplementary 2). We tested whether this could be a result of brain atrophy, but structural brain analysis did not confirm this, as no volumetric differences were detected in these regions (Supplementary 3). Moreover, our results did not identify a significant difference in the FW in the white matter of depressed patients compared to the healthy control group.

4.6.1 Relevance of FW for depression

Although most of the studies in the literature did not attempt to measure FW directly, the integrity of microstructures in the white matter computed by the FA as a DTI index was used to measure the isotropic axis of the degree of diffusion for the white matter in the brain (Bergamino et al., 2017). The reduction shown in the FA was reported to reflect changes in the integrity of myelination (Lyall et al., 2018), and the FA has been found to be sensitive to various biological conditions including axonal degeneration, demyelination, and increases in extracellular water volume (Assaf and Pasternak, 2008). Some researchers have also discovered

reductions in the FA of MDD patients compared to healthy control groups, which reflect abnormalities in the white matter (Guo et al., 2012a, Guo et al., 2012b, Kieseppä et al., 2010, Korgaonkar et al., 2011, Han et al., 2014, Li et al., 2007, Zhu et al., 2011, Bergamino et al., 2016). Moreover, other studies have shown an increase in the microstructural abnormalities of the white matter in MDD patients when applying a FW correction, but not in the FW itself (Bergamino et al., 2016, Bergamino et al., 2017). We can conclude from these studies that the FA was influenced by tissue compartments, including the CSF and extracellular water (Bergamino et al., 2016, Bergamino et al., 2017). In contrast, no significant difference was detected between MDD patients and the healthy control group in terms of the FA in other studies (Olvet et al., 2016, Choi et al., 2014). As far as the microstructural studies of the ROIs is concerned, a reduction of the FA in the prefrontal white matter was found in young MDD patients compared to healthy controls (Li et al., 2007). However, a study by Olvet et al. (2016) showed no differences in the FA of depressed patients and the healthy control group in the white matter associated with the orbitofrontal and the ACC cortices in grey matter. The FA values were associated with the severity of depression and the age of depression onset, respectively (Olvet et al., 2016). Extending this analysis to other mental health conditions, there is strong evidence that an increase in the FW is possible with no attendant microstructural alterations in first-episode schizophrenia (Pasternak et al., 2012, Lyall et al., 2018), although other studies have shown high FW in the presence of microstructural alterations in chronic schizophrenia patients (Pasternak et al., 2015, Oestreich et al., 2017, Kraguljac et al., 2019). More importantly, the findings of the FA studies of white matter and its link to depression are inconsistent (Olvet et al., 2016), and the absence of any specific links necessitates the investigation of the FW in grey matter for depression patients.

In terms of the FW in grey matter, a previous analysis of the same sample used in the current study quantified the tissue-free water content of the grey matter using proton density, and no

significant difference was found between the MDD group and the healthy control group (Kitzbichler et al., 2021). However, clinical studies of neuroinflammation in multiple sclerosis, strokes, glioma, and hepatic encephalopathy have reported increases in proton density (PD), which is considered a proxy for extracellular fluid volume in the lesion area (Kikinis et al., 1999, Warach et al., 1995, Raschke et al., 2019, Shah et al., 2008). The PD method has shown that the signal elevation in the inflamed regions of the brain has no clear link with peripheral inflammation (Nettis et al., 2021a). More recent studies of the FW in a preclinical model of neuroinflammation (Di Biase et al., 2020) and in schizophrenia patients (Di Biase et al., 2021), validated the idea that the elevation of FW levels can be used as an imaging proxy for neuroinflammation. So far, FW measurements through FA and microstructures have been inconsistent, as was the inability to differentiate between increases in the FW in the brain due to inflammation, brain atrophy, and lesions. This implies that another method needs to be developed with better specificity and sensitivity to FW (Oestreich and O'Sullivan, 2022). This would involve using the NODDI method to investigate cellular architectures, including the densities and orientations of axons, dendritic and nutrients, as well as the random movement of free water molecules in extracellular space (Kraguljac et al., 2022). The NODDI method will help researchers to address the limitations of FW studies in distinguishing between the alteration of microstructures in the grey and white matter and the development of free water (Yi et al., 2019), which may provide a better understanding of FW formation and its link with neuroinflammation (Dowell et al., 2019, Kraguljac et al., 2022).

In the literature, no study has so far investigated the link between the free water fraction and depression using the NODDI metrics or tested its relationship with neuroinflammation. We found a reduction of the FW in the ACC of the low inflammation depression group compared to the high inflammation depression group and the healthy control group. Our findings are consistent with a study of patients with repeated traumatic brain injury (TBI), which showed a reduction in the FW in TBI subjects compared to the healthy control group (Reid et al., 2019).

However, another study of concussed athletes did not find any significant differences in the extracellular free water shown in the NODDI metrics, although it did show increases in the extra-neurite water volume with no corresponding alterations in the microstructures (Churchill et al., 2019). Depression has been the most prevalent prolonged response to TBI (Singh et al., 2018). TBI subjects, from months to years after the brain injury, have demonstrated microglial activation in addition to cognitive and behavioural impairments (Ramlackhansingh et al., 2011, Witcher et al., 2021, Coughlin et al., 2017). The activated microglia seem to be persistent for a period of time after TBI and have mediated the cognitive impairment (Muccigrosso et al., 2016). The chronic inflammation during TBI remission seems to be prompted by single or repeated severe to moderate brain injuries (Ramlackhansingh et al., 2011). Another study by Dowell et al. did not investigate changes in the FW NODDI metrics following an IFN-α injection for patients with hepatitis-C, but did find increases in the level of intracellular water, measured by NODDI matrices, which may indicate glial swelling (Dowell et al., 2019). Neuroinflammation appears to increase microglial and astrocyte volumes (Streit et al., 2004) in response to chronic inflammation linked to the pathophysiology of depression (Leonard, 2007), which may reduce the extracellular space.

A voxel wise analysis was also run on the free water maps in our study, and showed differences in the free water clusters in the motor cortices of depressed patients compared to the healthy controls. These clusters were no different in terms of voxel volume, in contrast to the results found in the literature, which showed links between the loss of brain tissue and increasing free water levels (Guo et al., 2012a, Guo et al., 2012b, Kieseppä et al., 2010, Korgaonkar et al., 2011, Han et al., 2014, Li et al., 2007, Zhu et al., 2011, Bergamino et al., 2016). Interestingly, newly medicated schizophrenia patients showed higher FW levels in the whole brain analysis as well as alterations to the white matter microstructures compared to the healthy controls, but no significant differences in the FW NODDI measurement were detected (Kraguljac et al., 2019). Systemic inflammation may

affect the water composition of the brain tissue (Kitzbichler et al., 2021, Dieleman et al., 2017). Finally, the sensitivity of NODDI in terms of detecting freely diffused water molecules in the extracellular space may explain the low free water levels in our sample, which was not seen in previous work on the same sample which investigated the tissue-free water component using MRI proton density (Kitzbichler et al., 2021).

4.6.2 FW and inflammation (central and peripheral)

Increases in the free water measured through NODDI were found to be attributed to neuroinflammation markers, including high tau and amyloid plaques (Fick et al., 2016). A preclinical study on transgenic rats with Alzheimer's disease (AD) showed increases in the FW in the hippocampus and the cingulate cortex (Fick et al., 2016). This increase in the FW was shown in brain tissue with high amyloid accumulation and strong neuroinflammation, although the FW decreased when the neuroinflammation was reduced in response to the remotion of the amyloid plaque (Fick et al., 2016). However, our results showed no association between FW, the neuroinflammation markers, and the TSPO PET signal. The lack of specificity of the TSPO in the microglia may contribute to the absence of any correlation with the FW (Betlazar et al., 2020, Vicente-Rodríguez et al., 2021).

The lack of correlation between the FW and peripheral inflammatory markers is consistent with previous results when measuring the TSPO signal, which showed no association either with the CRP or with other peripheral cytokines (Schubert et al., 2021b). This result is also consistent with Metzler-Baddeley et al.'s study of AD patients, which did not identify any association between the FW NODDI and the CRP or any other peripheral inflammatory markers (Metzler-Baddeley et al., 2019).

4.6.3 FW and brain barriers

One of our exploratory analyses showed an inverse association between the FW and CSF-blood barriers. The FW in the insula is associated with the low permeability of CSF-blood barriers, and the FW WM in our study was associated with the low permeability of the CSF blood barriers, as well as with the low signal levels in the lateral ventricles (Supplementary 4). The CSF-blood exchange marker is the only measured imaging that has been found to be associated with peripheral inflammatory markers (Turkheimer et al., 2020). Previous work has identified an association between the reduction of permeability in the CSF-blood barrier and increases in systemic inflammation (Turkheimer et al., 2020). Meanwhile, a different study of the MDD cohort showed a reduction in the water permeability measured by the recently developed Intrinsic Diffusivity Encoding of Arterial Labeled Spins (IDEALS) MRI technique (Wengler et al., 2019). These findings indicated a restriction on the permeability barrier in depressive patients (Wengler et al., 2019b), although the mechanism of transporting the water molecules and the TSPO PET signal (a small lipophilic molecule) are different (Hatty et al., 2014). Our result is consistent with previous findings which showed that peripheral inflammation may reduce the permeability of the blood-CSF barriers, and consequently decrease the CSF-mediated brain clearance (Turkheimer et al., 2020). This result is interesting, as it suggests that the FW in the brain could be linked with the processes of brain clearance.

No significant association was found between the FW fraction in any of the ROIs and the choroid plexus enlargement in our study. No other study has examined the association between FW and the choroid plexus. However, in one previous paper, the depression group showed enlargements in the choroid plexus volume, which were associated with microglial activation and with several pathways that were linked to neuroinflammatory response (Althubaity et al., 2022). A larger choroid plexus may reflect the impairment of the BCSFB, as this is associated with low CSF levels, as well as with a reduction in the CSF-blood exchange markers in response to peripheral inflammation (Althubaity et al., 2022). The current study

undertook a further investigation based on a whole brain analysis, which showed that some clusters in the free water maps are associated with CP enlargement (Supplementary 5). Interestingly, the CP plays a role in regulating ion levels and in balancing the FW in the brain (Wolburg and Paulus, 2010), as well as its involvement in the neuro-immune axis and its interaction with the peripheral immune and inflammatory systems (Lizano et al., 2019). Changes in the FW of the grey matter may indicate an alteration to the CSF circulation and production in response to mild inflammation, but these changes are not necessarily associated with the formation of oedemas, as systemic inflammation in severe neuroinflammation increases the likelihood of oedema formation (Dénes et al., 2011).

Finally, changes in the FW fraction can be combined with central inflammation without any clear identification of the mechanism behind the inflammation. These alterations in the free water volume may not necessarily be associated with MDD.

4.7 Limitations

Some limitations should be considered. Firstly, the effect of sociodemographic factors, including age and sex, on the inflammation may affect the level of brain inflammation (Vogelzangs et al., 2012). Secondly, the exclusion of the treatment response group from the study and uncertainties in the classification between the MDD groups in terms of responses to antidepressant treatments, prevented us from testing the effects of antidepressants on the brain tissue and therefore on the FW measures. Some antidepressant medications decrease the systemic inflammatory markers (Miller et al., 2009), while others, such as tricyclic antidepressants, increase the systemic inflammation (Hamer et al., 2011). Future research could investigate the FW fraction in drug-free MDD patients and compare them with patients' responses to different treatments. Thirdly, missing information regarding the medication status and the onset of illness of the MDD subjects meant that we were unable to specify the state of the inflammation or to determine whether it was acute or chronic.

Finally, the lack of standardisation in our multi-scanner MRI is a limitation of this study. Notably, between site differences can remain even after calibration and harmonisation of scanner (Clarke et al., 2018). In this study, the scan site was controlled statically in all analysis.

4.8 Conclusion

This study showed the presence of alterations in the free water fraction in the grey matter of the depressed cohort, although, contrary to our hypothesis, it was not possible to establish a clear link to the pathophysiology of depression or to the inflammatory processes. Future research should undertake an assessment of the free water in well-characterised acute and chronic inflammation groups regardless of a diagnosis of depression.

4.9 Contributions to Study 3

All data collection was conducted for a previous study and the data were re-analysed for this work. The free water volume for the specific ROI and for the total brain was extracted and calculated by Noha Althubaity. All data analysis and the reporting of these results were conducted by Noha Althubaity.

5 Chapter 5: Discussion

In this chapter, I will summarise and highlight the main findings of the three studies discussed above. This will be followed by a discussion of the results in terms of the aim and hypothesis of each study and their relationship with the literature. I will also discuss the research and clinical implications of the findings of this PhD project, as well as the relevance of my results for future research. Finally, I will summarise the limitations of the study and present the conclusion.

5.1 Summary of findings

The first study in this project (Chapter 2) was composed of two separate datasets. The first dataset included 51 depressive patients and 25 healthy control subjects (Schubert et al., 2021b). The second dataset involved 7 healthy volunteers injected with immune challenge IFNα (Nettis et al., 2020). Participants in both datasets were scanned via PET and MRI and the PET signal in the lateral ventricles was extracted. In Chapter 3, Study 2 combined the depression and healthy control groups used in Study 1. MRI was used to calculate the choroid plexus volume. Study 3 (Chapter 4) included a larger sample size composed of 79 depressed patients, whose age and sex matched those of 45 healthy control subjects. All the participants underwent 90 minutes of MRI scans involving structural and functional sequences to measure the free water volume.

A summary of the findings of this thesis is that a significant association between the reduction of the lateral ventricles PET signal and an increase in the systemic inflammatory marker was found for the first time, which reveals some alteration in the CSF dynamic in the depression group. This association increased across the patient group, specifically among depressive patients with high peripheral inflammation, which may indicate a reduction in CSF clearance. No significant difference was found in the lateral ventricles PET signals between the

depression group and the healthy control subjects. Also, no significant association was found between the PET signal in lateral ventricles and depression symptoms.

In contrast, the choroid plexus volume was significantly bigger in depressive patients compared to the healthy control group, and it was significantly associated with the central inflammation markers measured by the TSPO PET signal. The choroid plexus enlargement was also inversely associated with the PET signal perfusion in the lateral ventricles. This change in the choroid plexus structure may suggest a link with the alteration in the CSF clearance in depression, as well as the involvement of the choroid plexus in the model of the peripheral to the central immune axis.

An unexpected reduction in the free water volume was detected in the anterior cingulate cortex in the low inflammation depression group compared to the group with high inflammation depression and the healthy control subjects. This decrease in the free water volume was found in the total grey matter of the depression group compared to the healthy control group, when the analysis was extended to the whole brain. The alteration of the free water volume in the low inflammation group may reveal the contribution of neuroinflammation to the change in the microstructures of the brain tissue. Additionally, the free water volume was inversely associated with the lateral ventricles PET signal, which may indicate a disturbance in the CSF clearance. Finally, no associations were detected between the free water volume and peripheral inflammation markers or central inflammation markers. Likewise, no significant associations were found between the free water volume and depression clinical scores (Table 5.1).

Overall, these results indicate that CSF-mediated clearance alterations can be assessed using neuroimaging and exploring a modified model of the peripheral-to-central immune axis. The changes in the CSF clearance are associated with peripheral and central inflammation, but not necessarily with MDD. Also, these findings demonstrated the role of the brain barriers in

modulating neuroinflammation and mediating the communication between the peripheral and central immune system.

Table 5.1 A summary of main results of the thesis.

	Cohort	Biomarker	Type of study	Key findings	Interpretation
Study 1	51 DEP (30 low CRP, 21 high CRP) 25 HC	^{11}C-PK11195 PET in Lateral ventricles Structural MRI	Cross-sectional	No significant difference in the CSF clearance markers between the DEP and the HC ↓ LV PET signal with ↑ CRP level	Disrupted CSF dynamics by a reduction in permeability barriers in response to high peripheral inflammation markers in depression and HC. Reduced the barriers' permeability in response to increase the peripheral inflammation after injecting immune challenge IFN-α in healthy volunteer.
	7 HC	^{11}C-PBR28 PET in Lateral ventricles (Kinetic modelling) Structural MRI	Within -subject open label (before and after Interferonalpha injection)	↓ LV PET signal with ↑ CRP level	
Study 2	51 DEP (30 low CRP, 21 high CRP) 25 HC	Structural MRI CP Volume ^{11}C-PK11195 PET	Crosssectional	↑ CP volume in depression ↑ CP volume with ↓ LV PET signal ↑ CP volume ↑ DVR in ACC, PFC, INS ↑ CP volume ↑ DVR CP	CP structural changes associated with disrupted CSF clearance markers and with central inflammatory markers in depression and healthy control.

Study 3	79 DEP (47 low CRP, 32 high CRP) 45 HC	Multiple sell Diffusion MRI (NODDI) FW volume ^{11}C-PK11195 PET	Cross-sectional	↓ FW volume in ACC of depression with low CRP ↓ FW volume in GM of depression ↑ FW volume in INS with ↓ LV signal with	FW volume associated with disrupted CSF dynamics

Table 5.1: Summary of all the study results: DEP = depressed patients; CRP = C-reactive protein; CP = choroid plexus; CSF = cerebrospinal fluid; HC = healthy controls; LV = lateral ventricles; MRI = magnetic resonance imaging; PET = positron emission tomography; DVR = distributed volume ratio; ACC = anterior cingulate cortex; PFC = prefrontal cortex; INS = insula cortex; NODDI = Neurite Orientation Dispersion and Density Imaging; FW = free water volume.

5.2 CSF clearance measured by TSPO PET perfusion in lateral ventricles

The primary aim of Study 1 in Chapter 2 was to explore the clinical relevance of the [^{11}C]PK11195 PET signal of the lateral ventricles as a proxy of the CSF dynamics and as an indirect measurement of the CSF clearance, by comparing the signal magnitudes in lateral ventricles (SUVR in 60 minutes and AUC 30 to 60) in MDD patients and healthy controls. The study also sets out to assess the link between the CSF clearance marker measured by the [^{11}C]PK11195 TSPO signal in lateral ventricles to peripheral inflammatory markers and MDD symptoms. I hypothesised that the reduction of the lateral ventricle PET measure would be sensitive to the alterations of the CSF dynamic in depressed patients compared to healthy control subjects. Also, it was hypothesised that mild inflammation in depressive patients would reduce the CSF dynamic by closing the brain barriers in response to the peripheral inflammation. Finally, I hypothesised that the reduction of the CSF clearance would be associated with high depression symptoms.

The analysis did not show a significant difference in the PET signal perfused into the lateral ventricles in depressed patients compared to the control group. However, for the first time, a significant association between the reduction of the CSF dynamic and the increase of the systemic inflammatory marker in both depressed patients and healthy controls was found. Among depressed patients, the childhood trauma score was the only depression clinical score that was associated with the reduction of the CSF dynamic, although it did not survive multiple comparison corrections. In terms of the study of healthy volunteers injected with IFN-α, no significant difference in the PET signal in the lateral ventricles at the baseline and after the immune challenge injection was detected among the healthy volunteers. However, it was noted that the CRP level increased following the IFN-α injection and was inversely associated with the CSF dynamic measured by the PET signal perfused in the lateral ventricles (SUVR). Interestingly, the tracer kinetic modelling demonstrated a significant decrease in the volume distribution (V_T) of the tracer in the lateral ventricles and the grey matter following the inducement of the IFN-α. However, the difference in the blood to CSF tracer transportation kinetic parameter (K1) almost reached significant levels in the lateral ventricles, although a significant reduction of the V_T was seen in the grey matter. The findings of this study support the hypothesis that a decrease in the permeability barrier may mediate the reduction of the CSF clearance in response to the increase of peripheral inflammation.

In the literature, no previous study had investigated CSF clearance among depressed patients using the perfusion of the PET signal in the lateral ventricles as a proxy for CSF clearance. However, previous literature has demonstrated that patients with Alzheimer's disease (AD) and mild cognitive impairment (MCI) showed a significant reduction in the CSF clearance measures, which is associated with Aβ deposition, a distinctive characteristic of AD (De Leon et al., 2017, Schubert et al., 2019). On the other hand, multiple sclerosis (MS) patients (i.e., those with a condition where there is no presence of Aβ accumulation) also exhibited a

reduction in the CSF clearance measured by PET perfusion in the lateral ventricles (Schubert et al., 2019). Depression has been known to be a risk factor for AD and has shown a significant association with AD (Sáiz-Vázquez et al., 2021, Sanmugam, 2015), as well as being a comorbidity condition with MS (Feinstein et al., 2014). The clearance mechanism in depression needs more elucidation via a larger sample size.

Moreover, the methodological challenges of quantifying the PK11195 PET tracer may contribute to the lack of a significant difference between the patients and the healthy control (Turkheimer et al., 2015). As the PK11195 recorded high affinity to the alpha1-acid glycoprotein, an acute phase protein in plasma (Lockhart et al., 2003), PK11195 was found to be a carrier of lipophilic drugs (Fournier et al., 2000), chapter 2, the methodologic issue. The alpha1-acid glycoprotein synthesis in the liver is abundant in humans, and its concentration increases in response to systemic tissue injury, inflammation, and infection (Fournier et al., 2000). This may suggest a small amount of the tracer crossing into the brain tissue and ultimately percolating into the lateral ventricles due to an increase in the free plasma fraction. Therefore, the SUVR may underestimate the PET signal perfused in the lateral ventricles.

On the other hand, the study of the healthy volunteers who were injected with IFN-α used the PBR28 PET tracer, and did not show a significant difference in the PET measures in the lateral ventricles between the baseline and after the immune challenge. However, its results showed a significant reduction in the tracer distribution following the immune challenge, which may indicate a reduction in the solutes crossing the brain tissue into the lateral ventricles. Interestingly, IFN type 1 plays a role in modulating BBB integrity and contributes to the anti-inflammatory process (Jana et al., 2022). The MS patients were shown to rise on the vascular cell adhesion protein 1 (VCAM-1) following the treatment of IFN type 1 and expressed a reduction in the barriers' permeability as well as decreased lymphocyte infiltration (Billiau, 2006). On the other hand, IFN type 1 plays a role in the anti-inflammation process. The systemic induction of the IFN-

β (type 1 IFN) in the ischemic stroke rat model identified a reduction in the brain infarction, preserved the BBB integrity and decreased the peripheral immune cells trafficking into brain tissue (Veldhuis et al., 2003). Moreover, the astrocytes of MS patients and experimental autoimmune encephalomyelitis (EAE) exhibited a transcriptional response to the IFN type 1, which is signalling contributed to the anti-inflammation in MS patients (Rothhammer et al., 2016). Thus, the findings of the IFN-α study support the hypothesis that the decrease in solute clearance is a response to the high systemic inflammation. Further studies need to investigate the PET signal percolation in the lateral ventricles using the kinetic modelling method with different mild inflammation states and TSPO PET tracers.

The second aim of Study 1 in Chapter 2 was to assess the link between the reduction of CSF clearance and inflammation. I hypothesised that inflammation would reduce the CSF dynamic by closing the BBB and BCSFB, ultimately downgrading the CSF clearance. The results showed an inverse association between high CRP levels and the CSF dynamic measures (SUVR and AUC 30-60), which suggests that inflammation decreases the permeability of the molecules across the BBB and BCSFB. In addition, the IFN-α study exhibited an inverse association between the heightening of CRP following the IFN-α injection and the reduction of the CSF dynamic measure (SUVR). Moreover, the IFN-α study showed a reduction in the total volume of the tracer distribution in the lateral ventricles and in the grey matter after the immune challenge, which indicates a decrease in the blood-to-brain tracer transfer. These findings support the hypothesis that mild inflammation restricts the permeability of brain barriers, which may disrupt solute homeostasis.

In this study, while there was no assessment of the BBB leakage marker in the depressive and healthy control subjects, the VEGF exhibited a reduction in the depressive group compared to the healthy control group. In the IFN-α study, healthy volunteers demonstrated a decrease in S100$\boldsymbol{\beta}$ following the injection of the IFN-α, with a trend level of significance

following the induction of the immune challenge. These findings support the hypothesis that chronic inflammation reduces permeability barriers as a short-term protection mechanism which may alter the clearance process. Different methods were used in the literature to assess the permeability barriers in neuroinflammation states. One of them was the level of the quotient albumin in CSF, which originally synthesises in blood, and was found in high concentration in the CSF of septic meningitis patients (an acute inflammation state), suggesting an increased permeability barrier (Akaishi et al., 2015). This concentration decreased to the normal level in the chronic phase, which points to barriers to recovery (Akaishi et al., 2015). Also, the increase of S100$\boldsymbol{\beta}$ in the plasma (which originates in brain tissue) of cancer patients who used BBB disruption drugs before chemotherapy, indicated increased permeability barriers (Kapural et al., 2002). Mild inflammation seems to reduce the barriers integrity, as a vascular stiffness was associated with low-grade inflammation (Kusche-Vihrog et al., 2011b).

A recent study showed that the permeability of the leaky barriers on the ependymal cell decreased in the depressive animal model and in MDD patients (Seo et al., 2021). The study demonstrated a reduction in p11, pointing to the role of lower barrier permeability and CSF flow in inducing depression and anxiety-like behaviour. The p11, also known as S100A, is produced by astrocytes and plays a role in the polarisation of the ependymal cells, as well as contributing to the aetiology of depression (Svenningsson et al., 2013). Interestingly, it has been found to be reduced in MDD plasma (Cattaneo et al., 2013), suggesting a reduction in the clearance process. Combined, this evidence supports my hypothesis that mild chronic inflammation in depressive patients reduces the barrier permeability. The dysregulation of the brain barriers' permeability may support the different peripheral and central immune communication models in response to low-grade systemic inflammation. This model of the closure of brain permeability in response to increasing peripheral inflammatory cytokines, may

serve as a protective mechanism in the short-term, but may make the brain homeostasis unstable by altering solute clearance.

5.3 Choroid plexus volume

The aim of Study 2 in Chapter 3 was to investigate the choroid plexus volume and its relationship with peripheral and central inflammation using structural MRI in depressive patients and healthy controls. It was also anticipated that the CP enlargement would be associated with the reduction of the CSF clearance markers measured in Study 1 (Chapter 2), as well as the clinical scores relating to depression. I hypothesised that the CP volume would increase in depressed patients compared to healthy control subjects, and be associated with higher depressive symptoms. In addition, it was predicted that the CP volume would be associated with high peripheral inflammatory markers and a high TSPO PET uptake in the three ROIs: the anterior cingulate cortex, the prefrontal cortex, and the insula.

The results indicated that there is an increase in the CP volume in depressed patients when compared to healthy control subjects. The CP enlargement is associated with a reduction in CSF clearance, calculated by the PET signal prefusion in the lateral ventricles. Also, the CP enlargement correlated with a high PET radioactive signal in the three ROIs and in the choroid plexus used as a central inflammation marker. No significant association was found between the CP volume and the peripheral inflammation markers, including CRP, IL6, and TNF-α. Similarly, no significant association was found between the CP volume and the clinical scores of the depressive group, except the perceived stress score which did not survive the multiple comparison correction tests. Finally, the additional analysis used a brain map to explore the association between the CP volume, TSPO, and post-mortem gene expression. The analysis of the image transcriptome showed that the enrichment genes in excitatory neurons were involved in the neuroinflammation pathways. My results support the hypothesis that the choroid plexus may mediate the reduction of CSF clearance and fit into the model of peripheral-to-central

immune interaction. Moreover, the alteration of the morphology of the choroid plexus may contribute to the reduction of the CSF mediated clearance.

This is the first study that has investigated the CP morphology and its link to peripheral and central inflammation markers in a depression cohort, as well as its association with the reduction of CSF clearance markers. A significant increase in the CP volume in depressed patients compared to the healthy controls was detected in this analysis. This enlargement of the CP has been linked to CP dysfunction and neuroinflammation in a recent study of an animal model and MS patients (Fleischer et al., 2021). Moreover, CP enlargement correlated with a peripheral inflammatory marker in a study of a psychosis cohort (Lizano et al., 2019) and inflammation-mediated CSF hypersecretion (Zhang et al., 2020, Karimy et al., 2017). Therefore, the structural alteration of the CSF system may be linked to the inflammation and dysregulation of CSF composition and flow by reducing the BCSFB permeability, which may consequently impair the CSF clearance process. My finding is consistent with the literature, as an increase in CP volume was shown in different neuroinflammation conditions, including AD and Parkinson's disease (PD) (Tadayon et al., 2020), MS (Ricigliano et al., 2021), complex regional pain syndrome (Zhou et al., 2015), and psychosis (Lizano et al., 2019, Zhou et al., 2020). Interestingly, AD and MS patients also exhibited a reduction in the CSF clearance measured by the lateral ventricles PET signal (De Leon et al., 2017, Schubert et al., 2019).
This outcome may support arguments for the importance of the choroid plexus in regulating CSF clearance. We could not specify in which part of the choroid plexus the volume increased due to the limitation of the structural imaging. However, there are possible explanations for the enlargement of the CP. The amplification of the CP volume may be the result of an increase in the epithelial cells, as seen in brain injury (Barkho and Monuki, 2015), or an increase in the non-choroidal immune cell infiltration into the CP where the peripheral and central immune systems interact (Schwartz and Baruch, 2014). It might also be the result of associated oedema

formation in infectious diseases (Cho et al., 1998). The increase in the CP volume has also been explained as a result of inflammation, as interpreted in the study of complex regional pain syndrome (Zhou et al., 2015) or its association with IL-6 in psychotic cohorts (Lizano et al., 2019, Zhou et al., 2020). Inflammation plays an important role in the structural alteration of the choroid plexus and the BCSFB, and may translate this alteration into the changes in the CSF production and composition (Santos et al., 2019), as well as ultimately in the CSF clearance process.

The second main finding of Study 2 is that there is an inverse association between CP enlargement and the CSF clearance marker measured by TSPO PET signal percolation in the lateral ventricles (SUVR and AUC 30-60). There was no previous study in the literature that investigated the association between the structures of the CP and the CSF dynamic in depressive cohorts. However, there is evidence that other neuroinflammation conditions, including AD and MS, showed a decrease in the CSF clearance (De Leon et al., 2017, Schubert et al., 2019) and an enlargement in CP volume (Tadayon et al., 2020, Ricigliano et al., 2021). Chronic inflammation may gradually increase the CP volume and reduce the BCSFB permeability in response to high peripheral inflammation cytokines. The CP volume in the current study is associated inversely with the albumin plasma level, which is used as a marker of chronic inflammation (Don and Kaysen, 2004). Interestingly, the CP volume in the IFN-α study did not present a significant difference in the healthy volunteers at the baseline and 24 hours after the immune challenge administration ($t_{(6)} = 0.11$, $p = 0.91$), with the mean and the stander deviation as (951.2 ± 260) and (967.46 ± 242), respectively. Chronic inflammation seems to increase the choroid plexus volume gradually as an immune defensive response. On the other hand, the clearance process has been known to be enhanced during sleep (Benveniste et al., 2019), and disturbance of sleep was detected in patients with psychiatric disorders (Krystal et al., 2008). The choroid plexus also plays a role in the circadian clock by expressing

the rhythmic genes Per1 and Per2, which encode the period circadian protein homolog and play a major role in circadian rhythms (Quintela et al., 2018). The circadian rhythmicity generated by the choroid plexus is transported to the suprachiasmatic pacemaker in the hypothalamus, which is also involved in circadian rhythms (Quintela et al., 2018, Johanson and Johanson, 2018. The increase in the CP volume which is associated with lower barrier permeability may be linked to the irregular sleep reported in depressed patients (Berk, 2009), and might mirror the reduction in CSF clearance.

In my study, the CP volume did not correlate with the CRP, which is consistent with the result of the CP enlargement in the psychosis cohort, which was not correlated with the CRP (Lizano et al., 2019). However, the CP enlargement is associated inversely with CSF clearance markers, which were the only central markers that were inversely associated with the high CRP. The choroid plexus may mediate the peripheral-to-central immune axis by restricting the transfer of molecules across barriers in an indirect response to inflammation. Further studies need to investigate the association between the alteration in CP volume and a high concentration of CRP in patients with a long chronic inflammation status.

The depressive group in my study exhibited a significant reduction in the VEGF level. This observation is in line with the findings of previous studies of MDD sufferers, which showed a significant reduction in the VEGF level in plasma, with an inverse association with the peripheral TNF-α (Dome et al., 2009). Moreover, a study by Maharaj et al. (2008) demonstrated an inhibition of the VEGF, which led to a decrease in the choroid plexus vascular permeability, and was associated with the accumulation of fibrin in the choroid plexus (Maharaj et al., 2008). Interestingly, the blocking of the VEGF and the TGF-$\boldsymbol{\beta}$ showed a reduction in different measures, including the permeability of the BCSFB and the periventricular ependymal barrier, the disappearance of the ependymal microvilli, and a thickening in the capillary

endothelial cells, which indicated an alteration in the CSF flow (Maharaj et al., 2008). Moreover, post-mortem depression studies showed a downgrading in the CP transcriptome which regulated the TGF-$\boldsymbol{\beta}$ permeability (Turner et al., 2014). The VEGF and the TGF-$\boldsymbol{\beta}$ receptors were found in the CP and ependymal cells, and are involved in the regulation of endothelial and ependymal cell functions and periventricular permeability (Maharaj et al., 2008). Furthermore, the TGF-$\boldsymbol{\beta}$ plays a role in the anti-inflammatory process, acting as an immune modulator to T-cell activation by inhibiting the self-reactive proliferation and differentiation of CD4+ and CD8+ T-cells (Sanjabi et al., 2009), and it is involved in the immune responses through its regulation of cytokine production (Oliveira et al., 2014). Therefore, the alteration of the CP morphology and the integrity of permeability barriers may be a defensive method in response to inflammation and an imbalance of the brain in homeostasis. The choroid plexus appears to be involved in the workings of the peripheral-to-central immune mechanism, although no significant association was detected with the peripheral inflammation markers.

My study also demonstrates, for the first time, significant associations between the CP volume and the central inflammation markers represented by the TSPO PET uptake in the brain parenchyma and in the CP in the depressive cohort. These findings corroborate the findings among remitting-relapse MS patients where the CP enlargement was associated with the TSPO PET signal in the CP (Ricigliano et al., 2021). Moreover, the MS patients and the two MS animal models studied by Ricigliano et al. (2021), confirmed the association between CP enlargement and glial activation, and used the CP volume as both a marker for disease progression and as a response to neuroinflammation (Fleischer et al., 2021). Hence, CP enlargement fits into the peripheral-to-central immune axis and can be used as a neuroinflammation marker.

No significant association between the CP volume and depression clinical scores was found, except the perceived stress score which did not pass the multiple correction test. My finding is consistent with other studies that did not find significant associations between CP enlargement and psychotic clinical scores (Lizano et al., 2019), as well as with CP volumes and the score of relapse-remittent MS and disease duration (Ricigliano et al., 2021).

5.4 Free water volume

The aim of Study 3 in Chapter 4 was to assess the free water volume in three regions of interest calculated by the multiple shell diffusion weight image of the MRI (NODDI) in depressed/healthy control groups, and use it as an alternative neuroinflammation biomarker of the TSPO PET signal. The association of the free water volume with peripheral and central inflammation markers was also investigated. Lastly, the study set out to assess the associations between the free water volume and the markers of CSF-mediated clearance measured in Study 1, the choroid plexus volume measured in Study 2, as well as with depression symptoms. I hypothesised an increase in the free water volume in the three regions of interest (the anterior cingulate cortex, the prefrontal cortex, and the insula), as well as in the total grey matter of depressed patients compared to healthy control subjects. It is believed that this alteration in the free water volume is linked to the marker of CSF clearance markers, including the TSPO PET signal perfused in the lateral ventricles and the CP enlargement.

The analysis revealed that there is an unexpected reduction in the free water volume in the anterior cingulate cortex (ACC) of the depressive cohort, with low inflammation compared to the depression group with high inflammation and the healthy control subjects. When I investigated the free water volume in the total grey and white matter, I found only a significant reduction in the free water volume of the total grey matter in depressive patients compared to the healthy control subjects. In terms of CSF clearance, I found that the free water volume in the insular cortex and in the white matter was inversely associated with low TSPO

PET perfusion in the lateral ventricles (the clearance marker). However, no significant associations were detected between the free water volume in the three ROIs and the CP enlargement. I extended the analysis to the whole brain, and found significant clusters in the free water map associated with the CP enlargement. Finally, I did not find any significant association between the free water volume, peripheral and central inflammation markers, or depression clinical scores.

The reduction of the free water volume NODDI measures in the low inflammation depression group in this study is a novel result, as no previous research has investigated free water volume using NODDI for depressive patients. The reduction in the volume of extracellular free water was seen in repeated traumatic brain injury (TBI) subjects who exhibited activated microglia and morphologic alteration detected by structural MRI (Reid et al., 2019). It is important to note that chronic inflammation activates microglia and astrocytes in the neuroinflammation by increasing their size and number (Streit, 2006). The excessive volume of glial cells in mild inflammation may explain the increase in the intracellular free water and therefore also explain the reduction of the extracellular space (Dowell et al., 2019). More detail found in Chapter 4, Discussion section.

My findings did not demonstrate a significant association between the free water volume and the central inflammation markers measured by the TSPO PET signal in brain parenchyma. Similarly, the reduction of the free water volume in repetitive TBI did not show a significant association with the central inflammation marker (Reid et al., 2019). Both TBI and depression patients exhibited chronic inflammation and a heightening of the peripheral inflammatory cytokines (Risbrough et al., 2022), which may participate in a comparable mechanism of neuroinflammation (Bodnar et al., 2018, Speer et al., 2018) and reveal the same response to the mild inflammation by reducing the extracellular space and increasing the intracellular free water. The lack of association between the free water volume and the TSPO

PET signal may be because of the unspecified TSPO in the microglia, or, as assumed in Study 1 in Chapter 2, the activation of the microglia is a secondary result of the brain solute imbalance. The free water volume in my study did not correlate with the peripheral inflammation marker. This finding is consistent with the literature, as no study has found any association between the free water volume and peripheral inflammation markers.

One of the main findings of this study is the inverse association between the free water volume in the insula and the CSF clearance marker measured by TSPO PET perfusion in the lateral ventricles. Moreover, the free water volume of the total white matter showed an inverse association with the CSF clearance marker (Chapter 4, Discussion). The reduction of the barriers permeability in response to increased inflammation may support the hypothesis that mild inflammation closes the brain barriers and consequently alters the solute clearance.

Additionally, the peripheral and central immune systems have been shown to interact with the infiltration of the peripheral cytokines from different pathways, which is an action that triggers neuroinflammation. Neuroinflammation promotes changes in the astrocytes, the glial cells that support the brain barriers and regulate water and ion transportations through the AQP4 (Colombo and Farina, 2016). The astrocytes also control the exchange of extracellular components via the CSF clearance pathways in addition to their role in immune cell trafficking (Colombo and Farina, 2016). A change in the astrocytes due to neuroinflammation may reflect the dysregulation of the water movement across the brain parenchyma, which therefore contributes to the imbalance of the CSF flow and ultimately to the clearance process. Further studies using the NODDI compartmental methods to assess the microstructural alteration in neuroinflammation conditions are advisable.

To extend the investigation of the association between the free water volume and the CP volume, the study did not find a significant correlation between the free water volume in

any of the ROIs and the CP volume. However, the CP volume was found to positively correlate with the free water volume in the total grey and white matter: ($r = 0.25$, $p = 0.005$) and ($r = 0.24$, $p = 0.008$), respectively. The correlation remained when the study was restricted to the depression groups with high and low CRP in the grey matter ($r = 0.32$, $p = 0.004$) and white matter ($r = 0.25$, $p = 0.03$). The associations between the CP volume and the free water in the grey and white matter did not survive the multiple correction tests. Furthermore, the whole brain voxel-wise analysis demonstrated that some clusters in the free water map are associated with CP enlargement (Chapter 4, Discussion). No previous study has been found which has tested the association between CP enlargement and the increase of the free water volume. The choroid plexus is involved in water and ion regulation in the brain, which contains the aquaporin 1 water channel, as well as the vasopressin receptor (Wolburg and Paulus, 2010). Vasopressin is a hormone released by the pituitary gland that regulates the water/ion balance in the CNS (Kozniewska and Romaniuk, 2008). Its receptors are highly distributed throughout the different structures of the brain, including the choroid plexus (Kozniewska and Romaniuk, 2008). Different studies confirm an increase in vasopressin and its receptors following strokes and subarachnoid haemorrhages which induce oedemas (Barreca et al., 2001, Kozniewska and Romaniuk, 2008). It is important to note that stroke patients demonstrated CP enlargement (Egorova et al., 2019), and post-stroke patients who showed depressive symptoms also revealed an increase in free water (Oestreich et al., 2020). The association between the free water clusters and the choroid plexus volume indicates that neuroinflammation is associated with changes in the CSF structural system and may therefore alter CSF clearance. Further research is needed to investigate the other compartments of NODDI in terms of different neuroinflammation conditions in order to assess how neuroinflammation may change the microstretches and consequently alter CSF clearance. More research is also needed to explore

NODDI measures and use them as an alternative biomarker for neuroinflammation. These findings showed a link to neuroinflammation, but not particularly to depression.

6 Research implications

The results from this project have highlighted several findings relating to CSF clearance, specifically in relation to assessing CSF dynamics through the PET signal in the lateral ventricles. Additional research on PET tracers combined with a kinetic compartmental method using blood sampling in depressed patients may provide an accurate magnitude for the solute measure, including a tracer rate across tissue and blood, ultimately percolating into the lateral ventricles. Although the PET quantification method based on reference regions simplifies the experimental procedure and avoids the need for arterial blood sampling, it is unable to return a full compartmental description of the system under investigation. The CSF clearance measures in this project were found to reduce when systemic inflammation increased. Future research also needs to investigate CSF clearance in chronic inflammation conditions, considering that the onset and duration of the disease may help to understand the mechanism of how mild neuroinflammation reduces CSF clearance. In terms of the choroid plexus volume measurement, developing an accurate automatic technique to segment the choroid plexus and extract the volume using structural MRI may provide an accessible and fast method to calculate the choroid plexus volume in a larger sample size. The findings from this project have confirmed the role of the choroid plexus in mediating neuroinflammation and the CSF clearance process. Further studies are needed to assess the choroid plexus in different neuroinflammation states and their individual relations with the peripheral and central inflammation markers. Indeed, using the NODDI technique to extract the microstructural and free water volume is a revolution in neuroimaging. NODDI is a fast and safe procedure that allows for the extraction of the structural and functional alterations linked to brain inflammation. Further research needs to design studies which analyse the NODDI

compartments in different neuroinflammations in order to be used as an alternative biological marker for brain inflammation.

7 Clinical implications

Although the findings of this project did not find a link to depression, the greatest clinical implication of this study is the exploration of a new peripheral-to-central inflammation model. This model will help to enhance our knowledge about the mechanism of inflammation in depression, as well as develop therapeutic targets, and biomarkers particularly in depression patients with antidepressant resistance. Furthermore, as the results of this project support the contribution of inflammation in the aetiology of depression, this model suggests the possible use of anti-inflammatory medication alongside the standard antidepressant drugs, which may increase the efficacy of the standard antidepressant medication, especially for treatment resistant depression patients.

8 Limitations

Several limitations in this work need to be considered. This is a summary of all of the limitations of this project. Firstly, methodological challenges were found in the quantification of the [^{11}C]PK11195 PET signal percolation in the lateral ventricles in Study 1 (Chapter 2). The lack of arterial blood sampling made it impossible to estimate the tracer kinetics in blood (e.g. plasma-to-blood ratio, free plasma fraction) and quantify the blood-to-brain transfer exchange kinetic rates. The simplified procedures used in the study, based on a reference region approach (i.e. SUVR and DVR), may underestimate the signal magnitude in the lateral ventricles. This may explain the lack of significant difference between the groups, although the depression group showed a modest increase of the [^{11}C]PK11195 PET signal compared to the healthy control group (Schubert et al., 2021b). We compensated for this limitation by using another dataset composed of 7 healthy volunteers challenged with IFN-α. The PET images of

the7 healthy volunteers who were injected with [^{11}C] PBR28 were re-analysed to test the effect of an increase in the systemic inflammation marker in the tracer which percolates into the lateral ventricles from the brain tissue and blood, using arterial blood sampling. Both the compartmental modelling and the simplified metric SUVR demonstrated an inverse association with the PET signal in the lateral ventricles and a high CRP, although no increase in the TSPO PET in the brain was detected (Nettis et al., 2020).

TSPO expression in the brain showed individual variability (Notter et al., 2018), and it was involved in the synthesis and metabolism of the neuroactive steroid, which was affected by age and hormonal steroid function (Giatti et al., 2019). The TSPO is involved in cholesterol transportation across the mitochondrial membrane, which is essential for steroid production (Papadopoulos et al., 2006). A preclinical study of rat brains showed higher TSPO expression in some regions of male rat brains than female ones, while other brain regions demonstrated similar TSPO levels in both males and females (Giatti et al., 2019); another study showed differences in microglial cells between male and female mice, which indicated sex-specific gene expression (Villa et al., 2018). On the other hand, human studies had mixed results in the expression of the TSPO PET signal in terms of sex: no significant differences were found between males and females; however, a study with a small sample size found a higher signal in females compared to males (Notter et al., 2018, Paul et al., 2019, Collste et al., 2017). Similarly, there were significant differences between males and females in TSPO levels in all brain areas, and females had higher TSPO binding levels (Tuisku et al., 2019). In this project, the TSPO PET signal did not significantly differ between males and females in the whole group or independently in the healthy control or depressive group. The results were tested before and after controlling for the sex, and they were unchanged. Fewer males were studied than females in this project; however, the sex was matched and not significantly different between the healthy control subjects and depressive sufferers. It would be beneficial

to have an equal number of males and females for further assessment of the impact sex has on the TSPO PET signal.

Another limitation of this study is related to incomplete information about the onset and duration of depression in the patients. This information may help to evaluate the structural changes in the brain tissue and measure the CSF clearance markers in both the early phase of the inflammation and throughout its lifetime in depressive patients. Also, the lack of CSF cytokines and CSF composition impeded us in terms of assessing the association between the central inflammatory cytokines and the blood-to-CSF exchanged marker. Moreover, a CSF composition may help to show whether the alteration of the permeability barriers may alter the CSF composition. In terms of the treatment response to the antidepressant medication, depressed patients who responded to the antidepressants were excluded from the study's recruitment in line with the study design. The missing information regarding this group prevented us from assessing the effect of the medication on the CSF clearance. It should, however, be noted that some antidepressant medication plays an inflammatory role and has shown a reduction in some peripheral inflammatory cytokines in depressed patients (Więdłocha et al., 2018), in addition to reducing depressive symptoms (Hannestad et al., 2011). The depression cohort in this project was categorised into two groups based on CRP level, and the recruitment included only untreated and treatment-resistant patients, while the treatment responsive were excluded due to their low CRP level.

An additional limitation is the potential introduction of bias due patient subgrouping based on continuous variable dichotomisation, as it is the case for low and high CRP MDD groups. This effect can be mitigated by increasing the number of categories, but information within each category is always ignored. Therefore, participants above or below a certain threshold are treated equally, despite the possibility of greatly differing outcomes (Naggara *et al*., 2011). Indeed, the use of a hard CRP threshold for the analysis of inflammation in

depression has been the subject of much debate (Munkholm and Paludan-Müller, 2021, Nettis et al., 2021b). The likelihood of a subgroup effect being real depends upon a variety of factors, and may be considered as a continuum ranging from very unlikely to highly plausible (Munkholm and Paludan-Müller, 2021). In terms of the CRP cut-off point, previous research on depression has demonstrated some variability in the group stratification based on the CRP level, although the predefined limit used was originally suggested by the American Society of Heart Disease for the evaluation of systemic inflammation, and thus may have reduced relevance (Raison *et al*., 2010, Uher *et al*., 2014, Wysokiński *et al*., 2015, Wium-Andersen *et al*., 2013). Additionally, the suggested threshold aligns with the idea that CRP levels above 3 mg/L indicate low-grade inflammation, which is linked to an increased risk of cardiovascular and depressive disorders, and has been associated with higher central inflammatory markers and treatment resistance in depression (Nettis *et al*., 2021b). in the BIODEP study, the researchers who participated in the study considered the CRP level threshold during data analysis before data collection was completed, following the method applied in a previous study (Nettis *et al*., 2021a). Since CRP levels are assessed in many local laboratories, group categorisation can be supported. CRP is produced by the hepatic cells and promoted by the elevation of cytokines, including IL-6 (Kimura and Kishimoto, 2010); therefore assessment of the relative immune cytokine was deemed relevant to this study.

Another limitation was the use of manual segmentation for the choroid plexus (Study 2 in Chapter 3). While this is still considered the gold standard for choroid plexus neuroimaging studies at the moment (Tadayon et al., 2020), it is time-consuming and difficult to apply to a larger sample size. Automated segmentation methods for the choroid plexus exist and allow one to investigate the choroid plexus volume in larger sample sizes (Lizano et al., 2019). However, they have repeatedly been found inaccurate for some brain regions with an undefined contrast, including the choroid plexus (Guenette et al., 2018). The improved auto-segmentation

methods which were developed using the Gaussian Mixture Model (GMM) performed better in terms of the choroid plexus segmentation and have a high similarity to the manual segmentation method (Tadayon et al., 2020). This was applied in Study 3 (Chapter 4) of this project in order to calculate the choroid plexus volume.

Finally, sociodemographic factors, including age, sex, and BMI, and the lack of standardisation in the multi-scanner MRI may contribute to collinearity in the third study of this work.

9 Future research

The findings of this work motivated me to continue investigating the CSF dynamic in other neurological and neuropsychiatric disorders which have shown an alteration in the choroid plexus and are linked to neuroinflammation. Further neuroimaging methods such as the use of a CSF contrast enhancement via MRI to assess the CSF clearance, or the use of non-invasive methods such as applying multiple echo time (multi-TE) to arterial spin labelling (ASL) to measure the CSF flow (Ohene et al., 2019), may enrich our existing knowledge about therapeutic drug delivery in the CNS (Ringstad et al., 2018). The combined PET and MRI methods may provide strong evidence of the CSF clearance markers.

CSF clearance pathways have been known to extend and increase the clearance process during natural sleeping periods and general anaesthesia. It would be beneficial to extend the investigation of the CSF clearance markers using the PET and MRI methods for subjects suffering from sleep disorders. The results of the free water volume studies should encourage further investigation into the NODDI compartment in acute and chronic neuroinflammation conditions in order to assess how inflammation changes the microstructures. Additionally, there should also be further research into how antidepressant drugs induce an alteration of the brain tissue (Korgaonkar et al., 2015) and manipulate the inflammation level in depressed patients. It would be useful to examine the NODDI compartments in drug-naive and clear treatment

responses in depression groups. Finally, as the choroid plexus seems to respond to chronic inflammation, it would be valuable to conduct a longitudinal study to assess the choroid plexus volume and its association with peripheral and central inflammation markers.

10 Conclusion

Overall, this study has explored, for the first time, the CSF-mediated clearance levels in depression by using neuroimaging. The results show a reduction in the blood-to-CSF exchange measured by the PET signal perfused in the lateral ventricles as the marker of CSF clearance, as previously proposed for different neuroinflammation conditions (De Leon et al., 2017, Schubert et al., 2019). The choroid plexus enlargement also suggests some structural changes linked to the lateral ventricles PET signal and neuroinflammation markers. The results also support the argument that changes in these measures can be associated with peripheral and central inflammation markers, but not necessarily with depression. Future research might focus on expanding the investigation of the lateral ventricles PET signal and its association with different parenchymal changes, including the choroid plexus and the permeability barriers in several neuroinflammation conditions. Such future research might help us to understand how inflammation might relate to solute clearance and ultimately to brain homeostasis, as well as potentially providing new insights into therapeutic targets in neuroinflammation conditions.

11 References

ABBOTT, N. J. 2005. Dynamics of CNS barriers: evolution, differentiation, and modulation. *Cellular and molecular neurobiology,* 25**,** 5-23.

ABBOTT, R., WHEAR, R., NIKOLAOU, V., BETHEL, A., COON, J. T., STEIN, K. & DICKENS, C. 2015. Tumour necrosis factor-α inhibitor therapy in chronic physical illness: A systematic review and meta-analysis of the effect on depression and anxiety. *Journal of psychosomatic research,* 79**,** 175-184.

ACABCHUK, R. L., SUN, Y., WOLFERZ JR, R., EASTMAN, M. B., LENNINGTON, J. B., SHOOK, B. A., WU, Q. & CONOVER, J. C. 2015. 3D modeling of the lateral ventricles and histological characterization of periventricular tissue in humans and mouse. *JoVE (Journal of Visualized Experiments)***,** e52328.

AKAISHI, T., NARIKAWA, K., SUZUKI, Y., MITSUZAWA, S., TSUKITA, K., KURODA, H., NAKASHIMA, I., FUJIHARA, K. & AOKI, M. 2015. Importance of the quotient of albumin, quotient of immunoglobulin G and Reibergram in inflammatory neurological disorders with disease-specific patterns of blood–brain barrier permeability. *Neurology and clinical Neuroscience,* 3**,** 94-100.

AKIRA, S., UEMATSU, S. & TAKEUCHI, O. 2006. Pathogen recognition and innate immunity. *Cell,* 124**,** 783-801.

ALBRECHT, D. S., NORMANDIN, M. D., SHCHERBININ, S., WOOTEN, D. W., SCHWARZ, A. J., ZÜRCHER, N. R., BARTH, V. N., GUEHL, N. J., AKEJU, O. & ATASSI, N. 2018. Pseudoreference regions for glial imaging with 11C-PBR28: investigation in 2 clinical cohorts. *Journal of Nuclear Medicine,* 59**,** 107-114.

ALEXANDER-BLOCH, A., GIEDD, J. N. & BULLMORE, E. 2013a. Imaging structural co-variance between human brain regions. *Nat Rev Neurosci,* 14**,** 322-36.

ALEXANDER-BLOCH, A., RAZNAHAN, A., BULLMORE, E. & GIEDD, J. 2013b. The convergence of maturational change and structural covariance in human cortical networks. *J Neurosci,* 33**,** 2889-99.

ALTHUBAITY, N., SCHUBERT, J., MARTINS, D., YOUSAF, T., NETTIS, M. A., MONDELLI, V., PARIANTE, C., HARRISON, N. A., BULLMORE, E. T. & DIMA, D. 2022. Choroid plexus enlargement is associated with neuroinflammation and reduction of blood brain barrier permeability in depression. *NeuroImage: Clinical,* 33**,** 102926.

AMANN, B. L., CANALES-RODRÍGUEZ, E., MADRE, M., RADUA, J., MONTE, G., ALONSO-LANA, S., LANDIN-ROMERO, R., MORENO-ALCÁZAR, A., BONNIN, C. & SARRÓ, S. 2016. Brain structural changes in schizoaffective disorder compared to schizophrenia and bipolar disorder. *Acta Psychiatrica Scandinavica,* 133**,** 23-33.

AMBREE, O., BERGINK, V., GROSSE, L., ALFERINK, J., DREXHAGE, H. A., ROTHERMUNDT, M., AROLT, V. & BIRKENHAGER, T. K. 2015. S100B Serum Levels Predict Treatment Response in Patients with Melancholic Depression. *Int J Neuropsychopharmacol,* 19**,** pyv103.

ANDERSSON, J. L., SKARE, S. & ASHBURNER, J. 2003. How to correct susceptibility distortions in spin-echo echo-planar images: application to diffusion tensor imaging. *Neuroimage,* 20**,** 870-888.

ANNEQUIN, M., WEILL, A., THOMAS, F. & CHAIX, B. 2015. Environmental and individual characteristics associated with depressive disorders and mental health care use. *Annals of Epidemiology,* 25**,** 605-612.

ARNATKEVICIUTE, A., FULCHER, B. D. & FORNITO, A. 2019. A practical guide to linking brain-wide gene expression and neuroimaging data. *Neuroimage,* 189**,** 353-367.

AROLT, V., PETERS, M., ERFURTH, A., WIESMANN, M., MISSLER, U., RUDOLF, S., KIRCHNER, H. & ROTHERMUNDT, M. 2003. S100B and response to treatment in major depression: a pilot study. *Eur Neuropsychopharmacol,* 13**,** 235-9.

ARORA, P., SAGAR, R., MEHTA, M., PALLAVI, P., SHARMA, S. & MUKHOPADHYAY, A. K. 2019. Serum S100B levels in patients with depression. *Indian journal of psychiatry,* 61**,** 70.

ASHBURNER, J. 2007. A fast diffeomorphic image registration algorithm. *Neuroimage,* 38**,** 95-113.

ASSAF, Y. & PASTERNAK, O. 2008. Diffusion tensor imaging (DTI)-based white matter mapping in brain research: a review. *Journal of molecular neuroscience,* 34**,** 51-61.

ATTWELLS, S., SETIAWAN, E., WILSON, A. A., RUSJAN, P. M., MILER, L., XU, C., HUTTON, C., HUSAIN, M. I., KISH, S., VASDEV, N., HOULE, S. & MEYER, J. H. 2019. Replicating predictive serum correlates of greater translocator protein distribution volume in brain. *Neuropsychopharmacology*.

BAGCHI, S., CHHIBBER, T., LAHOOTI, B., VERMA, A., BORSE, V. & JAYANT, R. D. 2019. In-vitro blood-brain barrier models for drug screening and permeation studies: an overview. *Drug Des Devel Ther,* 13**,** 3591-3605.

BAGLIONI, C., NANOVSKA, S., REGEN, W., SPIEGELHALDER, K., FEIGE, B., NISSEN, C., REYNOLDS, C. F. & RIEMANN, D. 2016. Sleep and mental disorders: A meta-analysis of polysomnographic research. *Psychological bulletin,* 142**,** 969-990.

BAI, S., GUO, W., FENG, Y., DENG, H., LI, G., NIE, H., GUO, G., YU, H., MA, Y. & WANG, J. 2020. Efficacy and safety of anti-inflammatory agents for the treatment of major depressive disorder: a systematic review and meta-analysis of randomised controlled trials. *Journal of Neurology, Neurosurgery & Psychiatry,* 91**,** 21-32.

BAINS, N. & ABDIJADID, S. 2022. Major depressive disorder. *StatPearls [Internet].* StatPearls Publishing.

BAKKER, E. N., BACSKAI, B. J., ARBEL-ORNATH, M., ALDEA, R., BEDUSSI, B., MORRIS, A. W., WELLER, R. O. & CARARE, R. O. 2016. Lymphatic clearance of the brain: perivascular, paravascular and significance for neurodegenerative diseases. *Cellular and molecular neurobiology,* 36**,** 181-194.

BARKHO, B. Z. & MONUKI, E. S. 2015. Proliferation of cultured mouse choroid plexus epithelial cells. *PLoS One,* 10**,** e0121738.

BARRECA, T., GANDOLFO, C., CORSINI, G., DEL SETTE, M., CATALDI, A., ROLANDI, E. & FRANCESCHINI, R. 2001. Evaluation of the secretory pattern of plasma arginine vasopressin in stroke patients. *Cerebrovascular Diseases,* 11**,** 113-118.

BARRETT, P. H., BELL, B. M., COBELLI, C., GOLDE, H., SCHUMITZKY, A., VICINI, P. & FOSTER, D. M. 1998. SAAM II: Simulation, Analysis, and Modeling Software for tracer and pharmacokinetic studies. *Metabolism,* 47**,** 484-92.

BAUMEISTER, D., AKHTAR, R., CIUFOLINI, S., PARIANTE, C. M. & MONDELLI, V. 2016. Childhood trauma and adulthood inflammation: a meta-analysis of peripheral C-reactive protein, interleukin-6 and tumour necrosis factor-alpha. *Mol Psychiatry,* 21**,** 642-9.

BAUMEISTER, D., RUSSELL, A., PARIANTE, C. M. & MONDELLI, V. 2014. Inflammatory biomarker profiles of mental disorders and their relation to clinical, social and lifestyle factors. *Social psychiatry and psychiatric epidemiology,* 49**,** 841-849.

BECHTER, K., REIBER, H., HERZOG, S., FUCHS, D., TUMANI, H. & MAXEINER, H. G. 2010. Cerebrospinal fluid analysis in affective and schizophrenic spectrum disorders: identification of subgroups with immune responses and blood-CSF barrier dysfunction. *J Psychiatr Res,* 44**,** 321-30.

BEKHBAT, M., CHU, K., LE, N.-A., WOOLWINE, B. J., HAROON, E., MILLER, A. H. & FELGER, J. C. 2018. Glucose and lipid-related biomarkers and the antidepressant response to infliximab in patients with treatment-resistant depression. *Psychoneuroendocrinology,* 98**,** 222-229.

BELMAKER, R. H. & AGAM, G. 2008. Major depressive disorder. *New England Journal of Medicine,* 358**,** 55-68.

BENVENISTE, H., HEERDT, P. M., FONTES, M., ROTHMAN, D. L. & VOLKOW, N. D. 2019. Glymphatic system function in relation to anesthesia and sleep states. *Anesthesia & Analgesia,* 128**,** 747-758.

BERGAMINO, M., KUPLICKI, R., VICTOR, T. A., CHA, Y. H. & PAULUS, M. P. 2017. Comparison of two different analysis approaches for DTI free-water corrected and uncorrected maps in the study of white matter microstructural integrity in individuals with depression. *Human brain mapping,* 38**,** 4690-4702.

BERGAMINO, M., PASTERNAK, O., FARMER, M., SHENTON, M. E. & HAMILTON, J. P. 2016. Applying a free-water correction to diffusion imaging data uncovers stress-related neural pathology in depression. *NeuroImage: Clinical,* 10**,** 336-342.

BERING, E. A. 1962. Circulation of the cerebrospinal fluid: demonstration of the choroid plexuses as the generator of the force for flow of fluid and ventricular enlargement. *Journal of neurosurgery,* 19**,** 405-413.

BERK, M. 2009. Sleep and depression-theory and practice. *Australian family physician,* 38**,** 302-304.

BETLAZAR, C., HARRISON-BROWN, M., MIDDLETON, R. J., BANATI, R. & LIU, G. J. 2018. Cellular Sources and Regional Variations in the Expression of the Neuroinflammatory Marker Translocator Protein (TSPO) in the Normal Brain. *Int J Mol Sci,* 19.

BETLAZAR, C., MIDDLETON, R. J., BANATI, R. & LIU, G.-J. 2020. The translocator protein (TSPO) in mitochondrial bioenergetics and immune processes. *Cells,* 9**,** 512.

BILLIAU, A. 2006. Anti-inflammatory properties of Type I interferons. *Antiviral research,* 71**,** 108-116.

BLOOM, D. E., CAFIERO, E., JANÉ-LLOPIS, E., ABRAHAMS-GESSEL, S., BLOOM, L. R., FATHIMA, S., FEIGL, A. B., GAZIANO, T., HAMANDI, A. & MOWAFI, M. 2012. The global economic burden of noncommunicable diseases. Program on the Global Demography of Aging.

BLOOMFIELD, P., BRIGADOI, S., RIZZO, G. & VERONESE, M. 2017. *Basic Neuroimaging: A Guide to the Methods and Their Applications*, CreateSpace Independent Publishing Platform.

BLOOMFIELD, P. S., SELVARAJ, S., VERONESE, M., RIZZO, G., BERTOLDO, A., OWEN, D. R., BLOOMFIELD, M. A., BONOLDI, I., KALK, N., TURKHEIMER, F., MCGUIRE, P., DE PAOLA, V. & HOWES, O. D. 2016. Microglial Activity in People at Ultra High Risk of Psychosis and in Schizophrenia: An [(11)C]PBR28 PET Brain Imaging Study. *Am J Psychiatry,* 173**,** 44-52.

BODNAR, C. N., MORGANTI, J. M. & BACHSTETTER, A. D. 2018. Depression following a traumatic brain injury: uncovering cytokine dysregulation as a pathogenic mechanism. *Neural regeneration research,* 13**,** 1693.

BORA, E., FORNITO, A., PANTELIS, C. & YÜCEL, M. 2012. Gray matter abnormalities in major depressive disorder: a meta-analysis of voxel based morphometry studies. *Journal of affective disorders,* 138**,** 9-18.

BOUYAGOUB, S., DOWELL, N. G., GABEL, M. & CERCIGNANI, M. 2021. Comparing multiband and singleband EPI in NODDI at 3 T: what are the implications for reproducibility and study sample sizes? *Magnetic Resonance Materials in Physics, Biology and Medicine,* 34**,** 499-511.

BRADBURY, M. W. & CSERR, H. F. 1985. Drainage of cerebral interstitial fluid and of cerebrospinal fluid into lymphatics. *Experimental Biology of the lymphatic circulation,* 9**,** 355-394.

BRINKER, T., STOPA, E., MORRISON, J. & KLINGE, P. 2014. A new look at cerebrospinal fluid circulation. *Fluids and Barriers of the CNS,* 11**,** 10.

BROSSERON, F., KRAUTHAUSEN, M., KUMMER, M. & HENEKA, M. T. 2014. Body fluid cytokine levels in mild cognitive impairment and Alzheimer's disease: a comparative overview. *Molecular neurobiology,* 50**,** 534-544.

BROWN, P., DAVIES, S., SPEAKE, T. & MILLAR, I. 2004. Molecular mechanisms of cerebrospinal fluid production. *Neuroscience,* 129**,** 955-968.

BROWNELL, G. L. 1999. A history of positron imaging. *Physics Research Laboratory, Massachusetts General Hospital, MIT,* 1.

BURGOS, N., CARDOSO, M. J., THIELEMANS, K., MODAT, M., PEDEMONTE, S., DICKSON, J., BARNES, A., AHMED, R., MAHONEY, C. J., SCHOTT, J. M., DUNCAN, J. S., ATKINSON, D., ARRIDGE, S. R., HUTTON, B. F. & OURSELIN, S. 2014. Attenuation correction synthesis for hybrid PET-MR scanners: application to brain studies. *IEEE Trans Med Imaging,* 33**,** 2332-41.

CAGNIN, A., KASSIOU, M., MEIKLE, S. R. & BANATI, R. B. 2007. Positron emission tomography imaging of neuroinflammation. *Neurotherapeutics,* 4**,** 443-452.

CATTANEO, A., GENNARELLI, M., UHER, R., BREEN, G., FARMER, A., AITCHISON, K. J., CRAIG, I. W., ANACKER, C., ZUNSZTAIN, P. A. & MCGUFFIN, P. 2013. Candidate genes expression profile associated with antidepressants response in the GENDEP study: differentiating between baseline 'predictors' and longitudinal 'targets'. *Neuropsychopharmacology,* 38**,** 377-385.

CHAMBERLAIN, S. R., CAVANAGH, J., DE BOER, P., MONDELLI, V., JONES, D. N., DREVETS, W. C., COWEN, P. J., HARRISON, N. A., POINTON, L. & PARIANTE, C. M. 2019. Treatment-resistant depression and peripheral C-reactive protein. *The British Journal of Psychiatry,* 214**,** 11-19.

CHEN, L., ELIAS, G., YOSTOS, M. P., STIMEC, B., FASEL, J. & MURPHY, K. 2015. Pathways of cerebrospinal fluid outflow: a deeper understanding of resorption. *Neuroradiology,* 57**,** 139-147.

CHEN, M.-K. & GUILARTE, T. R. 2008. Translocator protein 18 kDa (TSPO): Molecular sensor of brain injury and repair. *Pharmacology & Therapeutics,* 118**,** 1-17.

CHERRY, S. R., DAHLBOM, M., CHERRY, S. R. & DAHLBOM, M. 2006. *PET: physics, instrumentation, and scanners*, Springer.

CHO, I., CHANG, K., KIM, Y. H., KIM, S., YU, I. & HAN, M. 1998. MRI features of choroid plexitis. *Neuroradiology,* 40**,** 303-307.

CHOI, K. S., HOLTZHEIMER, P. E., FRANCO, A. R., KELLEY, M. E., DUNLOP, B. W., HU, X. P. & MAYBERG, H. S. 2014. Reconciling variable findings of white matter integrity in major depressive disorder. *Neuropsychopharmacology,* 39**,** 1332-1339.

CHURCHILL, N. W., CAVERZASI, E., GRAHAM, S. J., HUTCHISON, M. G. & SCHWEIZER, T. A. 2019. White matter during concussion recovery: Comparing diffusion tensor imaging (DTI) and neurite orientation dispersion and density imaging (NODDI). *Human brain mapping,* 40**,** 1908-1918.

CLARK-RAYMOND, A. & HALARIS, A. 2013. VEGF and depression: a comprehensive assessment of clinical data. *Journal of psychiatric research,* 47**,** 1080-1087.

CLARKE, W., MOUGIN, O., DRIVER, I., RUA, C., CARPENTER, A. & MUIR, K. 2018. The UK7T Network–optimized design of a multi-site, multivendor travelling heads study. *Proc 26th Meet Int Soc Magn Reson Med*.

COLLSTE, K., PLAVÉN-SIGRAY, P., FATOUROS-BERGMAN, H., VICTORSSON, P., SCHAIN, M., FORSBERG, A., AMINI, N., AEINEHBAND, S., ERHARDT, S. & HALLDIN, C. 2017. Lower levels of the glial cell marker TSPO in drug-naive first-episode psychosis patients as measured using PET and [11C] PBR28. *Molecular psychiatry,* 22**,** 850-856.

COLOMBO, E. & FARINA, C. 2016. Astrocytes: key regulators of neuroinflammation. *Trends in immunology,* 37**,** 608-620.

COUGHLIN, J. M., WANG, Y., MINN, I., BIENKO, N., AMBINDER, E. B., XU, X., PETERS, M. E., DOUGHERTY, J. W., VRANESIC, M. & KOO, S. M. 2017. Imaging of glial cell activation and white matter integrity in brains of active and recently retired national football league players. *JAMA neurology,* 74**,** 67-74.

CRAIGHEAD, W. E. & DUNLOP, B. W. 2014. Combination psychotherapy and antidepressant medication treatment for depression: for whom, when, and how. *Annual review of psychology,* 65**,** 267-300.

CROESE, T., CASTELLANI, G. & SCHWARTZ, M. 2021. Immune cell compartmentalization for brain surveillance and protection. *Nature immunology,* 22**,** 1083-1092.

D'MELLO, C., LE, T. & SWAIN, M. G. 2009. Cerebral microglia recruit monocytes into the brain in response to tumor necrosis factorα signaling during peripheral organ inflammation. *Journal of Neuroscience,* 29**,** 2089-2102.

DABITAO, D., MARGOLICK, J. B., LOPEZ, J. & BREAM, J. H. 2011. Multiplex measurement of proinflammatory cytokines in human serum: comparison of the Meso Scale Discovery electrochemiluminescence assay and the Cytometric Bead Array. *J Immunol Methods,* 372**,** 71-7.

DAHL, J., ORMSTAD, H., AASS, H. C. D., MALT, U. F., BENDZ, L. T., SANDVIK, L., BRUNDIN, L. & ANDREASSEN, O. A. 2014. The plasma levels of various cytokines are increased during ongoing depression and are reduced to normal levels after recovery. *Psychoneuroendocrinology,* 45**,** 77-86.

DAMKIER, H. H., BROWN, P. D. & PRAETORIUS, J. 2013. Cerebrospinal fluid secretion by the choroid plexus. *Physiological reviews,* 93**,** 1847-1892.

DANTZER, R. 2009. Cytokine, sickness behavior, and depression. *Immunology and Allergy Clinics,* 29**,** 247-264.

DANTZER, R. 2018. Neuroimmune interactions: from the brain to the immune system and vice versa. *Physiological reviews,* 98**,** 477-504.

DANTZER, R., CASTANON, N., LESTAGE, J., MOREAU, M. & CAPURON, L. 2006. Inflammation, sickness behaviour and depression. *Inflammation,* 12**,** 12.

DANTZER, R., O'CONNOR, J. C., FREUND, G. G., JOHNSON, R. W. & KELLEY, K. W. 2008. From inflammation to sickness and depression: when the immune system subjugates the brain. *Nature reviews neuroscience,* 9**,** 46-56.

DE LEON, M. J., LI, Y., OKAMURA, N., TSUI, W. H., SAINT-LOUIS, L. A., GLODZIK, L., OSORIO, R. S., FORTEA, J., BUTLER, T. & PIRRAGLIA, E. 2017. Cerebrospinal fluid clearance in Alzheimer disease measured with dynamic PET. *Journal of Nuclear Medicine,* 58**,** 1471-1476.

DEL BIGIO, M. R. 1995. The ependyma: a protective barrier between brain and cerebrospinal fluid. *Glia,* 14**,** 1-13.

DÉNES, Á., FERENCZI, S. & KOVÁCS, K. J. 2011. Systemic inflammatory challenges compromise survival after experimental stroke via augmenting brain inflammation, blood-brain barrier damage and brain oedema independently of infarct size. *Journal of neuroinflammation,* 8**,** 1-13.

DESIKAN, R. S., SEGONNE, F., FISCHL, B., QUINN, B. T., DICKERSON, B. C., BLACKER, D., BUCKNER, R. L., DALE, A. M., MAGUIRE, R. P., HYMAN, B. T., ALBERT, M. S. & KILLIANY, R. J. 2006. An automated labeling system for subdividing the human cerebral cortex on MRI scans into gyral based regions of interest. *Neuroimage,* 31**,** 968-80.

DEVORAK, J., TORRES-PLATAS, S. G., DAVOLI, M. A., PRUD'HOMME, J., TURECKI, G. & MECHAWAR, N. 2015. Cellular and molecular inflammatory profile of the choroid plexus in depression and suicide. *Frontiers in psychiatry,* 6**,** 138.

DI BIASE, M. A., KATABI, G., PIONTKEWITZ, Y., CETIN-KARAYUMAK, S., WEINER, I. & PASTERNAK, O. 2020. Increased extracellular free-water in adult male rats following in utero exposure to maternal immune activation. *Brain, behavior, and immunity,* 83**,** 283-287.

DI BIASE, M. A., ZALESKY, A., CETIN-KARAYUMAK, S., RATHI, Y., LV, J., BOERRIGTER, D., NORTH, H., TOONEY, P., PANTELIS, C. & PASTERNAK, O. 2021. Large-scale evidence for an association between peripheral inflammation and white matter free water in schizophrenia and healthy individuals. *Schizophrenia bulletin,* 47**,** 542-551.

DIELEMAN, N., KOEK, H. L. & HENDRIKSE, J. 2017. Short-term mechanisms influencing volumetric brain dynamics. *NeuroImage: Clinical,* 16**,** 507-513.

DOME, P., TELEKI, Z., RIHMER, Z., PETER, L., DOBOS, J., KENESSEY, I., TOVARI, J., TIMAR, J., PAKU, S. & KOVACS, G. 2009. Circulating endothelial progenitor cells and depression: a possible novel link between heart and soul. *Molecular psychiatry,* 14**,** 523-531.

DON, B. R. & KAYSEN, G. Poor nutritional status and inflammation: serum albumin: relationship to inflammation and nutrition. Seminars in dialysis, 2004. Wiley Online Library, 432-437.
DOORDUIN, J., DE VRIES, E. F., DIERCKX, R. A. & KLEIN, H. C. 2008. PET imaging of the peripheral benzodiazepine receptor: monitoring disease progression and therapy response in neurodegenerative disorders. *Current pharmaceutical design,* 14**,** 3297-3315.
DOWELL, N. G., BOUYAGOUB, S., TIBBLE, J., VOON, V., CERCIGNANI, M. & HARRISON, N. A. 2019. Interferon-alpha-Induced Changes in NODDI Predispose to the Development of Fatigue. *Neuroscience,* 403**,** 111-117.
DREXHAGE, R. C., HOOGENBOEZEM, T. H., VERSNEL, M. A., BERGHOUT, A., NOLEN, W. A. & DREXHAGE, H. A. 2011. The activation of monocyte and T cell networks in patients with bipolar disorder. *Brain, behavior, and immunity,* 25**,** 1206-1213.
EGOROVA, N., GOTTLIEB, E., KHLIF, M. S., SPRATT, N. J. & BRODTMANN, A. 2019. Choroid plexus volume after stroke. *International Journal of Stroke,* 14**,** 923-930.
ELWOOD, E., LIM, Z., NAVEED, H. & GALEA, I. 2017. The effect of systemic inflammation on human brain barrier function. *Brain Behav Immun,* 62**,** 35-40.
ENACHE, D., PARIANTE, C. M. & MONDELLI, V. 2019. Markers of central inflammation in major depressive disorder: A systematic review and meta-analysis of studies examining cerebrospinal fluid, positron emission tomography and post-mortem brain tissue. *Brain Behav Immun,* 81**,** 24-40.
ESPOSITO, P., GHEORGHE, D., KANDERE, K., PANG, X., CONNOLLY, R., JACOBSON, S. & THEOHARIDES, T. C. 2001. Acute stress increases permeability of the blood-brain-barrier through activation of brain mast cells. *Brain Res,* 888**,** 117-127.
FAULSTICH, M. E. 1991. Brain imaging in dementia of the Alzheimer type. *International journal of neuroscience,* 57**,** 39-49.
FEINSTEIN, A. 2011. Multiple sclerosis and depression. *Multiple Sclerosis Journal,* 17**,** 1276-1281.
FEINSTEIN, A., MAGALHAES, S., RICHARD, J.-F., AUDET, B. & MOORE, C. 2014. The link between multiple sclerosis and depression. *Nature Reviews Neurology,* 10**,** 507-517.
FELGER, J. C., HAROON, E., PATEL, T. A., GOLDSMITH, D. R., WOMMACK, E. C., WOOLWINE, B. J., LE, N. A., FEINBERG, R., TANSEY, M. G. & MILLER, A. H. 2018. What does plasma CRP tell us about peripheral and central inflammation in depression? *Mol Psychiatry*.
FERRARI, A. J., CHARLSON, F. J., NORMAN, R. E., PATTEN, S. B., FREEDMAN, G., MURRAY, C. J., VOS, T. & WHITEFORD, H. A. 2013. Burden of depressive disorders by country, sex, age, and year: findings from the global burden of disease study 2010. *PLoS medicine,* 10**,** e1001547.
FICK, R. H., DAIANU, M., PIZZOLATO, M., WASSERMANN, D., JACOBS, R. E., THOMPSON, P. M., TOWN, T. & DERICHE, R. Comparison of biomarkers in transgenic alzheimer rats using multi-shell diffusion MRI. International Conference on Medical Image Computing and Computer-Assisted Intervention, 2016. Springer, 187-199.
FISCHL, B., SALAT, D. H., BUSA, E., ALBERT, M., DIETERICH, M., HASELGROVE, C., VAN DER KOUWE, A., KILLIANY, R., KENNEDY, D. & KLAVENESS, S. 2002. Whole brain segmentation: automated labeling of neuroanatomical structures in the human brain. *Neuron,* 33**,** 341-355.
FLEISCHER, V., GONZALEZ-ESCAMILLA, G., CIOLAC, D., ALBRECHT, P., KÜRY, P., GRUCHOT, J., DIETRICH, M., HECKER, C., MÜNTEFERING, T. & BOCK, S. 2021. Translational value of choroid plexus imaging for tracking neuroinflammation in mice and humans. *Proceedings of the National Academy of Sciences,* 118.
FOURNIER, T., MEDJOUBI-N, N. & PORQUET, D. 2000. Alpha-1-acid glycoprotein. *Biochimica et Biophysica Acta (BBA) - Protein Structure and Molecular Enzymology,* 1482**,** 157-171.
FRIED, E. I., EPSKAMP, S., NESSE, R. M., TUERLINCKX, F. & BORSBOOM, D. 2016. What are'good'depression symptoms? Comparing the centrality of DSM and non-DSM symptoms of depression in a network analysis. *Journal of affective disorders,* 189**,** 314-320.

FRIED, E. I. & NESSE, R. M. 2015. Depression sum-scores don't add up: why analyzing specific depression symptoms is essential. *BMC medicine,* 13**,** 1-11.

FRIEDMAN, A., KAUFER, D., SHEMER, J., HENDLER, I., SOREQ, H. & TUR-KASPA, I. 1996. Pyridostigmine brain penetration under stress enhances neuronal excitability and induces early immediate transcriptional response. *Nat Med,* 2**,** 1382-5.

FRIEDRICH, M. J. 2017. Depression is the leading cause of disability around the world. *Jama,* 317**,** 1517-1517.

FRISK-HOLMBERG, M. & VAN DER KLEIJN, E. 1972. The relationship between the lipophilic nature of tricyclic neuroleptics and antidepressants, and histamine release. *Eur J Pharmacol,* 18**,** 139-47.

GABEREL, T., GAKUBA, C., GOULAY, R., DE LIZARRONDO, S. M., HANOUZ, J.-L., EMERY, E., TOUZE, E., VIVIEN, D. & GAUBERTI, M. 2014. Impaired glymphatic perfusion after strokes revealed by contrast-enhanced MRI: a new target for fibrinolysis? *Stroke,* 45**,** 3092-3096.

GAVARD, J. A., LUSTMAN, P. J. & CLOUSE, R. E. 1993. Prevalence of depression in adults with diabetes: an epidemiological evaluation. *Diabetes care,* 16**,** 1167-1178.

GELENBERG, A. J., FREEMAN, M., MARKOWITZ, J., ROSENBAUM, J., THASE, M., TRIVEDI, M. & VAN RHOADS, R. 2010. American Psychiatric Association practice guidelines for the treatment of patients with major depressive disorder. *Am J Psychiatry,* 167**,** 9-118.

GERNER, R. H., FAIRBANKS, L., ANDERSON, G. M., YOUNG, J. G., SCHEININ, M., LINNOILA, M., HARE, T. A., SHAYWITZ, B. A. & COHEN, D. J. 1984. CSF neurochemistry in depressed, manic, and schizophrenic patients compared with that of normal controls. *The American journal of psychiatry*.

GHERSI-EGEA, J.-F., STRAZIELLE, N., CATALA, M., SILVA-VARGAS, V., DOETSCH, F. & ENGELHARDT, B. 2018a. Molecular anatomy and functions of the choroidal blood-cerebrospinal fluid barrier in health and disease. *Acta neuropathologica,* 135**,** 337-361.

GHERSI-EGEA, J. F., STRAZIELLE, N., CATALA, M., SILVA-VARGAS, V., DOETSCH, F. & ENGELHARDT, B. 2018b. Molecular anatomy and functions of the choroidal blood-cerebrospinal fluid barrier in health and disease. *Acta Neuropathol,* 135**,** 337-361.

GIATTI, S., DIVICCARO, S., GARCIA-SEGURA, L. M. & MELCANGI, R. C. 2019. Sex differences in the brain expression of steroidogenic molecules under basal conditions and after gonadectomy. *Journal of neuroendocrinology,* 31**,** e12736.

GIMENO, D., KIVIMAKI, M., BRUNNER, E. J., ELOVAINIO, M., DE VOGLI, R., STEPTOE, A., KUMARI, M., LOWE, G. D., RUMLEY, A., MARMOT, M. G. & FERRIE, J. E. 2009. Associations of C-reactive protein and interleukin-6 with cognitive symptoms of depression: 12-year follow-up of the Whitehall II study. *Psychol Med,* 39**,** 413-23.

GOLDEN, J., O'DWYER, A. M. & CONROY, R. M. 2005. Depression and anxiety in patients with hepatitis C: prevalence, detection rates and risk factors. *General hospital psychiatry,* 27**,** 431-438.

GOLDIN, P. R., MCRAE, K., RAMEL, W. & GROSS, J. J. 2008. The neural bases of emotion regulation: reappraisal and suppression of negative emotion. *Biological psychiatry,* 63**,** 577-586.

GOYAL, M. S., HAWRYLYCZ, M., MILLER, J. A., SNYDER, A. Z. & RAICHLE, M. E. 2014. Aerobic glycolysis in the human brain is associated with development and neotenous gene expression. *Cell metabolism,* 19**,** 49-57.

GREEN, C., SHEN, X., STEVENSON, A. J., CONOLE, E. L., HARRIS, M. A., BARBU, M. C., HAWKINS, E. L., ADAMS, M. J., HILLARY, R. F. & LAWRIE, S. M. 2021. Structural brain correlates of serum and epigenetic markers of inflammation in major depressive disorder. *Brain, behavior, and immunity,* 92**,** 39-48.

GREEN, R. C., CUPPLES, L. A., KURZ, A., AUERBACH, S., GO, R., SADOVNICK, D., DUARA, R., KUKULL, W. A., CHUI, H. & EDEKI, T. 2003. Depression as a risk factor for Alzheimer disease: the MIRAGE Study. *Archives of neurology,* 60**,** 753-759.

GUDMUNDSSON, P., SKOOG, I., WAERN, M., BLENNOW, K., PALSSON, S., ROSENGREN, L. & GUSTAFSON, D. 2007. The relationship between cerebrospinal fluid biomarkers and depression in elderly women. *Am J Geriatr Psychiatry,* 15**,** 832-8.

GUENETTE, J. P., STERN, R. A., TRIPODIS, Y., CHUA, A. S., SCHULTZ, V., SYDNOR, V. J., SOMES, N., KARMACHARYA, S., LEPAGE, C. & WROBEL, P. 2018. Automated versus manual segmentation of brain region volumes in former football players. *Neuroimage: clinical,* 18**,** 888-896.

GUO, W.-B., LIU, F., CHEN, J.-D., XU, X.-J., WU, R.-R., MA, C.-Q., GAO, K., TAN, C.-L., SUN, X.-L. & XIAO, C.-Q. 2012a. Altered white matter integrity of forebrain in treatment-resistant depression: a diffusion tensor imaging study with tract-based spatial statistics. *Progress in Neuro-Psychopharmacology and Biological Psychiatry,* 38**,** 201-206.

GUO, W.-B., LIU, F., XUE, Z.-M., GAO, K., WU, R.-R., MA, C.-Q., LIU, Z.-N., XIAO, C.-Q., CHEN, H.-F. & ZHAO, J.-P. 2012b. Altered white matter integrity in young adults with first-episode, treatment-naive, and treatment-responsive depression. *Neuroscience letters,* 522**,** 139-144.

HAAPAKOSKI, R., MATHIEU, J., EBMEIER, K. P., ALENIUS, H. & KIVIMÄKI, M. 2015. Cumulative meta-analysis of interleukins 6 and 1β, tumour necrosis factor α and C-reactive protein in patients with major depressive disorder. *Brain, behavior, and immunity,* 49**,** 206-215.

HAMER, M., BATTY, G. D., MARMOT, M. G., SINGH-MANOUX, A. & KIVIMÄKI, M. 2011. Anti-depressant medication use and C-reactive protein: results from two population-based studies. *Brain, behavior, and immunity,* 25**,** 168-173.

HAMILTON, M. 1960. The Hamilton Depression Scale—accelerator or break on antidepressant drug discovery. *Psychiatry,* 23**,** 56-62.

HAN, K.-M., CHOI, S., JUNG, J., NA, K.-S., YOON, H.-K., LEE, M.-S. & HAM, B.-J. 2014. Cortical thickness, cortical and subcortical volume, and white matter integrity in patients with their first episode of major depression. *Journal of affective disorders,* 155**,** 42-48.

HANNESTAD, J., DELLAGIOIA, N. & BLOCH, M. 2011. The effect of antidepressant medication treatment on serum levels of inflammatory cytokines: a meta-analysis. *Neuropsychopharmacology,* 36**,** 2452-2459.

HANNESTAD, J., DELLAGIOIA, N., GALLEZOT, J.-D., LIM, K., NABULSI, N., ESTERLIS, I., PITTMAN, B., LEE, J.-Y., O'CONNOR, K. C. & PELLETIER, D. 2013. The neuroinflammation marker translocator protein is not elevated in individuals with mild-to-moderate depression: a [11C] PBR28 PET study. *Brain, behavior, and immunity,* 33**,** 131-138.

HARRISON, N. A., BRYDON, L., WALKER, C., GRAY, M. A., STEPTOE, A. & CRITCHLEY, H. D. 2009. Inflammation causes mood changes through alterations in subgenual cingulate activity and mesolimbic connectivity. *Biological psychiatry,* 66**,** 407-414.

HATTY, C. R., LE BRUN, A. P., LAKE, V., CLIFTON, L. A., LIU, G. J., JAMES, M. & BANATI, R. B. 2014. Investigating the interactions of the 18kDa translocator protein and its ligand PK11195 in planar lipid bilayers. *Biochimica et Biophysica Acta (BBA) - Biomembranes,* 1838**,** 1019-1030.

HAWRYLYCZ, M. J., LEIN, E. S., GUILLOZET-BONGAARTS, A. L., SHEN, E. H., NG, L., MILLER, J. A., VAN DE LAGEMAAT, L. N., SMITH, K. A., EBBERT, A. & RILEY, Z. L. 2012. An anatomically comprehensive atlas of the adult human brain transcriptome. *Nature,* 489**,** 391-399.

HEILIG, M. 2004. The NPY system in stress, anxiety and depression. *Neuropeptides,* 38**,** 213-224.

HEINEN, R., BOUVY, W. H., MENDRIK, A. M., VIERGEVER, M. A., BIESSELS, G. J. & DE BRESSER, J. 2016. Robustness of automated methods for brain volume measurements across different MRI field strengths. *PloS one,* 11**,** e0165719.

HERISSON, F., FRODERMANN, V., COURTIES, G., ROHDE, D., SUN, Y., VANDOORNE, K., WOJTKIEWICZ, G. R., MASSON, G. S., VINEGONI, C. & KIM, J. 2018. Direct vascular channels connect skull bone marrow and the brain surface enabling myeloid cell migration. *Nature neuroscience,* 21**,** 1209-1217.

HLADKY, S. B. & BARRAND, M. A. 2016. Fluid and ion transfer across the blood-brain and blood-cerebrospinal fluid barriers; a comparative account of mechanisms and roles. *Fluids Barriers CNS,* 13**,** 19.

HODES, G. E., KANA, V., MENARD, C., MERAD, M. & RUSSO, S. J. 2015. Neuroimmune mechanisms of depression. *Nat Neurosci,* 18**,** 1386-93.

HOLMES, S. E., HINZ, R., CONEN, S., GREGORY, C. J., MATTHEWS, J. C., ANTON-RODRIGUEZ, J. M., GERHARD, A. & TALBOT, P. S. 2018. Elevated translocator protein in anterior cingulate in major depression and a role for inflammation in suicidal thinking: a positron emission tomography study. *Biological psychiatry,* 83**,** 61-69.

HOWREN, M. B., LAMKIN, D. M. & SULS, J. 2009. Associations of depression with C-reactive protein, IL-1, and IL-6: a meta-analysis. *Psychosomatic medicine,* 71**,** 171-186.

HSUCHOU, H., KASTIN, A. J., MISHRA, P. K. & PAN, W. 2012. C-reactive protein increases BBB permeability: implications for obesity and neuroinflammation. *Cell Physiol Biochem,* 30**,** 1109-19.

HUANG, J. T. J., LEWEKE, F. M., OXLEY, D., WANG, L., HARRIS, N., KOETHE, D., GERTH, C. W., NOLDEN, B. M., GROSS, S., SCHREIBER, D., REED, B. & BAHN, S. 2006. Disease biomarkers in cerebrospinal fluid of patients with first-onset psychosis. *PLoS medicine,* 3**,** e428-e428.

IANCU, S. C., WONG, Y. M., RHEBERGEN, D., VAN BALKOM, A. J. & BATELAAN, N. M. 2020. Long-term disability in major depressive disorder: a 6-year follow-up study. *Psychological Medicine,* 50**,** 1644-1652.

ILIFF, J. J. & NEDERGAARD, M. 2013. Is there a cerebral lymphatic system? *Stroke,* 44**,** S93-5.

ILIFF, J. J., WANG, M., LIAO, Y., PLOGG, B. A., PENG, W., GUNDERSEN, G. A., BENVENISTE, H., VATES, G. E., DEANE, R. & GOLDMAN, S. A. 2012. A paravascular pathway facilitates CSF flow through the brain parenchyma and the clearance of interstitial solutes, including amyloid β. *Science translational medicine,* 4**,** 147ra111-147ra111.

ILIFF, J. J., WANG, M., ZEPPENFELD, D. M., VENKATARAMAN, A., PLOG, B. A., LIAO, Y., DEANE, R. & NEDERGAARD, M. 2013. Cerebral arterial pulsation drives paravascular CSF-interstitial fluid exchange in the murine brain. *J Neurosci,* 33**,** 18190-9.

ISUNG, J., MOBARREZ, F., NORDSTRÖM, P., ÅSBERG, M. & JOKINEN, J. 2012. Low plasma vascular endothelial growth factor (VEGF) associated with completed suicide. *The World Journal of Biological Psychiatry,* 13**,** 468-473.

JANA, A., WANG, X., LEASURE, J. W., MAGANA, L., WANG, L., KIM, Y.-M., DODIYA, H., TOTH, P. T., SISODIA, S. S. & REHMAN, J. 2022. Increased Type I interferon signaling and brain endothelial barrier dysfunction in an experimental model of Alzheimer's disease. *Scientific Reports,* 12**,** 16488.

JANG, B. S., KIM, H., LIM, S. W., JANG, K. W. & KIM, D. K. 2008. Serum S100B Levels and Major Depressive Disorder: Its Characteristics and Role in Antidepressant Response. *Psychiatry Investig,* 5**,** 193-8.

JESSEN, N. A., MUNK, A. S. F., LUNDGAARD, I. & NEDERGAARD, M. 2015. The glymphatic system: a beginner's guide. *Neurochemical research,* 40**,** 2583-2599.

JOHANSON, C. E. & JOHANSON, N. L. 2018. Choroid plexus blood-CSF barrier: major player in brain disease modeling and neuromedicine. *Journal of Neurology & Neuromedicine,* 3.

JOHNSTON, M. & PAPAICONOMOU, C. 2002. Cerebrospinal fluid transport: a lymphatic perspective. *Physiology,* 17**,** 227-230.

JORDÃO, M. J. C., SANKOWSKI, R., BRENDECKE, S. M., SAGAR, LOCATELLI, G., TAI, Y.-H., TAY, T. L., SCHRAMM, E., ARMBRUSTER, S. & HAGEMEYER, N. 2019. Single-cell profiling identifies myeloid cell subsets with distinct fates during neuroinflammation. *Science,* 363**,** eaat7554.

JOVICICH, J., CZANNER, S., HAN, X., SALAT, D., VAN DER KOUWE, A., QUINN, B., PACHECO, J., ALBERT, M., KILLIANY, R. & BLACKER, D. 2009. MRI-derived measurements of human subcortical, ventricular and intracranial brain volumes: reliability effects of scan sessions, acquisition sequences, data analyses, scanner upgrade, scanner vendors and field strengths. *Neuroimage,* 46**,** 177-192.

KALLAUR, A. P., LOPES, J., OLIVEIRA, S. R., REICHE, E. M. V., DE ALMEIDA, E. R. D., MORIMOTO, H. K., DE PEREIRA, W. L. C. J., ALFIERI, D. F., BORELLI, S. D. & KAIMEN-MACIEL, D. R. 2016. Immune-inflammatory and oxidative and nitrosative stress biomarkers of depression symptoms in subjects with multiple sclerosis: increased peripheral inflammation but less acute neuroinflammation. *Molecular neurobiology,* 53**,** 5191-5202.

KAMAGATA, K., ZALESKY, A., HATANO, T., UEDA, R., DI BIASE, M. A., OKUZUMI, A., SHIMOJI, K., HORI, M., CAEYENBERGHS, K. & PANTELIS, C. 2017. Gray matter abnormalities in idiopathic P arkinson's disease: Evaluation by diffusional kurtosis imaging and neurite orientation dispersion and density imaging. *Human brain mapping,* 38**,** 3704-3722.

KAPURAL, M., KRIZANAC-BENGEZ, L., BARNETT, G., PERL, J., MASARYK, T., APOLLO, D., RASMUSSEN, P., MAYBERG, M. & JANIGRO, D. 2002. Serum S-100β as a possible marker of blood–brain barrier disruption. *Brain research,* 940**,** 102-104.

KARIMY, J. K., ZHANG, J., KURLAND, D. B., THERIAULT, B. C., DURAN, D., STOKUM, J. A., FUREY, C. G., ZHOU, X., MANSURI, M. S. & MONTEJO, J. 2017. Inflammation-dependent cerebrospinal fluid hypersecretion by the choroid plexus epithelium in posthemorrhagic hydrocephalus. *Nature medicine,* 23**,** 997-1003.

KAUR, C., RATHNASAMY, G. & LING, E. A. 2016. The Choroid Plexus in Healthy and Diseased Brain. *J Neuropathol Exp Neurol,* 75**,** 198-213.

KEALY, J., GREENE, C. & CAMPBELL, M. 2020. Blood-brain barrier regulation in psychiatric disorders. *Neuroscience letters,* 726**,** 133664.

KENNEDY, S. H. 2022. Core symptoms of major depressive disorder: relevance to diagnosis and treatment. *Dialogues in clinical neuroscience*.

KHASAWNEH, A. H., GARLING, R. J. & HARRIS, C. A. 2018. Cerebrospinal fluid circulation: What do we know and how do we know it? *Brain circulation,* 4**,** 14.

KIESEPPÄ, T., EEROLA, M., MÄNTYLÄ, R., NEUVONEN, T., POUTANEN, V.-P., LUOMA, K., TUULIO-HENRIKSSON, A., JYLHÄ, P., MANTERE, O. & MELARTIN, T. 2010. Major depressive disorder and white matter abnormalities: a diffusion tensor imaging study with tract-based spatial statistics. *Journal of affective disorders,* 120**,** 240-244.

KIKINIS, R., GUTTMANN, C. R., METCALF, D., WELLS III, W. M., ETTINGER, G. J., WEINER, H. L. & JOLESZ, F. A. 1999. Quantitative follow-up of patients with multiple sclerosis using MRI: technical aspects. *Journal of Magnetic Resonance Imaging: An Official Journal of the International Society for Magnetic Resonance in Medicine,* 9**,** 519-530.

KIMURA, A. & KISHIMOTO, T. 2010. IL-6: regulator of Treg/Th17 balance. *European journal of immunology,* 40**,** 1830-1835.

KING, E., O'BRIEN, J., DONAGHY, P., WILLIAMS-GRAY, C. H., LAWSON, R. A., MORRIS, C. M., BARNETT, N., OLSEN, K., MARTIN-RUIZ, C. & BURN, D. 2019. Inflammation in mild cognitive impairment due to Parkinson's disease, Lewy body disease, and Alzheimer's disease. *International journal of geriatric psychiatry,* 34**,** 1244-1250.

KITZBICHLER, M. G., ARULDASS, A. R., BARKER, G. J., WOOD, T. C., DOWELL, N. G., HURLEY, S. A., MCLEAN, J., CORREIA, M., CLARKE, C. & POINTON, L. 2021. Peripheral inflammation is associated with micro-structural and functional connectivity changes in depression-related brain networks. *Molecular psychiatry***,** 1-9.

KÖHLER, O., BENROS, M. E., NORDENTOFT, M., FARKOUH, M. E., IYENGAR, R. L., MORS, O. & KROGH, J. 2014. Effect of anti-inflammatory treatment on depression, depressive symptoms,

and adverse effects: a systematic review and meta-analysis of randomized clinical trials. *JAMA psychiatry,* 71**,** 1381-1391.
KORCZAK, D., PEREIRA, S., KOULAJIAN, K., MATEJCEK, A. & GIACCA, A. 2011. Type 1 diabetes mellitus and major depressive disorder: evidence for a biological link. *Diabetologia,* 54**,** 2483-2493.
KORGAONKAR, M. S., GRIEVE, S. M., KOSLOW, S. H., GABRIELI, J. D., GORDON, E. & WILLIAMS, L. M. 2011. Loss of white matter integrity in major depressive disorder: Evidence using tract-based spatial statistical analysis of diffusion tensor imaging. *Human brain mapping,* 32**,** 2161-2171.
KOZNIEWSKA, E. & ROMANIUK, K. 2008. Vasopressin in vascular regulation and water homeostasis in the brain. *J Physiol Pharmacol,* 59**,** 109-116.
KRAGULJAC, N. V., ANTHONY, T., MONROE, W. S., SKIDMORE, F. M., MORGAN, C. J., WHITE, D. M., PATEL, N. & LAHTI, A. C. 2019. A longitudinal neurite and free water imaging study in patients with a schizophrenia spectrum disorder. *Neuropsychopharmacology,* 44**,** 1932-1939.
KRAGULJAC, N. V., GUERRERI, M., STRICKLAND, M. J. & ZHANG, H. 2022. Neurite Orientation Dispersion and Density Imaging (NODDI) in Psychiatric Disorders–A Systematic Literature Review and a Technical Note. *Biological Psychiatry Global Open Science*.
KRESS, B. T., ILIFF, J. J., XIA, M., WANG, M., WEI, H. S., ZEPPENFELD, D., XIE, L., KANG, H., XU, Q. & LIEW, J. A. 2014. Impairment of paravascular clearance pathways in the aging brain. *Annals of neurology,* 76**,** 845-861.
KRYSTAL, A. D., THAKUR, M. & ROTH, T. 2008. Sleep disturbance in psychiatric disorders: effects on function and quality of life in mood disorders, alcoholism, and schizophrenia. *Annals of Clinical Psychiatry,* 20**,** 39-46.
KUSCHE-VIHROG, K., URBANOVA, K., BLANQUE, A., WILHELMI, M., SCHILLERS, H., KLICHE, K., PAVENSTADT, H., BRAND, E. & OBERLEITHNER, H. 2011a. C-reactive protein makes human endothelium stiff and tight. *Hypertension,* 57**,** 231-7.
KUSCHE-VIHROG, K., URBANOVA, K., BLANQUÉ, A., WILHELMI, M., SCHILLERS, H., KLICHE, K., PAVENSTÄDT, H., BRAND, E. & OBERLEITHNER, H. 2011b. C-reactive protein makes human endothelium stiff and tight. *Hypertension,* 57**,** 231-237.
LACKIE, J. 2010. *A dictionary of biomedicine*, Oxford University Press.
LAKE, B. B., CHEN, S., SOS, B. C., FAN, J., KAESER, G. E., YUNG, Y. C., DUONG, T. E., GAO, D., CHUN, J., KHARCHENKO, P. V. & ZHANG, K. 2018. Integrative single-cell analysis of transcriptional and epigenetic states in the human adult brain. *Nat Biotechnol,* 36**,** 70-80.
LAMMERTSMA, A. A. & HUME, S. P. 1996. Simplified reference tissue model for PET receptor studies. *Neuroimage,* 4**,** 153-158.
LARSON, S., NEMOIANU, A., LAWRENCE, D. F., TROUP, M. A., GIONFRIDDO, M. R., POUSTI, B., SUN, H., RIAZ, F., WAGNER, E. S. & CHRONES, L. 2022. Characterizing primary care for patients with major depressive disorder using electronic health records of a US-based healthcare provider. *Journal of Affective Disorders,* 300**,** 377-384.
LEONARD, B. E. 2007. Inflammation, depression and dementia: are they connected? *Neurochemical research,* 32**,** 1749-1756.
LI, L., MA, N., LI, Z., TAN, L., LIU, J., GONG, G., SHU, N., HE, Z., JIANG, T. & XU, L. 2007. Prefrontal white matter abnormalities in young adult with major depressive disorder: a diffusion tensor imaging study. *Brain research,* 1168**,** 124-128.
LIASKOU, E., WILSON, D. V. & OO, Y. H. 2012. Innate immune cells in liver inflammation. *Mediators of inflammation,* 2012.
LIDDELOW, S. A. 2015. Development of the choroid plexus and blood-CSF barrier. *Frontiers in neuroscience,* 9**,** 32.

LINDSTRÖM, L. H. 1985. Low HVA and normal 5HIAA CSF levels in drug-free schizophrenic patients compared to healthy volunteers: correlations to symptomatology and family history. *Psychiatry Research,* 14**,** 265-273.
LISANTI, C. J., ASBACH, P. & BRADLEY, W. G. 2005. The ependymal "Dot-dash" sign: an MR imaging finding of early multiple sclerosis. *American journal of neuroradiology,* 26**,** 2033-2036.
LIZANO, P., LUTZ, O., LING, G., LEE, A. M., EUM, S., BISHOP, J. R., KELLY, S., PASTERNAK, O., CLEMENTZ, B., PEARLSON, G., SWEENEY, J. A., GERSHON, E., TAMMINGA, C. & KESHAVAN, M. 2019. Association of Choroid Plexus Enlargement With Cognitive, Inflammatory, and Structural Phenotypes Across the Psychosis Spectrum. *The American journal of psychiatry,* 176**,** 564-572.
LOCKHART, A., DAVIS, B., MATTHEWS, J. C., RAHMOUNE, H., HONG, G., GEE, A., EARNSHAW, D. & BROWN, J. 2003. The peripheral benzodiazepine receptor ligand PK11195 binds with high affinity to the acute phase reactant α1-acid glycoprotein: implications for the use of the ligand as a CNS inflammatory marker. *Nuclear medicine and biology,* 30**,** 199-206.
LOMBARDO, G., ENACHE, D., GIANOTTI, L., SCHATZBERG, A. F., YOUNG, A. H., PARIANTE, C. M. & MONDELLI, V. 2019. Baseline cortisol and the efficacy of antiglucocorticoid treatment in mood disorders: A meta-analysis. *Psychoneuroendocrinology,* 110**,** 104420.
LOTRICH, F. E. 2009. Major depression during interferon-α treatment: vulnerability and prevention. *Dialogues in clinical neuroscience,* 11**,** 417.
LOUVEAU, A., PLOG, B. A., ANTILA, S., ALITALO, K., NEDERGAARD, M. & KIPNIS, J. 2017. Understanding the functions and relationships of the glymphatic system and meningeal lymphatics. *J Clin Invest,* 127**,** 3210-3219.
LYALL, A. E., PASTERNAK, O., ROBINSON, D. G., NEWELL, D., TRAMPUSH, J. W., GALLEGO, J. A., FAVA, M., MALHOTRA, A. K., KARLSGODT, K. H. & KUBICKI, M. 2018. Greater extracellular free-water in first-episode psychosis predicts better neurocognitive functioning. *Molecular psychiatry,* 23**,** 701-707.
MAENG, S. H. & HONG, H. 2019. Inflammation as the potential basis in depression. *International Neurourology Journal,* 23**,** S63.
MAHARAJ, A. S., WALSHE, T. E., SAINT-GENIEZ, M., VENKATESHA, S., MALDONADO, A. E., HIMES, N. C., MATHARU, K. S., KARUMANCHI, S. A. & D'AMORE, P. A. 2008. VEGF and TGF-β are required for the maintenance of the choroid plexus and ependyma. *The Journal of experimental medicine,* 205**,** 491-501.
MARQUES, F. & SOUSA, J. C. 2015. The choroid plexus is modulated by various peripheral stimuli: implications to diseases of the central nervous system. *Frontiers in cellular neuroscience,* 9**,** 136.
MARQUES, F., SOUSA, J. C., COPPOLA, G., FALCAO, A. M., RODRIGUES, A. J., GESCHWIND, D. H., SOUSA, N., CORREIA-NEVES, M. & PALHA, J. A. 2009. Kinetic profile of the transcriptome changes induced in the choroid plexus by peripheral inflammation. *Journal of Cerebral Blood Flow & Metabolism,* 29**,** 921-932.
MARQUES, T. R., ASHOK, A. H., PILLINGER, T., VERONESE, M., TURKHEIMER, F. E., DAZZAN, P., SOMMER, I. E. C. & HOWES, O. D. 2019. Neuroinflammation in schizophrenia: meta-analysis of in vivo microglial imaging studies. *Psychol Med,* 49**,** 2186-2196.
MARTINEZ, J. M., GARAKANI, A., YEHUDA, R. & GORMAN, J. M. 2012. Proinflammatory and "resiliency" proteins in the CSF of patients with major depression. *Depression and anxiety,* 29**,** 32-38.
MARTINS, D., DIPASQUALE, O., VERONESE, M., TURKHEIMER, F., LOGGIA, M. L., MCMAHON, S., HOWARD, M. A. & WILLIAMS, S. C. R. 2021. Transcriptional and cellular signatures of cortical morphometric similarity remodelling in chronic pain. *bioRxiv***,** 2021.03.24.436777.
MASON, J. M., HANCOCK, H. C., CLOSE, H., MURPHY, J. J., FUAT, A., DE BELDER, M., SINGH, R., TEGGERT, A., WOOD, E., BRENNAN, G., HUSSAIN, N., KUMAR, N., MANSHANI, N.,

HODGES, D., WILSON, D. & HUNGIN, A. P. 2013. Utility of biomarkers in the differential diagnosis of heart failure in older people: findings from the heart failure in care homes (HFinCH) diagnostic accuracy study. *PLoS One,* 8**,** e53560.
MATCHAM, F., RAYNER, L., STEER, S. & HOTOPF, M. 2013. The prevalence of depression in rheumatoid arthritis: a systematic review and meta-analysis. *Rheumatology,* 52**,** 2136-2148.
MCCRONE, P., ROST, F., KOESER, L., KOUTOUFA, I., STEPHANOU, S., KNAPP, M., GOLDBERG, D., TAYLOR, D. & FONAGY, P. 2018. The economic cost of treatment-resistant depression in patients referred to a specialist service. *Journal of Mental Health,* 27**,** 567-573.
MECHAWAR, N. & SAVITZ, J. 2016. Neuropathology of mood disorders: do we see the stigmata of inflammation? *Translational psychiatry,* 6**,** e946-e946.
MEDZHITOV, R. & JANEWAY JR, C. A. 1997. Innate immunity: impact on the adaptive immune response. *Current opinion in immunology,* 9**,** 4-9.
MEEKER, R. B., WILLIAMS, K., KILLEBREW, D. A. & HUDSON, L. C. 2012. Cell trafficking through the choroid plexus. *Cell adhesion & migration,* 6**,** 390-396.
MENARD, C., PFAU, M. L., HODES, G. E., KANA, V., WANG, V. X., BOUCHARD, S., TAKAHASHI, A., FLANIGAN, M. E., ALEYASIN, H., LECLAIR, K. B., JANSSEN, W. G., LABONTE, B., PARISE, E. M., LORSCH, Z. S., GOLDEN, S. A., HESHMATI, M., TAMMINGA, C., TURECKI, G., CAMPBELL, M., FAYAD, Z. A., TANG, C. Y., MERAD, M. & RUSSO, S. J. 2017. Social stress induces neurovascular pathology promoting depression. *Nat Neurosci,* 20**,** 1752-1760.
METZLER-BADDELEY, C., MOLE, J. P., LEONAVICIUTE, E., SIMS, R., KIDD, E. J., ERTEFAI, B., KELSO-MITCHELL, A., GIDNEY, F., FASANO, F. & EVANS, J. 2019. Sex-specific effects of central adiposity and inflammatory markers on limbic microstructure. *Neuroimage,* 189**,** 793-803.
MEYERS, C. A., ALBITAR, M. & ESTEY, E. 2005. Cognitive impairment, fatigue, and cytokine levels in patients with acute myelogenous leukemia or myelodysplastic syndrome. *Cancer,* 104**,** 788-793.
MILLER, A. H., MALETIC, V. & RAISON, C. L. 2009. Inflammation and its discontents: the role of cytokines in the pathophysiology of major depression. *Biological psychiatry,* 65**,** 732-741.
MILLER, A. H. & RAISON, C. L. 2016. The role of inflammation in depression: from evolutionary imperative to modern treatment target. *Nature reviews immunology,* 16**,** 22-34.
MILLER, D. H., THOMPSON, A. J., MORRISSEY, S. P., MACMANUS, D. G., MOORE, S. G., KENDALL, B. E., MOSELEY, I. F. & MCDONALD, W. I. 1992. High dose steroids in acute relapses of multiple sclerosis: MRI evidence for a possible mechanism of therapeutic effect. *J Neurol Neurosurg Psychiatry,* 55**,** 450-3.
MIZUI, T., HATTORI, K., ISHIWATA, S., HIDESE, S., YOSHIDA, S., KUNUGI, H. & KOJIMA, M. 2019. Cerebrospinal fluid BDNF pro-peptide levels in major depressive disorder and schizophrenia. *Journal of psychiatric research,* 113**,** 190-198.
MOBASHERI, A. & MARPLES, D. 2004. Expression of the AQP-1 water channel in normal human tissues: a semiquantitative study using tissue microarray technology. *American Journal of Physiology-Cell Physiology*.
MONDELLI, V., VERNON, A. C., TURKHEIMER, F., DAZZAN, P. & PARIANTE, C. M. 2017. Brain microglia in psychiatric disorders. *The Lancet Psychiatry,* 4**,** 563-572.
MOSSER, D. M. & EDWARDS, J. P. 2008. Exploring the full spectrum of macrophage activation. *Nature reviews immunology,* 8**,** 958-969.
MOTIVALA, S. J., SARFATTI, A., OLMOS, L. & IRWIN, M. R. 2005. Inflammatory markers and sleep disturbance in major depression. *Psychosomatic medicine,* 67**,** 187-194.
MUCCIGROSSO, M. M., FORD, J., BENNER, B., MOUSSA, D., BURNSIDES, C., FENN, A. M., POPOVICH, P. G., LIFSHITZ, J., WALKER, F. R. & EIFERMAN, D. S. 2016. Cognitive deficits

develop 1 month after diffuse brain injury and are exaggerated by microglia-associated reactivity to peripheral immune challenge. *Brain, behavior, and immunity,* 54**,** 95-109.
MÜLLER, N. 2019. The Role of Intercellular Adhesion Molecule-1 in the Pathogenesis of Psychiatric Disorders. *Frontiers in pharmacology,* 10**,** 1251-1251.
MUNKHOLM, K. & PALUDAN-MÜLLER, A. S. 2021. Caution is advised when interpreting subgroup analyses. *Neuropsychopharmacology,* 46**,** 1551-1551.
NAGELHUS, E. A. & OTTERSEN, O. P. 2013. Physiological roles of aquaporin-4 in brain. *Physiological reviews,* 93**,** 1543-1562.
NAGGARA, O., RAYMOND, J., GUILBERT, F., ROY, D., WEILL, A. & ALTMAN, D. G. 2011. Analysis by categorizing or dichotomizing continuous variables is inadvisable: an example from the natural history of unruptured aneurysms. *American Journal of Neuroradiology,* 32**,** 437-440.
NAIR, A., VERONESE, M., XU, X., CURTIS, C., TURKHEIMER, F., HOWARD, R. & REEVES, S. 2016. Test-retest analysis of a non-invasive method of quantifying [(11)C]-PBR28 binding in Alzheimer's disease. *EJNMMI Res,* 6**,** 72.
NEMEROFF, C. B., WIDERLOV, E., BISSETTE, G., WALLEUS, H., KARLSSON, I., EKLUND, K., KILTS, C. D., LOOSEN, P. T. & VALE, W. 1984. Elevated concentrations of CSF corticotropin-releasing factor-like immunoreactivity in depressed patients. *Science,* 226**,** 1342-1344.
NERURKAR, L., SIEBERT, S., MCINNES, I. B. & CAVANAGH, J. 2019. Rheumatoid arthritis and depression: an inflammatory perspective. *The Lancet Psychiatry,* 6**,** 164-173.
NETTIS, M. A., LOMBARDO, G., HASTINGS, C., ZAJKOWSKA, Z., MARIANI, N., NIKKHESLAT, N., WORRELL, C., ENACHE, D., MCLAUGHLIN, A. & KOSE, M. 2021a. Augmentation therapy with minocycline in treatment-resistant depression patients with low-grade peripheral inflammation: results from a double-blind randomised clinical trial. *Neuropsychopharmacology***,** 1-10.
NETTIS, M. A., PARIANTE, C. M. & MONDELLI, V. 2021b. Reply to Drs Munkholm and Paludan-Müller's comment on our paper "Augmentation therapy with minocycline in treatment-resistant depression patients with low-grade peripheral inflammation: results from a double-blind randomised clinical trial". *Neuropsychopharmacology,* 46**,** 1552-1553.
NETTIS, M. A., VERONESE, M., NIKKHESLAT, N., MARIANI, N., LOMBARDO, G., SFORZINI, L., ENACHE, D., HARRISON, N. A., TURKHEIMER, F. & MONDELLI, V. 2020. PET imaging shows no changes in TSPO brain density after IFN-α immune challenge in healthy human volunteers. *Translational psychiatry,* 10**,** 1-11.
NOTTER, T., COUGHLIN, J., SAWA, A. & MEYER, U. 2018. Reconceptualization of translocator protein as a biomarker of neuroinflammation in psychiatry. *Molecular psychiatry,* 23**,** 36-47.
NOTTER, T., SCHALBETTER, S. M., CLIFTON, N. E., MATTEI, D., RICHETTO, J., THOMAS, K., MEYER, U. & HALL, J. 2020. Neuronal activity increases translocator protein (TSPO) levels. *Mol Psychiatry*.
OESTREICH, L. K., LYALL, A. E., PASTERNAK, O., KIKINIS, Z., NEWELL, D. T., SAVADJIEV, P., BOUIX, S., SHENTON, M. E., KUBICKI, M. & BANK, A. S. R. 2017. Characterizing white matter changes in chronic schizophrenia: A free-water imaging multi-site study. *Schizophrenia research,* 189**,** 153-161.
OESTREICH, L. K. & O'SULLIVAN, M. J. 2022. Transdiagnostic in vivo magnetic resonance imaging markers of neuroinflammation. *Biological Psychiatry: Cognitive Neuroscience and Neuroimaging*.
OESTREICH, L. K., WRIGHT, P. & O'SULLIVAN, M. J. 2020. Microstructural changes in the reward system are associated with post-stroke depression. *NeuroImage: Clinical,* 28**,** 102360.
OLIVEIRA, W. N., RIBEIRO, L. E., SCHRIEFFER, A., MACHADO, P., CARVALHO, E. M. & BACELLAR, O. 2014. The role of inflammatory and anti-inflammatory cytokines in the pathogenesis of human tegumentary leishmaniasis. *Cytokine,* 66**,** 127-132.

OLVET, D. M., DELAPARTE, L., YEH, F. C., DELORENZO, C., MCGRATH, P. J., WEISSMAN, M. M., ADAMS, P., FAVA, M., DECKERSBACH, T. & MCINNIS, M. G. 2016. A comprehensive examination of white matter tracts and connectometry in major depressive disorder. *Depression and anxiety,* 33**,** 56-65.

OPEL, N., CEARNS, M., CLARK, S., TOBEN, C., GROTEGERD, D., HEINDEL, W., KUGEL, H., TEUBER, A., MINNERUP, H. & BERGER, K. 2019. Large-scale evidence for an association between low-grade peripheral inflammation and brain structural alterations in major depression in the BiDirect study. *Journal of Psychiatry and Neuroscience,* 44**,** 423-431.

OSIMO, E. F., BAXTER, L. J., LEWIS, G., JONES, P. B. & KHANDAKER, G. M. 2019. Prevalence of low-grade inflammation in depression: a systematic review and meta-analysis of CRP levels. *Psychological medicine,* 49**,** 1958-1970.

OSIMO, E. F., PILLINGER, T., RODRIGUEZ, I. M., KHANDAKER, G. M., PARIANTE, C. M. & HOWES, O. D. 2020. Inflammatory markers in depression: a meta-analysis of mean differences and variability in 5,166 patients and 5,083 controls. *Brain, behavior, and immunity,* 87**,** 901-909.

OTTE, C., GOLD, S. M., PENNINX, B. W., PARIANTE, C. M., ETKIN, A., FAVA, M., MOHR, D. C. & SCHATZBERG, A. F. 2016. Major depressive disorder. *Nature reviews Disease primers,* 2**,** 1-20.

OUSMAN, S. S. & KUBES, P. 2012. Immune surveillance in the central nervous system. *Nature neuroscience,* 15**,** 1096-1101.

OWEN, D. R., YEO, A. J., GUNN, R. N., SONG, K., WADSWORTH, G., LEWIS, A., RHODES, C., PULFORD, D. J., BENNACEF, I., PARKER, C. A., STJEAN, P. L., CARDON, L. R., MOOSER, V. E., MATTHEWS, P. M., RABINER, E. A. & RUBIO, J. P. 2012. An 18-kDa translocator protein (TSPO) polymorphism explains differences in binding affinity of the PET radioligand PBR28. *J Cereb Blood Flow Metab,* 32**,** 1-5.

PAHWA, R., GOYAL, A. & JIALAL, I. 2021. Chronic inflammation. *StatPearls [Internet]*.

PANDEY, G. N., REN, X., RIZAVI, H. S. & ZHANG, H. 2015. Abnormal gene expression of proinflammatory cytokines and their receptors in the lymphocytes of patients with bipolar disorder. *Bipolar disorders,* 17**,** 636-644.

PAPADOPOULOS, V., BARALDI, M., GUILARTE, T. R., KNUDSEN, T. B., LACAPÈRE, J.-J., LINDEMANN, P., NORENBERG, M. D., NUTT, D., WEIZMAN, A. & ZHANG, M.-R. 2006. Translocator protein (18 kDa): new nomenclature for the peripheral-type benzodiazepine receptor based on its structure and molecular function. *Trends in pharmacological sciences,* 27**,** 402-409.

PARK, M.-G., KIM, M.-K., KIM, B.-K., BAIK, S. K. & PARK, K.-P. 2017. A case of contrast leakage mimicking intraventricular hemorrhage in a patient with intravenous thrombolysis. *Journal of Stroke and Cerebrovascular Diseases,* 26**,** e14-e17.

PASCO, J. A., NICHOLSON, G. C., WILLIAMS, L. J., JACKA, F. N., HENRY, M. J., KOTOWICZ, M. A., SCHNEIDER, H. G., LEONARD, B. E. & BERK, M. 2010. Association of high-sensitivity C-reactive protein with de novo major depression. *Br J Psychiatry,* 197**,** 372-7.

PASSARO, A. P., LEBOS, A. L., YAO, Y. & STICE, S. L. 2021. Immune response in neurological pathology: emerging role of central and peripheral immune crosstalk. *Frontiers in Immunology,* 12**,** 676621.

PASTERNAK, O., WESTIN, C.-F., DAHLBEN, B., BOUIX, S. & KUBICKI, M. 2015. The extent of diffusion MRI markers of neuroinflammation and white matter deterioration in chronic schizophrenia. *Schizophrenia research,* 161**,** 113-118.

PAUL, S., GALLAGHER, E., LIOW, J.-S., MABINS, S., HENRY, K., ZOGHBI, S. S., GUNN, R. N., KREISL, W. C., RICHARDS, E. M. & ZANOTTI-FREGONARA, P. 2019. Building a database for brain 18 kDa translocator protein imaged using [11C] PBR28 in healthy subjects. *Journal of Cerebral Blood Flow & Metabolism,* 39**,** 1138-1147.

PAUL, W. E. 2012. *Fundamental immunology*, Lippincott Williams & Wilkins.

PETRALIA, M. C., MAZZON, E., FAGONE, P., BASILE, M. S., LENZO, V., QUATTROPANI, M. C., DI NUOVO, S., BENDTZEN, K. & NICOLETTI, F. 2020. The cytokine network in the pathogenesis of major depressive disorder. Close to translation? *Autoimmunity reviews,* 19**,** 102504.

PINTZKA, C. W. S., HANSEN, T. I., EVENSMOEN, H. R. & HÅBERG, A. K. 2015. Marked effects of intracranial volume correction methods on sex differences in neuroanatomical structures: a HUNT MRI study. *Frontiers in neuroscience,* 9**,** 238.

PLOG, B. A. & NEDERGAARD, M. 2018. The Glymphatic System in Central Nervous System Health and Disease: Past, Present, and Future. *Annu Rev Pathol,* 13**,** 379-394.

POLLAK, T. A., DRNDARSKI, S., STONE, J. M., DAVID, A. S., MCGUIRE, P. & ABBOTT, N. J. 2018. The blood–brain barrier in psychosis. *The Lancet Psychiatry,* 5**,** 79-92.

POMARA, N., BRUNO, D., SARREAL, A. S., HERNANDO, R. T., NIERENBERG, J., PETKOVA, E., SIDTIS, J. J., WISNIEWSKI, T. M., MEHTA, P. D. & PRATICO, D. 2012. Lower CSF amyloid beta peptides and higher F2-isoprostanes in cognitively intact elderly individuals with major depressive disorder. *American Journal of Psychiatry,* 169**,** 523-530.

PRINZ, M. & PRILLER, J. 2017. The role of peripheral immune cells in the CNS in steady state and disease. *Nature neuroscience,* 20**,** 136-144.

QUAN, N. & BANKS, W. A. 2007. Brain-immune communication pathways. *Brain, behavior, and immunity,* 21**,** 727-735.

QUINTELA, T., ALBUQUERQUE, T., LUNDKVIST, G., CARMINE BELIN, A., TALHADA, D., GONÇALVES, I., CARRO, E. & SANTOS, C. R. 2018. The choroid plexus harbors a circadian oscillator modulated by estrogens. *Chronobiology International,* 35**,** 270-279.

RAISON, C., BORISOV, A., WOOLWINE, B., MASSUNG, B., VOGT, G. & MILLER, A. 2010. Interferon-α effects on diurnal hypothalamic–pituitary–adrenal axis activity: relationship with proinflammatory cytokines and behavior. *Molecular psychiatry,* 15**,** 535-547.

RAISON, C. L., CAPURON, L. & MILLER, A. H. 2006. Cytokines sing the blues: inflammation and the pathogenesis of depression. *Trends in immunology,* 27**,** 24-31.

RAISON, C. L., DEMETRASHVILI, M., CAPURON, L. & MILLER, A. H. 2005. Neuropsychiatric adverse effects of interferon-α. *CNS drugs,* 19**,** 105-123.

RAMEZANI, M., ABOLMAESUMI, P., TAHMASEBI, A., BOSMA, R., TONG, R., HOLLENSTEIN, T., HARKNESS, K. & JOHNSRUDE, I. 2015. Fusion analysis of first episode depression: Where brain shape deformations meet local composition of tissue. *NeuroImage: Clinical,* 7**,** 114-121.

RAMLACKHANSINGH, A. F., BROOKS, D. J., GREENWOOD, R. J., BOSE, S. K., TURKHEIMER, F. E., KINNUNEN, K. M., GENTLEMAN, S., HECKEMANN, R. A., GUNANAYAGAM, K. & GELOSA, G. 2011. Inflammation after trauma: microglial activation and traumatic brain injury. *Annals of neurology,* 70**,** 374-383.

RANSOHOFF, R. M., KIVISÄKK, P. & KIDD, G. 2003. Three or more routes for leukocyte migration into the central nervous system. *Nature Reviews Immunology,* 3**,** 569-581.

RASCHKE, F., BARRICK, T. R., JONES, T. L., YANG, G., YE, X. & HOWE, F. A. 2019. Tissue-type mapping of gliomas. *NeuroImage: Clinical,* 21**,** 101648.

RASMUSSEN, M. K., MESTRE, H. & NEDERGAARD, M. 2018. The glymphatic pathway in neurological disorders. *Lancet Neurol,* 17**,** 1016-1024.

REID, B. E., DI BIASE, M., POMPER, M. G., SHENTON, M. E., DU, Y., COUGHLIN, J. M. & PASTERNAK, O. Examining links between free water and a TSPO-PET marker of neuroinflammation. Proceedings of the ISMRM 27th Annual Meeting and Exhibition, 2019.

RENÚ, A., LAREDO, C., LOPEZ-RUEDA, A., LLULL, L., TUDELA, R., SAN-ROMAN, L., URRA, X., BLASCO, J., MACHO, J. & OLEAGA, L. 2017. Vessel Wall enhancement and blood–cerebrospinal fluid barrier disruption after mechanical thrombectomy in acute ischemic stroke. *Stroke,* 48**,** 651-657.

RICHARDS, D. A., EKERS, D., MCMILLAN, D., TAYLOR, R. S., BYFORD, S., WARREN, F. C., BARRETT, B., FARRAND, P. A., GILBODY, S. & KUYKEN, W. 2016. Cost and Outcome of Behavioural Activation versus Cognitive Behavioural Therapy for Depression (COBRA): a randomised, controlled, non-inferiority trial. *The Lancet,* 388**,** 871-880.

RICHARDS, E. M., ZANOTTI-FREGONARA, P., FUJITA, M., NEWMAN, L., FARMER, C., BALLARD, E. D., MACHADO-VIEIRA, R., YUAN, P., NICIU, M. J. & LYOO, C. H. 2018. PET radioligand binding to translocator protein (TSPO) is increased in unmedicated depressed subjects. *EJNMMI research,* 8**,** 1-9.

RICIGLIANO, V. A., MORENA, E., COLOMBI, A., TONIETTO, M., HAMZAOUI, M., POIRION, E., BOTTLAENDER, M., GERVAIS, P., LOUAPRE, C. & BODINI, B. 2021. Choroid plexus enlargement in inflammatory multiple sclerosis: 3.0-T MRI and translocator protein PET evaluation. *Radiology,* 301**,** 166-177.

RISBROUGH, V. B., VAUGHN, M. N. & FRIEND, S. F. 2022. Role of inflammation in traumatic brain injury–associated risk for neuropsychiatric disorders: state of the evidence and where do we go from here. *Biological psychiatry,* 91**,** 438-448.

ROSZKOWSKI, M. & BOHACEK, J. 2016. Stress does not increase blood-brain barrier permeability in mice. *J Cereb Blood Flow Metab,* 36**,** 1304-15.

ROTHHAMMER, V., MASCANFRONI, I. D., BUNSE, L., TAKENAKA, M. C., KENISON, J. E., MAYO, L., CHAO, C.-C., PATEL, B., YAN, R. & BLAIN, M. 2016. Type I interferons and microbial metabolites of tryptophan modulate astrocyte activity and central nervous system inflammation via the aryl hydrocarbon receptor. *Nature medicine,* 22**,** 586-597.

SACKEIM, H. A., AARONSON, S. T., BUNKER, M. T., CONWAY, C. R., DEMITRACK, M. A., GEORGE, M. S., PRUDIC, J., THASE, M. E. & RUSH, A. J. 2019. The assessment of resistance to antidepressant treatment: rationale for the antidepressant treatment history form: short form (ATHF-SF). *Journal of psychiatric research,* 113**,** 125-136.

SÁIZ-VÁZQUEZ, O., GRACIA-GARCÍA, P., UBILLOS-LANDA, S., PUENTE-MARTÍNEZ, A., CASADO-YUSTA, S., OLAYA, B. & SANTABÁRBARA, J. 2021. Depression as a risk factor for Alzheimer's disease: a systematic review of longitudinal meta-analyses. *Journal of Clinical Medicine,* 10**,** 1809.

SAKKA, L., COLL, G. & CHAZAL, J. 2011. Anatomy and physiology of cerebrospinal fluid. *European annals of otorhinolaryngology, head and neck diseases,* 128**,** 309-316.

SANDER, C., TORRADO-CARVAJAL, A., BOVO, S., HOOKER, J. & LOGGIA, M. Transient modulation of cerebral blood flow does not alter [C-11] PBR28 radiotracer binding. JOURNAL OF CEREBRAL BLOOD FLOW AND METABOLISM, 2019. SAGE PUBLICATIONS INC 2455 TELLER RD, THOUSAND OAKS, CA 91320 USA, 605-606.

SANJABI, S., ZENEWICZ, L. A., KAMANAKA, M. & FLAVELL, R. A. 2009. Anti-inflammatory and pro-inflammatory roles of TGF-β, IL-10, and IL-22 in immunity and autoimmunity. *Current opinion in pharmacology,* 9**,** 447-453.

SANMUGAM, K. 2015. Depression is a risk factor for Alzheimer disease-review. *Research Journal of Pharmacy and Technology,* 8**,** 1056.

SANTHA, P., VESZELKA, S., HOYK, Z., MESZAROS, M., WALTER, F. R., TOTH, A. E., KISS, L., KINCSES, A., OLAH, Z., SEPRENYI, G., RAKHELY, G., DER, A., PAKASKI, M., KALMAN, J., KITTEL, A. & DELI, M. A. 2015. Restraint Stress-Induced Morphological Changes at the Blood-Brain Barrier in Adult Rats. *Front Mol Neurosci,* 8**,** 88.

SANTOS, C., DUARTE, A., COSTA, A., TOMÁS, J., QUINTELA, T. & GONÇALVES, I. 2019. The senses of the choroid plexus. *Progress in Neurobiology,* 182**,** 101680.

SARTORIUS, N. 2022. Depression and diabetes. *Dialogues in clinical neuroscience*.

SAUNDERS, N. R., LIDDELOW, S. A. & DZIEGIELEWSKA, K. M. 2012. Barrier mechanisms in the developing brain. *Frontiers in pharmacology,* 3**,** 46.

SAVITZ, J., FRANK, M. B., VICTOR, T., BEBAK, M., MARINO, J. H., BELLGOWAN, P. S., MCKINNEY, B. A., BODURKA, J., TEAGUE, T. K. & DREVETS, W. C. 2013. Inflammation and neurological disease-related genes are differentially expressed in depressed patients with mood disorders and correlate with morphometric and functional imaging abnormalities. *Brain, behavior, and immunity,* 31**,** 161-171.

SCHEDLOWSKI, M., ENGLER, H. & GRIGOLEIT, J.-S. 2014. Endotoxin-induced experimental systemic inflammation in humans: a model to disentangle immune-to-brain communication. *Brain, behavior, and immunity,* 35**,** 1-8.

SCHMAAL, L., POZZI, E., HO, T. C., VAN VELZEN, L. S., VEER, I. M., OPEL, N., VAN SOMEREN, E. J., HAN, L. K., AFTANAS, L. & ALEMAN, A. 2020. ENIGMA MDD: seven years of global neuroimaging studies of major depression through worldwide data sharing. *Translational psychiatry,* 10**,** 1-19.

SCHROETER, M. L., ABDUL-KHALIQ, H., DIEFENBACHER, A. & BLASIG, I. E. 2002. S100B is increased in mood disorders and may be reduced by antidepressive treatment. *Neuroreport,* 13**,** 1675-8.

SCHUBERT, J., TONIETTO, M., TURKHEIMER, F., ZANOTTI-FREGONARA, P. & VERONESE, M. 2021a. Supervised clustering for TSPO PET imaging. *European Journal of Nuclear Medicine and Molecular Imaging***,** 1-12.

SCHUBERT, J., VERONESE, M., FRYER, T. D., MANAVAKI, R., KITZBICHLER, M. G., NETTIS, M., MONDELLI, V., PARIANTE, C. M., BULLMORE, E. T. & TURKHEIMER, F. E. 2020. A modest increase in 11C-PK11195-PET TSPO binding in depression is not associated with serum C-reactive protein or body mass index. *medRxiv*.

SCHUBERT, J. J., VERONESE, M., FRYER, T. D., MANAVAKI, R., KITZBICHLER, M. G., NETTIS, M. A., MONDELLI, V., PARIANTE, C. M., BULLMORE, E. T. & TURKHEIMER, F. E. 2021b. A modest increase in 11C-PK11195-PET TSPO binding in depression is not associated with serum C-reactive protein or body mass index. *Biological Psychiatry: Cognitive Neuroscience and Neuroimaging*.

SCHUBERT, J. J., VERONESE, M., FRYER, T. D., MANAVAKI, R., KITZBICHLER, M. G., NETTIS, M. A., MONDELLI, V., PARIANTE, C. M., BULLMORE, E. T. & WLAZLY, D. 2021c. A Modest Increase in 11C-PK11195-Positron Emission Tomography TSPO Binding in Depression Is Not Associated With Serum C-Reactive Protein or Body Mass Index. *Biological Psychiatry: Cognitive Neuroscience and Neuroimaging*.

SCHUBERT, J. J., VERONESE, M., MARCHITELLI, L., BODINI, B., TONIETTO, M., STANKOFF, B., BROOKS, D. J., BERTOLDO, A., EDISON, P. & TURKHEIMER, F. 2019. Dynamic 11C-PiB PET shows cerebrospinal fluid flow alterations in Alzheimer's disease and multiple sclerosis. *Journal of Nuclear Medicine***,** jnumed. 118.223834.

SCHWARTZ, M. & BARUCH, K. 2014. The resolution of neuroinflammation in neurodegeneration: leukocyte recruitment via the choroid plexus. *The EMBO journal,* 33**,** 7-22.

SEO, J.-S., MANTAS, I., SVENNINGSSON, P. & GREENGARD, P. 2021. Ependymal cells-CSF flow regulates stress-induced depression. *Molecular psychiatry,* 26**,** 7308-7315.

SETIAWAN, E., ATTWELLS, S., WILSON, A. A., MIZRAHI, R., RUSJAN, P. M., MILER, L., XU, C., SHARMA, S., KISH, S., HOULE, S. & MEYER, J. H. 2018. Association of translocator protein total distribution volume with duration of untreated major depressive disorder: a cross-sectional study. *The Lancet Psychiatry,* 5**,** 339-347.

SETIAWAN, E., WILSON, A. A., MIZRAHI, R., RUSJAN, P. M., MILER, L., RAJKOWSKA, G., SURIDJAN, I., KENNEDY, J. L., REKKAS, P. V. & HOULE, S. 2015. Role of translocator protein density, a marker of neuroinflammation, in the brain during major depressive episodes. *JAMA psychiatry,* 72**,** 268-275.

SHAH, N. J., NEEB, H., KIRCHEIS, G., ENGELS, P., HÄUSSINGER, D. & ZILLES, K. 2008. Quantitative cerebral water content mapping in hepatic encephalopathy. *Neuroimage,* 41**,** 706-717.

SHANKMAN, S. A., FUNKHOUSER, C. J., KLEIN, D. N., DAVILA, J., LERNER, D. & HEE, D. 2018. Reliability and validity of severity dimensions of psychopathology assessed using the Structured Clinical Interview for DSM-5 (SCID). *International journal of methods in psychiatric research,* 27**,** e1590.

SHECHTER, R., LONDON, A., VAROL, C., RAPOSO, C., CUSIMANO, M., YOVEL, G., ROLLS, A., MACK, M., PLUCHINO, S. & MARTINO, G. 2009. Infiltrating blood-derived macrophages are vital cells playing an anti-inflammatory role in recovery from spinal cord injury in mice. *PLoS medicine,* 6**,** e1000113.

SHEN, M. D. 2018. Cerebrospinal fluid and the early brain development of autism. *J Neurodev Disord,* 10**,** 39.

SIEGERT, R. J. & ABERNETHY, D. 2005. Depression in multiple sclerosis: a review. *Journal of Neurology, Neurosurgery & Psychiatry,* 76**,** 469-475.

SIERKSMA, A. S., VAN DEN HOVE, D. L., STEINBUSCH, H. W. & PRICKAERTS, J. 2010. Major depression, cognitive dysfunction and Alzheimer's disease: is there a link? *European Journal of Pharmacology,* 626**,** 72-82.

SINGH, R., MASON, S., LECKY, F. & DAWSON, J. 2018. Prevalence of depression after TBI in a prospective cohort: the SHEFBIT study. *Brain injury,* 32**,** 84-90.

SIYAHHAN, B., KNOBLOCH, V., DE ZÉLICOURT, D., ASGARI, M., SCHMID DANERS, M., POULIKAKOS, D. & KURTCUOGLU, V. 2014. Flow induced by ependymal cilia dominates near-wall cerebrospinal fluid dynamics in the lateral ventricles. *Journal of the Royal Society Interface,* 11**,** 20131189.

SKIPOR, J. & THIERY, J. C. 2008. The choroid plexus--cerebrospinal fluid system: undervaluated pathway of neuroendocrine signaling into the brain. *Acta Neurobiol Exp (Wars),* 68**,** 414-28.

SMITH, D. A. 2004. C-reactive protein was a moderate predictor of coronary heart disease. *ACP J Club,* 141**,** 51.

SOLÁR, P., ZAMANI, A., KUBÍČKOVÁ, L., DUBOVÝ, P. & JOUKAL, M. 2020. Choroid plexus and the blood–cerebrospinal fluid barrier in disease. *Fluids and Barriers of the CNS,* 17**,** 1-29.

SOLEIMANI, L., OQUENDO, M. A., SULLIVAN, G. M., MATHÉ, A. A. & MANN, J. J. 2014. Cerebrospinal fluid neuropeptide Y levels in major depression and reported childhood trauma. *International Journal of Neuropsychopharmacology,* 18**,** pyu023.

SONG, E., MAO, T., DONG, H., BOISSERAND, L. S. B., ANTILA, S., BOSENBERG, M., ALITALO, K., THOMAS, J.-L. & IWASAKI, A. 2020. VEGF-C-driven lymphatic drainage enables immunosurveillance of brain tumours. *Nature,* 577**,** 689-694.

SONINO, N., FAVA, G. A., RAFFI, A. R., BOSCARO, M. & FALLO, F. 1998. Clinical correlates of major depression in Cushing's disease. *Psychopathology,* 31**,** 302-6.

SOSVOROVA, L., KANCEVA, R., VCELAK, J., KANCHEVA, L., MOHAPL, M., STARKA, L. & HAVRDOVA, E. 2015. The comparison of selected cerebrospinal fluid and serum cytokine levels in patients with multiple sclerosis and normal pressure hydrocephalus. *Neuroendocrinol Lett,* 36**,** 564-571.

SPEER, K., UPTON, D., SEMPLE, S. & MCKUNE, A. 2018. Systemic low-grade inflammation in post-traumatic stress disorder: a systematic review. *Journal of inflammation research,* 11**,** 111.

SPINDLER, K. R. & HSU, T.-H. 2012. Viral disruption of the blood–brain barrier. *Trends in microbiology,* 20**,** 282-290.

SPROSTON, N. R. & ASHWORTH, J. J. 2018. Role of C-Reactive Protein at Sites of Inflammation and Infection. *Front Immunol,* 9**,** 754.

STIEGLITZ, J., TRUMBLE, B. C., THOMPSON, M. E., BLACKWELL, A. D., KAPLAN, H. & GURVEN, M. 2015. Depression as sickness behavior? A test of the host defense hypothesis in a high pathogen population. *Brain, behavior, and immunity,* 49**,** 130-139.

STRAWBRIDGE, R., ARNONE, D., DANESE, A., PAPADOPOULOS, A., VIVES, A. H. & CLEARE, A. 2015. Inflammation and clinical response to treatment in depression: a meta-analysis. *European Neuropsychopharmacology,* 25**,** 1532-1543.

STREIT, W. J. 2006. Microglial senescence: does the brain's immune system have an expiration date? *Trends in neurosciences,* 29**,** 506-510.

STREIT, W. J., MRAK, R. E. & GRIFFIN, W. S. T. 2004. Microglia and neuroinflammation: a pathological perspective. *Journal of neuroinflammation,* 1**,** 1-4.

STUHRMANN, A., SUSLOW, T. & DANNLOWSKI, U. 2011. Facial emotion processing in major depression: a systematic review of neuroimaging findings. *Biology of mood & anxiety disorders,* 1**,** 1-17.

SU, L., FALUYI, Y. O., HONG, Y. T., FRYER, T. D., MAK, E., GABEL, S., HAYES, L., SOTERIADES, S., WILLIAMS, G. B. & ARNOLD, R. 2016. Neuroinflammatory and morphological changes in late-life depression: the NIMROD study. *The British journal of psychiatry,* 209**,** 525-526.

SULLIVAN, G. M., MANN, J. J., OQUENDO, M. A., LO, E. S., COOPER, T. B. & GORMAN, J. M. 2006. Low cerebrospinal fluid transthyretin levels in depression: correlations with suicidal ideation and low serotonin function. *Biological psychiatry,* 60**,** 500-506.

SUN, T., CHEN, X., SHI, S., LIU, Q. & CHENG, Y. 2019. Peripheral blood and cerebrospinal fluid cytokine levels in Guillain Barre syndrome: a systematic review and meta-analysis. *Frontiers in Neuroscience,* 13**,** 717.

SVENNINGSSON, P., KIM, Y., WARNER-SCHMIDT, J., OH, Y.-S. & GREENGARD, P. 2013. p11 and its role in depression and therapeutic responses to antidepressants. *Nature Reviews Neuroscience,* 14**,** 673-680.

SZMYDYNGER-CHODOBSKA, J., STRAZIELLE, N., GANDY, J. R., KEEFE, T. H., ZINK, B. J., GHERSI-EGEA, J.-F. & CHODOBSKI, A. 2012. Posttraumatic invasion of monocytes across the blood—cerebrospinal fluid barrier. *Journal of cerebral blood flow & metabolism,* 32**,** 93-104.

TADAYON, E., PASCUAL-LEONE, A., PRESS, D., SANTARNECCHI, E. & INITIATIVE, A. S. D. N. 2020. Choroid plexus volume is associated with levels of CSF proteins: relevance for Alzheimer's and Parkinson's disease. *Neurobiology of aging,* 89**,** 108-117.

TAKIZAWA, K., MATSUMAE, M., HAYASHI, N., HIRAYAMA, A., SANO, F., YATSUSHIRO, S. & KURODA, K. 2018. The choroid plexus of the lateral ventricle as the origin of CSF pulsation is questionable. *Neurologia medico-chirurgica,* 58**,** 23-31.

TOMIYAMA, H., KOJI, Y., YAMBE, M., MOTOBE, K., SHIINA, K., GULNISA, Z., YAMAMOTO, Y. & YAMASHINA, A. 2005. Elevated C-reactive protein augments increased arterial stiffness in subjects with the metabolic syndrome. *Hypertension,* 45**,** 997-1003.

TORRES-PLATAS, S. G., CRUCEANU, C., CHEN, G. G., TURECKI, G. & MECHAWAR, N. 2014. Evidence for increased microglial priming and macrophage recruitment in the dorsal anterior cingulate white matter of depressed suicides. *Brain, behavior, and immunity,* 42**,** 50-59.

TOURNIER, B. B., TSARTSALIS, S., CEYZERIAT, K., MEDINA, Z., FRASER, B. H., GREGOIRE, M. C., KOVARI, E. & MILLET, P. 2019. Fluorescence-activated cell sorting to reveal the cell origin of radioligand binding. *J Cereb Blood Flow Metab***,** 271678X19860408.

TOWNEND, W. J., GUY, M. J., PANI, M. A., MARTIN, B. & YATES, D. W. 2002. Head injury outcome prediction in the emergency department: a role for protein S-100B? *J Neurol Neurosurg Psychiatry,* 73**,** 542-6.

TSAI, M.-C. & HUANG, T.-L. 2016. Increased activities of both superoxide dismutase and catalase were indicators of acute depressive episodes in patients with major depressive disorder. *Psychiatry research,* 235**,** 38-42.

TUISKU, J., PLAVÉN-SIGRAY, P., GAISER, E. C., AIRAS, L., AL-ABDULRASUL, H., BRÜCK, A., CARSON, R. E., CHEN, M.-K., COSGROVE, K. P. & EKBLAD, L. 2019. Effects of age, BMI and sex on the glial cell marker TSPO—A multicentre [11 C] PBR28 HRRT PET study. *European journal of nuclear medicine and molecular imaging,* 46**,** 2329-2338.

TURKHEIMER, F. E., ALTHUBAITY, N., SCHUBERT, J., NETTIS, M. A., COUSINS, O., DIMA, D., MONDELLI, V., BULLMORE, E. T., PARIANTE, C. & VERONESE, M. 2020. Increased serum peripheral C-reactive protein is associated with reduced brain barriers permeability of TSPO radioligands in healthy volunteers and depressed patients: implications for inflammation and depression. *Brain, Behavior, and Immunity*.

TURKHEIMER, F. E., EDISON, P., PAVESE, N., RONCAROLI, F., ANDERSON, A. N., HAMMERS, A., GERHARD, A., HINZ, R., TAI, Y. F. & BROOKS, D. J. 2007. Reference and target region modeling of [11C]-(R)-PK11195 brain studies. *Journal of Nuclear Medicine,* 48**,** 158-167.

TURKHEIMER, F. E., EDISON, P., PAVESE, N., RONCAROLI, F., HAMMERS, A., GERHARD, A., HINZ, R., TAI, Y. & BROOKS, D. 2006. Supervised reference region extraction for the quantification of [11C]-(R)-PK11195 brain studies. *NeuroImage,* 31**,** T18.

TURKHEIMER, F. E., RIZZO, G., BLOOMFIELD, P. S., HOWES, O., ZANOTTI-FREGONARA, P., BERTOLDO, A. & VERONESE, M. 2015. The methodology of TSPO imaging with positron emission tomography. *Biochemical Society transactions,* 43**,** 586-592.

TURKHEIMER, F. E., SELVARAJ, S., HINZ, R., MURTHY, V., BHAGWAGAR, Z., GRASBY, P., HOWES, O., ROSSO, L. & BOSE, S. K. 2012. Quantification of ligand PET studies using a reference region with a displaceable fraction: application to occupancy studies with [11C]-DASB as an example. *Journal of Cerebral Blood Flow & Metabolism,* 32**,** 70-80.

TURNER, C. A., THOMPSON, R. C., BUNNEY, W. E., SCHATZBERG, A. F., BARCHAS, J. D., MYERS, R. M., AKIL, H. & WATSON, S. J. 2014. Altered choroid plexus gene expression in major depressive disorder. *Front Hum Neurosci,* 8**,** 238.

TYRING, S., GOTTLIEB, A., PAPP, K., GORDON, K., LEONARDI, C., WANG, A., LALLA, D., WOOLLEY, M., JAHREIS, A. & ZITNIK, R. 2006. Etanercept and clinical outcomes, fatigue, and depression in psoriasis: double-blind placebo-controlled randomised phase III trial. *The Lancet,* 367**,** 29-35.

UHER, R., TANSEY, K. E., DEW, T., MAIER, W., MORS, O., HAUSER, J., DERNOVSEK, M. Z., HENIGSBERG, N., SOUERY, D. & FARMER, A. 2014. An inflammatory biomarker as a differential predictor of outcome of depression treatment with escitalopram and nortriptyline. *American Journal of Psychiatry,* 171**,** 1278-1286.

VAISHNAVI, S. N., VLASSENKO, A. G., RUNDLE, M. M., SNYDER, A. Z., MINTUN, M. A. & RAICHLE, M. E. 2010. Regional aerobic glycolysis in the human brain. *Proceedings of the National Academy of Sciences,* 107**,** 17757-17762.

VALKANOVA, V., EBMEIER, K. P. & ALLAN, C. L. 2013. CRP, IL-6 and depression: a systematic review and meta-analysis of longitudinal studies. *J Affect Disord,* 150**,** 736-44.

VARVEL, N. H., NEHER, J. J., BOSCH, A., WANG, W., RANSOHOFF, R. M., MILLER, R. J. & DINGLEDINE, R. 2016. Infiltrating monocytes promote brain inflammation and exacerbate neuronal damage after status epilepticus. *Proceedings of the National Academy of Sciences,* 113**,** E5665-E5674.

VASA, F., SEIDLITZ, J., ROMERO-GARCIA, R., WHITAKER, K. J., ROSENTHAL, G., VERTES, P. E., SHINN, M., ALEXANDER-BLOCH, A., FONAGY, P., DOLAN, R. J., JONES, P. B., GOODYER, I. M., CONSORTIUM, N., SPORNS, O. & BULLMORE, E. T. 2018. Adolescent Tuning of Association Cortex in Human Structural Brain Networks. *Cereb Cortex,* 28**,** 281-294.

VELDHUIS, W. B., DERKSEN, J. W., FLORIS, S., VAN DER MEIDE, P. H., DE VRIES, H. E., SCHEPERS, J., VOS, I. M., DIJKSTRA, C. D., KAPPELLE, L. J. & NICOLAY, K. 2003. Interferon-beta blocks infiltration of inflammatory cells and reduces infarct volume after ischemic stroke in the rat. *Journal of Cerebral Blood Flow & Metabolism,* 23**,** 1029-1039.

VERCELLINO, M., VOTTA, B., CONDELLO, C., PIACENTINO, C., ROMAGNOLO, A., MEROLA, A., CAPELLO, E., MANCARDI, G. L., MUTANI, R. & GIORDANA, M. T. 2008. Involvement of the choroid plexus in multiple sclerosis autoimmune inflammation: a neuropathological study. *Journal of neuroimmunology,* 199**,** 133-141.

VERONESE, M., REIS MARQUES, T., BLOOMFIELD, P. S., RIZZO, G., SINGH, N., JONES, D., AGUSHI, E., MOSSES, D., BERTOLDO, A. & HOWES, O. 2018. Kinetic modelling of [11C] PBR28 for 18 kDa translocator protein PET data: a validation study of vascular modelling in the brain using XBD173 and tissue analysis. *Journal of Cerebral Blood Flow & Metabolism,* 38**,** 1227-1242.

VICENTE-RODRÍGUEZ, M., SINGH, N., TURKHEIMER, F., PERIS-YAGUE, A., RANDALL, K., VERONESE, M., SIMMONS, C., HAJI-DHEERE, A. K., BORDOLOI, J. & SANDER, K. 2021. Resolving the cellular specificity of TSPO imaging in a rat model of peripherally-induced neuroinflammation. *Brain, behavior, and immunity,* 96**,** 154-167.

VICHAYA, E. G., MALIK, S., SOMINSKY, L., FORD, B. G., SPENCER, S. J. & DANTZER, R. 2020. Microglia depletion fails to abrogate inflammation-induced sickness in mice and rats. *Journal of Neuroinflammation,* 17**,** 1-14.

VILLA, A., GELOSA, P., CASTIGLIONI, L., CIMINO, M., RIZZI, N., PEPE, G., LOLLI, F., MARCELLO, E., SIRONI, L. & VEGETO, E. 2018. Sex-specific features of microglia from adult mice. *Cell reports,* 23**,** 3501-3511.

VINJE, V., RINGSTAD, G., LINDSTRØM, E. K., VALNES, L. M., ROGNES, M. E., EIDE, P. K. & MARDAL, K.-A. 2019. Respiratory influence on cerebrospinal fluid flow–a computational study based on long-term intracranial pressure measurements. *Scientific reports,* 9**,** 1-13.

VOGELZANGS, N., DUIVIS, H. E., BEEKMAN, A. T., KLUFT, C., NEUTEBOOM, J., HOOGENDIJK, W., SMIT, J. H., DE JONGE, P. & PENNINX, B. W. 2012. Association of depressive disorders, depression characteristics and antidepressant medication with inflammation. *Translational psychiatry,* 2**,** e79-e79.

WARACH, S., GAA, J., SIEWERT, B., WIELOPOLSKI, P. & EDELMAN, R. R. 1995. Acute human stroke studied by whole brain echo planar diffusion-weighted magnetic resonance imaging. *Annals of Neurology: Official Journal of the American Neurological Association and the Child Neurology Society,* 37**,** 231-241.

WATZLAWIK, J., WARRINGTON, A. E. & RODRIGUEZ, M. 2010. Importance of oligodendrocyte protection, BBB breakdown and inflammation for remyelination. *Expert review of neurotherapeutics,* 10**,** 441-457.

WEBER, M. D., GODBOUT, J. P. & SHERIDAN, J. F. 2017. Repeated Social Defeat, Neuroinflammation, and Behavior: Monocytes Carry the Signal. *Neuropsychopharmacology,* 42**,** 46-61.

WENGLER, K., CHEN, K., CANLI, T., DELORENZO, C., SCHWEITZER, M. E. & HE, X. 2019. Abnormal Blood-Brain Barrier Water Permeability in Major Depressive Disorder. *ISRM 27th, Montreal, QC, Canada*.

WERRY, E. L., BRIGHT, F. M., PIGUET, O., ITTNER, L. M., HALLIDAY, G. M., HODGES, J. R., KIERNAN, M. C., LOY, C. T., KRIL, J. J. & KASSIOU, M. 2019. Recent developments in TSPO PET imaging as a biomarker of neuroinflammation in neurodegenerative disorders. *International journal of molecular sciences,* 20**,** 3161.

WESTMAN, E., MUEHLBOECK, J.-S. & SIMMONS, A. 2012. Combining MRI and CSF measures for classification of Alzheimer's disease and prediction of mild cognitive impairment conversion. *Neuroimage,* 62**,** 229-238.

WHITAKER, K. J., VERTES, P. E., ROMERO-GARCIA, R., VASA, F., MOUTOUSSIS, M., PRABHU, G., WEISKOPF, N., CALLAGHAN, M. F., WAGSTYL, K., RITTMAN, T., TAIT, R., OOI, C., SUCKLING, J., INKSTER, B., FONAGY, P., DOLAN, R. J., JONES, P. B., GOODYER, I. M., CONSORTIUM, N. & BULLMORE, E. T. 2016. Adolescence is associated with genomically

patterned consolidation of the hubs of the human brain connectome. *Proc Natl Acad Sci U S A,* 113**,** 9105-10.

WIĘDŁOCHA, M., MARCINOWICZ, P., KRUPA, R., JANOSKA-JAŹDZIK, M., JANUS, M., DĘBOWSKA, W., MOSIOŁEK, A., WASZKIEWICZ, N. & SZULC, A. 2018. Effect of antidepressant treatment on peripheral inflammation markers–A meta-analysis. *Progress in Neuro-Psychopharmacology and Biological Psychiatry,* 80**,** 217-226.

WITCHER, K. G., BRAY, C. E., CHUNCHAI, T., ZHAO, F., O'NEIL, S. M., GORDILLO, A. J., CAMPBELL, W. A., MCKIM, D. B., LIU, X. & DZIABIS, J. E. 2021. Traumatic brain injury causes chronic cortical inflammation and neuronal dysfunction mediated by microglia. *Journal of Neuroscience,* 41**,** 1597-1616.

WIUM-ANDERSEN, M. K., ØRSTED, D. D., NIELSEN, S. F. & NORDESTGAARD, B. G. 2013. Elevated C-reactive protein levels, psychological distress, and depression in 73 131 individuals. *JAMA psychiatry,* 70**,** 176-184.

WOELFER, M., KASTIES, V., KAHLFUSS, S. & WALTER, M. 2019. The Role of Depressive Subtypes within the Neuroinflammation Hypothesis of Major Depressive Disorder. *Neuroscience,* 403**,** 93-110.

WOHLEB, E. S., POWELL, N. D., GODBOUT, J. P. & SHERIDAN, J. F. 2013. Stress-induced recruitment of bone marrow-derived monocytes to the brain promotes anxiety-like behavior. *J Neurosci,* 33**,** 13820-33.

WOLBURG, H. & LIPPOLDT, A. 2002. Tight junctions of the blood–brain barrier: development, composition and regulation. *Vascular pharmacology,* 38**,** 323-337.

WOLBURG, H. & PAULUS, W. 2010. Choroid plexus: biology and pathology. *Acta neuropathologica,* 119**,** 75-88.

WONG, M.-L. & LICINIO, J. 2001. Research and treatment approaches to depression. *Nature Reviews Neuroscience,* 2**,** 343-351.

WUNDERLICH, M. T., WALLESCH, C. W. & GOERTLER, M. 2004. Release of neurobiochemical markers of brain damage is related to the neurovascular status on admission and the site of arterial occlusion in acute ischemic stroke. *J Neurol Sci,* 227**,** 49-53.

WYSOKIŃSKI, A., MARGULSKA, A., STRZELECKI, D. & KŁOSZEWSKA, I. 2015. Levels of C-reactive protein (CRP) in patients with schizophrenia, unipolar depression and bipolar disorder. *Nordic journal of psychiatry,* 69**,** 346-353.

XIE, L., KANG, H., XU, Q., CHEN, M. J., LIAO, Y., THIYAGARAJAN, M., O'DONNELL, J., CHRISTENSEN, D. J., NICHOLSON, C. & ILIFF, J. J. 2013. Sleep drives metabolite clearance from the adult brain. *science,* 342**,** 373-377.

YANG, A. C., KERN, F., LOSADA, P. M., AGAM, M. R., MAAT, C. A., SCHMARTZ, G. P., FEHLMANN, T., STEIN, J. A., SCHAUM, N. & LEE, D. P. 2021. Dysregulation of brain and choroid plexus cell types in severe COVID-19. *Nature***,** 1-10.

YI, S. Y., BARNETT, B. R., TORRES-VELÁZQUEZ, M., ZHANG, Y., HURLEY, S. A., ROWLEY, P. A., HERNANDO, D. & YU, J.-P. J. 2019. Detecting microglial density with quantitative multi-compartment diffusion MRI. *Frontiers in neuroscience,* 13**,** 81.

YUSHKEVICH, P. A., PIVEN, J., HAZLETT, H. C., SMITH, R. G., HO, S., GEE, J. C. & GERIG, G. 2006. User-guided 3D active contour segmentation of anatomical structures: significantly improved efficiency and reliability. *Neuroimage,* 31**,** 1116-1128.

ZHANG, B., KIROV, S. & SNODDY, J. 2005. WebGestalt: an integrated system for exploring gene sets in various biological contexts. *Nucleic Acids Res,* 33**,** W741-8.

ZHANG, C., LIN, J., WEI, F., SONG, J., CHEN, W., SHAN, L., XUE, R., WANG, G., TAO, J. & ZHANG, G. 2018a. Characterizing the glymphatic influx by utilizing intracisternal infusion of fluorescently conjugated cadaverine. *Life sciences,* 201**,** 150-160.

ZHANG, E., INMAN, C. & WELLER, R. 1990. Interrelationships of the pia mater and the perivascular (Virchow-Robin) spaces in the human cerebrum. *Journal of anatomy,* 170**,** 111.

ZHANG, F. F., PENG, W., SWEENEY, J. A., JIA, Z. Y. & GONG, Q. Y. 2018b. Brain structure alterations in depression: Psychoradiological evidence. *CNS neuroscience & therapeutics,* 24**,** 994-1003.

ZHANG, H., SCHNEIDER, T., WHEELER-KINGSHOTT, C. A. & ALEXANDER, D. C. 2012. NODDI: practical in vivo neurite orientation dispersion and density imaging of the human brain. *Neuroimage,* 61**,** 1000-1016.

ZHANG, Z., TAN, Q., GUO, P., JIA, Z., LIU, X. & FENG, H. 2020. NLRP3 inflammasome-mediated cerebrospinal fluid hypersecretion in choroid plexus contributes to hydrocephalus after hemorrhage.

ZHOU, G., HOTTA, J., LEHTINEN, M. K., FORSS, N. & HARI, R. 2015. Enlargement of choroid plexus in complex regional pain syndrome. *Scientific reports,* 5**,** 1-5.

ZHOU, Y.-F., HUANG, J.-C., ZHANG, P., FAN, F.-M., CHEN, S., FAN, H.-Z., CUI, Y.-M., LUO, X.-G., TAN, S.-P. & WANG, Z.-R. 2020. Choroid plexus enlargement and allostatic load in schizophrenia. *Schizophrenia Bulletin,* 46**,** 722-731.

ZHU, X., WANG, X., XIAO, J., ZHONG, M., LIAO, J. & YAO, S. 2011. Altered white matter integrity in first-episode, treatment-naive young adults with major depressive disorder: a tract-based spatial statistics study. *Brain research,* 1369**,** 223-229.

12 Appendix

Appendix A:

Increased serum peripheral C-reactive protein is associated with reduced brain barriers permeability of TSPO radioligands in healthy volunteers an depressed patients: implications for inflammation and depression

Brain, Behavior, and Immunity 91 (2021) 487–497

Contents lists available at ScienceDirect

Brain Behavior and Immunity

journal homepage: www.elsevier.com/locate/ybrbi

Increased serum peripheral C-reactive protein is associated with reduced brain barriers permeability of TSPO radioligands in healthy volunteers and depressed patients: implications for inflammation and depression

Federico E. Turkheimer [a,*], Noha Althubaity [a], Julia Schubert [a], Maria A. Nettis [b], Oliver Cousins [a], Danai Dima [a,c], Valeria Mondelli [b], Edward T. Bullmore [d,e], Carmine Pariante [b], Mattia Veronese [a]

[a] Department of Neuroimaging, Institute of Psychiatry, Psychology and Neuroscience, King's College London, London, UK
[b] Department of Neuroimaging, Institute of Psychiatry, Psychology and Neuroscience, King's College London, London, UK
[c] Department of Psychology, School of Arts and Social Sciences, City, University of London, London, UK
[d] Department of Psychiatry, School of Clinical Medicine, University of Cambridge, UK
[e] Cambridgeshire and Peterborough NHS Foundation Trust, Cambridge, UK

ARTICLE INFO

Keywords:
Inflammation
Depression
BBB permeability
CSF
Choroid plexus
PET
Tracer percolation

ABSTRACT

The relationship between peripheral and central immunity and how these ultimately may cause depressed behaviour has been the focus of a number of imaging studies conducted with Positron Emission Tomography (PET). These studies aimed at testing the immune-mediated model of depression that proposes a direct effect of peripheral cytokines and immune cells on the brain to elicit a neuroinflammatory response via a leaky blood–brain barrier and ultimately depressive behaviour. However, studies conducted so far using PET radioligands targeting the neuroinflammatory marker 18 kDa translocator protein (TSPO) in patient cohorts with depression have demonstrated mild inflammatory brain status but no correlation between central and peripheral immunity.

To gain a better insight into the relationship between heightened peripheral immunity and neuroinflammation, we estimated blood-to-brain and blood-to-CSF perfusion rates for two TSPO radiotracers collected in two separate studies, one large cross-sectional study of neuroinflammation in normal and depressed cohorts (N = 51 patients and N = 25 controls) and a second study where peripheral inflammation in N = 7 healthy controls was induced via subcutaneous injection of interferon (IFN)-α. In both studies we observed a consistent negative association between peripheral inflammation, measured with c-reactive protein P (CRP), and radiotracer perfusion into and from the brain parenchyma and CSF. Importantly, there was no association of this effect with the marker of BBB leakage S100β, that was unchanged.

These results suggest a different model of peripheral-to-central immunity interaction whereas peripheral inflammation may cause a reduction in BBB permeability. This effect, on the long term, is likely to disrupt brain homeostasis and induce depressive behavioural symptoms.

1. Introduction

The relationship between peripheral and central inflammation and depressed behaviour has been investigated by a number of in vivo studies using Positron Emission Tomography (PET) and radioligands targeting the 18 kDa translocator protein (TSPO) in patients with depression. The TSPO is a mitochondrial protein that is expressed in a number of cells (endothelial, astrocyte as well as neurons) of the central nervous system (CNS) (Notter et al., 2020) but is particularly enriched in activated microglia, the brain-resident macrophages (Betlazar et al., 2018; Tournier et al., 2019). However, TSPO PET studies in depressed cohorts have returned mixed results demonstrating either negative (Zhang et al., 2018), null (Hannestad et al., 2013) or mild TSPO elevations (Holmes et al., 2018; Richards et al., 2018; Setiawan et al., 2015; Su et al., 2016; Zhang et al., 2018), with elevation being more evident in unmedicated subjects (Richards et al., 2018) and in those with suicidal

* Corresponding author: Institute of Psychiatry, Psychology and Neuroscience, King's College London Centre for Neuroimaging Sciences SE5 9RT London, UK.
E-mail address: federico.turkheimer@kcl.ac.uk (F.E. Turkheimer).

https://doi.org/10.1016/j.bbi.2020.10.025
Received 21 June 2020; Received in revised form 30 October 2020; Accepted 31 October 2020
Available online 5 November 2020

thoughts (Holmes et al., 2018). More importantly, so far no study has demonstrated a consistent and replicable association between TSPO brain concentration and peripheral inflammatory mediators (Enache et al., 2019; Mondelli et al., 2017). A positive association was found in a sample of 48 patients with major depressive disorder between plasma adiponectin (an anti-inflammatory protein) and TSPO PET imaging in anterior cingulate cortex, but the analysis was only exploratory and did not survive correction for multiple comparisons (Richards et al., 2018). More recently, a negative association between CRP and brain TSPO expression was found by Attwells (Attwells et al., 2019), suggesting that patients with depression and high peripheral inflammation would have less microglia activation than those with normal level blood CRP. This disagrees with the immune-mediated model of depression for which depressive symptoms can be induced by peripheral cytokines and immune cells acting on the brain to elicit a neuroinflammatory response via a leaky blood–brain barrier (BBB) (Dantzer, 2009; Miller and Raison, 2016; Schedlowski et al., 2014). The evidence above prompted us to re-evaluate the data collected in TSPO imaging studies in normal and depressed cohorts by focusing on the relationship with one particular peripheral inflammatory marker, C-reactive protein (CRP), in order to propose an alternative model for the mechanism of action between peripheral and CNS immunity.

Meta-analysis of cross-sectional and longitudinal studies on the relationship between peripheral immunity and depression have highlighted the relevance of pro-inflammatory cytokines such as tumour necrosis factor-α (TNF-α), interleukin-1β (IL-1β) and interleukin-6 (IL-6) but also of the acute phase protein, CRP (Valkanova et al., 2013). CRP is an acute phase reactant, a protein primarily made by the liver that is released into the blood within a few hours after tissue injury, the start of an infection or other inflammatory insults (Sproston and Ashworth, 2018). The concentration of CRP in blood has been increasingly used to quantify levels of systemic inflammation and associated levels of risks for a number of conditions, with concentrations>3 mg/L indicating a high risk of cardiovascular disease (Smith, 2004).

In-vitro and preclinical models have shown that high concentrations of CRP (10 to 20 mg/L) are associated with BBB disruption, increasing its permeability (Hsuchou et al., 2012). However, the clinical relevance of this literature to the in-vivo human context remains to be shown, as in most instances CRP levels in depressed cohorts are below the 10 mg/L mark, which is on the low to moderate spectrum of the peripheral inflammatory range (Elwood et al., 2017); in particular, we note that higher CRP levels increase BBB porosity to plasma proteins (measured as cerebrospinal fluid/serum albumin ratio) but only in those instances when CSF also exhibited abnormalities (Elwood et al., 2017). At the same time, other in-vitro work has reported that milder CRP plasma concentrations may stiffen endothelial cells and reduce endothelial permeability (Kusche-Vihrog et al., 2011; Tomiyama et al., 2005).

Hence, we hypothesized that, in normal volunteers and patients with depression but no other BBB impairment, the levels of CRP in the range observed in these cohorts (range 3–10 mg/l, equivalent to 'low-grade inflammation') are associated with reduced blood to brain permeability. To test this hypothesis, we evaluated previously acquired data on the perfusion of TSPO radiotracers across the blood–brain interface (e.g., the BBB) and the blood-cerebrospinal fluid (CSF) interface (e.g., the choroid plexus).

Specifically, we quantified radiotracer perfusion from blood into parenchyma (via the BBB) and from blood and parenchyma into the CSF (via epithelial barriers and the choroid plexus) from TSPO PET data collected in two separate studies, one large cross-sectional study of neuroinflammation in normal controls and depressed patients (Schubert et al., 2020b) and a second study where peripheral inflammation in normal volunteers was induced via subcutaneous injection of interferon (IFN)-α and CNS inflammation was measured with PET (Nettis et al., 2020).

2. Methods

2.1. Datasets

Two independent TSPO PET datasets collected from two separate neuroimaging studies were considered in this work.

Dataset 1 includes 51 subjects with major depressive disorder (MDD) (36/15 women/men; mean age: 36.2 ± 7.4 years) and 25 matched healthy controls (HC) (14/11 women/men; mean age: 37.3 ±7.8 years) as part of the Biomarkers in Depression Study (BIODEP, NIMA consortium, https://www.neuroimmunology.org.uk/) to investigate the contribution of neuroinflammation in depression. Patients aged 25 to 50 (inclusive) that were taking anti-depressant treatment and had a total Hamilton Depression (HAMD) score > 13 or were untreated and had a total HAMD > 17 were included. The final sample consisted of 9 untreated patients and 42 taking medications. MDD patients were further classified based on their blood CRP level, CRP > 3 mg/L corresponding to the *high CRP group* (20 patients, 36.9 ± 7.6 years) and CRP<=3mg/L corresponding to *low CRP group* (31 patients, 35.7 ± 7.2 years). Of the 9 untreated patients 4 were in the high CRP group and 5 in the low CRP group. In the treated group, 17 were in the high CRP group, 25 in the low CRP group. 33 patients were treatment resistant (15 and 18 respectively in the high and low CRP group) while of the remaining 9, 2 had high CRP values and 7 low. CRP concentrations for controls were no different to the ones for low CRP group (t = 0.017, p = 0.99). MDD cases and HC with a lifetime history of other neurological disorders, active drug and/or alcohol abuse, participation in clinical drug trials within the previous year, concurrent medication or medical disorder that could compromise the interpretation of results, and those who were pregnant or breast-feeding were excluded. HC subjects had no personal history of clinical depression requiring treatment and were age- and sex-matched with the patient group. On the contrary, BMI was significantly higher for the depression group (BMI_{MDD}: 27.2±4.0) kg/m; BMI_{HC} 24.2±4.8 kg/m^2; p-value = 0.001). For patients detailed characteristics and demographics please refer to Table S1 in Supplementary Materials and the original publication (Schubert et al., 2020a).

Dataset 2 includes data from 7 healthy males (demographic data presented in Table S2 in Supplementary Materials) to image microglia activation in the CNS before and ~ 24 h after one subcutaneous injection of the immune challenge IFN-α 2a (Roferon-A 3 million IU/0.5 ml solution for injection). The study aimed to investigate putative changes in brain microglia activity and their relationship with changes in peripheral inflammation and in mood. Eligible participants were non-smokers, drank no>5 alcohol drinks per week, had no history of significant medical illness and did not meet the criteria for any current or past psychiatric or substance-dependence diagnosis. Subjects were excluded if they had an infection in the last month or had regularly used anti-inflammatory drugs. All subjects were TSPO high-affinity binders (HABs) as determined by single-nucleotide polymorphism rs6971 genotyping (Owen et al., 2012).

All imaging protocols were approved by the local ethics committee and participants gave written informed consent prior to data collection.

2.2. Image acquisition and analysis

Dataset 1 - All subjects underwent 60-minute dynamic PET scan on a GE SIGNA PET/MR scanner (GE healthcare, Waukesha, USA) after an intravenous bolus injection of [^{11}C]PK11195 (target dose ~ 350 MBq, injected dose 361±53 MBq). Data were reconstructed using multi-subject atlas method and improvements for the MRI brain coil component (Burgos et al., 2014). Data were corrected for scatter, randoms and deadtime using the scanner GE software. No arterial blood data was collected during the PET imaging consistent with best practice of [^{11}C]PK11195 PET imaging (Turkheimer et al., 2007). Full experimental details are reported in the original reference (Schubert et al., 2020b).

Dataset 2 – All the subjects underwent two 90-minute dynamic PET scans on a Siemens Biograph™ True Point™ PET/CT scanner (Siemens Medical Systems, Germany) after receiving a bolus injection of [^{11}C]PBR28 (target dose ~350 Mbq, injected dose 341 ± 15). Images were reconstructed using filtered back projection and corrected tissue attenuation, scatter and random coincidences, and deadtime using scanner software. In parallel to the PET acquisition, arterial blood sampling was performed to generate metabolite-free arterial input function consistently with previous studies using the same tracer (Bloomfield et al., 2016). Ligand free-plasma fraction (fp), or the portion of [11C]PBR28 unbound to plasma proteins, was determined for all scans using a ultrafiltration-based method as previously described (Hannestad et al., 2013). Full experimental details are reported in the original reference (Nettis et al., 2020).

In both datasets, all subjects also had structural T1-weighted brain MRI, either collected during the PET acquisition as in *dataset 1* or acquired just before the PET session as in *dataset 2*. These MRI images were used for PET data processing including grey matter (GM) and white matter (WM) tissue segmentation, brain masking, and atlas-based region extraction. These pre-processing steps as well as the PET inter-frame motion correction were performed using MIAKAT™ (www.miakat.org) a MATLAB-based software combining tools from SPM12 and FSL for PET/MRI imaging analysis. For the [^{11}C]PK11195 PET studies TSPO density was assessed using BPnd parameter calculated by using a supervised clustering reference region approach (Turkheimer et al., 2007). For the [^{11}C]PBR28 PET study, instead, the tracer tissue kinetics was described with full compartmental modelling (Rizzo et al., 2019, 2014). The tracer blood to tissue exchange rate (K_1) and tracer volume of distribution (V_T) were used as main parameters of interest to measure the tracer perfusion and TSPO availability, respectively.

2.3. Quantification of blood to CSF tracer exchange

TSPO tracer exchange between blood and CSF through CP was calculated from the PET imaging using the validated analysis protocol defined in (de Leon et al., 2017; Schubert et al., 2019). The method has shown to be sensitive to CSF dynamics, returning evidence for altered CSF-mediated clearance in dementia and multiple sclerosis (de Leon et al., 2017; Schubert et al., 2019). Briefly, manual lateral ventricle ROIs were generated for all subjects using the subject T1-weighted structural MRI data and the ITK-SNAP (Yushkevich et al., 2006) (itksnap.org) snake tool, following previously described guidelines for lateral ventricle extraction (Acabchuk et al., 2015). The lateral ventricle ROIs were then eroded by two voxels (5.2 mm) using the erode function given by FSL's 'fslmaths' utility package in order to reduce partial volume effects of the surrounding tissues.

For both datasets, standardized uptake value ratios (SUVRs) at 60 min (activity at 60 mins normalized to counts of a reference region) and the area-under-curve from 30 to 60 min (AUC30-60, e.g. integrated activity between 30 and 60 mins) were calculated from the PET images using the eroded lateral ventricle activity as target region and supervised reference region (dataset 1) or whole brain gray matter (dataset 2) as normative region.

In dataset 2, for which metabolite-free arterial input function was also available, we implemented the compartmental modelling approach to quantitatively describe the rates of exchanges of the tracer from blood to lateral ventricle (*K1*), from tissue into lateral ventricle and clearance (*kClearance*) as well as the tracer specific biding in the lateral ventricle (*kon* and *koff*) (Fig. 1). The volume of distribution of the [11C]PBR28 into lateral ventricles was calculate as $V_T = K_1/\text{kClearance}*(1 + \text{kon}/\text{koff})$. Interestingly, it was not possible to model a specific tracer

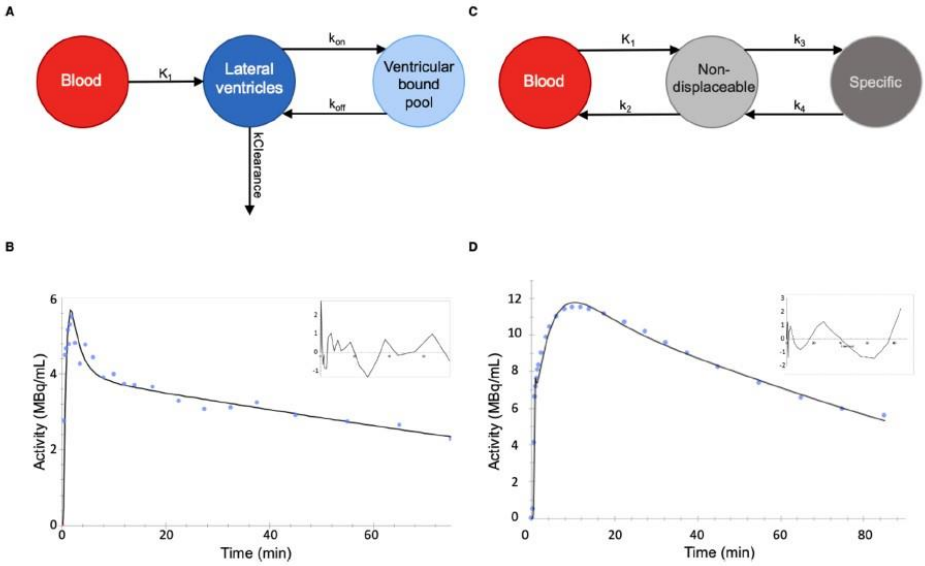

Fig. 1. – Compartmental modelling of [11C]PBR28 tracer kinetic in lateral ventricles and parenchima. *A) Compartmental model and kinetic parameters for lateral ventricles. K1 represents the rate of transfer from plasma to the lateral ventricles. Given the low extraction of the tracer into parenchima in respect to blood (1%) the rate of transfer of the tracer from parenchima into the lateral ventricles was not detectable. The parameters kon and koff represent the rate of binding on and off the binding sites in the ventricles; These binding sites are so far unknown and could be specific to cells lining the ventricles or simply non-specific (lipids) due to the lipophilicity of PET tracer. The parameter KClearance compounds the rate of flux of the tracer back into blood or, potentially in parenchima – the two not being identifiable by the model in this context B) Representative data fit for a ventricle time-course (healthy control, baseline). C) Compartmental model and kinetic parameters for brain parenchima. K1 and k2 represent the rates of transfer from blood to tissue and viceversa while k3 and k4 denote the on and off rate of binding to the TSPO. D) Representative data fit for a tissue time-course (healthy control, baseline).*

exchange from tissue to CSF as in the original paper describing [11C]PIB kinetics into lateral ventricles (Schubert et al., 2019); this may be possibly due to a poorer extraction of the radiotracer whereas the radioactivity in tissue is ~ 1% of the one in blood hence its contribution to the kinetics in the ventricles is undetectable (Sander et al., 2019). Consistent with a previous publication the model was implemented using SAAM II software (Barrett et al., 1998).

2.4. High sensitivity C-reactive protein measurement

For both datasets venous blood samples were collected from each participant for the CRP analysis In study 1, a venous blood sample was collected after an overnight fast between 08:00 and 10:00 on the day of clinical assessment. Participants had refrained from exercise for 72 h and had been lying supine for 0.5 h prior to venipuncture (Chamberlain et al., 2019). For study 2, blood samples were collected at the time of PET scans, i.e. at baseline and ~ 24 h after IFN-α injection. High sensitivity CRP (hsCRP) was used to assess peripheral inflammation. For both projects, blood samples were collected in clot activator containing tubes for measurement. The samples were allowed to coagulate for 30–60 min, then centrifuged at 1600 Relative Centrifugal Force (RCF) for 15 min. For the first project (BIODEP), serum samples were separated and transported to a central laboratory (Q2Solutions) where analyzed on the day of receipt. Samples were exposed to anti-CRP-antibodies on latex particles, and the increase in light absorption due to complex formation was used to quantify hsCRP levels, using Turbidimetry on Beckman Coulter AU analyzers. Inter and intra-assay coefficients of variation were < 10%. For the second project (FLAME) after blood collection, the serum was separated, aliquoted and stored at − 80 °C before use. It was later assayed on the Siemens Advia 2400 Chemistry analyser (Siemens Healthcare Diagnostics, Frimley, UK) (Mason et al., 2013). Inter and intra-assay co-efficient of variations were also < 10%. In both datasets there were no missing data or values below detection limit.

2.5. VEGF and S100B measurement

Forth both datasets, VEGF-A was measured using Meso Scale Discovery (MSD) V-PLEX sandwich immunoassays (Dabitao et al., 2011) (King et al., 2019), and plates read on an MSD QuickPlex SQ 120. The results were analyzed using MSD DISCOVERY WORKBENCH analysis software. Intra-assay and inter assay coefficients of variation were 7% and 15% respectively, and in both datasets there were no missing data or values below detection limit.

In dataset 2 (FLAME), levels of serum S100B protein were also measured in serum using a S100B kit distributed by Diasorin, Charles House, Toutley Road, Wokingham, Berkshire, run on the Liaison XL chemiluminescence analyser (Townend et al., 2002; Wunderlich et al., 2004). Intra assay and inter assay coefficients of variation were < 7% and < 11% respectively. 7% of the values were undetected, so they we replaced with the lowest detectable validated value (0.02 μg/L).

2.6. Statistics

SPSS (version 24.0, Chicago, IL) was used to perform all statistical analyses. Normality of the data was tested using Shapiro-Wilk's W test. For *dataset 1*, blood to CSF exchange measures (i.e. SUVR and AUC30-60) were investigated using analysis of variance (ANOVA) to test for group differences between MDD at different CRP levels and HC, while covarying for possible confounding factors (e.g. age, BMI, tracer injected dose, or lateral ventricle volume). Group differences were further investigated using independent samples t-tests, while association between CSF-mediated clearance measures and clinical scores (i.e. HAMDI, Childhood trauma, and Perceived Stress Score) were investigated with bivariate correlations. Correlation of these metrics with the blood brain barrier permeability marker (VEGF) was also explored. For *Dataset 2*, we explored the relationship between CRP changes and blood to CSF exchange measures (i.e. SUVR and AUC30-60) before and after IFN-α challenge. We also compared K_1 and V_T, both into lateral ventricles and GM parenchyma between conditions. The latter was chosen as representation of the parenchymal tracer uptake independent from lateral ventricles. Correlation of these metrics with CRP levels, peripheral tracer plasma protein binding and the blood brain barrier integrity markers (VEGF and S100β) were also explored. We implemented the Durbin-Watson test to exclude outliers.

3. Results

3.1. Marked inverse association between blood-to-CSF exchange measures and CRP in patients with depression

Results from the analysis of dataset 1 indicated the presence of a reduction in blood to CSF TSPO ligand perfusion as shown by an inverse association between blood-to-CSF exchange parameters and CRP, with higher CRP levels corresponding to both lower SUVR and lower AUC30-60 (Fig. 2) in both MDD patients and HC. Considering the whole population (HC and MDD cases) the association remained significant, once corrected for lateral ventricle volumes using partial correlations, for both SUVR ($r = -0.233$, $p = 0.045$) and AUC30-60 ($r = -0.277$, $p = 0.016$). There was no effect of age, tracer injected dose and subject BMI on SUVR and AUC30-60 ($p > 0.4$).

These associations between CRP and CSF radiotracer activity became stronger when considering MDD patients only, both with SUVR (partial correlation r: −0.300, $p = 0.034$) and AUC30-60 (partial correlation r: −0.338, $p = 0.016$). The relationship between these variables became more evident by restricting the analysis to the MDD-high CRP group only. Controlling for lateral ventricle volume SUVR-CRP partial correlation was −0.447 ($p = 0.048$) while AUC30-60-CRP partial correlation was −0.579 ($p = 0.007$). As for the whole sample, there was no effect of age, tracer injected dose and subject BMI on SUVR and AUC30-60 correlation with CRP.

No correlations between CSF-mediated clearance measures and HAMD score, Childhood trauma or Perceived Stress Score were found. The only exception was a significant inverse association between AUC30-60 and Childhood trauma score (Spearman's rho = -0.32, p: 0.02) although it did not survive to multiple comparison correction.

No correlation between VEGF and CSF-mediated clearance measures or CRP was found ($p > 0.5$) although MDD cases reported a significantly lower VEGF value compared to HC (t_{44}: 2.90, $p < 0.01$).

3.2. Peripheral CRP increase is associated with reduction of blood to brain tracer percolation after IFN-α injection

In dataset 2, we found that the CRP increase following the peripheral IFN-α challenge was inversely associated with lateral ventricular SUVR measure (R^2: 0.72, $p = 0.015$) (Fig. 3A) indicating a reduction on blood-to-CSF small molecule transfer. This association was not replicated by AUC30-60 (Fig. 3B).

The most interesting results were obtained for the compartmental modelling analysis (Fig. 3C and D). When we considered the tracer kinetics into lateral ventricle CSF we found that V_T was significantly reduced after IFN-α injection (-18 ± 12%, $p = 0.01$) while the difference in blood to CSF tracer transportation K_1 almost reached significance (–23 ± 20%, $p = 0.05$). No significant difference was found for the other kinetic parameters (kClearance: 1 ± 49%, kon: 19 ± 56%; koff: 2 ± 10%).

A stronger effect of interferon-α was found also for the kinetic parameters describing tracer kinetics with brain GM. Particularly we found that both blood to GM tracer transportation K_1 (-27 ± 15%, $p < 0.01$) and GM V_T (–22 ± 10%, $p < 0.01$) were significantly reduced after the challenge. Given the effect that blood proteins have on the TSPO tracer availability (Lockhart et al., 2003), we explored whether these reductions were associated with CRP changes or with tracer plasma

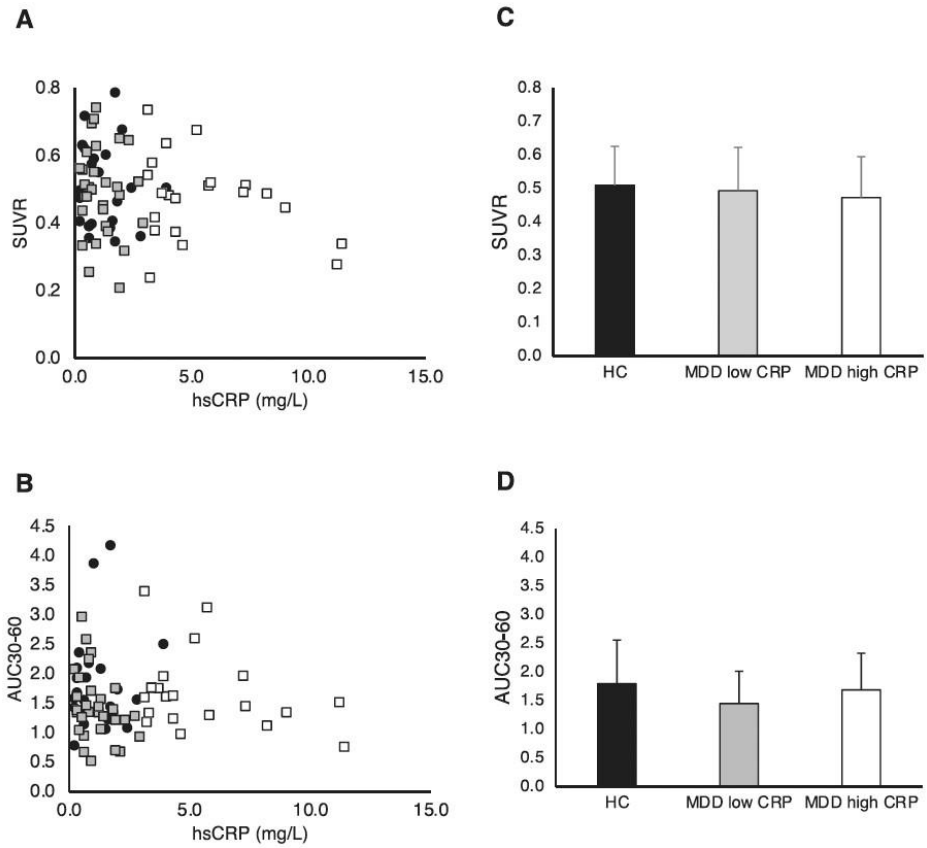

Fig. 2. – CSF-mediated clearance parameters and peripheral CRP in MDD. The results refer to [11C]PK11195 PET study (dataset 1). Patients are identified by low CRP group (<3mg/L, grey bar) and high CRP group (>3mg/L, white bar). Healthy matched controls are reported in black. Panel A and B show the distribution of SUVR (activity at 60 mins normalized to counts of a reference region) and AUC30-60 (total integrated activity between 30 and 60 mins) as function of CRP, respectively. Panel C and D show the SUVR and AUC30-60 group averages and standard deviations.

protein binding (Fig. 4). We found that both variables were associated with reduction of tracer percolation into GM (Pearson's R = -0.73, $p < 0.01$) and into lateral ventricle CSF (Spearman rho = -0.53, p = 0.04).

Given the collinearity between plasma protein binding and CRP ($R^2 = 0.32$, p = 0.03) we studied their interaction with K_1 as the dependent variable. Partial regression between K_1 and CRP controlling for plasma protein binding (fp) showed significant association for GM tissue (Pearson's R = -0.65,$p < 0.01$) but not for CSF (Spearman rho = -0.37, p = 0.11). However, when we directly corrected the transfer rate K_1 by multiplication with fp, we still found the same significant associations between the tracer perfusion and CRP for both CSF and GM.

In term of BBB permeability markers, there were positive associations between VEGF and K_1 parameters (R = 0.63, p = 0.02 for CSF and R = 0.53, p = 0.05 for GM) but no association was found between S100β and any kinetic parameter (both K_1 and tracer clearance from lateral ventricle) (Fig. 5). Interestingly S100β and VEGF were positively associated (R = 0.55, p = 0.04) but only VEGF was significantly reduced after interferon-α (from 134.5 ± 52.5 at 1 h before IFN-α to 93.5 ± 34.9 at 24 h after; paired *t*-test, t = 5.15, p = 0.002).

4. Discussion

This work has demonstrated that, contrary to expectations, high levels of the peripheral inflammatory marker CRP are associated with reduced influx of TSPO PET radiotracers into brain spaces. Influx rates K1, whether they represent the rate of transfer of the tracer from plasma to parenchyma through the BBB or from blood to the CSF through the choroid plexus, are the product of two factors: cerebral blood flow (*CBF*) and tracer extraction (*E*). Hence reduction in influx in the MDD cohorts can be explained by reduction of either *CBF* or *E* or both. A review of the literature seems to point to a likely reduction in extraction; a very recent MRI imaging technique called IDEALS (intrinsic diffusivity encoding of arterial labeled spin) (Wengler et al., 2019a) now allows the direct and simultaneous measurement of *CBF* and BBB water extraction. Preliminary data obtained with IDEALS indicate that in MDD *CBF* is unchanged but *E* is reduced by about 20% (Wengler et al., 2019b).

It is important to note that BBB permeability of water is not the same as the permeability of a PET radioligand. The BBB is constituted by three layers; the endothelial layer where cell-to-cell contact is through the tight junctions, the basal membrane upon which the endothelial cells lie,

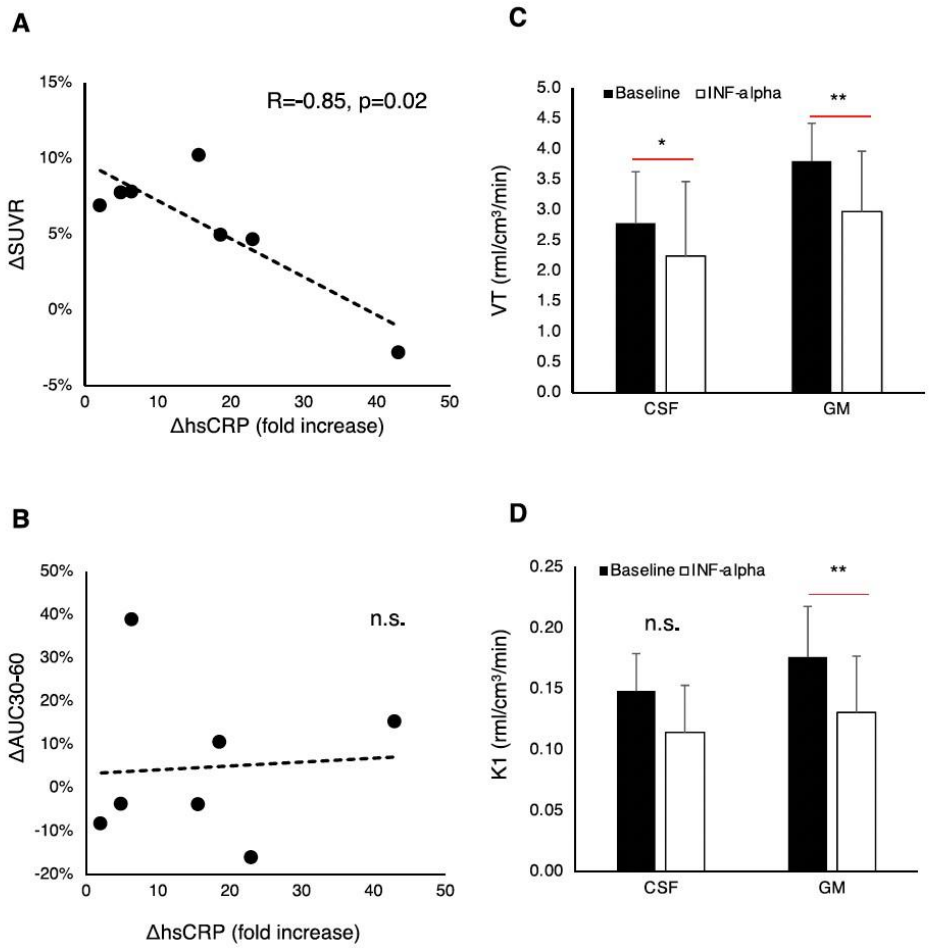

Fig. 3. - *CSF-mediated clearance after IFN-α immune challenge. The results refer to [11C]PBR28 PET study (dataset 2). A) Association between CRP and SUVR variations at baseline and after 24 h IFN-α injection. B) Association between CRP and AUC30-60 variations at baseline and after 24 h IFN-α injection. C) Comparison of the volume of distributions (V_T) for GM and lateral ventricle CSF at baseline and after 24 h IFN-α injection. D) Comparison of blood to tissue rates (K_1) for GM and lateral ventricle CSF at baseline and after 24 h IFN-α injection.*

and the final layer made of pericytes and the astrocytic end-feet (Hladky and Barrand, 2016). Aqueous transport across the endothelial layer is thought to be paracellular across the tight junction while PET radioligands, that are generally quite lipophilic, are thought to use a transcellular route (Bagchi et al., 2019). Less is known about the transfer of substances through the remaining layers and a number of models considering passage through the clefts between astrocytic end-feet or through aquaporin channels have been proposed (Hladky and Barrand, 2016). Data so far do not allow the clarification of the mechanism involved in the observed changes in permeability in MDD and further studies are granted.

However it is very worth noting that TSPO ligands have molecular weight (~300 g/mol) and lipophilicity similar to that of other lipid-soluble drugs like antidepressants (Frisk-Holmberg and van der Kleijn, 1972) and thus it is interesting to consider the possibility that reduced paracellular perfusion of small lipophilic molecule into the brain could be a mechanism of drug resistance. In fact, in those instances where MDD cohorts demonstrate increases in BBB porosity, drug response seems associated with increased levels of the marker S100β (Ambree et al., 2015; Arolt et al., 2003) although this is debated (Jang et al., 2008).

In addition, on a technical level, our findings are relevant in the context of the difficulties encountered in the quantification of the binding of TSPO PET tracers in the study of patient cohorts with inflamed peripheral status where the volume of distribution, e.g. the estimated ratio between the target and the plasma tracer concentrations, will be lowered by the decreased perfusion and this may be mistakenly interpreted as a reduction in the target TSPO density. This further complicates the interpretation of TSPO neuroimaging studies, which is already methodological challenging (Turkheimer et al., 2015).

It is notable that the findings here do not fit with the previous models of peripheral-to-central immune interaction in depression. For example,

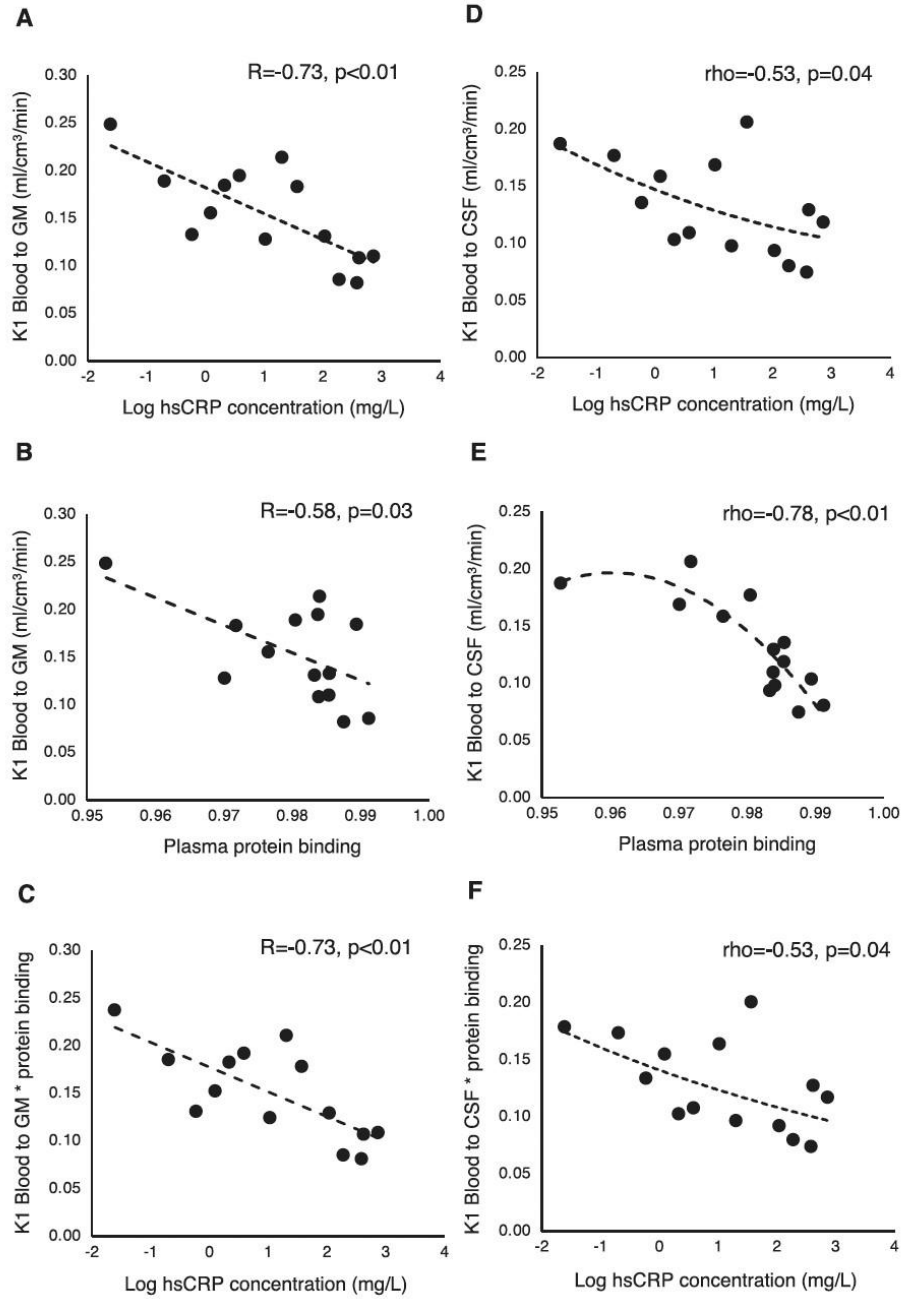

Fig. 4. – Association between blood to tissue tracer percolations, plasma protein binding and CRP. A-C) Blood to tissue transport into brain GM. D-F) Blood to tissue transport into lateral ventricle CSF. Please note that independent variables in plots B and E are linear while they are logarithmic in the others.

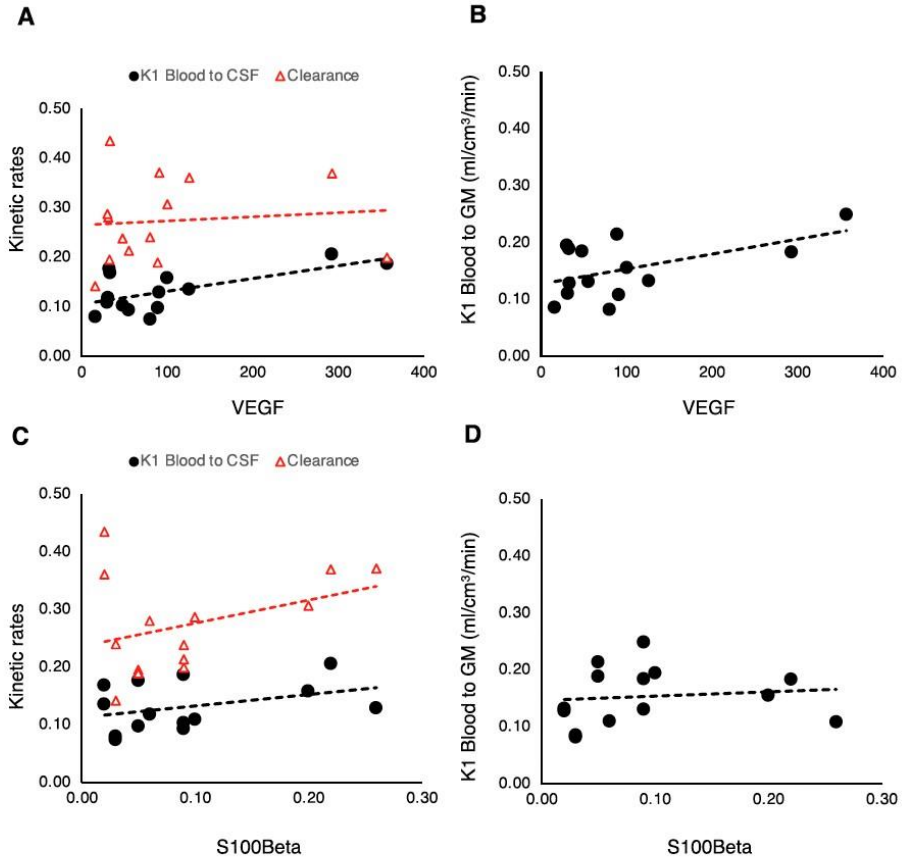

Fig. 5. – Association between blood to tissue tracer percolations and BBB integrity (VEGF and S100β). A) Tracer kinetics in lateral ventricles (black circles = K_1, red triangle = kClearance). B) Blood to GM transport (black circles = K_1). (For interpretation of the references to colour in this figure legend, the reader is referred to the web version of this article.)

depression's main environmental risk factor is chronic stress and one prevalent model proposes that peripheral myeloid cells or pro-inflammatory cytokines generated during prolonged stress conditions can diffuse into the brain either through saturable transport mechanisms or through stress-induced increase of BBB permeability (Quan and Banks, 2007); a large body of literature exists on this matter, particularly on the latter (Esposito et al., 2001; Friedman et al., 1996; Hodes et al., 2015; Menard et al., 2017; Santha et al., 2015; Weber et al., 2017; Wohleb et al., 2013) although this link is still controversial (Roszkowski and Bohacek, 2016) and clinical evidence is sparse (Bechter et al., 2010; Gudmundsson et al., 2007). In this paper, patients in the BIODEP cohort did not demonstrate biomarkers of BBB disruption (e.g. VEGF was actually reduced). In the FLAME study, the HC after the IFN-α challenge did not exhibit evidence of BBB leakage as measured by serum levels of S100β.

If the reduction in BBB permeability in MDD extends beyond lipophilic molecules then a different model can be put forward positing a reduction of the permeability of the healthy BBB in reaction to increased peripheral inflammation as indexed by CRP.

Hence, we may then speculate that the mild inflammatory state observed by PET imaging in the brain of clinically depressed patients may be the result of disturbed homeostasis due to the much-reduced transfer of solutes across the BBB. This reduction of BBB permeability may be protective on the short-term but may lead to disturbed homeostasis in the case of prolonged/chronic inflammatory states. If this were proven to be the case, then the mechanism of interaction between peripheral cytokines and CNS immune activity would be indirect, e.g., mediated by the BBB closure and ensuing disturbance to CSF dynamics.

Importantly, the activation of microglia in MDD would be the secondary outcome of disturbed homeostasis. To support further this model, Dantzer and colleagues have very recently demonstrated that sickness behaviour generated in mice and rats by peripheral immune challenges is not mediated by microglia (Vichaya et al., 2020).

Further support to this model comes from the observation that in MDD peripheral circulating glucocorticoids are increased (Lombardo et al., 2019), and conditions with high endogenous glucocorticoids, such as Cushing's disease, are associated with depression (Sonino et al., 1998). Within neuroinflammatory diseases such as multiple sclerosis use of high dose glucocorticoid treatment is thought to reduce BBB permeability and therefore reduce the flow of inflammatory mediators from

the blood into the CNS (Miller et al., 1992). Anti-glucocorticoid treatments have also been used with some benefit in the treatment of MDD in patients with high serum glucocorticoids (Lombardo et al., 2019). Therefore, increases in circulating glucocorticoids in MDD, although not measured in this study, could potentially explain the reduction in BBB permeability demonstrated and therefore changes in BBB permeability could explain the mechanism of their actions.

The observation of reduced transfer across the choroid plexus into CSF also supports our proposed model; amongst its various functions, the choroid plexus regulates the access for chemical substances from blood to the CSF playing a key role in neurotransmitter volumetric transmission (Skipor and Thiery, 2008). Molecular and gene-expression analysis of choroid plexus gene expressions in MDD has suggested alterations to calcium signalling as well as to immune activity in MDD (Devorak et al., 2015; Turner et al., 2014).

Finally, it is also of note the significant negative correlation between reduced CSF tracer exchange in ventricles and increased childhood trauma scores observed in the secondary analysis; this correlation did not survive multiple comparison correction but it is suggestive that early life events may translate into BBB porosity becoming a trait in the following years, most likely because of an increased inflammatory state (Baumeister et al., 2016), and become a risk factor for adult depression. Further investigations on the issue are needed in a much larger dataset.

4.1. Methodological issues

To measures the perfusion of the tracers from blood to CSF we focused on the amount of radioactivity percolating into the lateral ventricles. Generally, the source of this radioactivity is both the fraction of the radiotracer in parenchyma flowing in the interstitial spaces and then across the ependymal cells that line the ventricular spaces and the radiotracer flowing directly from blood through the choroid-plexus (Schubert et al., 2019). Kinetic modelling of the [11C]PBR28 data evidenced that in the case of TSPO tracers, likely due to their poor tissue extraction, radioactivity in the lateral ventricles is predominantly sourced from blood.

Given the variability across subjects in the BIODEP dataset as well as the un-availability of arterial blood data for [11C]PK11195 study, we then turned to another dataset where inflammation was experimentally controlled via IFN-α challenge in normal volunteers and measured with [11C]PBR28 with arterial sampling. Here we also observed a strong inverse linear relationship between peripheral CRP levels and radioactivity in ventricles measured both with SUVR and via kinetic modelling through the blood to lateral ventricle CSF transport. In these data as in the previous set, the effect was amplified non-linearly for abnormal CRP levels. Although we do not know whether CRP is directly inducing the observed reduction in tracer delivery, this modulation, that was consistently observed across the two datasets, possibly indicates a threshold effect with barriers becoming less permeable for inflammatory states corresponding to CRP levels>3–5 mg/L.

In the [11C]PBR28 dataset, the same association between CRP and reduction in tracer delivery to the lateral ventricles was observed in the blood-to-brain transfer constant K_1. This also suggests that in the BIODEP dataset the SUVR for the lateral ventricles may actually underestimate the reduction of delivery into those spaces given that is likely that the delivery to parenchyma was also reduced; this would explain the lack of group difference between controls and patients. Note that an alternative explanation is that the observed associations are confounded by changes in the free fraction of the radiotracer in plasma. Lockart et al., (Lockhart et al., 2003) demonstrated an affinity of PK11195, a quinoline, to the reactant alpha1-acid glycoprotein which, although not measured in these two datasets, is also likely to be positively associated with peripheral inflammatory states. There was indeed an association between tracer delivery into brain and CSF and plasma free fractions of [11C]PBR28, the latter being highly collinear with CRP levels. However, the range of changes in free fractions did not explain a significant portion of the variability of blood-to-tissue transport (as measured by K_1) either in CSF or in GM.

The inverse association between TSPO tracer perfusion and peripheral inflammatory status indexed by CRP may explain why brain TSPO density quantified with a plasma input function has shown reductions or no differences in MDD cases versus HC as the parameter used, the volume of distribution, is dependent on the target TSPO density but also on the perfusion of the tracer into tissue. Reference tissue approaches to quantification, that are not dependent on plasma-to-tissue transfer, may be more suitable for the quantification task in these cohorts (Marques et al., 2019).

Overall, the observed changes in free plasma fraction and brain perfusion, combined with the moderate-to-low variations observed in MDD and psychiatric cohorts, underlie the difficulty of obtaining robust quantification in these studies.

5. Limitations

The use of PET tracer percolation into lateral ventricle is an indirect way to quantify CSF dynamics and suffers from the low PET signal measurable in this anatomical area. However, when we tested the reproducibility of our metrics (both SUVR and AUC30-60) in a test–retest [11C]PBR28 brain PET dataset of 5 patient with mild AD (Nair et al., 2016) we found good performances: for SUVR parameter the test–retest absolute variability was 8%±4%, corresponding to an intra-class correlation coefficient (ICC) = 0.97, while for AUC30-60 test–retest absolute variability was 12%±7% (ICC = 0.86). These numbers are in line with those obtained for SUV in whole GM for which absolute variability was 6%±3% and ICC = 0.94 (Nair et al., 2016).

6. Conclusion

We have demonstrated a strong association between (increased) peripheral inflammation indexed by CRP and (reduced) blood-to-brain and blood-to-CSF transfer of TSPO-PET radiotracers. These results may be expanded to implicate a mechanism of reduced permeability of the BBB and BCSFB that may be harmful if protracted by chronic inflammatory states. This mechanism should be further tested to assess the effect of peripheral inflammatory messengers on BBB permeability for a wider range of molecules as well as antidepressant medications.

Acknowledgements

The BIODEP study (dataset 1) was sponsored by the Cambridgeshire and Peterborough NHS Foundation Trust and the University of Cambridge, and funded by a strategic award from the Wellcome Trust (104025) in partnership with Janssen, GlaxoSmithKline, Lundbeck and Pfizer. Recruitment of participants was supported by the National Institute of Health Research (NIHR) Clinical Research Network: Kent, Surrey and Sussex & Eastern. Additional funding was provided by the National Institute for Health Research (NIHR) Biomedical Research Centre at South London and Maudsley NHS Foundation Trust and King's College London, and by the NIHR Cambridge Biomedical Research Centre (Mental Health). The FLAME study (dataset 2) was sponsored by the NIHR Biomedical Research Centre at South London and Maudsley NHS Foundation Trust and King's College London in partnership whit Janssen Pharmaceutical Companies of Johnson&Johnson. We would like to gratefully thank all study participants, research teams and laboratory staff, without whom this research would not have been possible.

Finally, we would like to thank the three anonymous reviewers for their very insightful and valuable comments that have substantially improved the paper.

Compliance with ethical standards

All procedures performed in studies involving human participants

were in accordance with the ethical standards of the institutional and/or national research committee and with the 1964 Helsinki declaration and its later amendments or comparable ethical standards. Written informed consent was obtained from all individual participants included in the studies. The BIODEP study was approved by the NRES Committee East of England Cambridge Central (REC reference:15/EE/0092) and the UK Administration of Radioactive Substances Advisory Committee. The FLAME study was approved by the Queen Square London Ethical committee (REC reference. 16/LO/1520)

Appendix A. Supplementary data

Supplementary data to this article can be found online at https://doi.org/10.1016/j.bbi.2020.10.025.

References

Acabchuk, R.L., Sun, Y., Wolferz Jr., R., Eastman, M.B., Lennington, J.B., Shook, B.A., Wu, Q., Conover, J.C., 2015. 3D Modeling of the Lateral Ventricles and Histological Characterization of Periventricular Tissue in Humans and Mouse. J Vis Exp e52328.

Ambree, O., Bergink, V., Grosse, L., Alferink, J., Drexhage, H.A., Rothermundt, M., Arolt, V., Birkenhager, T.K., 2015. S100B Serum Levels Predict Treatment Response in Patients with Melancholic Depression. Int J Neuropsychopharmacol 19, pyv103.

Arolt, V., Peters, M., Erfurth, A., Wiesmann, M., Missler, U., Rudolf, S., Kirchner, H., Rothermundt, M., 2003. S100B and response to treatment in major depression: a pilot study. Eur Neuropsychopharmacol 13, 235–239.

Attwells, S., Setiawan, E., Wilson, A.A., Rusjan, P.M., Miler, L., Xu, C., Hutton, C., Husain, M.I., Kish, S., Vasdev, N., Houle, S., Meyer, J.H., 2019. Replicating predictive serum correlates of greater translocator protein distribution volume in brain. Neuropsychopharmacology.

Bagchi, S., Chhibber, T., Lahooti, B., Verma, A., Borse, V., Jayant, R.D., 2019. In-vitro blood-brain barrier models for drug screening and permeation studies: an overview. Drug Des Devel Ther 13, 3591–3605.

Barrett, P.H., Bell, B.M., Cobelli, C., Golde, H., Schumitzky, A., Vicini, P., Foster, D.M., 1998. SAAM II: Simulation, Analysis, and Modeling Software for tracer and pharmacokinetic studies. Metabolism 47, 484–492.

Baumeister, D., Akhtar, R., Ciufolini, S., Pariante, C.M., Mondelli, V., 2016. Childhood trauma and adulthood inflammation: a meta-analysis of peripheral C-reactive protein, interleukin-6 and tumour necrosis factor-alpha. Mol Psychiatry 21, 642–649.

Bechter, K., Reiber, H., Herzog, S., Fuchs, D., Tumani, H., Maxeiner, H.G., 2010. Cerebrospinal fluid analysis in affective and schizophrenic spectrum disorders: identification of subgroups with immune responses and blood-CSF barrier dysfunction. J Psychiatr Res 44, 321–330.

Betlazar, C., Harrison-Brown, M., Middleton, R.J., Banati, R., Liu, G.J., 2018. Cellular Sources and Regional Variations in the Expression of the Neuroinflammatory Marker Translocator Protein (TSPO) in the Normal Brain. Int. J. Mol. Sci. 19.

Bloomfield, P.S., Selvaraj, S., Veronese, M., Rizzo, G., Bertoldo, A., Owen, D.R., Bloomfield, M.A., Bonoldi, I., Kalk, N., Turkheimer, F., McGuire, P., de Paola, V., Howes, O.D., 2016. Microglial Activity in People at Ultra High Risk of Psychosis and in Schizophrenia: An [(11)C]PBR28 PET Brain Imaging Study. Am J Psychiatry 173, 44–52.

Burgos, N., Cardoso, M.J., Thielemans, K., Modat, M., Pedemonte, S., Dickson, J., Barnes, A., Ahmed, R., Mahoney, C.J., Schott, J.M., Duncan, J.S., Atkinson, D., Arridge, S.R., Hutton, B.F., Ourselin, S., 2014. Attenuation correction synthesis for hybrid PET-MR scanners: application to brain studies. IEEE Trans Med Imaging 33, 2332–2341.

Chamberlain, S.R., Cavanagh, J., de Boer, P., Mondelli, V., Jones, D.N.C., Drevets, W.C., Cowen, P.J., Harrison, N.A., Pointon, L., Pariante, C.M., Bullmore, E.T., 2019. Treatment-resistant depression and peripheral C-reactive protein. Br J Psychiatry 214, 11–19.

Dabitao, D., Margolick, J.B., Lopez, J., Bream, J.H., 2011. Multiplex measurement of proinflammatory cytokines in human serum: comparison of the Meso Scale Discovery electrochemiluminescence assay and the Cytometric Bead Array. J. Immunol. Methods 372, 71–77.

Dantzer, R., 2009. Cytokine, sickness behavior, and depression. Immunol Allergy Clin North Am 29, 247–264.

de Leon, M.J., Li, Y., Okamura, N., Tsui, W.H., Saint-Louis, L.A., Glodzik, L., Osorio, R.S., Fortea, J., Butler, T., Pirraglia, E., Fossati, S., Kim, H.J., Carare, R.O., Nedergaard, M., Benveniste, H., Rusinek, H., 2017. Cerebrospinal Fluid Clearance in Alzheimer Disease Measured with Dynamic PET. J Nucl Med 58, 1471–1476.

Devorak, J., Torres-Platas, S.G., Davoli, M.A., Prud'homme, J., Turecki, G., Mechawar, N., 2015. Cellular and Molecular Inflammatory Profile of the Choroid Plexus in Depression and Suicide. Front Psychiatry 6, 138.

Elwood, E., Lim, Z., Naveed, H., Galea, I., 2017. The effect of systemic inflammation on human brain barrier function. Brain Behav Immun 62, 35–40.

Enache, D., Pariante, C.M., Mondelli, V., 2019. Markers of central inflammation in major depressive disorder: A systematic review and meta-analysis of studies examining cerebrospinal fluid, positron emission tomography and post-mortem brain tissue. Brain Behav Immun 81, 24–40.

Esposito, P., Gheorghe, D., Kandere, K., Pang, X., Connolly, R., Jacobson, S., Theoharides, T.C., 2001. Acute stress increases permeability of the blood-brain-barrier through activation of brain mast cells. Brain Res 888, 117–127.

Friedman, A., Kaufer, D., Shemer, J., Hendler, I., Soreq, H., Tur-Kaspa, I., 1996. Pyridostigmine brain penetration under stress enhances neuronal excitability and induces early immediate transcriptional response. Nat Med 2, 1382–1385.

Frisk-Holmberg, M., van der Kleijn, E., 1972. The relationship between the lipophilic nature of tricyclic neuroleptics and antidepressants, and histamine release. Eur J Pharmacol 18, 139–147.

Gudmundsson, P., Skoog, I., Waern, M., Blennow, K., Palsson, S., Rosengren, L., Gustafson, D., 2007. The relationship between cerebrospinal fluid biomarkers and depression in elderly women. Am J Geriatr Psychiatry 15, 832–838.

Hannestad, J., DellaGioia, N., Gallezot, J.D., Lim, K., Nabulsi, N., Esterlis, I., Pittman, B., Lee, J.Y., O'Connor, K.C., Pelletier, D., Carson, R.E., 2013. The neuroinflammation marker translocator protein is not elevated in individuals with mild-to-moderate depression: a [(1)(1)C]PBR28 PET study. Brain Behav Immun 33, 131–138.

Hladky, S.B., Barrand, M.A., 2016. Fluid and ion transfer across the blood-brain and blood-cerebrospinal fluid barriers; a comparative account of mechanisms and roles. Fluids Barriers CNS 13, 19.

Hodes, G.E., Kana, V., Menard, C., Merad, M., Russo, S.J., 2015. Neuroimmune mechanisms of depression. Nat Neurosci 18, 1386–1393.

Holmes, S.E., Hinz, R., Conen, S., Gregory, C.J., Matthews, J.C., Anton-Rodriguez, J.M., Gerhard, A., Talbot, P.S., 2018. Elevated Translocator Protein in Anterior Cingulate in Major Depression and a Role for Inflammation in Suicidal Thinking: A Positron Emission Tomography Study. Biol Psychiatry 83, 61–69.

Hsuchou, H., Kastin, A.J., Mishra, P.K., Pan, W., 2012. C-reactive protein increases BBB permeability: implications for obesity and neuroinflammation. Cell Physiol Biochem 30, 1109–1119.

Jang, B.S., Kim, H., Lim, S.W., Jang, K.W., Kim, D.K., 2008. Serum S100B Levels and Major Depressive Disorder: Its Characteristics and Role in Antidepressant Response. Psychiatry Investig 5, 193–198.

King, E., O'Brien, J., Donaghy, P., Williams-Gray, C.H., Lawson, R.A., Morris, C.M., Barnett, N., Olsen, K., Martin-Ruiz, C., Burn, D., Yarnall, A.J., Taylor, J.P., Duncan, G., Khoo, T.K., Thomas, A., 2019. Inflammation in mild cognitive impairment due to Parkinson's disease, Lewy body disease, and Alzheimer's disease. Int J Geriatr Psychiatry 34, 1244–1250.

Kusche-Vihrog, K., Urbanova, K., Blanque, A., Wilhelmi, M., Schillers, H., Kliche, K., Pavenstadt, H., Brand, E., Oberleithner, H., 2011. C-reactive protein makes human endothelium stiff and tight. Hypertension 57, 231–237.

Lockhart, A., Davis, B., Matthews, J.C., Rahmoune, H., Hong, G., Gee, A., Earnshaw, D., Brown, J., 2003. The peripheral benzodiazepine receptor ligand PK11195 binds with high affinity to the acute phase reactant alpha1-acid glycoprotein: implications for the use of the ligand as a CNS inflammatory marker. Nucl Med Biol 30, 199–206.

Lombardo, G., Enache, D., Gianotti, L., Schatzberg, A.F., Young, A.H., Pariante, C.M., Mondelli, V., 2019. Baseline cortisol and the efficacy of antiglucocorticoid treatment in mood disorders: A meta-analysis. Psychoneuroendocrinology 110, 104420.

Marques, T.R., Ashok, A.H., Pillinger, T., Veronese, M., Turkheimer, F.E., Dazzan, P., Sommer, I.E.C., Howes, O.D., 2019. Neuroinflammation in schizophrenia: meta-analysis of in vivo microglial imaging studies. Psychol Med 49, 2186–2196.

Mason, J.M., Hancock, H.C., Close, H., Murphy, J.J., Fuat, A., de Belder, M., Singh, R., Teggert, A., Wood, E., Brennan, G., Hussain, N., Kumar, N., Manzhani, N., Hodges, D., Wilson, D., Hungin, A.P., 2013. Utility of biomarkers in the differential diagnosis of heart failure in older people: findings from the heart failure in care homes (HFinCH) diagnostic accuracy study. PLoS ONE 8, e53560.

Menard, C., Pfau, M.L., Hodes, G.E., Kana, V., Wang, V.X., Bouchard, S., Takahashi, A., Flanigan, M.E., Aleyasin, H., LeClair, K.B., Janssen, W.G., Labonte, B., Parise, E.M., Lorsch, Z.S., Golden, S.A., Heshmati, M., Tamminga, C., Turecki, G., Campbell, M., Fayad, Z.A., Tang, C.Y., Merad, M., Russo, S.J., 2017. Social stress induces neurovascular pathology promoting depression. Nat Neurosci 20, 1752–1760.

Miller, A.H., Raison, C.L., 2016. The role of inflammation in depression: from evolutionary imperative to modern treatment target. Nat Rev Immunol 16, 22–34.

Miller, D.H., Thompson, A.J., Morrissey, S.P., MacManus, D.G., Moore, S.G., Kendall, B. E., Moseley, I.F., McDonald, W.I., 1992. High dose steroids in acute relapses of multiple sclerosis: MRI evidence for a possible mechanism of therapeutic effect. J Neurol Neurosurg Psychiatry 55, 450–453.

Mondelli, V., Vernon, A.C., Turkheimer, F., Dazzan, P., Pariante, C.M., 2017. Brain microglia in psychiatric disorders. Lancet Psychiatry 4, 563–572.

Nair, A., Veronese, M., Xu, X., Curtis, C., Turkheimer, F., Howard, R., Reeves, S., 2016. Test-retest analysis of a non-invasive method of quantifying [(11)C]-PBR28 binding in Alzheimer's disease. EJNMMI Res 6, 72.

Nettis, M.A., Veronese, M., Nikkheslat, N., Mariani, N., Lombardo, G., Sforzini, L., Enache, D., Harrison, N.A., Turkheimer, F.E., Mondelli, V., Pariante, C.M., 2020. PET imaging shows no changes in TSPO brain density after IFN-alpha immune challenge in healthy human volunteers. Transl Psychiatry 10, 89.

Notter, T., Schalbetter, S.M., Clifton, N.E., Mattei, D., Richetto, J., Thomas, K., Meyer, U., Hall, J., 2020. Neuronal activity increases translocator protein (TSPO) levels. Mol Psychiatry.

Owen, D.R., Yeo, A.J., Gunn, R.N., Song, K., Wadsworth, G., Lewis, A., Rhodes, C., Pulford, D.J., Bennacef, I., Parker, C.A., StJean, P.L., Cardon, L.R., Mooser, V.E., Matthews, P.M., Rabiner, E.A., Rubio, J.P., 2012. An 18-kDa translocator protein (TSPO) polymorphism explains differences in binding affinity of the PET radioligand PBR28. J Cereb Blood Flow Metab 32, 1–5.

Quan, N., Banks, W.A., 2007. Brain-immune communication pathways. Brain Behav Immun 21, 727–735.

Richards, E.M., Zanotti-Fregonara, P., Fujita, M., Newman, L., Farmer, C., Ballard, E.D., Machado-Vieira, R., Yuan, P., Niciu, M.J., Lyoo, C.H., Henter, I.D., Salvadore, G.,

Drevets, W.C., Kolb, H., Innis, R.B., Zarate Jr., C.A., 2018. PET radioligand binding to translocator protein (TSPO) is increased in unmedicated depressed subjects. EJNMMI Res 8, 57.
Rizzo, G., Veronese, M., Tonietto, M., Bodini, B., Stankoff, B., Wimberley, C., Lavisse, S., Bottlaender, M., Bloomfield, P.S., Howes, O., Zanotti-Fregonara, P., Turkheimer, F. E., Bertoldo, A., 2019. Generalization of endothelial modelling of TSPO PET imaging: Considerations on tracer affinities. J Cereb Blood Flow Metab 39, 874–885.
Rizzo, G., Veronese, M., Tonietto, M., Zanotti-Fregonara, P., Turkheimer, F.E., Bertoldo, A., 2014. Kinetic Modeling without Accounting for the Vascular Component Impairs the Quantification of [11C]PBR28 Brain PET Data. J. Cereb. Blood Flow Metab. 34, 1060–1069.
Roszkowski, M., Bohacek, J., 2016. Stress does not increase blood-brain barrier permeability in mice. J Cereb Blood Flow Metab 36, 1304–1315.
Sander, C., Torrado-Carvajal, A., Bovo, S., Hooker, J., Loggia, M., 2019. Transient modulation of cerebral blood flow does not alter [C-11] PBR28 radiotracer binding. J Cereb Blood Flow Metab 605–606.
Santha, P., Veszelka, S., Hoyk, Z., Meszaros, M., Walter, F.R., Toth, A.E., Kiss, L., Kincses, A., Olah, Z., Seprenyi, G., Rakhely, G., Der, A., Pakaski, M., Kalman, J., Kittel, A., Deli, M.A., 2015. Restraint Stress-Induced Morphological Changes at the Blood-Brain Barrier in Adult Rats. Front Mol Neurosci 8, 88.
Schedlowski, M., Engler, H., Grigoleit, J.S., 2014. Endotoxin-induced experimental systemic inflammation in humans: a model to disentangle immune-to-brain communication. Brain Behav Immun 35, 1–8.
Schubert, J., Veronese, M., Fryer, T.D., Manavaki, R., Kitzbichler, M.G., Nettis, M., Mondelli, V., Pariante, C.M., Bullmore, E.T., Turkheimer, F.E., 2020a. A modest increase in 11C-PK11195-PET TSPO binding in depression is not associated with serum C-reactive protein or body mass index, 2020.2006.2004.20099556.
Schubert, J., Veronese, M., Fryer, T.D., Manavaki, R., Kitzbichler, M.G., Nettis, M., Mondelli, V., Pariante, C.M., Bullmore, E.T., Turkheimer, F.E., 2020b. A modest increase in 11C-PK11195-PET TSPO binding in depression is not associated with serum C-reactive protein or body mass index. medRxiv, 2020.2006.2004.20099556.
Schubert, J.J., Veronese, M., Marchitelli, L., Bodini, B., Tonietto, M., Stankoff, B., Brooks, D.J., Bertoldo, A., Edison, P., Turkheimer, F.E., 2019. Dynamic (11)C-PiB PET Shows Cerebrospinal Fluid Flow Alterations in Alzheimer Disease and Multiple Sclerosis. J Nucl Med 60, 1452–1460.
Setiawan, E., Wilson, A.A., Mizrahi, R., Rusjan, P.M., Miler, L., Rajkowska, G., Suridjan, I., Kennedy, J.L., Rekkas, P.V., Houle, S., Meyer, J.H., 2015. Role of translocator protein density, a marker of neuroinflammation, in the brain during major depressive episodes. JAMA Psychiatry 72, 268–275.
Skipor, J., Thiery, J.C., 2008. The choroid plexus–cerebrospinal fluid system: undervaluated pathway of neuroendocrine signaling into the brain. Acta Neurobiol Exp (Wars) 68, 414–428.
Smith, D.A., 2004. C-reactive protein was a moderate predictor of coronary heart disease. ACP J Club 141, 51.
Sonino, N., Fava, G.A., Raffi, A.R., Boscaro, M., Fallo, F., 1998. Clinical correlates of major depression in Cushing's disease. Psychopathology 31, 302–306.
Sproston, N.R., Ashworth, J.J., 2018. Role of C-Reactive Protein at Sites of Inflammation and Infection. Front Immunol 9, 754.
Su, L., Faluyi, Y.O., Hong, Y.T., Fryer, T.D., Mak, E., Gabel, S., Hayes, L., Soteriades, S., Williams, G.B., Arnold, R., Passamonti, L., Rodriguez, P.V., Surendranathan, A., Bevan-Jones, R.W., Coles, J., Aigbirhio, F., Rowe, J.B., O'Brien, J.T., 2016. Neuroinflammatory and morphological changes in late-life depression: the NIMROD study. Br J Psychiatry 209, 525–526.
Tomiyama, H., Koji, Y., Yambe, M., Motobe, K., Shiina, K., Gulnisa, Z., Yamamoto, Y., Yamashina, A., 2005. Elevated C-reactive protein augments increased arterial stiffness in subjects with the metabolic syndrome. Hypertension 45, 997–1003.
Tournier, B.B., Tsartsalis, S., Ceyzeriat, K., Medina, Z., Fraser, B.H., Gregoire, M.C., Kovari, E., Millet, P., 2019. Fluorescence-activated cell sorting to reveal the cell origin of radioligand binding. J Cereb Blood Flow Metab 271678X19860408.
Townend, W.J., Guy, M.J., Pani, M.A., Martin, B., Yates, D.W., 2002. Head injury outcome prediction in the emergency department: a role for protein S-100B? J Neurol Neurosurg Psychiatry 73, 542–546.
Turkheimer, F.E., Edison, P., Pavese, N., Roncaroli, F., Anderson, A.N., Hammers, A., Gerhard, A., Hinz, R., Tai, Y.F., Brooks, D.J., 2007. Reference and target region modeling of [11C]-(R)-PK11195 brain studies. J Nucl Med 48, 158–167.
Turkheimer, F.E., Rizzo, G., Bloomfield, P.S., Howes, O., Zanotti-Fregonara, P., Bertoldo, A., Veronese, M., 2015. The methodology of TSPO imaging with positron emission tomography. Biochem Soc Trans 43, 586–592.
Turner, C.A., Thompson, R.C., Bunney, W.E., Schatzberg, A.F., Barchas, J.D., Myers, R. M., Akil, H., Watson, S.J., 2014. Altered choroid plexus gene expression in major depressive disorder. Front Hum Neurosci 8, 238.
Valkanova, V., Ebmeier, K.P., Allan, C.L., 2013. CRP, IL-6 and depression: a systematic review and meta-analysis of longitudinal studies. J Affect Disord 150, 736–744.
Vichaya, E.G., Malik, S., Sominsky, L., Ford, B.G., Spencer, S.J., Dantzer, R., 2020. Microglia depletion fails to abrogate inflammation-induced sickness in mice and rats. J Neuroinflammation 17, 172.
Weber, M.D., Godbout, J.P., Sheridan, J.F., 2017. Repeated Social Defeat, Neuroinflammation, and Behavior: Monocytes Carry the Signal. Neuropsychopharmacology 42, 46–61.
Wengler, K., Bangiyev, L., Canli, T., Duong, T.Q., Schweitzer, M.E., He, X., 2019. 3D MRI of whole-brain water permeability with intrinsic diffusivity encoding of arterial labeled spin (IDEALS). Neuroimage 189, 401–414.
Wengler, K., Chen, K., Canli, T., DeLorenzo, C., Schweitzer, M.E., He, X., 2019b. Abnormal Blood-Brain Barrier Water Permeability in Major Depressive Disorder. ISRM 27th, Montreal, QC, Canada.
Wohleb, E.S., Powell, N.D., Godbout, J.P., Sheridan, J.F., 2013. Stress-induced recruitment of bone marrow-derived monocytes to the brain promotes anxiety-like behavior. J Neurosci 33, 13820–13833.
Wunderlich, M.T., Wallesch, C.W., Goertler, M., 2004. Release of neurobiochemical markers of brain damage is related to the neurovascular status on admission and the site of arterial occlusion in acute ischemic stroke. J Neurol Sci 227, 49–53.
Yushkevich, P.A., Piven, J., Hazlett, H.C., Smith, R.G., Ho, S., Gee, J.C., Gerig, G., 2006. User-guided 3D active contour segmentation of anatomical structures: significantly improved efficiency and reliability. Neuroimage 31, 1116–1128.
Zhang, C., Lin, J., Wei, F., Song, J., Chen, W., Shan, L., Xue, R., Wang, G., Tao, J., Zhang, G., Xu, G.Y., Wang, L., 2018. Characterizing the glymphatic influx by utilizing intracisternal infusion of fluorescently conjugated cadaverine. Life Sci 201, 150–160.

Appendix B:

Choroid plexus enlargement is associated with neuroinflammation and reduction of blood brain barrier permeability in depression

NeuroImage: Clinical 33 (2022) 102926

Contents lists available at ScienceDirect

NeuroImage: Clinical

journal homepage: www.elsevier.com/locate/ynicl

Choroid plexus enlargement is associated with neuroinflammation and reduction of blood brain barrier permeability in depression

Noha Althubaity [a,b,*], Julia Schubert [a], Daniel Martins [a], Tayyabah Yousaf [a], Maria A. Nettis [c], Valeria Mondelli [c], Carmine Pariante [c], Neil A. Harrison [d,e], Edward T. Bullmore [f,g,h], Danai Dima [a,i], Federico E. Turkheimer [a], Mattia Veronese [a,j]

[a] Department of Neuroimaging, Institute of Psychiatry, Psychology and Neuroscience, King's College London, London, UK
[b] Department of Radiological Sciences, College of Applied Medical Science, King Saud bin Abdulaziz University for Health Sciences, Riyadh, Saudi Arabia
[c] Department of Psychological Medicine, Institute of Psychiatry, Psychology and Neuroscience, King's College London, London, UK
[d] Cardiff University Brain Research Imaging Centre (CUBRIC), Cardiff University, Cardiff, UK
[e] Department of Neuroscience, Brighton and Sussex Medical School, University of Sussex, UK
[f] Department of Psychiatry, School of Clinical Medicine, University of Cambridge, UK
[g] Cambridgeshire and Peterborough NHS Foundation Trust, Cambridge, UK
[h] Immuno-Psychiatry, Immuno-Inflammation Therapeutic Area Unit, GlaxoSmithKline R&D, Stevenage, UK
[i] Department of Psychology, School of Arts and Social Sciences, City University of London, London, UK
[j] Department of Information Engineering, University of Padua, Padua, Italy

ARTICLE INFO

Keywords:
Choroid Plexus
Neuroinflammation
Depression
Blood brain barrier

ABSTRACT

Background: Recent studies have shown that choroid plexuses (CP) may be involved in the neuro-immune axes, playing a role in the interaction between the central and peripheral inflammation. Here we aimed to investigate CP volume alterations in depression and their associations with inflammation.

Methods: 51 depressed participants (HDRS score > 13) and 25 age- and sex-matched healthy controls (HCs) from the Wellcome Trust NIMA consortium were re-analysed for the study. All the participants underwent full peripheral cytokine profiling and simultaneous [11C]PK11195 PET/structural MRI imaging for measuring neuroinflammation and CP volume respectively.

Results: We found a significantly greater CP volume in depressed subjects compared to HCs ($t_{(76)} = +2.17$) that was positively correlated with [^{11}C]PK11195 PET binding in the anterior cingulate cortex ($r = 0.28$, $p = 0.02$), prefrontal cortex ($r = 0.24$, $p = 0.04$), and insular cortex ($r = 0.24$, $p = 0.04$), but not with the peripheral inflammatory markers: CRP levels ($r = 0.07$, $p = 0.53$), IL-6 ($r = -0.08$, $p = 0.61$), and TNF-α ($r = -0.06$, $p = 0.70$). The CP volume correlated with the [^{11}C]PK11195 PET binding in CP ($r = 0.34$, $p = 0.005$). Integration of transcriptomic data from the Allen Human Brain Atlas with the brain map depicting the correlations between CP volume and PET imaging found significant gene enrichment for several pathways involved in neuroinflammatory response.

Conclusion: This result supports the hypothesis that changes in brain barriers may cause reduction in solute exchanges between blood and CSF, disturbing the brain homeostasis and ultimately contributing to inflammation in depression. Given that CP anomalies have been recently detected in other brain disorders, these results may not be specific to depression and might extend to other conditions with a peripheral inflammatory component.

1. Introduction

Major Depressive Disorder (MDD) is a neuropsychiatric disorder associated with significant psychosocial impairment, recognized by the WHO as the leading cause of disability worldwide (Petralia et al., 2020). MDD is associated with mood changes such as sadness, crying, irritability, and anhedonia as well as psychophysiological symptoms such as insomnia, slowness of speech and action, loss of appetite, constipation, diminished sexual desire, and suicidal thoughts (Belmaker and Agam, 2008). Available antidepressant medications, which largely target

* Corresponding author at: Department of Neuroimaging, Institute of Psychiatry, Psychology and Neuroscience, King's College London, London, UK.
E-mail address: noha.althubaity@kcl.ac.uk (N. Althubaity).

https://doi.org/10.1016/j.nicl.2021.102926
Received 23 September 2021; Received in revised form 8 December 2021; Accepted 21 December 2021
Available online 27 December 2021

monoamine pathways, are effective; however, >30% of depressed patients fail to achieve remission despite multiple treatment trials (Nettis et al., 2021). Treatment resistance in MDD has been associated with heighted peripheral immunity (Bekhbat et al., 2018).

MDD patients who experienced treatment resistance exhibit most of the cardinal features of inflammation, including elevations in inflammatory cytokines, acute phase proteins, chemokines, adhesion molecules, and inflammatory mediators such as prostaglandins in peripheral blood and CSF (Miller et al., 2009). Different studies have shown significant associations between inflammatory cytokines, in particular IL-1, TNF- α, and IL-6 that are markers of innate immune response, and depressive symptoms (Miller and Raison, 2016; Enache et al., 2019). Evidence of direct relationship between peripheral heightened immunity and MDD is supplied by the reproducible observation that the acute and chronic administration of cytokines (or cytokine inducers such as lipopolysaccharide (LPS) or vaccination) can cause behavioural symptoms that overlap with those found in MDD (Miller and Raison, 2016). For example, 20% to 50% of patients receiving chronic IFN-alpha therapy for the treatment of infectious diseases or cancer develop MDD (Lotrich, 2009). Moreover, inducing acute IFN-alpha in healthy subjects results in the elevation of peripheral inflammation immune markers such as C-reactive protein, TNF-alpha, and IL-6 and is accompanied with depressive symptoms (Nettis et al., 2020).

The mechanisms linking peripheral immunity to changes in central nervous system and mood changes in MDD are still under investigation. The hypothesis of a potential direct action of peripheral cytokines trespassing the blood brain barrier (BBB) to activate brain microglia (D'Mello et al., 2009) has spurred a number of imaging studies of neuroinflammation in the central nervous system (CNS) in MDD that have been conducted using positron emission tomography (PET) and radiotracers targeting the 18 kDa mitochondrial translocator protein (TSPO), a protein that is consistently upregulated in activated microglia (see review in (Mondelli et al., 2017)). These have revealed mild microglial activity in depressed subjects (Schubert et al., 2021b); however, evidence of a relationship between central and peripheral inflammation for PET imaging has been lacking (Schubert et al., 2021b). Instead, there is very recent evidence of a relationship between heightened peripheral immunity and the reduction of the brain barriers permeability, both for the BBB and blood-CSF barrier (BCSFB) at the choroid plexus (CP) (Turkheimer et al., 2021).

This has led us to hypothesize a different model of peripheral-to-central inflammatory interaction whereas brain barriers react to increases in circulating inflammatory messengers by reducing peripheral-to-central solute transfer (Turkheimer et al., 2021). This may be protective in the short term but, if the inflammatory status becomes chronic, may disturb brain homeostasis and induce microglia to react to the disturbed environment. Very recent work on immune peripheral activation via LPS in mice and rats supports this view by showing that sickness behaviour is not mediated by microglia, hence their activation is a secondary result of the peripheral immune challenge (Vichaya et al., 2020).

The model above leads to a novel focus on a particular brain structure, the CP, that is an important part of the brain barriers, plays an active role in immune responses in the nervous system (Meeker et al., 2012) and, importantly, can be measured in-vivo using MRI imaging: the choroid plexus (Fig. 1).

The primary role of the CP is to produce the cerebrospinal fluid (CSF) and form the BCSFB (Liddelow, 2015). The CP is an epithelial-endothelial convolute, consisting of a highly vascularised stroma with connective tissue and epithelial cells and is located in the basal lamina of the four brain ventricles (Shen, 2018; Brown et al., 2004; Khasawneh et al., 2018). It is responsible for producing 75% of CSF, and through the action of active transporters and channels mediates the movement of water and solutes across the epithelium (Ghersi-Egea et al., 2018b). CP epithelial cells are connected via tight junctions, which play a fundamental role in regulating the permeability and integrity of the BCSFB

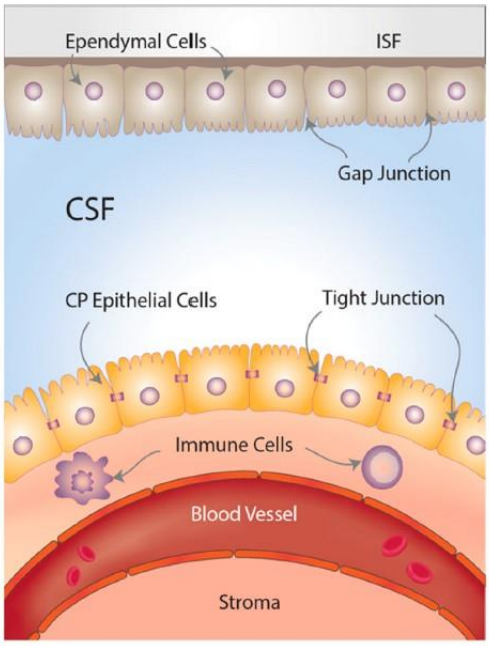

Fig. 1. Choroid plexus (CP) and brain-CSF-barriers (BCSFB). The CP is located at the base of each of the four brain ventricles and is composed of epithelial cells surrounded by connective stroma and blood vasculature, which forms the BCSFB. The epithelial cells are connected by tight junctions in the apical border which face the cerebrospinal fluid (CSF) and are covered by microvilli, while the basolateral border faces the blood vasculature. The ependymal cells cover the roof of the ventricles and are connected by gap junctions, which facilitate the exchange of electrolytes and some solutes between the CSF and the interstitial fluid (ISF).

(Ghersi-Egea et al., 2018a). The fenestrations in the choroidal vessels are less restricted compared to cerebral vessels, and allow ions and small molecules such as amino acids to diffuse into the CP epithelial cells, which can then be actively transported actively into the CSF (Maharaj et al., 2008; Liddelow, 2015). The BCSFB together with the BBB control the traffic between the blood, the CSF, and the brain parenchyma (Saunders et al., 2012). There has been a recent increase of interest in the CP due to its important role in regulating brain homeostasis and, particularly, the neuroinflammatory response (Schwartz and Baruch, 2014). CP immune cells and intraventricular macrophages provide the first line of defence against brain infections and inflammation (Pollak et al., 2018; Yang et al., 2021). Prolonged inflammation may contribute to the infiltration of the CP by immune cells, and subsequently into the CSF and into the brain parenchyma (Marques and Sousa, 2015).

There is a growing body of literature that recognises the importance of CP morphology in psychiatric conditions. In subjects with schizophrenia, CP enlargement has been found to be associated with chronic stress (Zhou et al., 2020), a condition often associated with MDD and inflammation. A more direct correlation between CP volume and levels of peripheral IL-6 has been documented by Lizano and colleagues in psychosis (Lizano et al., 2019) whereas CP enlargement was also associated with reductions in gray matter and amygdala volume as well as ventricle enlargement and consequential deteriorated cognitive status (Lizano et al., 2019). Note that CP enlargement is also observed in patients with mild cognitive impairment and Alzheimer's disease, for

which MDD is a known prodrome (Tadayon et al., 2020). However, few studies suggest a potential direct link between CP structural and functional alterations and depression. Gene expression analysis from a cross-sectional post-mortem study has identified multiple differential mRNA expression in CP samples obtained from MDD patients (Turner et al., 2014; Devorak et al., 2015). ICAM-1 and VEGF transcripts are notable examples as they are known to play an important role in depression, being part of the tissue inflammatory response. They are also known to affect BBB permeability and in fact their peripheral measures serve as inflammatory markers (Müller, 2019; Clark-Raymond and Halaris, 2013)

In this study we wanted to test the model of peripheral-to-central inflammation sketched above by investigating for the first time the association between CP volume and neuroinflammation in a depressed cohort, using structural MRI and 18 kDa translocator protein (TSPO) positron emission tomography (PET) data. We hypothesized that if the BCSFB were indeed a mediator between peripheral and central inflammation in depression, we would observe a direct correlation between central inflammation, here marked by TSPO parenchymal expression, and CP volume.

2. Methods

2.1. Dataset

Data for this study were collected from a network of clinical research sites in the United Kingdom as part of the Biomarkers in Depression Study (BIODEP, NIMA consortium, https://www.neuroimmunology.org.uk/) and included 51 depressed participants and 25 healthy controls (HCs). Depressed subjects who had taken anti-depressive treatment with Hamilton Depression Rating scale (HDRS) > 13 and untreated subjects with HDRS > 17 were included. In total, there were 9 untreated subject and 42 were medicated. An overview of demographic and clinical characteristic data is reported in Table 1, while full details of the dataset are outlined in the previous publication (Schubert et al., 2021b).

Table 1
Demographics and clinical characteristics for depressed subjects and healthy controls (HCs).

Variable	Depressed subjects (n = 51)	Healthy controls (n = 25)	p Value
Demographics			
Age, mean ± SD, years	36.2 ± 7.3	37.3 ± 7.8	0.56
Male, No. (%)	15 (29)	11 (44)	0.21
Weight, mean ± SD, kg	80.3 ± 14.4	73.7 ± 15.1	0.1
BMI, mean ± SD, kg/m^2	27.2 ± 4.0	24.2 ± 4.8	<0.01*
Blood Variables, (MDD No.; HC No.), mean ± SD:			
CRP mg/L (51; 25)	2.9 ± 2.8	1.1 ± 0.9	<0.01*
IL6 (35;12)	1.1 ± 1.63	0.6 ± 0.4	0.35
TNF-α (34;11)	2.7 ± 0.9	2.3 ± 0.5	0.25
IFN-γ (35;11)	4.0 ± 0.7	4.2 ± 0.0	0.26
IP-10 (49;22)	402 ± 152	428 ± 101	0.46
Lymphocytes (47;23)	30.9 ± 7.2	30.2 ± 10.2	0.79
Monocytes (47;23)	6.8 ± 2.1	6.6 ± 2.5	0.78
Neutrophil's total (47;23)	58.8 ± 8.3	59.3 ± 11.3	0.8
Neutrophils absolute (47;23)	3.9 ± 1.5	4.1 ± 1.4	0.48
Albumin (47;23)	44.8 ± 2.7	45.3 ± 2.1	0.44
Cholesterol (47;23)	5.2 ± 1.2	4.9 ± 1.2	0.35
VEGF (35;11)	82 ± 55.5	136 ± 47.8	<0.01*
Depressive Clinical Scores, (MDD No.), mean + SD:			
HDRS (51)	18.5 ± 3.7	0.6 ± 0.9	<0.001*
Childhood Trauma score (50)	54.3 ± 14	38.2 ± 5.4	<0.001*
Perceived Stress score (48)	26.7 ± 4.3	10 ± 5.9	<0.001*
ICV, mean ± SD, mm^3	1,562,594 ± 137,333	1,550,724 ± 185,887	0.76

Abbreviations: NA, not applicable.

Participant's inclusion criteria were as follows: no history of other neurological disorder, no current alcohol and/or drug abuse, no contribution in any clinical drug trials during the previous year. Participants were not experiencing any other medical disorders or undergoing any treatment that could affect the accuracy of the study's results. Pregnant or breastfeeding women were excluded. HC subjects were age- and sex-matched with the depressed subjects, and they did not have a history of clinical depression or antidepressant treatment. Ethical approval was obtained from the Institutional and/or National research committee and and with the 1964 Helsinki declaration and its later amendments or comparable ethical standards. All participants provided written informed consent prior to the study. The BIODEP study was approved by the NRES Committee East of England Cambridge Central (REC reference:15/EE/0092) and the UK Administration of Radioactive Substances Advisory Committee.

2.2. Clinical assessments

For the clinical evaluation of depression, HCs and depressed subjects underwent a number of psychiatric assessments: the Hamilton Depression Rating scale (HDRS), the Standard Clinical Interview for DSM-5, the Beck Depression Inventory, the Spielberger State-Trait Anxiety Rating Scale, the Chalder Fatigue Scale, the Snaith-Hamilton Pleasure Scale, the Childhood Trauma score, and the Perceived Stress score. A venous blood sample was collected from all participants to assess peripheral blood parameters including interlukin-6 (IL-6), tumor necrosis factor-alpha (TNF-α), interferon gamma (IFN-γ), interferon gamma-induced protein 10 (IP-10), lymphocytes, monocytes, neutrophil's total, neutrophils absolute, albumin, cholesterol, VEGF, and C-reactive protein (CRP) concentration. CRP was used as the main marker of a peripheral inflammation, consistent with other studies in MDD (Howren et al., 2009; Haapakoski et al., 2015).

2.3. MRI and PET imaging

For all the subjects, imaging data were obtained using a GE SIGNA simultenous PET/MR scanner (GE Healthcare, Waukesha, USA). All MRI acquisitions included a high resolution T1-weighted image for structural imaging. PET imaging consisted in a bolus injection of [^{11}C]PK11195 (target dose ~ 350 MBq, mean injected dose 361 + 53 MBq) followed by a 60-minute dynamic acqusition. A multi-subject atlas method was used for attenuation correction and included improvement for the MRI brain coil component (Burgos et al., 2014). Additional corrections (including scatter, random, normalisation, and deadtime correction), were performed using the standard console software that applied PET/MR reconstruction algorithm correction. Additional information on the PET and MRI protocols can be found in the original report on these data (Schubert et al., 2021a).

2.4. CP volume and brain volume measurement

The CP of the lateral ventricles of all subjects was manually segmented on the axial, sagittal, and coronal planes of the high resolution T1- weighted image using the Analyze software (v.12, https://analyzedirect.com) (Fig. 2. The image intensity was adjusted to assist in the localization of the region of interest and its anatomical boundaries. The CP was traced slice by slice starting from the axial plane followed by coronal and sagittal planes. After the region contouring, the CP volume was calculated for each subject using the Analyze software. The SPM12 (http://www.fil.ion.ucl.ac.uk/spm) was used to perform tissue segmentation for gray matter, white matter, and CSF (Heinen et al., 2016). High resolution T1 weighted images were smoothed and normalised into MNI standard space using the DARTEL algorithm via the SPM12 for brain volume calculation (Ashburner, 2007). The total brain volume was obtained by the sum of gray and white matter volume (Heinen et al., 2016). Additionally, the Freesurfer software (v.6.0, http:

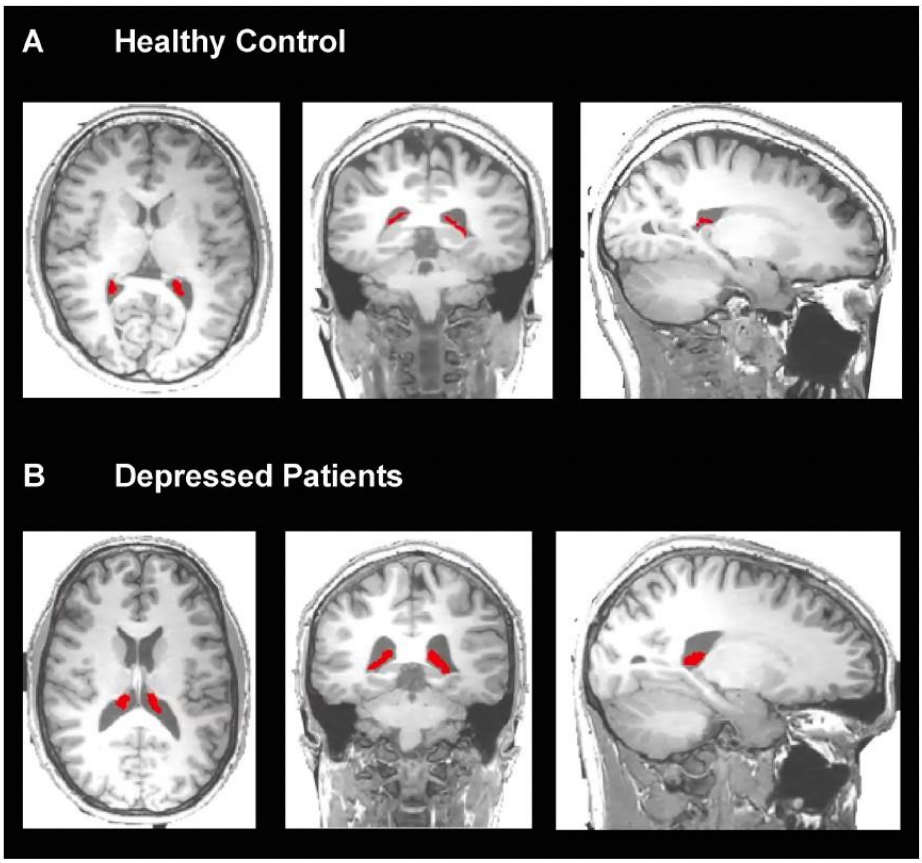

Fig. 2. Choroid plexus (CP) segmentation in HCs and depressedsubject. T1-weighted MRI images with the manual segmentation of the left and right CP (red) on the axial, coronal, and sagittal planes for one representative control (A) and one depressed subject (B). (For interpretation of the references to colour in this figure legend, the reader is referred to the web version of this article.)

//surfer.nmr.mgh.harvard.edu/), was used to estimate the total intracranial volume (ICV) (Fischl et al., 2002; Jovicich et al., 2009), which was used as a covariate in the statistical analysis (Pintzka et al., 2015).

2.5. PET analysis

The pre-processing of the [^{11}C]PK11195 PET imaging including frame-by-frame motion correction, PET-MRI alignment, brain masking, and atlas-based region extraction was performed using the MIAKAT software (www.miakat.org). Processed data were hence used for both the quantification of TSPO distribution in brain parenchyma (as a proxy of neuroinflammation) as well as to assess the tracer exchange between blood and CSF in the lateral ventricles. This second method had been previously validated and used to demonstrate CSF dynamic alterations in Alzheimer's disease (De Leon et al., 2017, Schubert et al., 2019) and multiple sclerosis (Schubert et al., 2019). The lateral ventricles were manually segmented using T1-weighted structural MRI and ITK-SNAP software as was done in the original reference (Schubert et al., 2019; Acabchuk et al., 2015), and then eroded by two voxels in native space (5.2 mm) to reduce the effect of the partial volume (Yushkevich et al., 2006; Turkheimer et al., 2021). Consistently with original publication, the [^{11}C]PK11195 PET activity extracted from the eroded lateral ventricles was used to calculate the standardized uptake value ratio (SUVR) normalized by a reference region at 60 min, and the area-under-curve (AUC) which included activity of the lateral ventricles between 30 and 60 min ($AUC_{30\text{-}60}$) (Turkheimer et al., 2021). The supervised reference tissue was computed at individual level and was identified by a set of grey matter voxels with tracer-activity comparable to non-inflamed grey matter tissue (Schubert et al., 2021a). For the quantification of TSPO, the simplified reference tissue model was used to calculate the distribution volume ratio (DVR) of [^{11}C]PK11195 in brain (Schubert et al., 2021b; Turkheimer et al., 2007). The DVR estimates for the anterior cingulate cortex (ACC), prefrontal cortex (PFC), and insula (INS), were extracted to assess the level of brain inflammation as these regions serve important roles in mood regulation (Goldin et al., 2008), and the ACC has been previously shown to be involved in inflammation-associated mood deterioration (Harrison et al., 2009; Torres-Platas et al., 2014). The [^{11}C]PK11195 DVR in CP was estimated from the parametric maps after performing partial volume correction using the Richardson-Lucy deconvolution method with 6 mm point spread function provided by

the PETPVC toolbox (Thomas et al., 2016). For both methods, the same reference region derived from a supervised clustering of dynamic PET images was applied (Schubert et al., 2021a). Additional details about the PET image processing and quantification are found in our previous studies (Schubert et al., 2021a).

2.6. Statistical analysis

Statistical analyses were performed using SPSS software (version 25.0, Chicago, IL). The Shapiro-Wilk's test was used to test for normality of the data. An independent sample *t*-test was used to examine the difference of CP volume between the HCs and depressed subjects. Partial correlations were used to analyse the relationship between CP volume and depressive clinical scores (HDRS, the Childhood Trauma, and Perceived Stress score), while covarying for ICV. Partial correlation tests were used to investigate the association between the CP volume and blood to CSF exchange measures (SUVR and $AUC_{30\text{-}60}$) while covarying for the ICV and group. Partial correlation of CP volume measures and brain TSPO values (ACC, PFC, and INS) and brain volume were also investigated while covarying for possible confounding factors including ICV and group. The same analyses were repeated voxelwise with SPM12, using FWE for multiple comparison corrections.

2.7. Imaging transcriptomics

We leveraged transcriptomic data from the Allen Human Brain Atlas (AHBA) (Hawrylycz et al., 2012) to explore possible associations between the brain map depicting the correlations between CP volume and TSPO and post-mortem brain gene expression. With this analysis, we aimed to gain further insight about potential biological pathways explaining regional vulnerability to spatial variability in the association between CP volume and brain TSPO across subjects.

We used the *abagen* toolbox (https://github.com/netneurolab/abagen) to process and map the transcriptomic data to 83 parcellated brain regions from the DK atlas (Desikan et al., 2006), as described in Martins et al. (2021). We applied the normalization for cortical and subcortical regions separately, as suggested by Arnatkeviciute et al., 2019 (Arnatkeviciute et al., 2019). After pre-processing, we retained regional gene expression data from 15,633 genes, corresponding to genes with expression higher than background noise. We then used partial least square regression (PLS) to investigate associations between the t-statistics quantifying the regional correlations between CP volume and TSPO and brain gene expression. We focused on both cortical and subcortical regions from the left hemisphere only. This choice was motivated by scarcity of data in the AHBA for the right hemisphere.

Partial least square regression ranks all genes by their multivariate spatial alignment with the regional strength of the association between CP volume and TSPO. The first PLS component (PLS_1) is the linear combination of the weighted gene expression scores that have a brain expression map that covaries the most with the map of the association between CP volume and TSPO. We confirmed PLS_1 explained the largest amount of variance by testing across a range of PLS components (between 1 and 15) and quantifying the relative variance explained by each component. The statistical significance of the variance explained by each PLS model was tested by permuting the response variables 1,000 times, while considering the spatial dependency of the data by using a spin test (Alexander-Bloch et al., 2013a; Alexander-Bloch et al., 2013b; Vasa et al., 2018). Since PLS_1 alone explained the largest amount of variance in the imaging dependent variable, we focused our following analyses on this component.

The error in estimating each gene's PLS_1 weight was assessed by bootstrapping (resampling with replacement of the 34 brain regions), and the ratio of the weight of each gene to its bootstrap standard error was used to calculate the *Z* scores and, hence, rank the genes according to their contribution to PLS_1 (Whitaker et al., 2016). Genes with large positive PLS_1 weights correspond to genes that have higher than average expression in regions where the association between CP volume and TSPO is more strongly positive. Mid-rank PLS weights showed expression gradients that are weakly related to the pattern of the regional association between CP volume and TSPO.

We then used the list of genes ranked by the respective weights according to the PLS_1 component to perform gene set enrichment analyses for biological pathways (gene ontology) and genes expressed in different brain cell types, as identified in a previous single-cell transcriptomic study of the human brain (Lake et al., 2018). We implemented these analyses using the GSEA method of interest of the Web-based gene set analysis toolkit (*WebGestalt*) (Zhang et al., 2005).

For comparative purposes, we used the same method to understand the spatial variability of changes in brain TSPO between subjects with depression and HCs.

3. Result

3.1. Demographic and clinical characteristics

Subjects with depression and HCs were matched in terms of age ($p = 0.56$) and sex ($p = 0.21$), and no difference was shown in terms of the ICV between groups ($p = 0.76$). BMI was significantly higher in depressed subjects compared to HCs ($t_{(76)} = 3.52$, $p = 0.001$).

Peripheral blood parameters were all comparable between two groups (Table 1, with the exception of CRP and VEGF levels. Depressed subjects had higher blood CRP ($t_{(76)} = 3.14$, $p = 0.002$) and lower VEGF ($t_{(46)} = -2.90$, $p = 0.006$) levels compared to HCs. While CRP differences were expected given the recruitment parameters (Schubert et al., 2021b), the difference in VEGF level was not.

In terms of clinical variables, the HDRS, Childhood Trauma scores, and the Perceived Stress score were significantly higher in depressed subjects compared to HCs ($t_{(76)} = 23.6$, $p < 0.001$), ($t_{(75)} = 5.5$, $p < 0.001$), ($t_{(73)} = 13.8$, $p < 0.001$) respectively (Table 1.

3.2. Depressed subjects have larger CPs compared to HCs

The CP volume was log10-transformed to induce normality in the data distribution as confirmed by Shapiro-Wilk's test ($W_{(76)} = 0.98$, $p = 0.23$). The CP volume was greater in patients with depression compared to HCs (mean value of depressed patients:1710.29 ± 408.80; mean value HCs: 1513.96 ± 459.80; $t_{(76)} = 2.17$, $p = 0.03$) (Fig. 3. In both groups, the CP volume was strongly correlated with ICV ($r = 0.25$, $p = 0.03$) and sex ($F = 4.7$, $p = 0.03$), but not with age ($p = 0.72$) or BMI ($p = 0.19$). However, when both ICV and sex were included as covariates, only ICV remained significant. After adjusting for ICV, the CP volume remained significantly higher in depressed subjects compared with HCs ($F_{(76)} = 4.6$, $p = 0.04$) (Fig. 3.

After adjusting for ICV, the CP volume of depressed subjects showed a negative association with Perceived Stress score ($r = -0.30$, $p = 0.05$); however, the association was not significant following multiple comparisons correction. No association was found with any other clinical variable.

To investigate the relationship between the CP enlargement and disease duration, we considered a subset of 42 depressive patients with known onset of depressive symptoms. This showed no significant associations between CP volume and disease duration ($r = -0.27$, $p = 0.08$). However, the disease duration was inversely associated with LV SUVR ($r = -0.4$, $p = 0.006$) and and positively associate with CSF volume ($r = 0.43$, $p = 0.005$).

3.3. CP volume is not associated with peripheral inflammatory markers

When using the full sample, the CP volume was not associated with the CRP levels ($r = 0.07$, $p = 0.53$), IL-6 ($r = -0.08$, $p = 0.61$), TNF-α ($r = -0.06$, $p = 0.70$), or VEGF ($r = 0.12$, $p = 0.39$). Similarly, no association between CP volume and peripheral inflammatory markers was found

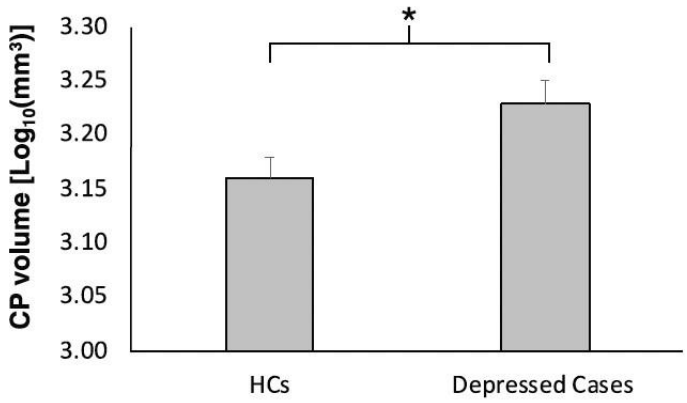

Fig. 3. Choroid plexus (CP) volume in depressed subjects and healthy controls (HCs) Mean difference of CP volumes between HC and depressed groups ($F = 5.30$, $p = 0.02$). Error bars indicate standard error. The analysis is corrected for the intracranial volume.

when depressed and HC groups were analysed separately. However, an inverse association was found between the albumin level in plasma and CP volume ($r = 0.27$, $p = 0.03$) after adjusting the ICV, lateral ventricles volume and group. The association was not significant following multiple comparisons correction.

3.4. CP volume is positively associated with central inflammation and inversely with CSF clearance

Using the full dataset ($N = 76$), CP volume measures were positively correlated with [^{11}C]PK11195 DVR in the ACC ($r = 0.28$, $p = 0.02$), PFC ($r = 0.24$, $p = 0.04$) and INS ($r = 0.24$, $p = 0.04$) (Fig. 4. All these correlations were corrected for group and ICV, although only ICV was a significant covariate in the regression for ACC and INS (Fig. 4. When analysis was repeated in the depression cohort only, no correlation was detected between the CP volume and [^{11}C]PK11195 DVR in any of the main ROIs (ACC: $r = 0.20$, $p = 0.40$; PFC: $r = 0.18$, $p = 0.18$; INS: $r = 0.17$, $p = 0.2$). No correlation was found between CP volumes and total cortical [^{11}C]PK11195 DVR ($r = -0.21$, $p = 0.07$) nor with whole brain [^{11}C]PK11195 DVR ($r = -0.05$, $p = 0.56$). CP volume and [^{11}C]PK11195 DVR in CP were instead correlated both in the full sample ($r = 0.34$, $p = 0.005$) and in the depression cohort only ($r = 0.39$, $p = 0.001$), after correction for ICV, lateral ventricle volumes, and group.

The CP volume exhibited a negative association with the blood-to-CSF radiotracer exchange as measured by the lateral ventricle SUVR ($r = -0.23$, $p = 0.05$), following correction for group and ICV. A similar association was found for radiotracer $AUC_{30\text{-}60}$ in lateral ventricle ($r = -0.26$, $p = 0.02$) (Fig. 5. However, the depression cohort did not show a significant association between the CP volume and the SUVR ($r = -0.19$, $p = 0.19$) nor $AUC_{30\text{-}60}$ ($r = -0.20$, $p = 0.16$).

3.5. CP volume is not associated with brain volume

No association was detected between the CP volume and brain volume ($r = 0.16$, $p = 0.17$), nor with total grey matter volume ($r = 0.10$, $p = 0.38$) when depression and control groups were combined. Results were consistent with and without group and ICV as covariates.

3.6. Imaging transcriptomics

The first PLS component explained 26.01% of the spatial variability in the strength of the association between CP volume and TSPO and did so above chance ($r = 0.51$, $p_{spatial} = 0.006$) (Fig. 6. The list of genes

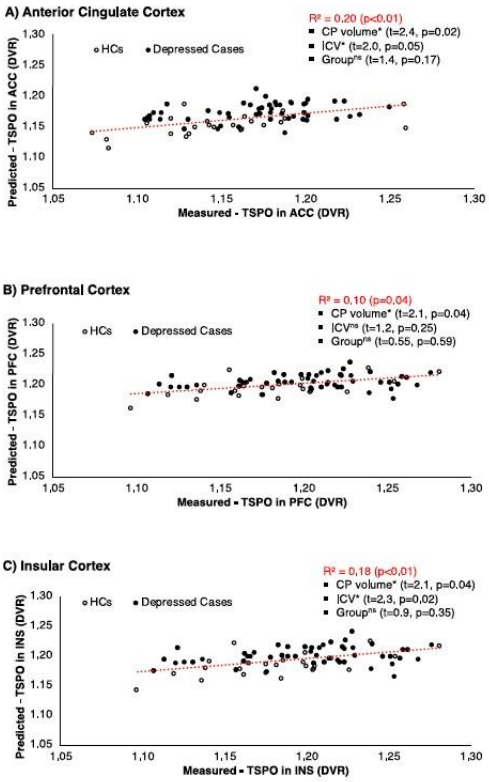

Fig. 4. Correlation between the choroid plexus (CP) volume and brain inflammation in healthy controls (HCs) and depressed subjects in ACC (A), PFC (B) and INS (C). *indicates statistical significance (p-value < 0.05). ^{ns} indicates non-significant results.

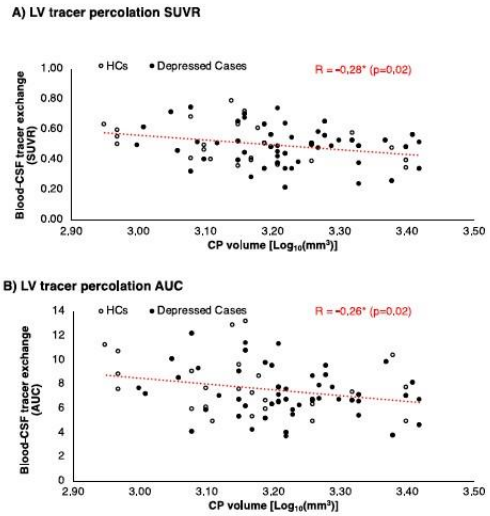

Fig. 5. Inverse association between choroid plexus (CP) volume and CSF-blood tracer exchange measured by [^{11}C]PK11195 PET uptake (SUVR and AUC, respectively) in lateral ventricles (LV). * indicates statistical significance (p-value < 0.05).

ranked by the respective PLS1 weights can be found in "Supplementary data - [*PLS1_weights_CP_TSPO_Corr*]". We found significant enrichment for six gene ontology (i.e. biological pathways terms among the top positively weighted genes), including "protein localization to endoplasmatic reticulum", "leukocyte activation involved in inflammatory response", "serotonin receptor signalling pathway", "gamma-amino-butyric acid signalling pathway", "neuroinflammatory response", and "interleukin-1 response". In the brain cell type enrichment analysis, we found enrichment among the top positively weighted genes mostly for genes from excitatory and inhibitory neurons, where the strongest positive enrichment hit was the subclass of excitatory neurons "Ex3e" (Fig. 6 (Full statistics can be found in "Supplementary data - [*GSEA_PLS1_CP_TSPO_Corr*]").

For the analyses on case-control differences in TSPO, PLS_1 explained 33.64% of the spatial variability in TSPO differences and did so above chance ($r = 0.58$, $p_{boot} = 0.001$) (Supplementary – Fig. 1). In the gene set enrichment analysis, we did not find significant enrichment for any gene ontology. In the brain cell type enrichment analysis, we also did not find significant enrichment among positively weighted genes for genes from any of the cell types we tested (Full statistics can be found in Supplementary [*PLS1_weights_TSPO_Differences*] and [*GSEA_PLS1_TSPO_Differences*]).

4. Discussion

We demonstrated for the first time the association between CP enlargement in depression and a reduction of brain barrier permeability reflected by blood-to-CSF radiotracer exchange parameters (SUVR). Moreover, we have also demonstrated that in the same patients CP volume is positively associated with increases in brain inflammation as measured by TSPO PET in key regions (ACC, PFC and Insular Cortex). There was no association between CP volume and peripheral inflammatory markers (CRP, IL6, and TNF- α) nor depression clinical scores (HDRS, Childhood Trauma score), but there was an association with Perceived Stress score. However, as this result was from exploratory analysis and did not survive multiple comparison testing correction, it should be taken with caution. Our results support the hypothesis that CP enlargement occurs in depressed cohorts, and this enlargement is associated with central inflammation.

The finding that CP volume is correlated with inflammation of the CNS but not with peripheral inflammation fits into the proposed model of the relationship between peripheral and central inflammation. We can speculate that CP volume may increase with time, likely together with the BBB dysfunction (Kealy et al., 2020) as a reaction to a

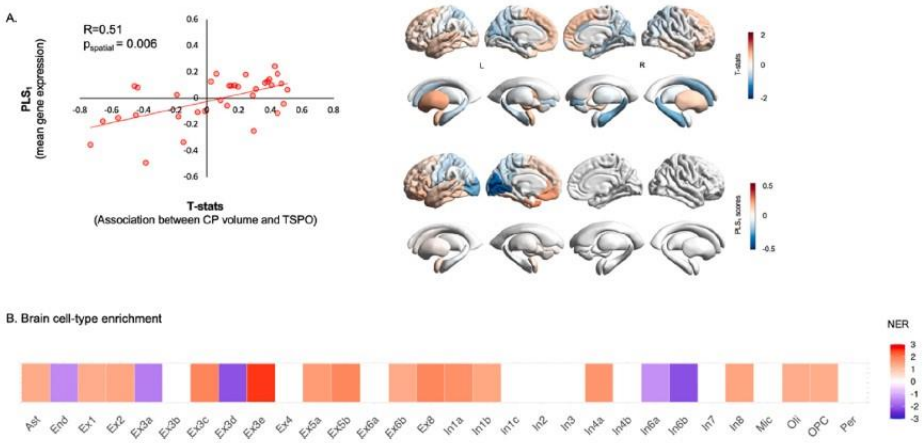

Fig. 6. Imaging transcriptomics decoding of regional variation in the association between choroid plexus (CP) volume and TSPO. Panel A: Left - scatter plot depicting a significant positive correlation between PLS1 gene expression weights and the t-statistics quantification the association between CP volume and TSPO for each region of the left hemisphere. Right – the upper brain map depicts the cortical distribution of the t-statistics quantifying the association between CP volume and TSPO; the lower brain map depicts the cortical distribution of the weights of PLS_1. Panel B: Table showing the results of the brain cell-type gene enrichment analysis. The colours depict normalized enrichment ratios; positive ratios indicate enrichment for genes of a specific cell class among those genes with the highest positive PLS_1 weights; the reverse applies to negative enrichment ratios. White squares indicate cell classes where enrichment did not survive $p_{FDR} < 0.05$. NER – Normalized enrichment ratio; CP – Choroid plexus.

heightened concentration of peripheral immune mediators. The lack of correlation between CP volume and CRP (which trends towards a positive association but does not achieve significance) is probably due to the CRP concentrations being an instantaneous measurement (Felger et al., 2020), while CP volume increase is likely the result of the integrated series of peripheral immune events across time (Marques and Sousa, 2015, Turner et al., 2014). Interestingly, CP volume increases were associated with reductions in plasma albumin which is a well established marker of chronic inflammation (Don and Kaysen, 2004). The enlargement of the CP volume in our result is associated with the reduction of the BCSFB permeability, which was identified as a reaction to the chronic inflammatory events in depressed subjects (Turkheimer et al., 2021). Similarly, the correlation between CP volume and brain inflammation may indicate that microglial activation is also the result of disturbed homeostasis across time (Enache et al., 2019). In our study, we did not see any elevation of CP [11C]PK11195 in depression, but we were able to replicate the association between CP volume and CP TSPO uptake as reported by in relapsing remitting multiple sclerosis patients (Ricigliano et al., 2021). The specificity to TSPO of tracer activity in CP was investigated in an independent [11C]PBR28 PET blocking study with XBD173 (Veronese et al., 2018). A significant reduction of tracer activity (-42%, $t_{(7)} = 2.6$, $p = 0.04$) was found after XBD173 administration. Unfortunately, we cannot comment on the origin of tracer-specific binding in CP, as it could be endothelial, vascular, or infiltration of immune cells (Veronese et al., 2018).

The spatial profile of the correlation pattern between CP volume and TSPO brain expression was positively associated with the neuronal distribution, twice stronger for excitatory neurons than for inhibitory ones (supplementary data). This result indicates that those brain areas metabolically more active are also those where inflammation is likely the result of reduced permeability of the barriers. These areas are known as "neotenic" as they contain a disproportionate density of synapses that have exceptionally high energy requirements and matching needs of efficient transport and clearance of metabolic substrates and products (Goyal et al., 2014; Vaishnavi et al., 2010). These results confirm an associative link between brain metabolism, brain barriers, permeability, and neuroinflammation. But further research is required to establish a causal link between these factors in MDD.

It is important to note that imaging data on the structure of CP do not explain the functional mechanism underlying such morphological modifications. Previous gene expression analysis from a cross-sectional post-mortem study has identified multiple differences in CP samples obtained from patients with depression, particularly in the down-regulation of genes related to the "transforming growth factors- beta" (TGF-B) pathway, which are known to interact with the production of the extracellular matrix, suggesting changes in the cytoskeleton of CP epithelial cells in patients with MDD (Turner et al., 2014). Reduction of VEGF, a neurotrophic factor which is produced by the CP epithelial cells and responsible for angiogenesis and vascular fenestration permeability, were found in serum of suicide victims with MDD (Isung et al., 2012) and in plasma of MDD patients (Dome et al., 2009). To date, however, CP alterations remain poorly understood and multiple mechanisms are put forward that include CP ependymal cell proliferation (Barkho and Monuki, 2015), infiltration of CP by peripheral immune cells or edema (Johanson and Johanson, 2018).

Finally, it is important to note that the findings above do not seem to be specific to depression. Hence, this peripheral-to-central immunity mechanism seems to be generalizable to all pathologies where peripheral inflammatory states are observed, such as in schizophrenic cohorts (Lizano et al., 2019; Zhou et al., 2020). Recenlty, strong evidences from multiple sclerosis patients, a cuprizone diet-related demyelination mouse model and the experimental autoimmune encephalomyelitis model demonstrated a cross-dependency between neuroinflammation and choroid plexus functional, cellular and morphological characteristics which included volume enlargement, glia hyperactivity and the up-regulation of functional pathways primary related to neuroinflammation and cell-to-cell interactions (Fleischer et al., 2021). Taken together, these results further support the use of CP volume as a reliable, *trans*-diagnostic marker of neuroinflammation.

5. Limitations

Some limitations have to be considered regarding our results. Manual CP segmentation is operator dependent but reanalysis of the CP volume with a second operator (JS) lead to an intraclass correlation coefficient ICC = 82% indicating robustness in our estimation. Automatic methods to measures CP volume exists but do not match well with manual extraction (Lizano et al., 2019) especially when applied to structural T1-weighted MRI data. The sample size in this study was small compared to recent big-data structural MRI studies in depression (N > 1,000) (Schmaal et al., 2020). However, this is one of the largest samples ever published in depression that combines MRI with TSPO PET imaging. Future studies should investigate the use of automatic methods for CP segmentation in order to scale up these analyses to a larger sample size. Moreover, the collection of TSPO PET data with arterial input function to quantify tracer kinetic exchange though BCSFB would be more accurate than static SUVR and AUC parameters (Schubert et al., 2019) for measuring CSF dynamics.

6. Conclusion

This study has identified for the first time in vivo a relationship between CP volumetric and brain inflammatory alterations in depression. The change on the CP morphology has been found in different neuroinflammation disorders, with support the role of CP enlargement in neuroinflammation. This study also provides further evidence to the model that reduced permeability of the BBB and BCSFB could alter brain homeostasis, becoming harmful if protracted by chronic inflammatory states. These findings do not seem to be specific to depression, but rather explain a more general mechanism of brain immune defence, in which CP plays a fundamental role.

Finally, we would like to acknowledge the King Saud bin Abdulaziz University for Health Sciences, Riyadh, Saudi Arabia, and the Saudi Arabia Cultural Bureau (SACB).

CRediT authorship contribution statement

Noha Althubaity: Conceptualization, Methodology, Software, Formal analysis, Investigation, Validation, Writing – original draft, Writing – review & editing. **Julia Schubert:** Conceptualization, Methodology, Software, Formal analysis, Investigation, Validation, Writing – original draft, Writing – review & editing. **Daniel Martins:** Conceptualization, Methodology, Software, Formal analysis, Investigation, Validation, Writing – original draft, Writing – review & editing. **Tayyabah Yousaf:** Formal analysis, Writing – review & editing. **Maria A. Nettis:** Formal analysis, Writing – review & editing. **Valeria Mondelli:** Formal analysis, Writing – review & editing. **Carmine Pariante:** Formal analysis, Writing – review & editing. **Neil A. Harrison:** Formal analysis, Writing – review & editing. **Edward T. Bullmore:** Formal analysis, Writing – review & editing. **Danai Dima:** Conceptualization, Methodology, Software, Formal analysis, Investigation, Validation, Writing – original draft, Writing – review & editing. **Federico E. Turkheimer:** Conceptualization, Methodology, Software, Formal analysis, Investigation, Validation, Writing – original draft, Writing – review & editing. **Mattia Veronese:** Conceptualization, Methodology, Software, Formal analysis, Investigation, Validation, Writing – original draft, Writing – review & editing.

Declaration of Competing Interest

The authors declare that they have no known competing financial interests or personal relationships that could have appeared to influence

the work reported in this paper.

Acknowledgements

The BIODEP study was sponsored by the Cambridgeshire and Peterborough NHS Foundation Trust and the University of Cambridge, and funded by a strategic award from the Wellcome Trust (104025) in partnership with Janssen, GlaxoSmithKline, Lundbeck and Pfizer. Recruitment of participants was supported by the National Institute of Health Research (NIHR) Clinical Research Network: Kent, Surrey and Sussex & Eastern. E Bullmore and CM Pariante are supported by a Senior Investigator award from the NIHR. Additional funding was provided by the National Institute for Health Research (NIHR) Biomedical Research Centre at South London and Maudsley NHS Foundation Trust and King's College London, and by the NIHR Cambridge Biomedical Research Centre (Mental Health). Study data were collected and managed using REDCap electronic data capture tools hosted at the University of Cambridge (70). We would like to gratefully thank all study participants, research teams and laboratory staff, without whom this research would not have been possible. We thank and acknowledge all members of the NIMA Consortium at the time of data collection: Dominika Wlazly, Amber Dickinson, Andy Foster, Clare Knight, Claire Leckey, Paul Morgan, Angharad Morgan, Caroline O'Hagan, Samuel Touchard, Shahid Khan, Phil Murphy, Christine Parker, Jai Patel, Jill Richardson, Paul Acton, Nigel Austin, Anindya Bhattacharya, Nick Carruthers, Peter de Boer, Wayne Drevets, John Isaac, Declan Jones, John Kemp, Hartmuth Kolb, Jeff Nye, Gayle Wittenberg, Gareth Barker, Anna Bogdanova, Heidi Byrom, Diana Cash, Annamaria Cattaneo, Daniela Enache, Tony Gee, Caitlin Hastings, Melisa Kose, Giulia Lombardo, Nicole Mariani, Anna McLaughlin, Valeria Mondelli, Maria Nettis, Naghmeh Nikkheslat, Carmine Pariante, Karen Randall, Julia Schubert, Luca Sforzini, Hannah Sheridan, Camilla Simmons, Nisha Singh, Federico Turkheimer, Vicky Van Loo, Mattia Veronese, Marta Vicente Rodriguez, Toby Wood, Courtney Worrell, Zuzanna Zajkowska, Brian Campbell, Jan Egebjerg, Hans Eriksson, Francois Gastambide, Karen Husted Adams, Ross Jeggo, Thomas Moeller, Bob Nelson, Niels Plath, Christian Thomsen, Jan Torleif Pederson, Stevin Zorn, Catherine Deith, Scott Farmer, John McClean, Andrew McPherson, Nagore Penandes, Paul Scouller, Murray Sutherland, Mary Jane Attenburrow, Jithen Benjamin, Helen Jones, Fran Mada, Akintayo Oladejo, Katy Smith, Rita Balice-Gordon, Brendon Binneman, James Duerr, Terence Fullerton, Veeru Goli, Zoe Hughes, Justin Piro, Tarek Samad, Jonathan Sporn, Liz Hoskins, Charmaine Kohn, Lauren Wilcock, Franklin Aigbirhio, Junaid Bhatti, Ed Bullmore, Roido Manavaki, Sam Chamberlain, Marta Correia, Anna Crofts, Tim Fryer, Martin Graves, Alex Hatton, Manfred Kitzbichler, Mary-Ellen Lynall, Christina Maurice, Ciara O'Donnell, Linda Pointon, Peter St George Hyslop, Lorinda Turner, Petra Vertes, Barry Widmer, Guy Williams, Jonathan Cavanagh, Alison McColl, Robin Shaw, Erik Boddeke, Alison Baird, Stuart Clare, Phil Cowen, I-Shu (Dante) Huang, Sam Hurley, Simon Lovestone, Alejo Nevado-Holgado, Elena Ribe, Anviti Vyas, Laura Winchester, Madeleine Cleal, Diego Gomez-Nicola, Renzo Mancuso, Hugh Perry, Mara Cercignani, Charlotte Clarke, Alessandro Colasanti, Neil Harrison, Rosemary Murray, Jason O'Connor, Howard Mount.

References

ACABCHUK, R. L., SUN, Y., WOLFERZ JR, R., EASTMAN, M. B., LENNINGTON, J. B., SHOOK, B. A., WU, Q. & CONOVER, J. C. 2015. 3D modeling of the lateral ventricles and histological characterization of periventricular tissue in humans and mouse. *JoVE (Journal of Visualized Experiments)*, e52328.

Alexander-Bloch, A., Giedd, J.N., Bullmore, E., 2013a. Imaging structural co-variance between human brain regions. Nat. Rev. Neurosci. 14, 322–336.

Alexander-Bloch, A., Raznahan, A., Bullmore, E., Giedd, J., 2013b. The convergence of maturational change and structural covariance in human cortical networks. J. Neurosci. 33, 2889–2899.

Arnatkeviciute, A., Fulcher, B.D., Fornito, A., 2019. A practical guide to linking brain-wide gene expression and neuroimaging data. Neuroimage 189, 353–367.

ASHBURNER, J. 2007. A fast diffeomorphic image registration algorithm. *Neuroimage*, 38, 95-113.

Barkho, B.Z., Monuki, E.S., 2015. Proliferation of cultured mouse choroid plexus epithelial cells. PLoS ONE 10, e0121738.

Bekhbat, M., Chu, K., Le, N.-A., Woolwine, B.J., Haroon, E., Miller, A.H., Felger, J.C., 2018. Glucose and lipid-related biomarkers and the antidepressant response to infliximab in patients with treatment-resistant depression. Psychoneuroendocrinology 98, 222–229.

Belmaker, R.H., Agam, G., 2008. Major depressive disorder. N. Engl. J. Med. 358, 55–68.

Brown, P., Davies, S., Speake, T., Millar, I., 2004. Molecular mechanisms of cerebrospinal fluid production. Neuroscience 129, 955–968.

Burgos, N., Cardoso, M.J., Thielemans, K., Modat, M., Pedemonte, S., Dickson, J., Barnes, A., Ahmed, R., Mahoney, C.J., Schott, J.M., Duncan, J.S., Atkinson, D., Arridge, S.R., Hutton, B.F., Ourselin, S., 2014. Attenuation correction synthesis for hybrid PET-MR scanners: application to brain studies. IEEE Trans. Med. Imaging 33, 2332–2341.

Clark-Raymond, A., Halaris, A., 2013. VEGF and depression: a comprehensive assessment of clinical data. J. Psychiat. Res. 47, 1080–1087.

de Leon, M.J., Li, Y., Okamura, N., Tsui, W.H., Saint-Louis, L.A., Glodzik, L., Osorio, R.S., Fortea, J., Butler, T., Pirraglia, E., 2017. Cerebrospinal fluid clearance in Alzheimer disease measured with dynamic PET. J. Nucl. Med. 58, 1471–1476.

Desikan, R.S., Segonne, F., Fischl, B., Quinn, B.T., Dickerson, B.C., Blacker, D., Buckner, R.L., Dale, A.M., Maguire, R.P., Hyman, B.T., Albert, M.S., Killiany, R.J., 2006. An automated labeling system for subdividing the human cerebral cortex on MRI scans into gyral based regions of interest. Neuroimage 31, 968–980.

Devorak, J., Torres-Platas, S.G., Davoli, M.A., Prud'homme, J., Turecki, G., Mechawar, N., 2015. Cellular and molecular inflammatory profile of the choroid plexus in depression and suicide. Front. Psychiat. 6, 138.

D'Mello, C., Le, T., Swain, M.G., 2009. Cerebral microglia recruit monocytes into the brain in response to tumor necrosis factorα signaling during peripheral organ inflammation. J. Neurosci. 29, 2089–2102.

Dome, P., Teleki, Z., Rihmer, Z., Peter, L., Dobos, J., Kenessey, I., Tovari, J., Timar, J., Paku, S., Kovacs, G., 2009. Circulating endothelial progenitor cells and depression: a possible novel link between heart and soul. Mol. Psychiatry 14, 523–531.

DON, B. R. & KAYSEN, G. Poor nutritional status and inflammation: serum albumin: relationship to inflammation and nutrition. Seminars in dialysis, 2004. Wiley Online Library, 432-437.

ENACHE, D., PARIANTE, C. & MONDELLI, V. 2019. Markers of central inflammation in major depressive disorder: A systematic review and meta-analysis of studies examining cerebrospinal fluid, positron emission tomography and post-mortem brain tissue. *Brain, behavior, and immunity*.

FELGER, J. C., HAROON, E., PATEL, T. A., GOLDSMITH, D. R., WOMMACK, E. C., WOOLWINE, B. J., LE, N. A., FEINBERG, R., TANSEY, M. G. & MILLER, A. H. 2018. What does plasma CRP tell us about peripheral and central inflammation in depression? *Mol Psychiatry*.

Fischl, B., Salat, D.H., Busa, E., Albert, M., Dieterich, M., Haselgrove, C., van der Kouwe, A., Killiany, R., Kennedy, D., Klaveness, S., 2002. Whole brain segmentation: automated labeling of neuroanatomical structures in the human brain. Neuron 33, 341–355.

Fleischer, V., Gonzalez-Escamilla, G., Ciolac, D., Albrecht, P., Küry, P., Gruchot, J., Dietrich, M., Hecker, C., Müntefering, T., Bock, S., 2021. Translational value of choroid plexus imaging for tracking neuroinflammation in mice and humans. In: Proceedings of the National Academy of Sciences, p. 118.

Ghersi-Egea, J.-F., Strazielle, N., Catala, M., Silva-Vargas, V., Doetsch, F., Engelhardt, B., 2018. Molecular anatomy and functions of the choroidal blood-cerebrospinal fluid barrier in health and disease. Acta Neuropathol. 135, 337–361.

Goldin, P.R., McRae, K., Ramel, W., Gross, J.J., 2008. The neural bases of emotion regulation: reappraisal and suppression of negative emotion. Biol. Psychiatry 63, 577–586.

Goyal, M.S., Hawrylycz, M., Miller, J.A., Snyder, A.Z., Raichle, M.E., 2014. Aerobic glycolysis in the human brain is associated with development and neotenous gene expression. Cell Metab. 19, 49–57.

Haapakoski, R., Mathieu, J., Ebmeier, K.P., Alenius, H., Kivimäki, M., 2015. Cumulative meta-analysis of interleukins 6 and 1β, tumour necrosis factor α and C-reactive protein in patients with major depressive disorder. Brain Behav. Immun. 49, 206–215.

Harrison, N.A., Brydon, L., Walker, C., Gray, M.A., Steptoe, A., Critchley, H.D., 2009. Inflammation causes mood changes through alterations in subgenual cingulate activity and mesolimbic connectivity. Biol. Psychiatry 66, 407–414.

Hawrylycz, M.J., Lein, E.S., Guillozet-Bongaarts, A.L., Shen, E.H., Ng, L., Miller, J.A., van de Lagemaat, L.N., Smith, K.A., Ebbert, A., Riley, Z.L., 2012. An anatomically comprehensive atlas of the adult human brain transcriptome. Nature 489, 391–399.

Heinen, R., Bouvy, W.H., Mendrik, A.M., Viergever, M.A., Biessels, G.J., de Bresser, J., 2016. Robustness of automated methods for brain volume measurements across different MRI field strengths. PLoS ONE 11, e0165719.

Howren, M.B., Lamkin, D.M., Suls, J., 2009. Associations of depression with C-reactive protein, IL-1, and IL-6: a meta-analysis. Psychosom. Med. 71, 171–186.

Isung, J., Mobarrez, F., Nordström, P., Åsberg, M., Jokinen, J., 2012. Low plasma vascular endothelial growth factor (VEGF) associated with completed suicide. World J. Biol. Psychiatry 13, 468–473.

Johanson, C.E., Johanson, N.L., 2018. Choroid plexus blood-CSF barrier: major player in brain disease modeling and neuromedicine. J. Neurol. Neuromed. 3.

Jovicich, Jorge, Czanner, Silvester, Han, Xiao, Salat, David, van der Kouwe, Andre, Quinn, Brian, Pacheco, Jenni, Albert, Marilyn, Killiany, Ronald, Blacker, Deborah, 2009. MRI-derived measurements of human subcortical, ventricular and intracranial brain volumes: reliability effects of scan sessions, acquisition sequences, data

analyses, scanner upgrade, scanner vendors and field strengths. Neuroimage 46 (1), 177–192.
Kealy, J., Greene, C., Campbell, M., 2020. Blood-brain barrier regulation in psychiatric disorders. Neurosci. Lett. 726, 133664.
Khasawneh, A.H., Garling, R.J., Harris, C.A., 2018. Cerebrospinal fluid circulation: What do we know and how do we know it? Brain circulation 4, 14.
Lake, B.B., Chen, S., Sos, B.C., Fan, J., Kaeser, G.E., Yung, Y.C., Duong, T.E., Gao, D., Chun, J., Kharchenko, P.V., Zhang, K., 2018. Integrative single-cell analysis of transcriptional and epigenetic states in the human adult brain. Nat. Biotechnol. 36, 70–80.
LIDDELOW, S. A. 2015. Development of the choroid plexus and blood-CSF barrier. *Frontiers in neuroscience*, 9, 32.
Lizano, P., Lutz, O., Ling, G., Lee, A.M., Eum, S., Bishop, J.R., Kelly, S., Pasternak, O., Clementz, B., Pearlson, G., Sweeney, J.A., Gershon, E., Tamminga, C., Keshavan, M., 2019. Association of choroid plexus enlargement with cognitive, inflammatory, and structural phenotypes across the psychosis spectrum. Am. J. Psychiatry 176, 564–572.
LOTRICH, F. E. 2009. Major depression during interferon-α treatment: vulnerability and prevention. *Dialogues in clinical neuroscience*, 11, 417.
Maharaj, A.S., Walshe, T.E., Saint-Geniez, M., Venkatesha, S., Maldonado, A.E., Himes, N.C., Matharu, K.S., Karumanchi, S.A., D'Amore, P.A., 2008. VEGF and TGF-β are required for the maintenance of the choroid plexus and ependyma. J. Exp. Med. 205, 491–501.
Marques, F., Sousa, J.C., 2015. The choroid plexus is modulated by various peripheral stimuli: implications to diseases of the central nervous system. Front. Cell. Neurosci. 9, 136.
MARTINS, D., DIPASQUALE, O., VERONESE, M., TURKHEIMER, F., LOGGIA, M. L., MCMAHON, S., HOWARD, M. A. & WILLIAMS, S. C. R. 2021. Transcriptional and cellular signatures of cortical morphometric similarity remodelling in chronic pain. *bioRxiv*, 2021.03.24.436777.
Miller, A.H., Raison, C.L., 2016. The role of inflammation in depression: from evolutionary imperative to modern treatment target. Nat. Rev. Immunol. 16, 22.
Meeker, R.B., Williams, K., Killebrew, D.A., Hudson, L.C., 2012. Cell trafficking through the choroid plexus. Cell Adhesi. Migrat. 6, 390–396.
Miller, A.H., Maletic, V., Raison, C.L., 2009. Inflammation and its discontents: the role of cytokines in the pathophysiology of major depression. Biol. Psychiatry 65, 732–741.
Mondelli, V., Vernon, A.C., Turkheimer, F., Dazzan, P., Pariante, C.M., 2017. Brain microglia in psychiatric disorders. Lancet Psychiatry 4, 563–572.
Müller, N., 2019. The Role of Intercellular Adhesion Molecule-1 in the Pathogenesis of Psychiatric Disorders. Front. Pharmacol. 10, 1251. https://doi.org/10.3389/fphar.2019.01251.
Nettis, Maria Antonietta, Lombardo, Giulia, Hastings, Caitlin, Zajkowska, Zuzanna, Mariani, Nicole, Nikkheslat, Naghmeh, Worrell, Courtney, Enache, Daniela, McLaughlin, Anna, Kose, Melisa, Sforzini, Luca, Bogdanova, Anna, Cleare, Anthony, Young, Allan H., Pariante, Carmine M., Mondelli, Valeria, 2021. Augmentation therapy with minocycline in treatment-resistant depression patients with low-grade peripheral inflammation: results from a double-blind randomised clinical trial. Neuropsychopharmacology 46 (5), 939–948.
Nettis, M.A., Veronese, M., Nikkheslat, N., Mariani, N., Lombardo, G., Sforzini, L., Enache, D., Harrison, N.A., Turkheimer, F., Mondelli, V., 2020. PET imaging shows no changes in TSPO brain density after IFN-α immune challenge in healthy human volunteers. Transl. Psychiatry 10, 1–11.
Petralia, M.C., Mazzon, E., Fagone, P., Basile, M.S, Lenzo, V., Quattropani, M.C., Bendtzen, K., Nicoletti, F., 2020. Pathogenic contribution of the Macrophage migration inhibitory factor family to major depressive disorder and emerging tailored therapeutic approaches. J. Affect. Disorder 263, 15–24.
Pintzka, C.W.S., Hansen, T.I., Evensmoen, H.R., Håberg, A.K., 2015. Marked effects of intracranial volume correction methods on sex differences in neuroanatomical structures: a HUNT MRI study. Front. Neurosci. 9, 238.
Pollak, T.A., Drndarski, S., Stone, J.M., David, A.S., McGuire, P., Abbott, N.J., 2018. The blood–brain barrier in psychosis. Lancet Psychiatry 5, 79–92.
Ricigliano, Vito A.G., Morena, Emanuele, Colombi, Annalisa, Tonietto, Matteo, Hamzaoui, Mariem, Poirion, Emilie, Bottlaender, Michel, Gervais, Philippe, Louapre, Céline, Bodini, Benedetta, Stankoff, Bruno, 2021. Choroid plexus enlargement in inflammatory multiple sclerosis: 3.0-T MRI and translocator protein PET evaluation. Radiology 301 (1), 166–177.
Saunders, N.R., Liddelow, S.A., Dziegielewska, K.M., 2012. Barrier mechanisms in the developing brain. Front. Pharmacol. 3, 46.
Schmaal, L., Pozzi, E., Ho, T.C., van Velzen, L.S., Veer, I.M., Opel, N., van Someren, E.J., Han, L.K., Aftanas, L., Aleman, A., 2020. ENIGMA MDD: seven years of global neuroimaging studies of major depression through worldwide data sharing. Transl. Psychiatry 10, 1–19.
Schubert, J., Tonietto, M., Turkheimer, F., Zanotti-Fregonara, P., Veronese, M., 2021a. Supervised clustering for TSPO PET imaging. Eur. J. Nucl. Med. Mol. Imaging 1–12.
Schubert, J.J., Veronese, M., Marchitelli, L., Bodini, B., Tonietto, M., Stankoff, B., Brooks, D.J., Bertoldo, A., Edison, P., Turkheimer, F., 2019. Dynamic 11C-PiB PET shows cerebrospinal fluid flow alterations in Alzheimer's disease and multiple sclerosis. J. Nucl. Med., jnumed. 118, 223834.
Schubert, J.J., Veronese, M., Fryer, T.D., Manavaki, R., Kitzbichler, M.G., Nettis, M.A., Mondelli, V., Pariante, C.M., Bullmore, E.T., Turkheimer, F.E., 2021b. A modest increase in 11C-PK11195-PET TSPO binding in depression is not associated with serum C-reactive protein or body mass index. Biol. Psychiatry Cognit. Neurosci. Neuroimag.
Schwartz, M., Baruch, K., 2014. The resolution of neuroinflammation in neurodegeneration: leukocyte recruitment via the choroid plexus. EMBO J. 33, 7–22.
SHEN, M. D. 2018. Cerebrospinal fluid and the early brain development of autism. *J Neurodev Disord*, 10, 39.
Tadayon, E., Pascual-Leone, A., Press, D., Santarnecchi, E., Initiative, A.S.D.N., 2020. Choroid plexus volume is associated with levels of CSF proteins: relevance for Alzheimer's and Parkinson's disease. Neurobiol. Aging 89, 108–117.
Thomas, B.A., Cuplov, V., Bousse, A., Mendes, A., Thielemans, K., Hutton, B.F., Erlandsson, K., 2016. PETPVC: a toolbox for performing partial volume correction techniques in positron emission tomography. Phys. Med. Biol. 61, 7975.
Torres-Platas, S.G., Cruceanu, C., Chen, G.G., Turecki, G., Mechawar, N., 2014. Evidence for increased microglial priming and macrophage recruitment in the dorsal anterior cingulate white matter of depressed suicides. Brain Behav. Immun. 42, 50–59.
Turkheimer, Federico E., Althubaity, Noha, Schubert, Julia, Nettis, Maria A., Cousins, Oliver, Dima, Danai, Mondelli, Valeria, Bullmore, Edward T., Pariante, Carmine, Veronese, Mattia, 2021. Increased serum peripheral C-reactive protein is associated with reduced brain barriers permeability of TSPO radioligands in healthy volunteers and depressed patients: implications for inflammation and depression. Brain Behav. Immun. 91, 487–497.
Turkheimer, F.E., Edison, P., Pavese, N., Roncaroli, F., Anderson, A.N., Hammers, A., Gerhard, A., Hinz, R., Tai, Y.F., Brooks, D.J., 2007. Reference and target region modeling of [11C]-(R)-PK11195 brain studies. J. Nucl. Med. 48, 158–167.
Turner, C.A., Thompson, R.C., Bunney, W.E., Schatzberg, A.F., Barchas, J.D., Myers, R. M., Akil, H., Watson, S.J., 2014. Altered choroid plexus gene expression in major depressive disorder. Front. Hum. Neurosci. 8, 238.
Vaishnavi, S.N., Vlassenko, A.G., Rundle, M.M., Snyder, A.Z., Mintun, M.A., Raichle, M. E., 2010. Regional aerobic glycolysis in the human brain. Proc. Natl. Acad. Sci. 107, 17757–17762.
Vasa, F., Seidlitz, J., Romero-Garcia, R., Whitaker, K.J., Rosenthal, G., Vertes, P.E., Shinn, M., Alexander-Bloch, A., Fonagy, P., Dolan, R.J., Jones, P.B., Goodyer, I.M., Consortium, N., Sporns, O., Bullmore, E.T., 2018. Adolescent tuning of association cortex in human structural brain networks. Cereb. Cortex 28, 281–294.
VERONESE, M., REIS MARQUES, T., BLOOMFIELD, P. S., RIZZO, G., SINGH, N., JONES, D., AGUSHI, E., MOSSES, D., BERTOLDO, A. & HOWES, O. 2018. Kinetic modelling of [11C] PBR28 for 18 kDa translocator protein PET data: a validation study of vascular modelling in the brain using XBD173 and tissue analysis. *Journal of Cerebral Blood Flow & Metabolism*, 38, 1227-1242.
Vichaya, E.G., Malik, S., Sominsky, L., Ford, B.G., Spencer, S.J., Dantzer, R., 2020. Microglia depletion fails to abrogate inflammation-induced sickness in mice and rats. J. Neuroinflamm. 17, 1–14.
Whitaker, K.J., Vertes, P.E., Romero-Garcia, R., Vasa, F., Moutoussis, M., Prabhu, G., Weiskopf, N., Callaghan, M.F., Wagstyl, K., Rittman, T., Tait, R., Ooi, C., Suckling, J., Inkster, B., Fonagy, P., Dolan, R.J., Jones, P.B., Goodyer, I.M., Consortium, N., Bullmore, E.T., 2016. Adolescence is associated with genomically patterned consolidation of the hubs of the human brain connectome. Proc. Natl. Acad. Sci. U.S. A. 113, 9105–9110.
Yang, A.C., Kern, F., Losada, P.M., Agam, M.R., Maat, C.A., Schmartz, G.P., Fehlmann, T., Stein, J.A., Schaum, N., Lee, D.P., 2021. Dysregulation of brain and choroid plexus cell types in severe COVID-19. Nature 1–10.
Yushkevich, Paul A., Piven, Joseph, Hazlett, Heather Cody, Smith, Rachel Gimpel, Ho, Sean, Gee, James C., Gerig, Guido, 2006. User-guided 3D active contour segmentation of anatomical structures: significantly improved efficiency and reliability. Neuroimage 31 (3), 1116–1128.
Zhang, B., Kirov, S., Snoddy, J., 2005. WebGestalt: an integrated system for exploring gene sets in various biological contexts. Nucleic Acids Res. 33, W741–W748.
Zhou, Y.-F., Huang, J.-C., Zhang, P., Fan, F.-M., Chen, S., Fan, H.-Z., Cui, Y.-M., Luo, X.-G., Tan, S.-P., Wang, Z.-R., 2020. Choroid plexus enlargement and allostatic load in schizophrenia. Schizophr. Bull. 46, 722–731.